

# Load interdependencies of flood defences

A new methodology for incorporating load  
interdependencies in flood risk analysis of lowland  
rivers

Master Thesis

Wouter Jan Klerk



Front page cover image: 2004 levee breach at Jones Tract, California.  
Retrieved October 2013 from: [http://www.deltanationalpark.org/images/images/jones\\_tract\\_breach.jpg](http://www.deltanationalpark.org/images/images/jones_tract_breach.jpg)

# Load interdependencies of flood defences

---

A new methodology for incorporating load interdependencies  
in flood risk analysis of lowland rivers

**Author** Wouter Jan Klerk  
**E-mail-adress** [w.j.klerk@gmail.com](mailto:w.j.klerk@gmail.com)  
**Phone number** +31 (0)630839508

This research has been done in partial fulfilment of requirements for the Master of Science degree in Civil Engineering, Track Hydraulic Engineering, Specialization Hydraulic Structures & Flood Risk at the faculty of Civil Engineering & Geosciences of **Delft University of Technology**, Delft, the Netherlands.

## Graduation committee

Prof. dr. ir. M. Kok Delft University of Technology  
*Department of Hydraulic Engineering*

Prof. dr. ir. S.N. Jonkman Delft University of Technology  
*Department of Hydraulic Engineering*

Dr. Ir. K.M. De Bruijn Deltares  
*Unit Scenarios and Policy Analysis*

Dr. Ir. P.J.A.T.M. van Overloop Delft University of Technology  
*Department of Water Management*



*“Interdependence is a fact, it's not an opinion”*

Peter Coyote



## Acknowledgements

This thesis is the final part of my master programme in Hydraulic Engineering at Delft University of Technology. The research presented here was executed at Deltares and supervised by both Deltares and TU Delft.

The goal of this research is to investigate load interdependencies of flood defences. Hopefully the methodology suggested and the conclusions can lead to a better understanding and management of flood risks in the future.

This thesis would not have been the same without the support of my graduation committee. First of all I want to thank Matthijs Kok for taking up the role as chairman of the graduation committee and providing many interesting thoughts during our discussions on my progress. The daily supervision by Karin de Bruijn was also very important with her thorough and constructive feedback throughout the process. The other members of the committee, Bas Jonkman and Peter-Jules van Overloop, were also very important in the discussions during the committee meetings.

At Deltares I also would like to express my acknowledgement to Ferdinand Diermanse, for helping me find my way through his neat Monte Carlo scripts. Also André Hendriks was very important in helping me with some programming which would have probably lead me to total desperation, if I would have done it myself. All in all it was a great pleasure to be working at Deltares with so many smart people around me. And of course I also want to thank Deltares in general for having me around.

At last I want to thank the people around me, and especially my parents, for their constant support and motivation throughout my studies. It is a privilege to have so much encouraging support from people around you.

## Summary

In the Netherlands flood risk is often assessed per dike ring area: a designated area protected against flooding by a system of primary flood defences (Waterwet, 2009). Although the approach is suitable for many areas it also has some disadvantages. One of the main disadvantages when zooming in on a small area in a large water system is that often the effect of the system on that small area is not, or cannot be, dealt with properly. Research has shown that for a set of cases in the Netherlands load interdependencies of flood defences have a significant influence on the outcome of flood risk analysis. Load interdependencies of flood defences are the effects that failures of certain dike reaches have on other dike reaches. Due to failures the loads at other locations are influenced. The aim of this research is to develop a framework which enables accounting for load interdependencies of flood defences. This is done by studying literature and defining the relevant factors of influence for these effects. After that the methodology is applied in a case study.

Load interdependencies are better known in the Netherlands by the term ‘system behaviour’, however due to the vagueness of this term, ‘load interdependencies’ is considered a better description of the phenomenon. In literature two types of load interdependencies are distinguished: positive and negative load interdependencies. In cases with positive interdependencies the failures of dikes increase the safety of dikes at other locations, for instance due to a decrease in river discharge. This principle is called load relief. Negative load interdependencies work the other way around: failure of a certain dike causes a higher than expected load at another dike. An example of the latter was found and studied for the ‘Land van Maas en Waal’ (Vrouwenvelder et al., 2010), where water from the Waal can increase water levels at the Maas by over a meter, this is called shortcutting. There is also another way in which negative load interdependencies can have an effect: so called cascade effects. In those cases flooding of one area causes consequential flooding of more downstream areas due to flow over land.

Previous research suggests several methods in order to deal with the effects of dike breaches on safety. However, these methods are only applied for specific cases or for river reaches with only positive load interdependencies. Based on literature it is concluded that load interdependencies have a significant effect on flood risk. Also nearly all articles (Apel et al., 2009a; De Bruijn et al., 2013; Diermanse et al., 2007; Van Mierlo, 2005a; van Mierlo et al., 2008; Vorogushyn et al., 2010; Vrouwenvelder et al., 2010) on the subject conclude that it is important to consider load interdependencies in future flood risk analysis, but that there is no general method to do so. When looking at the effects of load interdependencies on flood risks it is important to have a good overview of which factors of influence are most important. This is done using the case shown below, for which all types of interactions are possible.

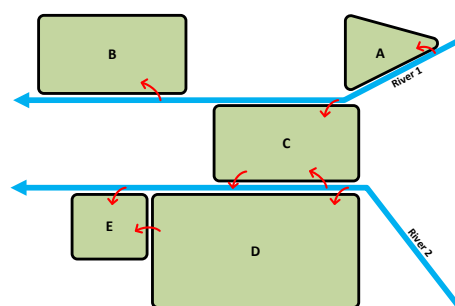
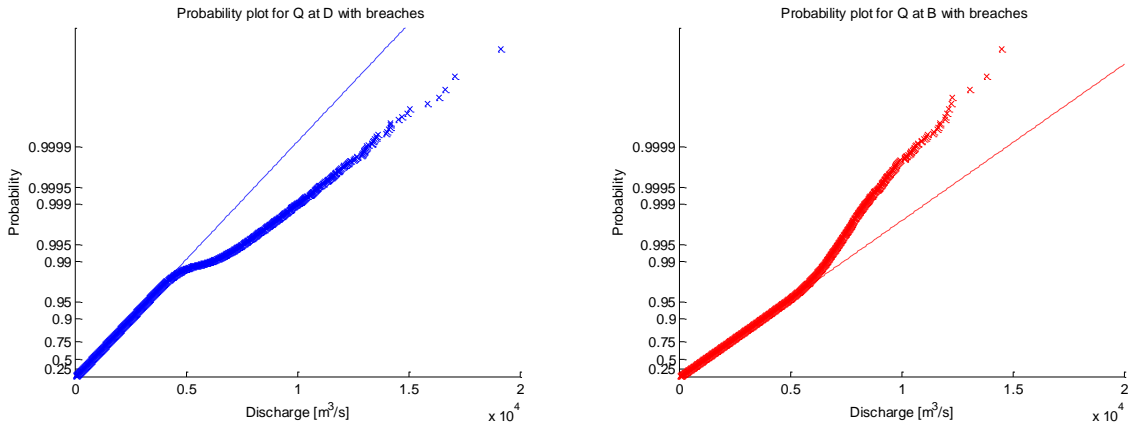


Figure 0-1 Conceptual case with different types of effects of load interdependencies

When considering the possible effects of load interdependencies, common factors such as width of the discharge wave, breach growth velocity, breach size and timing of discharge waves in cases with 2 rivers are identified as being influential. However, three main factors characteristic for mainly the effects of negative load interdependencies are identified: polder retention volume, time of breaching and polder side failures. The first is important as it determines the amount of relief on other locations but also the time before shortcutting occurs. The second one is important because time of breaching during the discharge wave has a large influence on the extent of the flood, and thus for the extent of potential shortcutting or cascade effects. The third is important because water flows over land and loads dikes from the polder side, which is quite unusual. In such cases, due to the dike profile, the dike might be considerably weaker, especially for macrostability failures. In the conceptual case the change in water level exceedence probabilities was a very good indicator for the effects of load interdependencies. In the conceptual case this is shown for both positive and negative load interdependencies, the trendline is a normal exponential distribution, the realizations can be observed to be shifted compared to this distribution: non-exceedence probabilities of high discharges become lower at the left, in case of negative interdependencies. For the right case, with positive interdependencies it is found to be the other way around.



**Figure 0-2 Non-exceedence probabilities of discharges from the conceptual model. At the left for negative load interdependencies, at the right for positive load interdependencies**

Based on the knowledge obtained from literature and the conceptual case a methodology was defined to deal with both positive and negative interdependencies. The set up of this new method is shown in Figure 0-3. The core of this method is a 1D model combined with a fast inundation model consisting of 1D branches and storage reservoirs. The fast inundation model is calibrated using 2D flood scenarios. In order to be able to use this model in a probabilistic context, fragility curves for dike strength and boundary conditions can be sampled using Monte Carlo simulation with Importance Sampling. Monte Carlo has an advantage in this case due to the many different scenarios, which gives it an edge over for instance FORM (First Order Reliability Method), which is considerably slower for cases with many variables (De Bruijn et al., 2013). By applying Importance Sampling only the runs with likely failures are selected to be run in the model.

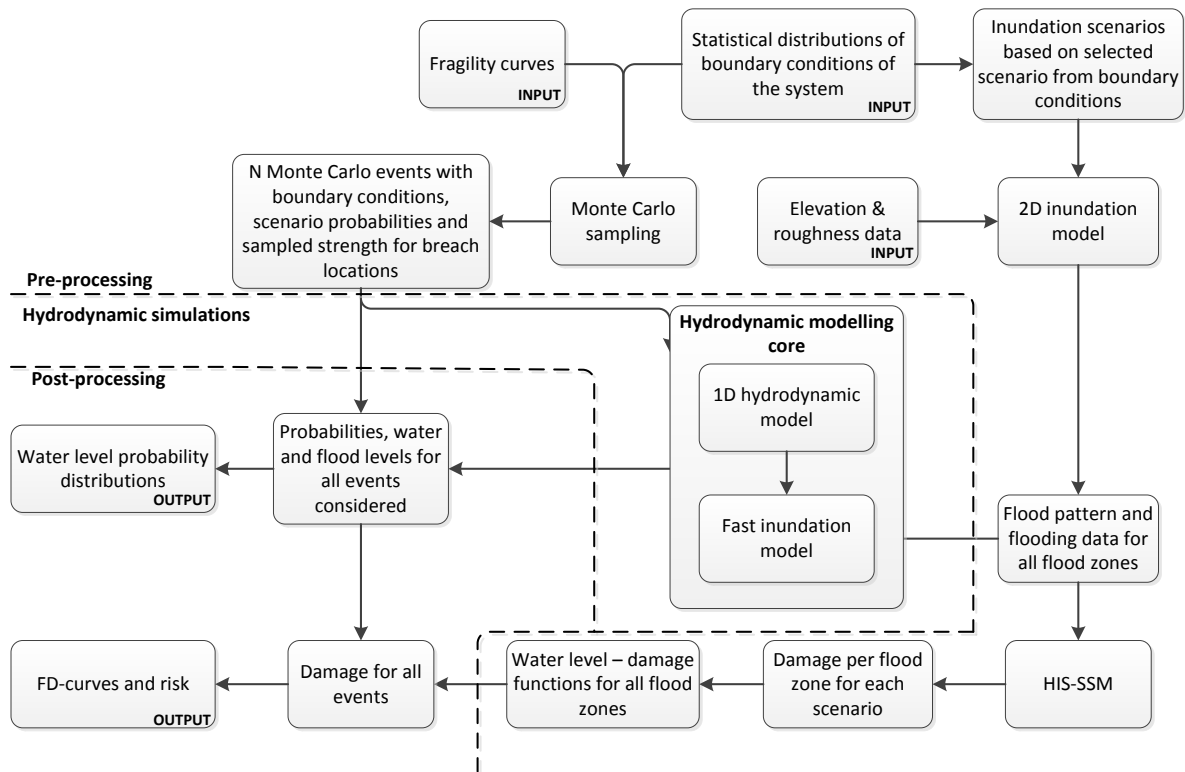


**Figure 0-3 Methodology for dealing with load interdependencies in risk analysis**

The methodology above is applied to a case for the Bovenrijn/IJssel, where load relief, shortcutting and cascade effects can occur. The fast inundation model is calibrated using data from 9 different 2D flood scenarios for each of the most important breach locations. By using HIS-SSM it is also possible to define water level – damage relationships for different ‘flood zones’ in the model, areas with a more or less uniform water level in case of a flood. The model contains 22 breach locations which can fail from both river and polder sides. For the dike strengths fragility curves are used, for polder side failures these were modified in order to account for the lower resistance against macrostability failures in those cases. Furthermore it was assumed that all dikes were at a 1/1.250 year design level, so the fragility curves were shifted to this level. The model performed quite well, although for some scenarios the calculated water levels were different from the ones calculated in the 2D scenarios. However, by using the water level – damage functions, and shifting these, it was possible to calculate the damage quite well.

For the case study area 5 different cases were analysed in the model: With/without breaches, with/without polder breaches (breaches induced by loading from the polder side), with/without outflow of polder and with/without cascade effects. From this case study it was shown that for the Bovenrijn/IJssel area load interdependencies can have significant effects, both positive and negative. Along the Bovenrijn the effects of breaches are generally positive while at the IJssel they can be both positive and negative, depending on the location in the river. For instance for the breach location at Giesbeek at the IJssel negative load interdependencies were found to be quite dominant, as can be seen from Figure 0-4, where the results for cases with breaches, without shortcutting and without breaches are compared. The negative effect in the case with breaches is caused by a large outflow of the breach.

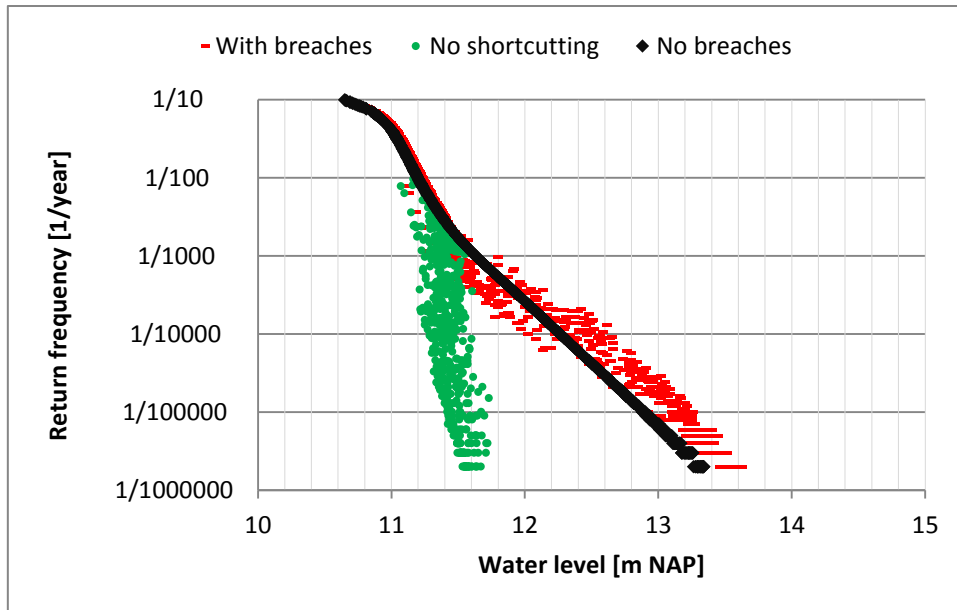


Figure 0-4 Water levels for the IJssel at Giesbeek

From this figure it can be seen that water levels are indeed lower in cases with positive load interdependencies. In this case the negative interdependencies were dominant in Scenario 1, although for other locations it was found that the positive effects were stronger.

In terms of economic risk the effect of load interdependencies on the total area is not that big: most effects compensate each other. For instance considering cascade effects decreases risk at certain locations while increasing it at others. In Figure 0-5 the FD-curve for the total area considered is shown for a set of scenarios. The net effect of considering cascade effects is not that big, shortcutting is found to be very important, especially for damage at the left bank of the IJssel.

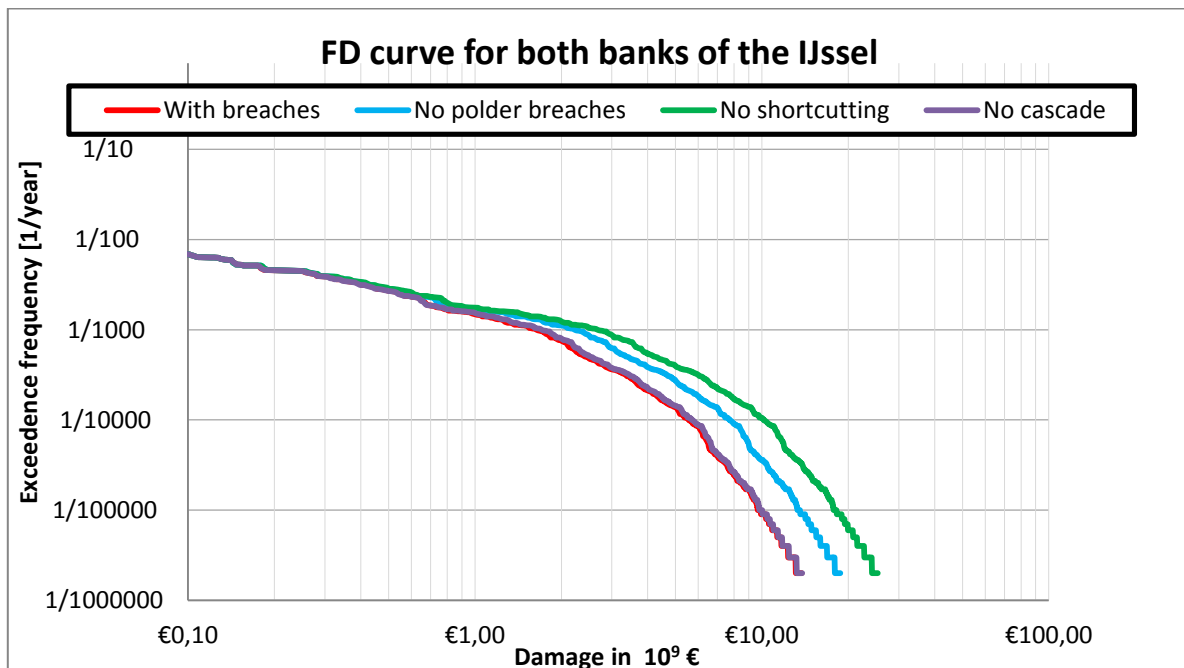


Figure 0-5 FD curve for the case study area

Cascade effects are found to have nearly no influence on the total risk of the area. However when considering separate dike rings it is found that the risk is redistributed. For instance for dike ring 48, the risk is found to be 20% higher when cascade effects are not taken into account.

In general the methodology performed well and the risk estimates found are quite reasonable. However, more case studies and further calibration of the model is necessary to give a full conclusion on the accuracy of these models. It can be concluded that this methodology is suitable for incorporating load interdependencies in risk analysis although improvements are suggested on the topics of calibrating breach outflows, investigating polder side failures and using more advanced failure mechanisms. Furthermore, it is suggested to develop an optimization model to enable better and faster calibration of these models using existing flood data. The effect of load interdependencies is found to be very important for proper risk estimates, although positive effects should not be accounted for in for instance dike design, as reinforcing one dike will cause the other dikes to not meet their standard anymore. Negative interdependencies are of importance in nearly all cases, but it is also suggested to further look into mitigating measures for these situations, such as controlled dike breaches, where water is diverted back into the river to prevent large negative effects.

## Table of Contents

Acknowledgements.....	vi
Summary.....	vii
List of figures .....	xvi
List of tables .....	xix
1. Introduction.....	1
1.1 Load interdependencies: a short introduction.....	2
1.2 Problem analysis.....	3
1.3 Context .....	3
1.4 Objective.....	3
1.5 Approach .....	4
1.6 Readers guide.....	4
2. Load interdependencies and their relevance for assessing flood risks.....	5
2.1 River system behaviour redefined .....	5
2.2 The concept of load interdependencies.....	6
2.3 Historical examples illustrating the relevance of load interdependencies.....	7
2.3.1 Load interdependencies in the Netherlands.....	7
2.3.2 System behaviour abroad.....	9
2.4 Studies on load interdependencies .....	12
2.4.1 Methodological approach, the Delft Cluster project.....	12
2.4.2 Flood risk analysis for the Bac Hung Hai polder, Vietnam.....	14
2.4.3 Influence of dike breaches on frequency of discharge waves .....	15
2.4.4 Dike breaches at the Elbe river by Vorogushyn et al.....	17
2.4.5 Effects of load interdependencies on different cases in the Netherlands .....	18
2.4.6 VNK2: safety of dike rings 14, 15 and 44 .....	18
2.5 Short conclusion on historic events and previous studies on effects of load interdependencies.....	19
2.6 Important aspects when considering interdependencies .....	20
2.6.1 When does the dike breach and under which conditions? .....	21
2.6.2 What happens in case of shortcutting? .....	23
2.6.3 What happens when water flows from River 1 into River 2?.....	26
3. General framework for flood risk analysis .....	28
3.1 Risk and its use in quantitative flood risk analysis.....	28
3.2 Methods for risk analysis in the Netherlands and abroad.....	28
3.2.1 Introduction .....	28

3.2.2	VNK2: How safe are we? .....	28
3.2.3	WV21: How safe should we be? .....	30
3.2.4	Risk analysis in the UK.....	31
3.3	Flood defences in risk analysis.....	32
3.3.1	Failure probabilities of dikes .....	32
3.3.2	Failure mechanisms .....	33
3.3.3	Spatial effects in flood defence reliability .....	35
3.3.4	Fragility curves .....	37
3.4	Methods for probabilistic analysis of flood defences.....	40
3.4.1	Type II: First-order reliability method (FORM) .....	40
3.4.2	Type III: Monte Carlo simulation.....	41
3.4.3	Comparison of methods .....	44
3.5	Quantifying flood risk .....	44
3.5.1	Societal risk .....	44
3.5.2	Economic damage .....	45
3.5.3	HIS-SSM.....	45
3.6	Flood modelling.....	46
3.6.1	Storage cell models.....	46
3.6.2	2D hydrodynamic modelling.....	46
3.6.3	3Di modelling.....	48
3.6.4	0D-models.....	48
3.6.5	Calculation speed .....	49
3.6.6	Conclusion.....	49
3.7	Dike breach modelling.....	49
3.7.1	Van der Knaap and Verheij-van der Knaap formulas.....	49
3.7.2	Use of statistical data on dike breaches.....	50
4.	New methodology for assessing load interdependencies of flood defences .....	51
4.1	Analysis of effects of load interdependencies.....	51
4.1.1	Positive load interdependencies in the conceptual model .....	52
4.1.2	Negative load interdependencies in the conceptual model.....	55
4.2	New methodology for incorporating load interdependencies in flood risk analysis .....	59
4.2.1	Possible outline of risk analysis .....	59
4.2.2	Computations with positive load interdependencies .....	59
4.2.3	Negative load interdependencies: modelling the interaction between land and river .....	60

4.2.4	Methodology for incorporating load interdependencies in flood risk analysis .....	63
5.	Application of the new methodology on the Bovenrijn/IJssel case.....	64
5.1	The Bovenrijn/IJssel area.....	64
5.2	Shortcutting at the Bovenrijn/IJssel area.....	65
5.3	Qualitative analysis of floods in the case study area.....	67
5.4	Set up of the models for inundation modelling.....	68
5.4.1	Available and used models.....	68
5.4.2	Boundary conditions .....	68
5.4.3	Comparison of hydraulic results of the model with the design water levels .....	68
5.5	Applying the method to the case study area .....	70
5.5.1	General outline.....	70
5.5.2	Pre-processing.....	72
5.5.3	Hydrodynamic modelling .....	77
5.5.4	Post-processing.....	82
5.5.5	Other important assumptions in the model.....	87
5.6	Results for the Bovenrijn/IJssel case study .....	88
5.6.1	Effects of load interdependencies on water levels.....	89
5.6.2	Effects of load interdependencies on number of breaches.....	94
5.6.3	Effects of load interdependencies on economic risk.....	95
5.6.4	Influence of load interdependencies on duration of the load.....	98
5.6.5	Computational performance of the new model.....	98
5.7	Conclusions and recommendations on the case study results .....	99
5.7.1	Conclusions.....	99
5.7.2	Recommendations .....	100
5.8	Applications of the method on flood risk management in the IJssel area.....	101
5.8.1	Dike design.....	101
5.8.2	Prioritization of reinforcement projects .....	103
5.8.3	Safety assessment.....	103
5.8.4	Calculations of Maximum Probable Damage .....	104
5.8.5	Estimating loss of life.....	104
6.	Conclusions and recommendations on the new methodology.....	105
7.	References .....	109
	Appendix.....	115
A	The societal risk assessment tool by Deltares.....	118
B	Dike stability in case of inner slope loading.....	122

C	MATLAB script used for the conceptual case .....	125
D	Building of the fast inundation model .....	129
E	Discharge waves .....	130
F	Fragility curves.....	133
G	Sobek input sheets.....	136
H	Profiles in the fast inundation model.....	139
I	Differences between 2D and 0D for different scenarios .....	147
J	Water level – damage curves.....	149
K	Water level differences for all breach locations .....	154
L	FD curves for dike rings 49, 50, 51 and 53 .....	159

## List of figures

Figure 0-1 Conceptual case with different types of effects of load interdependencies .....	vii
Figure 0-2 Non-exceedence probabilities of discharges from the conceptual model. At the left for negative load interdependencies, at the right for positive load interdependencies....	viii
Figure 0-3 Methodology for dealing with load interdependencies in risk analysis .....	ix
Figure 0-4 Water levels for the IJssel at Giesbeek.....	x
Figure 0-5 FD curve for the case study area .....	x
Figure 1-1 Current safety standards for dike ring areas in the Netherlands .....	1
Figure 1-2 Outline of thesis and report.....	4
Figure 2-1 Dike ring areas 14, 15 and 44 (ter Horst, 2012) .....	5
Figure 2-2 The three cases used in van der Wiel (2004).....	6
Figure 2-3 Historical drawing of a river flood in the Netherlands .....	7
Figure 2-4 Inundation 240 hours after the breach in the 1805 flood (Hesselink et al., 2003).....	8
Figure 2-5 Inundated areas in 1926 (van der Ham and van de Ven, 2004).....	8
Figure 2-6 Discharge hydrographs along the Elbe river, near Torgau (the blue line) a drop can be observed caused by several major dike breaches at that location (Infrastructure Development Institute, 2002).....	10
Figure 2-7 Water levels during the Jones Tract breach found from the DSM2 model (Mierzwa, 2005) .....	10
Figure 2-8 Map of the confluence of the Ohio and Mississippi rivers near Cairo, Illinois (Olson and Morton, 2012a).....	11
Figure 2-9 Conceptual Framework suggested by the Delft Cluster project on system behaviour (Vrouwenvelder et al., 2010) .....	13
Figure 2-10 Comparison between the results from the dynamic-probabilistic model and extreme value analysis for discharges with different return intervals along the river reach considered, from this figure the influence of dike breaches on extreme discharges is visible (Apel et al., 2009a) .....	15
Figure 2-11 Methodology used by Apel et al. (2009a) .....	16
Figure 2-12 Schematization of the methodology used (Vorogushyn et al., 2010).....	17
Figure 2-13 Hypothetical water system with load interdependencies .....	20
Figure 2-14 Inundation volumes compared to discharge peak levels and discharge during breaching in cases of rising or falling water levels for the case by Van der Wiel (2004) .....	21
Figure 2-15 Difference in inundation volume for two discharge waves with different lengths. The gray area is the total inundation volume.....	22
Figure 2-16 Distribution of failures over time during a standard shaped discharge wave. Please note that this is just a sketch to show the possible distribution of failures over time during a discharge wave.....	22
Figure 2-17 Case of a small retention capacity where the polder is filled up before the peak discharge.....	23
Figure 2-18 General cross section of Dutch river dike. ....	24
Figure 2-19 Failure mechanisms for load from river side .....	24
Figure 2-20 Loads on dike when polder is inundated .....	24
Figure 2-21 Loads on dike when polder is inundated and river at lower level .....	25
Figure 2-22 Time difference of discharge peak arrival between River 1 and 2 for two different correlation values.....	26

Figure 2-23 Conceptual inundation pattern when not considering additional dike breaches along River 2.....	27
Figure 2-24 Inundation pattern when considering additional dike breaches.....	27
Figure 3-1 Methodology used in VNK2 to assess the consequences of different flood scenarios (Jongejan et al., 2011).....	29
Figure 3-2 Economically optimal inundation probabilities for different dike reaches found from WV21 (Deltares, 2011).....	30
Figure 3-3 Generic process of the RASP methodology (Sayers and Meadowcroft, 2005).....	31
Figure 3-4 An overview of failure mechanisms (TAW, 1998).....	32
Figure 3-5 2D probability distribution for strength and loading of an element (TAW, 1998).....	33
Figure 3-6 Bishop sliding circle (Zwanenburg et al., 2013).....	35
Figure 3-7 Piping resistance: reality and observations (V NK2 project office, 2012).....	36
Figure 3-8 Principle of the length effect for a dike consisting of n elements (Kanning, 2012).....	36
Figure 3-9 Failure probability for a dike of n elements with various correlation coefficients (Kanning, 2012).....	36
Figure 3-10 Representation of a failure probability calculation using a water level distribution and a fragility curve (V NK2 project office, 2012).....	38
Figure 3-11 Fragility curves as found by Ter Horst (2005).....	38
Figure 3-12 3-dimensional seepage fragility curves for different durations in different water level intervals. The intervals represent portions of the total dike height and D(h) is the duration of the loading at a certain interval (Vorogushyn et al., 2009).....	39
Figure 3-13 Overview of the different parameters in a FORM analysis after normalization of the uncertain variables (V NK2 project office, 2012).....	40
Figure 3-14 Set of Monte Carlo simulations with their Z-values.....	41
Figure 3-15 Sampling strategy used in the societal risk tool (De Bruijn et al., 2013).....	42
Figure 3-16 Bias and standard deviation for Crude Monte Carlo and Monte Carlo with uniform Importance Sampling of river discharges at Lobith for the societal risk tool project at Deltares (De Bruijn et al., 2013).....	43
Figure 3-17 Example of an FN curve (Jonkman, 2007).....	45
Figure 3-18 Principle of water flow through a 1D2D model.....	47
Figure 3-19 Hierarchical quadtree ordering (Stelling, 2012).....	48
Figure 3-20 Example of the use of different grid scales in 1 model (Stelling, 2012).....	48
Figure 4-1 Hypothetical water system with load interdependencies.....	51
Figure 4-2 Case of positive load interdependence.....	52
Figure 4-3 Non-exceedence probabilities of the river discharge at different locations.....	53
Figure 4-4 Water levels and their exceedence probabilities with and without load interdependencies.....	54
Figure 4-5 Schematization of the mechanism of negative system behaviour.....	55
Figure 4-6 Non-exceedence probabilities with and without shortcutting from River 1.....	56
Figure 4-7 Non-exceedence probability plot for shortcutting with distinction between failures due to shortcutting and 'normal' failures.....	57
Figure 4-8 Event tree for failures at C and D.....	58
Figure 4-9 General outline of risk analysis.....	59
Figure 4-10 General outline of risk analysis including positive load interdependencies.....	60
Figure 4-11 Methodology for risk analysis accounting for both positive and negative load interdependencies.....	63
Figure 5-1 Overview of the IJssel area and surrounding dike rings considered in the case study64	

Figure 5-2 Effect of dike breaches at dike ring 48 on the discharges in the different river branches. Left: normal situation. Right: situation with a breach at the Bovenrijn. Please note that the time influence is ignored!.....	65
Figure 5-3 Separating canal and dikes between dike ring 49 and 50 .....	66
Figure 5-4 Elevations at the polders on the right bank of the IJssel .....	66
Figure 5-5 Flood depths for a breach at Spijk for a 1/10.000 year discharge from the 2D model.....	67
Figure 5-6 Water level differences between model and HR2006 for design discharge wave .....	69
Figure 5-7 Methodology as applied in the case study.....	70
Figure 5-8 Breach locations as used in the case study, all breach locations are at the right bank of the river except De Nijenstein, Terwolde, Hoven, 't Schol and Cortenoever .....	71
Figure 5-9 Discharge waves for the 2D simulations, the same discharge shape is used for the fast inundation model.....	73
Figure 5-10 Fragility curves for three failure mechanisms for Spijk.....	73
Figure 5-11 Method for shifting the fragility curves .....	74
Figure 5-12 Uniform importance sampling for Rhine discharges .....	75
Figure 5-13 Standard breach growth as used in both models .....	76
Figure 5-14 Comparison between 2D flood pattern and set up of the 0D model.....	77
Figure 5-15 Profiles and data for different types of nodes for the western part of dike ring 48 as used in the model .....	78
Figure 5-16 Breach discharges for 1,1000 year scenario at Gravenswaardsedam .....	80
Figure 5-17 Water level at flood zone 48_3 for both models in the case Germany_2 10,000 year t = 0 days.....	81
Figure 5-18 Flood zones used for determining the damage per area .....	83
Figure 5-19 HIS-SSM function for damage at low-rise buildings .....	83
Figure 5-20 Logarithmic water level - damage curve for flood zone 48_3 based on 13 water levels and damages for 13 2D scenarios.....	84
Figure 5-21 Procedure for calculation of the total risk.....	86
Figure 5-22 Breach locations in the model.....	88
Figure 5-23 Water levels and return frequencies at Giesbeek.....	90
Figure 5-24 Water levels and return frequencies at Deventer .....	90
Figure 5-25 Water levels and return frequencies at IJcentrale.....	91
Figure 5-26 Water level and return frequencies at Herwen.....	92
Figure 5-27 Uncertainty in water levels caused by interdependencies .....	93
Figure 5-28 FD curve total case study area.....	95
Figure 5-29 FD curve for dike ring 52 .....	96
Figure 5-30 FD curve for right bank of the IJssel .....	96
Figure 5-31 Discharge wave for a location near the downstream boundary of the IJssel. The time period is 2 months .....	98
Figure 5-32 Water levels in the conceptual case and the change in safety level in case upstream dikes are reinforced .....	102
Figure 5-33 Economically optimal inundation probabilities from WV21 .....	103

## List of tables

Table 2-1 Contribution of breaches in different dike rings on damage in dike rings in million € (ter Horst, 2012) .....	18
Table 2-2 Bishop Factor of Safety for a dike at dike ring 48 under inner and/or outer slope loading .....	25
Table 4-1 Dimensions of rivers 1 & 2 .....	52
Table 4-2 Discharges for 1/1.000 year return frequencies for all locations in the conceptual system .....	53
Table 4-3 Different methods and their advantages and disadvantages (ratings at scale between -- and ++).....	62
Table 5-1 Statistical description of discharge at Lobith (De Bruijn et al., 2013).....	72
Table 5-2 Inundation scenarios with their return period and time of breaching.....	76
Table 5-3 Differences in breach discharges of 0D and 2D model .....	79
Table 5-4 Water level differences between 0D and 2D for two scenarios .....	80
Table 5-5 Performance of water level – damage relations for 13 scenarios.....	85
Table 5-6 Performance of methods in calculation of risk for the 13 scenarios.....	85
Table 5-7 Scenarios used for comparing effects of load interdependencies.....	88
Table 5-8 Design water levels and actual return periods from the model.....	92
Table 5-9 Number of times breaches were triggered for different locations in the system.....	94
Table 5-10 Total risk for different areas in the case study .....	97





## 1. Introduction

For centuries water has formed and shaped the Netherlands. Economically, socially and politically it can be said that the Netherlands would be completely different without water. Currently, about two-thirds of the Netherlands is in danger of being flooded. It is not the goal of this paragraph to give a full overview of Dutch flood history, but one event is discerned since it shaped the Dutch flood risk management: the catastrophic flood of 1953. After these floods which took 1836 lives and caused enormous economic and societal damage the First Delta Committee was installed to come up with a renewed flood risk management strategy for the Netherlands. The First Delta Committee was the main driving force behind the execution of the Delta Works and in terms of risk management they also played a significant role. They reformed the standards of flood defences and determined these by looking at the potential consequences in case of a dike failure. By doing this they estimated an economic optimal probability of failure (van Dantzig, 1956) and with this knowledge experts set safety standards for different dike ring areas. For instance dike ring 14 (South Holland), with its large economic value has a safety standard of 1/10.000 year while other coastal dike rings only have a 1/4.000 year standard (Deltacommissie, 1961). The water level with a frequency of exceedance of 1/10.000 or 1/4.000 years was then used as basis for dike design (See Figure 1-1 for the current standards).

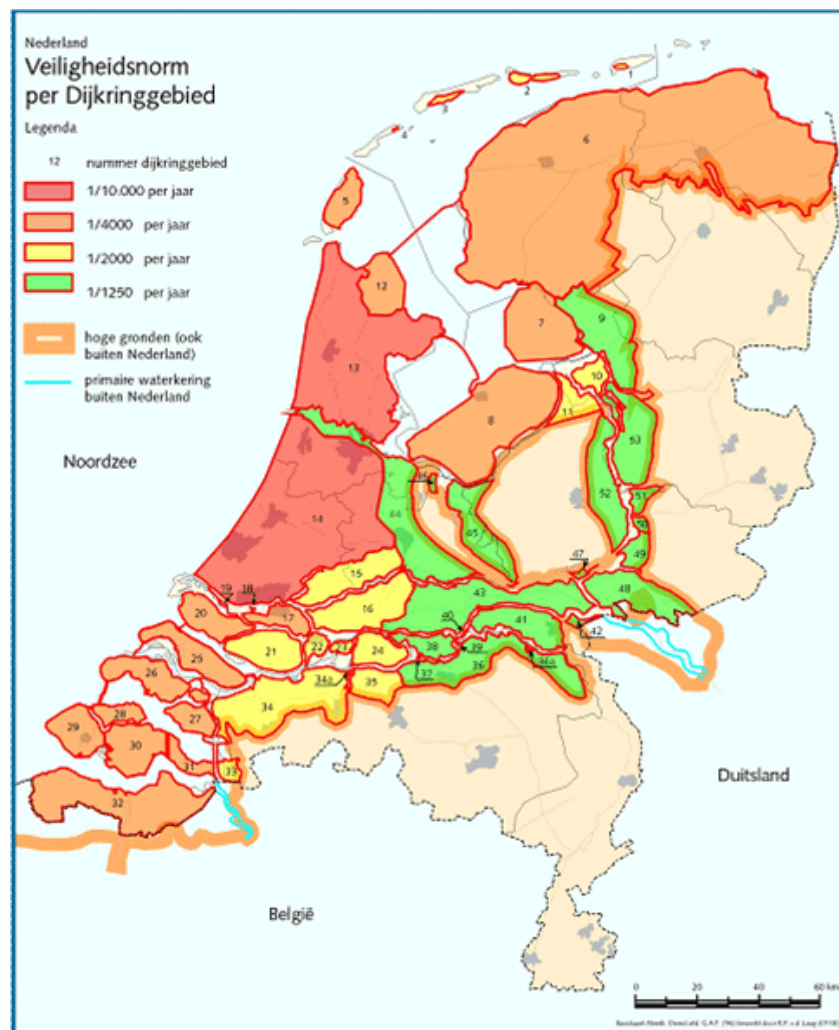


Figure 1-1 Current safety standards for dike ring areas in the Netherlands

During the decades after 1953 several committees were installed to review the flood risk management strategies, and one of the main changes over time was the change of the discharges and water levels corresponding with the design probabilities of the riverine areas. For different reasons these were lowered and raised during the years. For instance, after protests against dike reinforcement projects in the seventies, the Becht Committee lowered the design discharge for the river Rhine and subsequently the required safety standards for the river dikes. After the near flood disaster in 1993 the discharges were reviewed again and, after the near flood disasters in 1993 and 1995, the Room for the River project was started to increase the discharge capacity of the rivers. This was done by removing obstacles from the floodplain, widening flood plains and other discharge capacity increasing measures, rather than raising and improving dikes. After reports on climate change it was deemed realistic that the design discharge would have to be increased to 18.000 m<sup>3</sup>/s in 2050. During the last 20 years there have been more changes in flood risk management. In 2000 the TAW demonstrated that it is now possible to estimate the probability of flooding of a dike ring area (TAW, 2000). This report also implements the change suggested in 1995 by the Flood Defence Act to use the probability of flooding instead of the former used exceedance probabilities of water levels. After this the Dutch government commissioned a study to assess the probabilities and consequences of large scale floods. The VNK1 and VNK2 projects aim to assess all the dikes for their strength and calculate the risks in all the dike rings (Jongejan et al., 2011). In 2008 the 2nd Delta committee came with new advice on how to deal with flood risk in the Netherlands in the 21st century and in 2015 the Delta commissioner will deliver his conclusions on how to assess flood risks in the future. Part of this advice will be a new strategy for risk analysis and new flood protection standards. This report aims to explore the effects of an integrated risk analysis approach, where the system as a whole is considered.

### 1.1 Load interdependencies: a short introduction

In a river system people usually protect themselves from the danger of high water by living on higher grounds or building dikes around their cities, farmland and infrastructure. As was shown in the preceding paragraph the Dutch have been quite successful in protecting themselves from the water, despite some grave floods in the last centuries. The flood protection system in the Netherlands has developed to a network of dikes, forming so called dike ring areas, areas protected from the primary rivers, seas and lakes by a ring of dikes.

In risk analysis these dike rings are often analysed separately from each other, but research has shown that this is not always an accurate way to describe the actual situation (Van Mierlo, 2005a). Due to the fact that multiple dike rings protect land along the same river or a dike ring separates two rivers with different boundary conditions, dike rings influence each other and considering them separately is often an incorrect representation of the truth.

In past research these influences between dike rings were generally called river system behaviour. River system behaviour is a quite general term to describe interactions between different elements or subsystems in a larger system. Also in this context the term is quite vague and does not completely cover the subject. It is therefore necessary to reconsider the term 'river system behaviour'. As the goal of this research is to study the effect of breaches on loads elsewhere in the system the problem is better described by the term 'load interdependencies of flood defences'. A more extensive explanation of the use of this term is given in paragraph 2.1. When reference is made to past research the term system behaviour is sometimes used, however in those cases the meaning is the same.

## 1.2 Problem analysis

Although there is an extensive framework for assessing flood risks in the Netherlands, it does not include load interdependencies of flood defences. These interdependencies can have a significant influence on flood risks. VNK2 (VNK2 project office, 2012) assesses risks per dike ring but does not consider the number of other dike rings affected nor the damage in other dike rings during one event. This can potentially cause heavily underestimated or overestimated flood risks for the dike ring considered. It is also not possible to calculate flood risk accurately for the Netherlands as a whole by studying it in small isolated parts.

The main problem with load interdependencies is that it is a very complex, case-dependant phenomenon which can have influence in the entire system. To be able to assess these problems in a general framework either an enormous, unrealistic amount of computational capacity is required or simplifications in the modelling of these system effects have to be applied. There is however no clear view on which factors are most important, and whether it is possible to assess these types of problems in a model which spans for instance the whole Dutch water system. In order to do so a thorough understanding of the complexity of load interdependencies is required. Another aspect is that there is little insight in the effects of upstream dike rings on downstream dike rings in the Netherlands. This is also a factor which potentially leads to an overestimation of the risks in the downstream, mainly river-dominated dike rings. This is something which is especially very interesting for (re)insurance companies, emergency planners and other parties with interest in scenarios with extreme consequences.

## 1.3 Context

At Deltares a new tool has been developed which is able to assess the effects of positive load interdependencies on societal risk for the Netherlands as a whole (De Bruijn et al., 2013). This tool consists of a 1D model and a probabilistic framework to simulate multiple dike breaches in the system. In the context of this project, it is desired to enhance the knowledge on the influence of load interdependencies and system effects on flood risk, this report is a part of this. More information on the societal risk tool can be found in Appendix 0 and the report by De Bruijn et al. (2013).

## 1.4 Objective

In previous research load interdependencies have been investigated in specific cases and although there are some suggestions on how to deal with dike ring interactions by Delft Cluster (Vrouwenvelder et al., 2010), there is no general framework for incorporating these interdependencies in risk assessments. Especially for larger areas it is very difficult to incorporate load interdependencies in risk analysis, as it usually requires a lot of computational capacity.

The objective of this thesis is therefore:

*Develop a framework for flood risk analysis which enables accounting for load interdependencies of flood defences.*

The research is split up in the following sub-questions:

- How are load interdependencies considered in current flood risk management and past flood risk analysis and what can be improved?
- What are the main factors of influence in typical cases where load interdependencies are of importance?
- Based on the case study: what kind of simplifications are justified to still obtain reasonable results for flood depths and water levels and what are the consequences of interdependencies for the case study area?
- How can this framework be applied in further flood risk analysis, what should be improved to make it a universally applicable framework for flood risk analysis?

**1.5 Approach**

The first part of this research will deal with developing a general framework for incorporating load interdependencies of flood defences in flood risk analysis. The currently available analyses (Apel et al., 2009a; ter Horst, 2012; Van Mierlo and Vrouwenvelder, 2007; van Mierlo et al., 2008; Van Mierlo et al., 2003; Vorogushyn et al., 2010) will be analysed and compared, and if necessary new suggestions for approaches in flood risk analysis will be given. By using former studies and historic events the main factors in cases, with both negative and/or positive interdependencies, can be identified. If necessary the properties of cases with interdependencies are investigated using a conceptual case.

With the knowledge from the research done in the past and the new suggestions a new framework is developed to assess the load interdependencies. This is applied to the case of the IJssel/Bovenrijn and it is concluded whether the used approach has the potential to deal with the interactions of different dikes and whether this is usable in future risk analysis.

**1.6 Readers guide**

The setup of the report, the different steps, chapters and corresponding research questions are shown in Figure 1-2.

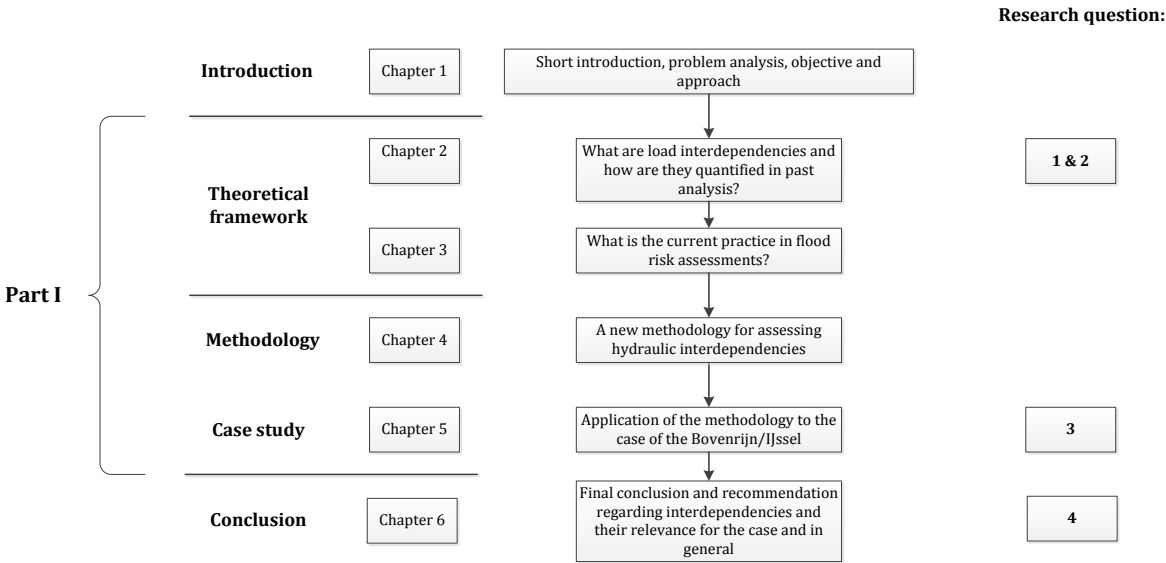


Figure 1-2 Outline of thesis and report

## 2. Load interdependencies and their relevance for assessing flood risks

In this chapter first the term river system behaviour is reconsidered and redefined to load interdependencies. Next, their importance in flood risk assessments is shown using historical examples and results from past studies. Also some remarks are made on the methodologies used in these studies and the governing factors of influence are also identified. As was done in most of the former studies the term system behaviour is sometimes used in this chapter, however, the effect of load interdependencies is meant.

### 2.1 River system behaviour redefined

System behaviour, which was introduced in paragraph 1.1, is an unclear term as it can describe virtually anything: the world is a system, consisting of many more smaller systems in different topics. One could think of organizational systems, water systems, computer systems, flood defence systems and many more. Narrowing the term down to 'river system behaviour' already gives a better idea of the processes described, however in a river system there can be many more systems described with the term, e.g. sediment processes or shipping. Van der Wiel (2004) describes it as 'the hydraulic interaction between dike ring areas' which is already a clearer description of the phenomenon. For the case considered this description was correct, but the use of the term dike ring narrows the subject down to only a few areas around the world, where flood protection systems are considered as systems of dike rings, such as in the Netherlands. This definition also brings along the problem that the occurrence of the phenomenon becomes dependent on the definition of the dike rings. Especially the second problem is important for the Netherlands, an example of this is the Dutch dike ring area 14, which was described before by the VNK2-study (ter Horst, 2012) and is shown in Figure 2-1.

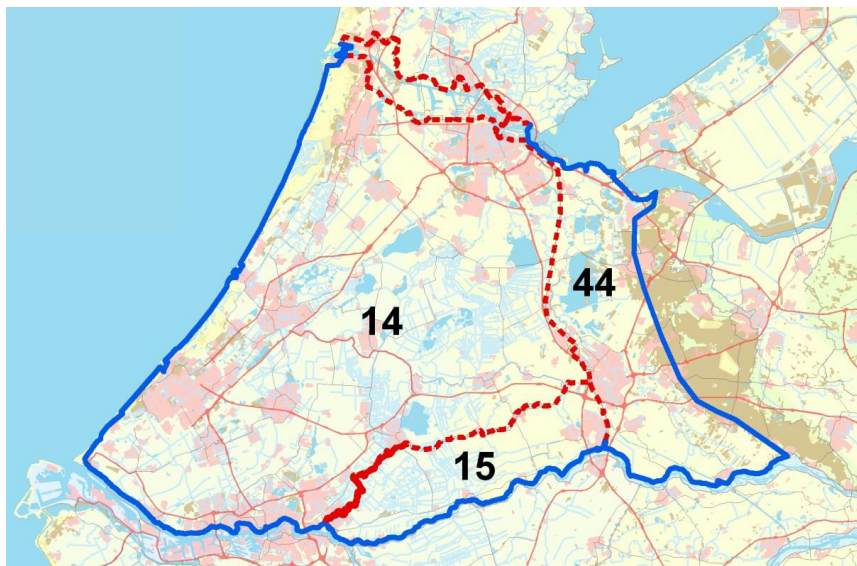


Figure 2-1 Dike ring areas 14, 15 and 44 (ter Horst, 2012)

The issue with this area is that the dike rings are defined separately but the separating dikes between 14 and 15 and 14 and 44 are category-c flood defences, meaning they are not directly protecting against flood water. In this case they are low and weak and an inundation of dike ring 15 or 44 means (partial) inundation of ring 14. However, when redefining this to one big dike ring there would be no system behaviour. This can also be the case with secondary or tertiary flood defences: redefining the categories can induce occurrence or disappearance of system behaviour and specifically cascade effects. The term dike ring is thus problematic in the

definition. Other, non-Dutch, authors who considered types of system behaviour did not use the term system behaviour nor dike ring interaction (Apel et al., 2009a; Vorogushyn et al., 2010). The principle of system behaviour is probably best seen as the de effect of failures on hydraulic conditions elsewhere in the system, as was described by Apel et al. (2009a). A way to deal with this is to redefine river system behaviour as: 'load interdependence of flood defences'. By using this term the problem with the definition of dike rings is eliminated and it also describes the mutual relations between different flood defences in the system in terms of hydraulic loads. Therefore this is the term used in this report. Dike rings are only used as definition when it is convenient, however in principle the definition of a dike ring as being an isolated area considered in a flood risk analysis is dropped.

## 2.2 The concept of load interdependencies

Van der Wiel (2004) did a conceptual research on the load interdependencies of dike rings. The aim of this study was to qualitatively assess the influence of the interaction of dike rings on each other in terms of risk and failure probability. Three cases are considered which are shown in Figure 2-2 and their total risk is compared using an isolated and an integrated approach. The isolated approach considers the dike rings separately and the integrated approach takes their interactions into account.

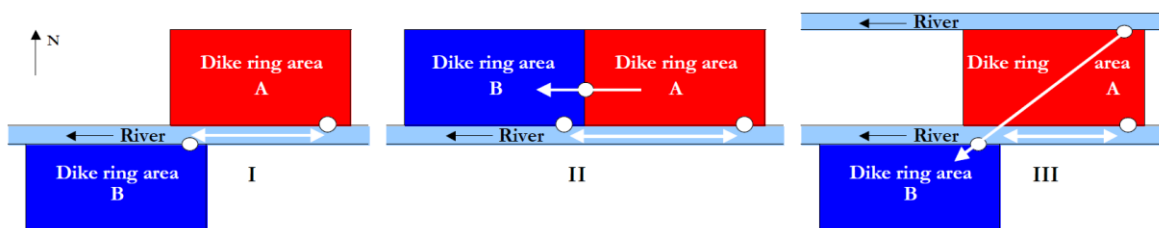


Figure 2-2 The three cases used in van der Wiel (2004)

Depending on the situation, load interdependencies can have both negative and positive effects; both are considered in the cases in this study. For instance: if dike ring A and dike ring B are on the same river and dike ring A breaches, the water flows into the polder protected by dike ring A. This reduces the flow in the river, thus the water level in the river and therefore reduces the load on the dike protecting B. This is an example of positive load interdependencies. However, if A and B are next to each other and are separated by a relatively weak compartment dike it could be that the inundation of A causes the compartment dike to fail. This is an example of negative load interdependencies, especially if the compartment dike is weaker than the river dike protecting area B; flooding of A can then cause flooding in B. A similar example of negative load interdependencies is if a dike ring separates two rivers with different design water levels: If the dike at the river with the high design water level fails this could lead to conditions far above design level at the river with the lower design water level and thus negative effects. As most systems of dike rings consist of more than 2 dike rings, usually it cannot be described by one case but is a combination of cases. Another important thing about the mechanisms is that it is also a matter of definition: for instance in case II, if the dike separating the dike rings is classified as primary defence, system effects occur, according to the definition in the research. If the separation dike is classified as secondary or tertiary defence, dike rings A and B become one dike ring and there is no system effect anymore. Therefore in paragraph 2.1 it was suggested to drop the definition of dike rings.

The main conclusion on case I was that both dike rings benefit from each other when load interdependencies are accounted for. The beneficial effect of the upstream dike ring is less in general, and decreases when dike ring B is further downstream. Furthermore, in the cases II and III the effect can be both negative and positive, depending on the probabilities and risks. Dike improvements always have a positive effect on the total failure probability of the system, however, depending on the distribution of the risk, the total risk can increase due to a dike upgrade. The final conclusion of the report by van der Wiel (2004) is:

*“Overall it can be concluded that both for a correct assessment of the current probabilities of failure and risks of dike ring areas as well as of the effects of possible future measures (dike improvement, emergency storage areas) the integrated risk assessment is required.”*

## 2.3 Historical examples illustrating the relevance of load interdependencies

### 2.3.1 Load interdependencies in the Netherlands

For nearly 100 years there have been no significant river floods in the Netherlands. This has several reasons: the flood defences have become stronger than before and another, very important reason, is the disappearance of ice dams, due to the increase in water temperature caused by industry cooling water from Germany. Before this increase in temperature most floods which occurred were caused by ice dams. A few of the, for this subject relevant, major floods in the last centuries will be briefly discussed here.



**Figure 2-3 Historical drawing of a river flood in the Netherlands**

In 1805 the ‘Land van Maas en Waal’, nowadays dike ring 41 was inundated due to a dike breach at the Waal (Hesselink et al., 2003). The flood was caused by an ice dam which blocked the water from flowing through the river and caused overloading of the dike. As the ‘Land van Maas en Waal’ was identified as a potentially dangerous location where river system behaviour could occur (van Mierlo et al., 2008) this is a particularly interesting case. However due to the ice dam the discharge into the polder is most likely higher than in the case of a ‘normal’ dike breach so the situations are not entirely comparable. In this case the discharge was at a high, but not abnormally high level, as it had occurred several times in the years before and after. It is concluded from the reconstruction that under these circumstances no shortcutting occurred and the flooding was restricted to the Land van Maas en Waal.

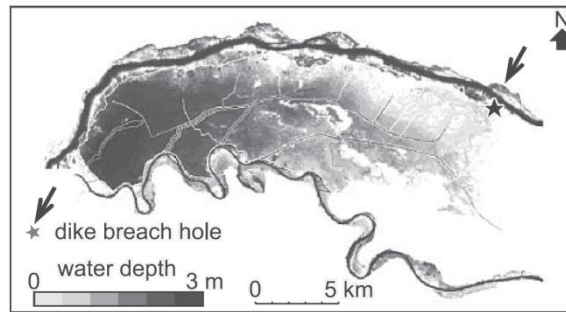


Figure 2-4 Inundation 240 hours after the breach in the 1805 flood (Hesselink et al., 2003)

In 1926 a series of floodings occurred due to abnormal high discharges. These were described by Ververs and Klijn (2004) and conclusions were drawn on the effect of emergency storage areas. In this case there was no negative system behaviour at the Waal and Maas, but it is suggested that this was caused by upstream dike breaches which lowered the water levels at the Waal river. During that time many polders functioned as emergency storage areas. However, the weirs controlling the inflow to these areas were raised in the years before and this has most likely caused the majority of the uncontrolled breaches in this case. Supposedly there was also extra discharge in the IJssel due to inundation of the Oude IJssel. It was estimated that the water level reduction caused by the upstream polders Ooijpolder and Rijnstrangen, was at least 26 centimetres, which prevented more failures downstream. It is thus concluded that emergency storage areas have the potential to decrease flood risks.

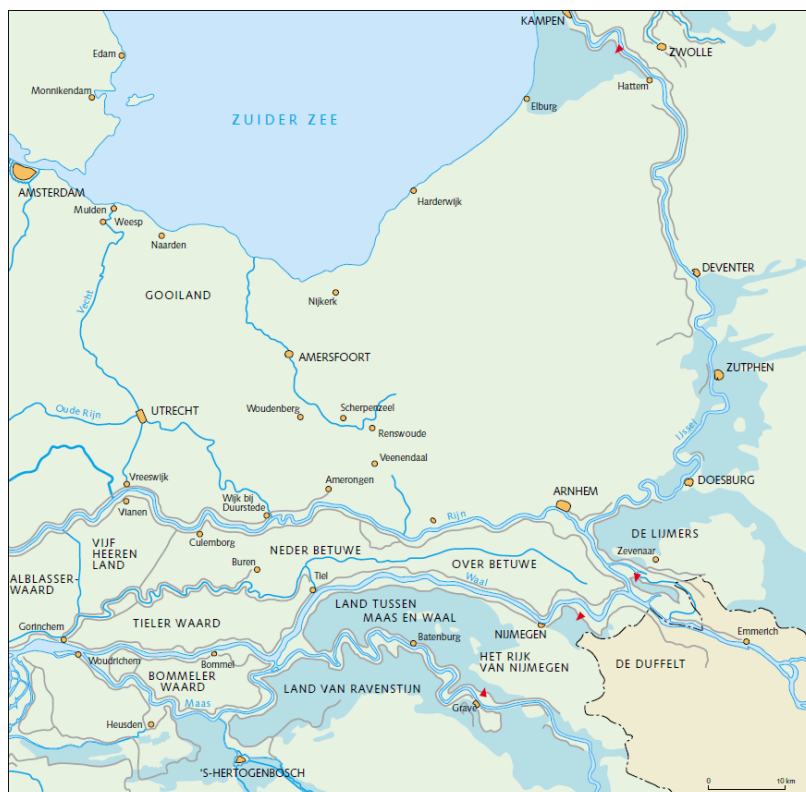


Figure 2-5 Inundated areas in 1926 (van der Ham and van de Ven, 2004)

The important question of course is: what can be learned from these events? First it has to be noted that there is only marginal negative system behaviour between Maas and Waal, this is most likely caused by the situation at Heerewaarden. Heerewaarden is currently the dike ring

area just downstream of the 'Land van Maas en Waal' where the Waal and Maas almost touch each other. Until 1899 Heerewaarden was a natural overflow area in which water from the Waal flowed to the Maas. Therefore the difference in high water levels between Maas and Waal was much smaller until the year it was closed. The overflow at Heerewaarden also caused a lot of ice dams due to the low flow velocities at that location in the river, these ice dams were one of the main reasons for inundations of the Land van Maas en Waal. The closure of Heerewaarden thus drastically changed the conditions at both the Maas and Waal. What can be learned from the 1926 flood is that, most likely due to the breaches upstream the water levels downstream were sufficiently lowered to prevent further inundations. A detailed description of the historical changes and floods in this part of the Dutch water system can be found in the report by van der Ham and van de Ven (2004).

#### *Emergency storage and the relation to load interdependencies*

As was shown in the preceding example there is a strong analogy between effects of load interdependencies and the effects of emergency storage areas. In the case of an emergency storage the discharge wave from a river can be topped off by using the storage area, which is practically the same as what happens in case of positive system behaviour caused by a dike failure and also what happened in for instance the flooding in 1926. The main difference is that for a dike breach it is unknown at which moment in the discharge wave it will happen, the breach is uncontrolled. Research in the past has shown that the timing of the dike breach is of major importance for the extent and influence of effects of load interdependencies (Van Mierlo et al., 2003).

#### **2.3.2 System behaviour abroad**

##### *Elbe floods in 2002*

In 2002 the Elbe catchment area in Germany suffered from extensive flooding due to heavy rainfall in the Czech Republic and Germany. At the German part of the Elbe catchment more than 130 dike breaches occurred (Vorogushyn et al., 2010), causing a total of 15 billion € of damage in Germany (Apel et al., 2009a). From Figure 2-6 it can be seen that dike breaches can have quite a large influence on discharges in rivers, given the drop in discharge near Torgau which was caused by dike breaches (Engel, 2002). Vorogushyn et al. (2010) however concluded that the influence of these upstream breaches on downstream dike loads, is not sufficient to cause a significant load relief in this case. The reason suggested was insufficient retention capacity in the upstream parts of the river. It can thus be concluded that the positive effect on downstream safety can become very small in cases with a small retention capacity or small dike rings. It is therefore very important to determine the typology of the river when considering the potential effects of load interdependencies on flood risk.

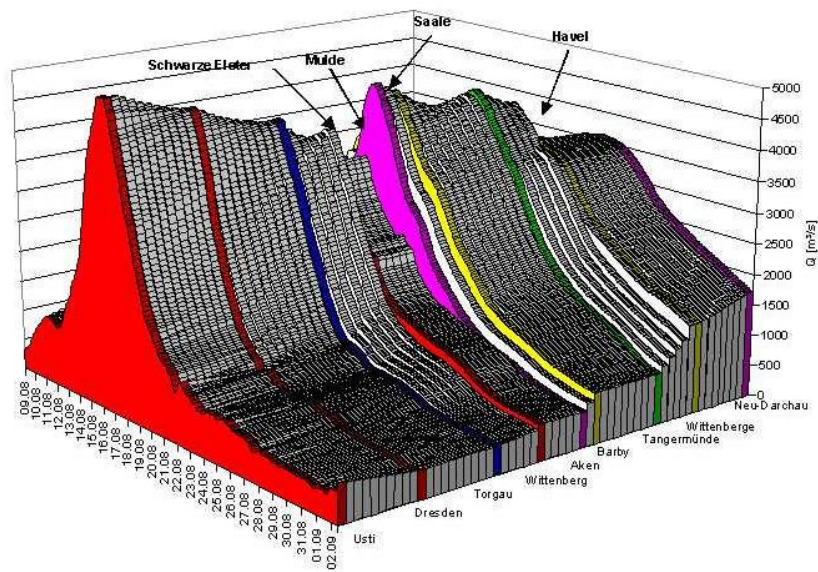


Figure 2-6 Discharge hydrographs along the Elbe river, near Torgau (the blue line) a drop can be observed caused by several major dike breaches at that location (Infrastructure Development Institute, 2002)

**Jones Tract breach, California**

In 2004 the dike protecting the Jones Tract dike ring near Stockton, California failed due to a combination of spring tide and rapid drawdown of the water. Although there is no evidence that the failure of the Jones Tract dike prevented other failures, a study using the Delta Simulation Model II by Mierzwa (2005) shows a significant drop in water level of almost 50 cm after the dike failure which can be seen in Figure 2-7. This shows that the influence of dike failures on water levels can be quite large.

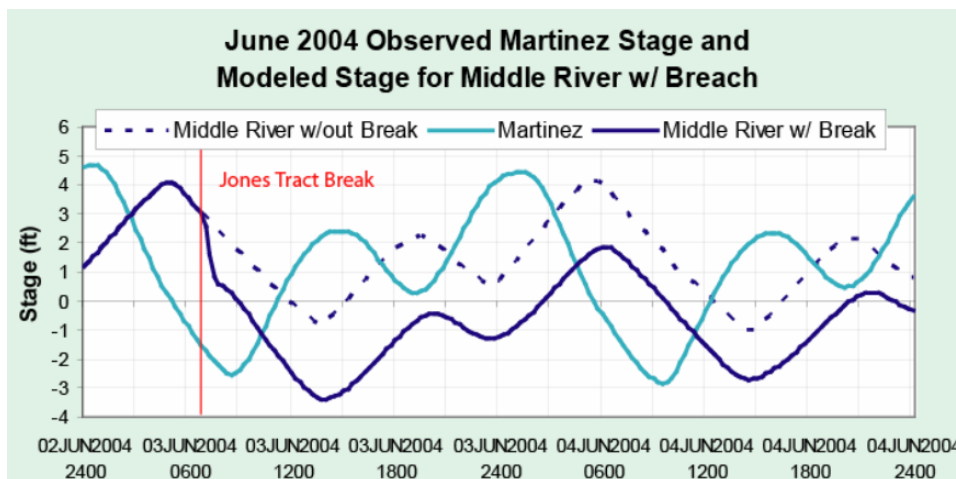


Figure 2-7 Water levels during the Jones Tract breach found from the DSM2 model (Mierzwa, 2005)

**Mississippi floods 2011: The controlled levee breach near Cairo**

In 2011 the Mississippi river reached one of its highest water levels in known history (Olson and Morton, 2012a). An important point in the Mississippi Delta is the confluence of the Mississippi and Ohio rivers near Cairo, Illinois. In 2011 the flood waves from both rivers arrived at the same time, causing extreme high water levels and an imminent dike failure given the occurrence of

sand boils. Due to the small area and the relatively large number of inhabitants and economic value behind the seawalls and levees protecting Cairo, it was decided by the USACE (United States Army Corps of Engineers) that the New Madrid Floodway, an emergency storage/discharge area had to be activated, in order to relieve the flood protection of Cairo and cause a general drop in flood levels along the Mississippi and Ohio rivers. After doing this the water levels near Cairo dropped by approximately 0,8 meters within 48 hours, thus relieving the flood protection of Cairo (Olson and Morton, 2012b). Also further upstream both the Ohio and Mississippi rivers, near Cape Girardeau, Missouri and Paducah, Kentucky the water levels were lowered by approximately 0,6 and 0,9 meters (Cape Girardeau can be found on the map in Figure 2-8, Paducah is at the Mississippi river, approximately 40 miles upstream of Cairo). The deliberate breach of the levees near Cairo is a typical example of relief due to positive load interdependencies. By using the relations between different water levels and areas it is possible to relieve an area with valuable assets (in this case the area near Cairo), by flooding an area with fewer assets (in this case the New Madrid Floodway), such that the potential damage of the flood is lowered.

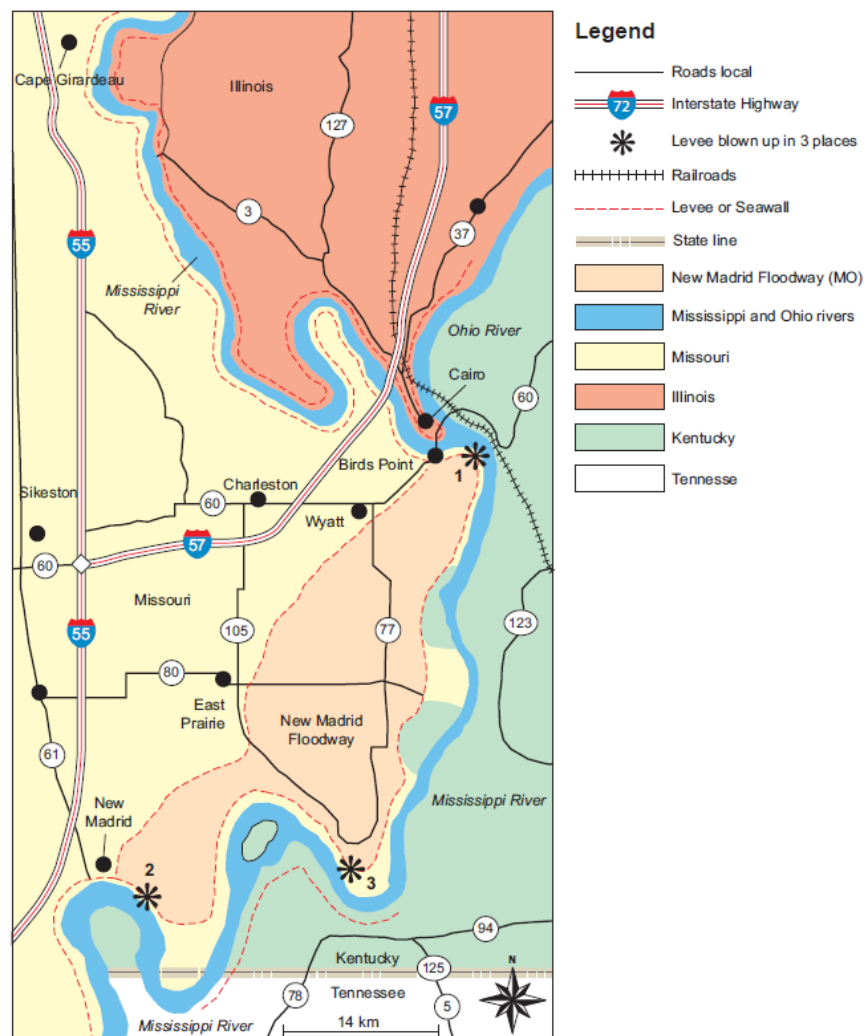


Figure 2-8 Map of the confluence of the Ohio and Mississippi rivers near Cairo, Illinois (Olson and Morton, 2012a)

## 2.4 Studies on load interdependencies

Due to its complexity and often case-specific behaviour there is no general theoretical framework to deal with effects of load interdependencies or system behaviour. A few studies on the subject have been conducted in the past. These will be discussed below. Some of them are methodologically relevant for this research, these will be discussed in more detail. Also more qualitative studies have been executed, these will also be discussed.

### 2.4.1 Methodological approach, the Delft Cluster project

The aim of this project (Van Mierlo et al., 2003) was to develop a Conceptual Framework enabling decision makers to evaluate the effects of safety-improvement measures on overall safety of the system. The case study was a fictive situation with 3 dike rings of which one was an emergency storage area (Van Mierlo and Vrouwenvelder, 2007). Two hypothetical cases were used, one with and one without the emergency storage. The final conclusion by Van Mierlo et al. (2003) states that for determining flood risks accurately it is a prerequisite that effects of load interdependencies are taken into account in flood risk assessments.

After this the Conceptual Framework was applied in a real case study on dike ring 41 'Land van Maas en Waal' (Vrouwenvelder et al., 2010), with as goal to show the use and limitations of the method and investigate the effects of high waters at the Waal on the risk along the Maas. This study showed that this framework was quite flexible and useful for assessing flood risks, and the case studies executed can be considered a proof of concept. However it is also noted that load interdependencies will become more complex when more dike rings and a larger system are considered. In a second case in the study, the number of breaches considered was increased, this caused a large variation in risk thus showing that the method used is very sensitive to the number of breaches considered.

#### *The methodology: its advantages and shortcomings*

The methodology by Vrouwenvelder et al. (2010) uses PC-Ring to determine the reliability of the flood defences, Sobek to determine the hydraulic loads and Prob2B to determine the failure scenarios. The input data needed are:

- Input flow at upper boundaries by flood wave generator and stage-discharge relationships at the downstream boundaries
- Dike strength parameters
- Digital Elevation Map
- Predefined dike breach locations

The calculation process is shown in Figure 2-9 the following: first the water levels without interdependencies are determined using Sobek, then, by using a Monte Carlo simulation of the dike reliability the breach locations are determined. Next, by using the Verheij/van der Knaap formula for breach growth the flooding is simulated and this can be translated to damage, casualties and risk for all scenarios using the HIS-SSM module (for a more detailed description of these elements and their background see Chapter 3).

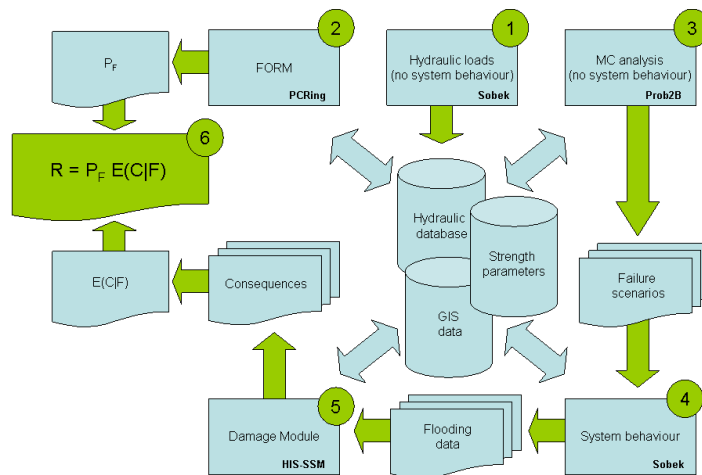


Figure 2-9 Conceptual Framework suggested by the Delft Cluster project on system behaviour (Vrouwenvelder et al., 2010)

The result for dike ring 41 was that the risk was found to be a factor 1.5 higher than in other studies not accounting for load interdependencies. However the methodology also has some shortcomings and uncertain factors. The most important ones are:

- *Dike breaches at other dike rings were not taken into account:* The only dike breaches taken into account were the ones at dike ring 41, the other dike rings along the Maas could only overtop. In reality it seems very likely that at least one dike at the Maas will also fail due to the increased load.
- *Symmetry of dikes was assumed:* It was assumed that the strength of the dike under loading at the inner slope was equal to the strength when loaded at the outer slope. It is debatable whether this is correct, as the situation when a dike is loaded from two sides is different from when it is loaded from one side. However, research on this subject is lacking.
- *Effect of dike breaches on water levels at other breach locations at other dike rings were not taken into account:* This can cause an incorrect damage calculation as the effect of relief is completely neglected. If for instance it is decided to raise the dike, this could decrease the safety of another, more valuable area (for an example of this principle see paragraph 2.4.2).
- *Fixed dike breach locations were used:* The second case, where the number of breach locations was increased, gave different results. The choice of breach locations is thus very important as some scenarios are very important for the final result.

In addition it has to be noted that the calculation times for the total analysis were quite large due to the use of 2D simulations, per model run they amounted up to 6 days. It might be worth to investigate other, faster, calculation methods, especially when using Monte Carlo techniques and considering larger areas.

Aside from these shortcomings the Delft Cluster approach seems to be an effective tool for assessing flood risk at locations where load interdependencies are of importance, especially

when the area to be considered is not too large. According to the final report (Vrouwenvelder et al., 2010) further research should focus upon:

- *Dealing consistently with length effects:* currently the breaches only represent one small location and the parts between the breaches are not considered. By applying length effects to the failure probabilities it could also be that the large difference found when increasing the number of dike breaches becomes smaller.
- *Studying dike failure mechanisms when loading is (also) on the inner slopes:* As was mentioned this is one of the shortcomings of the method.
- *Improving efficiency using Importance Sampling methods:* This can increase computational efficiency for the Monte Carlo calculations. This technique is already applied in the societal risk tool by Deltares (De Bruijn et al., 2013).
- *Calculating realistic sets of dike rings:* As was mentioned, currently the positive or negative effects in terms of determining failures at other dike rings is not considered. This can be very important for a correct risk estimation.
- *Making links to optimal dike improvement strategies:* By considering different safety levels for dikes, the improved risk estimation following from accounting for load interdependencies, can be used to define an optimal strategy for dike improvement.

#### 2.4.2 Flood risk analysis for the Bac Hung Hai polder, Vietnam

Diermanse et al. (2007) investigated the flood risk in the Bac Hung Hai polder in the Red River delta in Vietnam. In this analysis load interdependencies had a pivotal role, as one of the main objectives of the research was to investigate optimal dike improvement strategies. By incorporating load interdependencies it was shown that by raising dikes at the sections with the largest damage the flood damage at these sections was reduced but this was partly compensated by an increase in damage at other sections, due to an increase in failure probability there. The research showed that for determining optimal investment strategies load interdependencies are very important due to these effects.

##### *The methodology: its advantages and shortcomings*

The goal of this project was to rank different flood protection projects in terms of their effect on the total risk. The input parameters used were as usual the strength of the dikes and the discharges and water levels. An extra interesting part was that the economic damage was calculated using a formula relating damage and breach flow volume. This is a quite simple and quick method to determine damages, however it seems only useful for very homogeneous polders without too much spatial differences in terms of large cities and agricultural areas, as large spatial variations render large spatial variations in damages.

The calculation process is the following: the first step is to determine all Z-values for the dikes<sup>1</sup>, then determine the lowest Z-value and model a failure at that location. After determining the inflow volume, also the water level reduction in the river downstream of the breach can be determined using stage-discharge relations. This process continues until all Z-values are positive. The results showed indeed that interdependencies are important for effectivity of flood protection projects, it was even shown that, due to these interdependencies, dike improvements can cause an increase in total risk.

---

<sup>1</sup> Z is the resulting value of the standard reliability function  $Z=R-S$ . When Z is negative the structural element, in this case the dike section fails. More details can be found in paragraph 3.3.1

Because there was no hydrodynamic model but only the maximum water levels were considered, the influence of the time of breaching was neglected. As can be seen in for instance the study by van der Wiel (2004) this can have quite a large impact. Another possible shortcoming is the very simple description of the failure probabilities in the sense that they only depend on the water level, for instance time duration of high waters doesn't play a role. What also might influence the results is accounting for backwater effects caused by dike breaches. Both dike breaches itself (due to rising water levels in the inundating polders) and the river (due to a sudden change in discharge) will show backwater effects. As the water level effects are derived from stage-discharge relationships this might give slightly conservative results as also upstream the water levels will drop.

**2.4.3 Influence of dike breaches on frequency of discharge waves**

Apel et al. (2009a) investigated the effect of upstream dike breaches on downstream flood frequencies. The case study area was a section of the Rhine in Germany between Cologne and Rees. Along the river there were 41 breach locations, and the river flow was described by a set of flood waves composed from the Rhine flood wave and the flood waves from the two tributaries Ruhr and Lippe. The findings of the paper show that, by using a dynamic-probabilistic model which can account for discharge reduction due to dike breaches, dike breaches have a significant influence on the maximum discharges downstream. Especially for extreme events with an exceedance frequency lower than the design level of most of the dikes the influence is very large, as is shown in Figure 2-10. It can be observed that especially for the 1/5.000-year discharge the influence is big, resulting in a 2.000 m<sup>3</sup>/s reduction at Dusseldorf when using the dynamic-probabilistic approach instead of the standard flood frequency analysis (FFA) not accounting for dike breaches. The influence for 1/1.000-year discharges is already a lot smaller. For discharges with a lower return interval the results give slightly higher discharges due to the slightly different shapes of the distributions used at the downstream gauging stations. It is also shown that the maximum discharge when accounting for dike breaches can be described by an asymptotically approached maximum discharge which can be considered the maximum probable flood. An analysis in which the results are compared to specific discharges from different flood events in Europe also shows that the dynamic-probabilistic model gives more realistic results than the conventional lognormal analysis.

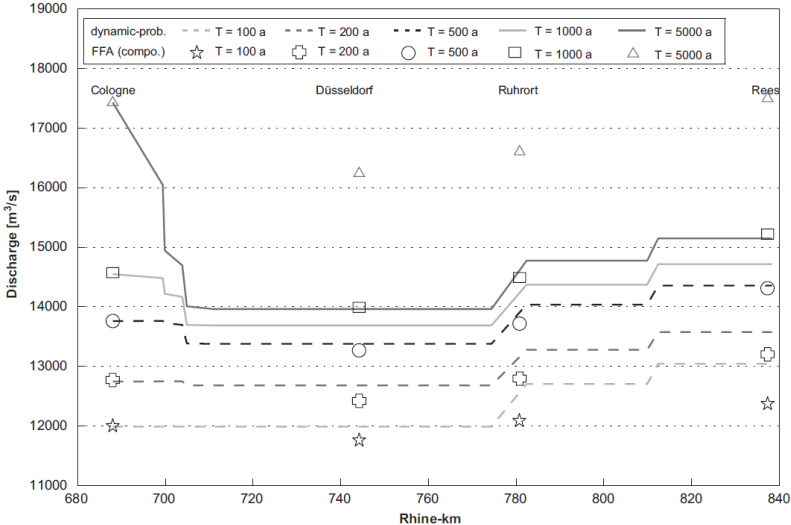


Figure 2-10 Comparison between the results from the dynamic-probabilistic model and extreme value analysis for discharges with different return intervals along the river reach considered, from this figure the influence of dike breaches on extreme discharges is visible (Apel et al., 2009a)

**Methodology: dynamic-probabilistic calculation**

As was said, the goal in this case was to determine the return intervals for discharges when considering upstream dike breaches. Because the case study area consists of a main river and two tributaries, the flood waves of these were combined. Other input data were the dike heights, the breach locations considered and a 2D fragility curve for overtopping, so in this case also the time dependency of failure was considered. The breach width was put in as a random variable. The breach locations were chosen based on 2D inundation models to ensure the right locations were used. The main part of the calculation consisted of a Monte Carlo simulation in which breaches were simulated. Once a breach occurred the flood wave reduction was accounted for in the final results. After the whole flood wave had passed all  $10^5$  times, the discharge frequencies were analysed for the whole length of the reach. This resulted in a significant decrease of the return intervals of high discharges, which clearly proved the relevance of relief due to dike breaches for flood risk analysis. In this case the stretching of the flood wave and attenuation of the peak were neglected based on simulations and also the routing effect in the river was not taken into account. The characteristics of the flood plain type also allowed neglecting the backwater effect of dike breaches. An uncertainty in the approach is the validity of the data as there have been numerous river training and retention measures along the river Rhine, which might cause the historical data to be incorrect. An overview of the total methodology is shown in Figure 2-11.

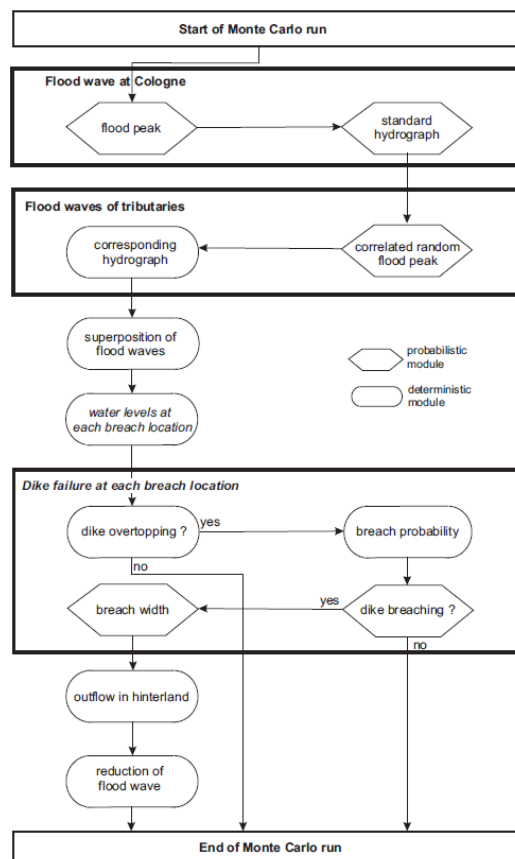


Figure 2-11 Methodology used by Apel et al. (2009a)

Of course the methodology used also has some shortcomings:

- The breach width: the width of the dike breaches is based upon breaches at the Rhine more than 100 years ago. As was said the river has changed a lot since then and the same will most likely hold for the geotechnical composition of the dikes.
- Very dependent on correct dike data: As was shown in the results, the flood frequency is heavily influenced by the failure probability of the dikes. A slight deviation might give completely different results due to a large increase or decrease in the amount of failures. Especially when only overtopping is taken into account this is an important factor, as the probability distribution for dike overtopping strength has a small standard deviation.

#### 2.4.4 Dike breaches at the Elbe river by Vorogushyn et al.

Vorogushyn et al. (2010) introduced a new methodology for assessing flood hazard, which considers interdependencies of loads for dike reaches along the Elbe river in Germany. In the research by Vorogushyn et al. (2012) the framework was applied to a case at the Elbe where the influence of a retention basin on dike failure probabilities downstream was considered. It was concluded that inundating the retention basin caused a decrease in flood probabilities downstream. However, when considering the discharges downstream of the retention basin no complete conclusion could be drawn, which was caused by a complex interdependence between failures at different locations. Also it was concluded that for sufficient relief, it is not only necessary to have many breaches but also a significant retention volume, as the inundation volumes have to be significant to have a serious impact on water levels and failure probabilities at other locations.

#### Methodology: Inundation Hazard Assessment Model

As core a Monte Carlo simulation was used which consisted of a 1D hydrodynamic model, a 2D storage cell inundation model and a probabilistic dike breach module based on dike breach data from the 2002 Elbe floods. Furthermore, input hydrographs and fragility curves for 3 different failure modes were used. An overview of the method is shown in Figure 2-12. It was concluded that the methodology succeeded in its goal to compute an extended spectrum of flood intensity indicators while considering dike failures and their interdependencies.

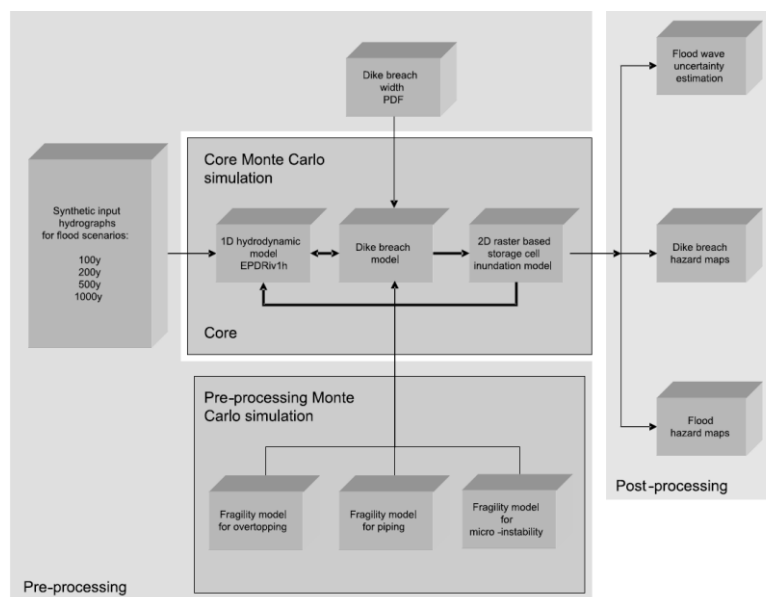


Figure 2-12 Schematization of the methodology used (Vorogushyn et al., 2010)

#### 2.4.5 Effects of load interdependencies on different cases in the Netherlands

Around 2005 and 2006 several studies on load interdependencies in different parts of the Netherlands were conducted by WL|Delft Hydraulics. This resulted in reports on the effects of load interdependencies at the Maas (Van Mierlo and van Buren, 2006a), upper Rhine area (Van Mierlo, 2005a) and the Netherlands in general (Van Mierlo and van Buren, 2006b). The reports are not detailed studies but are preliminary investigations on the influence of system behaviour on the design water levels.

These studies showed that due to negative load interdependencies in case of a dike breach at the Waal dike the design water level in the Maas can raise by about one meter, increasing the water levels to be dealt with from a 1/1.250-year to a 1/28.000-year return frequency. The same holds for the IJssel where the design water levels can increase by approximately 55 centimetres due to breaches along the Bovenrijn. The positive effects in the Rhine branches and the Maas are found to be at most 0,10 meters on the design water levels, however in particular scenario's it can make a much larger difference. In Zeeland the load interdependencies are more complex due to the presence of barriers and storm surges, therefore only positive effects have been considered. These can locally, in case of closed barriers, amount up to 1 meter lowering of the water level. The positive hydraulic effects caused by interdependencies at the IJssel lake can amount up to 2 meters. From the calculations in these reports it is concluded that, due to the major influence of negative system behaviour, it is wise to focus on accounting for especially negative system behaviour in further flood risk analysis (Van Mierlo, 2005b). Further research on the subject, already mentioned before in this chapter, emphasized these findings (Vrouwenvelder et al, 2010).

#### 2.4.6 VNK2: safety of dike rings 14, 15 and 44

Due to the relatively weak state of the so called category-c flood defences, dike rings 14, 15 and 44 behave as one single system (ter Horst, 2012). This was not considered in the VNK2 study since this only considers single dike ring areas but this study has shown that, for dike breaches at dike rings 15 and 44, a cascade effect to dike ring 14 occurs. This study also offers some solutions to increase the general safety of the three dike rings. This report is especially interesting in comparison to the main report by VNK, as the risk for dike ring 14 is for the main part determined by cascade effects from dike rings 15 and 44, as can be seen from Table 2-1. This study thus clearly shows the importance of hydraulic interactions in risk assessments and it also points out the main disadvantage of the VNK2 approach that dike rings are considered separately. It also shows that definition of different categories of flood defences can determine whether hydraulic interactions actually occur, if the area is considered as one dike ring there is no interdependence, if it is considered as separate dike rings there is. It has to be noted that, according to the definition used in paragraph 2.1 the interactions between these dike rings are not negative load interdependencies as they depend on the definition of the dike rings or reaches considered.

		Breach in dike ring...			Total
		14	15	44	
Leads to damage in dike ring area...	14	0,3	16	10	27
	15	-	75	1	76
	44	-	-	31	31
Total		0,3	91	42	134

Table 2-1 Contribution of breaches in different dike rings on damage in dike rings in million € (ter Horst, 2012)

## 2.5 Short conclusion on historic events and previous studies on effects of load interdependencies

The methods used in the different studies discussed in the preceding paragraphs use different ways to assess load interdependencies. However, usually the methods are only applied for a relatively small case (ter Horst, 2012; Van Mierlo et al., 2003; Vrouwenvelder et al., 2010) or for a river reach with only positive load interdependencies (Apel et al., 2009a). It is clear that there is no general method to take load interdependencies into account, when assessing risks in a system with several branches and dike ring areas. This is one of the main white spots in the current flood risk assessments in the Netherlands, as there is currently no quantification of the effect of the upstream dike rings on the downstream dike rings, as well as the interactions between rivers. Consequently these effects are not taken into account. The approaches used in literature are also quite different in terms of system characteristics. The approach by Delft Cluster for instance is for a lowland river and accounts for both negative and positive effects. The approaches by Apel et al. (2009a) and Vorogushyn et al. (2010) deal with positive effects for rivers higher upstream. All in all, it is concluded that load interdependencies are very important, but the application does not seem too widespread in risk assessments. There are also still quite some white spots.

So in short, past research has concluded and shown:

- Load interdependencies can have a significant effect on flood risk.
- It is important to consider load interdependencies in future flood risk analysis.
- There is no standard methodology to account for the effect of load interdependencies in flood risk analysis.

## 2.6 Important aspects when considering interdependencies

Compared to 'normal' flood risk analysis, only considering one particular area, analysis where interdependencies are taken into account bring along some extra aspects which are of importance.

In this paragraph some potential factors of influence are further elaborated based on the literature discussed above. Also some basic concepts are introduced which are important for effects of load interdependencies. To support this a conceptual case was used. In this case, which is shown in Figure 2-13 there are several different possible interactions between the areas, for instance shortcutting between River 1 and River 2, cascade effects between D and E and also load relief between dike rings at the same river. River 1 is assumed to have higher water levels than River 2, so in case of a failure at the northern dike of area C, water can flow from River 1 to River 2. The shortcutting between River 1 and River 2 through area C will be the most important event in this chapter as this is the most complex case. The findings of this chapter will be used to define a new methodology in Chapter 4.

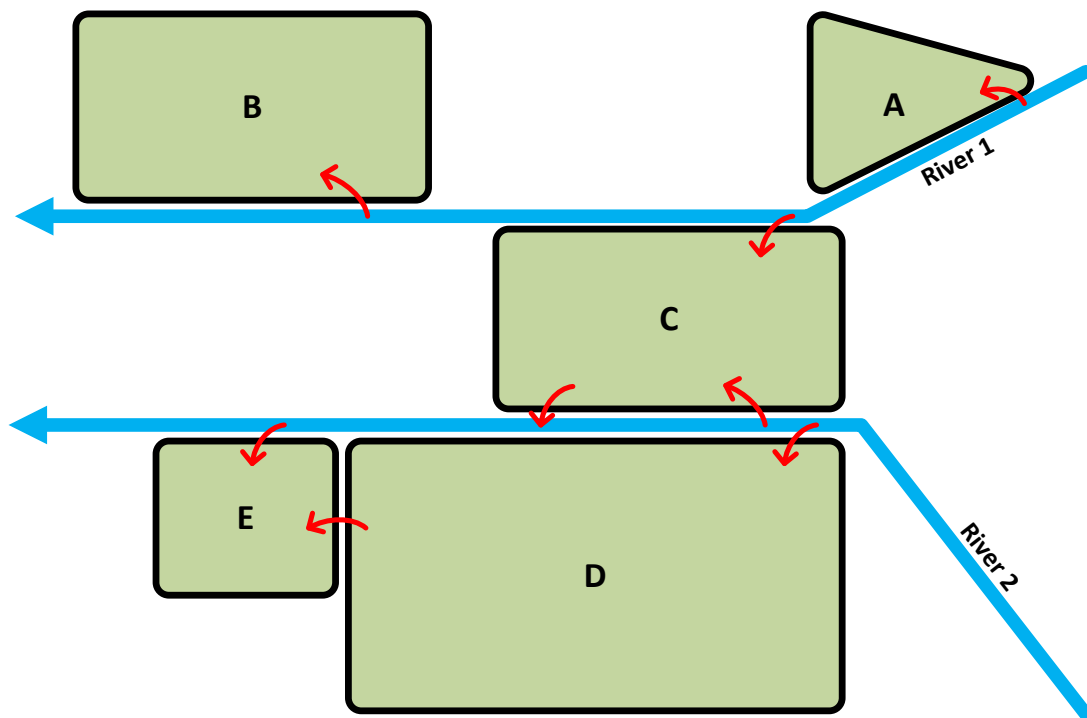


Figure 2-13 Hypothetical water system with load interdependencies

This paragraph is split up in a set of steps in the process of breaching and shortcutting:

- When does the dike breach and under which conditions?
- What happens when the dike breaches and what determines the consequences?
- In case of shortcutting, what happens when it occurs?
- What happens when water flows from River 1 into River 2?

### 2.6.1 When does the dike breach and under which conditions?

A dike breach is caused by overloading and a lack of strength to withstand the induced load. The most important factors when looking at the effect of a dike breach on other dike breaches, are the shape of the discharge wave, the time of breaching during the discharge wave and the retention capacity of the polder. These factors are very important for the extent of the flood (and thus the likelihood of shortcutting) and for the effects on water levels downstream.

#### Shape and time of failure during discharge wave

If a dike fails, it is of importance at which time it fails during the discharge wave and how long the high discharges hold on. Van der Wiel (2004) found that for breaches after the peak of the discharge wave the effects on downstream water levels as well as the total inundation volume of the breach are considerably lower. In Figure 2-14 the inundation volumes found by Van der Wiel (2004) are shown compared to the time of breaching during the discharge wave. From this it can be observed that for failures during rising water levels the inundation volume is considerably larger than during falling water levels.

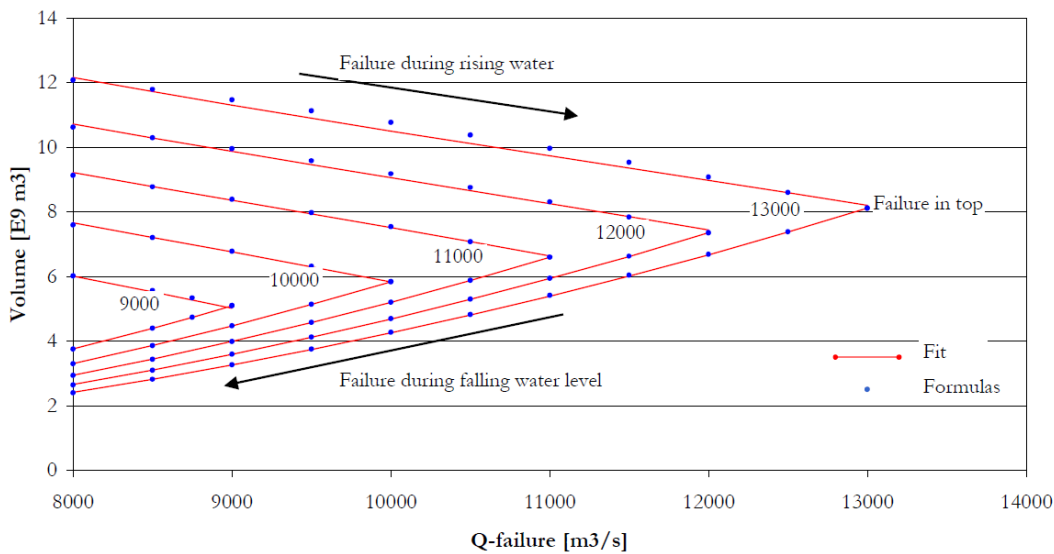


Figure 2-14 Inundation volumes compared to discharge peak levels and discharge during breaching in cases of rising or falling water levels for the case by Van der Wiel (2004)

When considering the shape of the discharge wave it can also be concluded that, when a discharge wave is of shorter duration, the inundation volume will be lower, as the total volume of the discharge wave is also lower. When comparing for instance the green and blue discharge waves in Figure 2-15, it can be seen that the total inundation volume in the case of a shorter discharge wave is smaller than for a longer wave, provided that the peak discharge is the same and the dike fails at the peak.

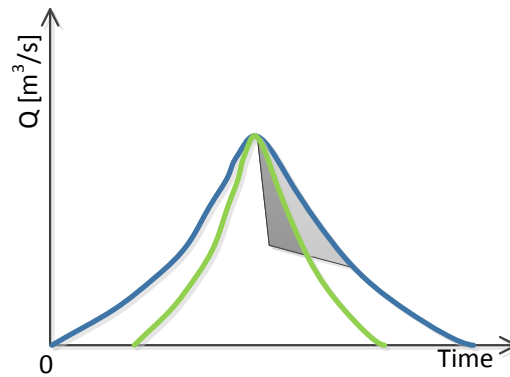


Figure 2-15 Difference in inundation volume for two discharge waves with different lengths. The gray area is the total inundation volume

In relation to failure mechanisms the above information is especially important for cases which are dominated by failure mechanisms for which the duration of the load is important, such as piping. For overtopping, failures after the top of the wave are not important. A schematic overview of this is given in Figure 2-16 for a case where overtopping and piping can occur and overtopping is caused by high water levels while piping is caused by a combination of a high water level and the load duration (more details on the different failure mechanisms can be found in paragraph 3.3.2).

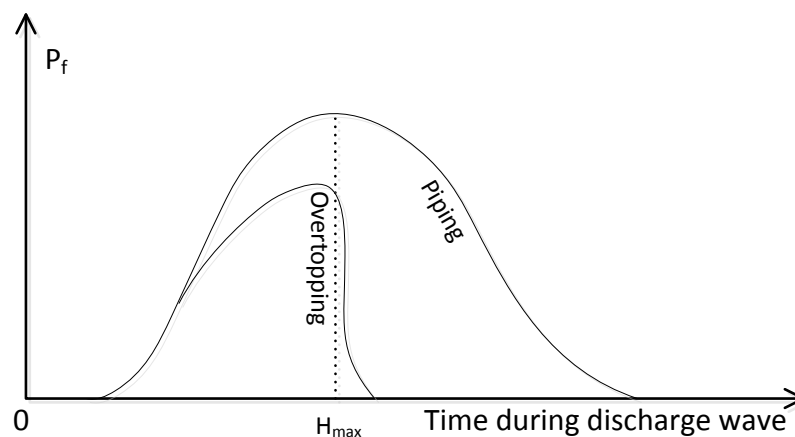


Figure 2-16 Distribution of failures over time during a standard shaped discharge wave. Please note that this is just a sketch to show the possible distribution of failures over time during a discharge wave.

The failure over time can be described by the following formula

$$P_f(t) = f(Z_{failure\ mechanisms}, H_{peak})$$

In a model this can be accounted for by using two different limit state functions, one for water level dependent overtopping and one for water level and load duration dependent piping failures. Failures due to piping will generally have less effect on high water levels and shortcutting mechanisms, as they often occur after the highest peak has already passed, due to their dependence on the load duration.

A last aspect is the retention volume of a polder. If we assume a case where a dike breaches some time before the peak of the flood wave a small retention volume can decrease the relief effects on other dike rings as, after some time the polder is full and the breach discharges

becomes 0. In Figure 2-17 a case is shown for which the maximum discharge stays the same despite a dike breach; due to a small retention capacity the polder is already filled up before the actual maximum water level is reached. A similar conclusion was drawn by Vorogushyn et al. (2010) in his study on the Elbe floods. It was suggested that one of the main reasons for not observing significant relief of other dikes was that the retention capacity of many of the flooded areas along the river was too small to have an impact.

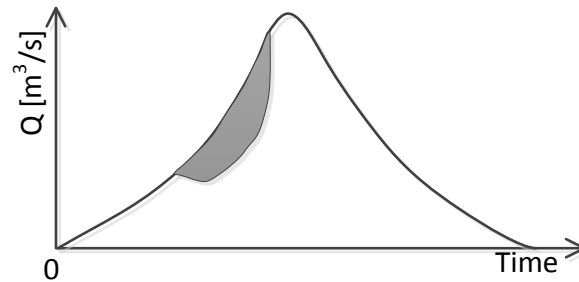


Figure 2-17 Case of a small retention capacity where the polder is filled up before the peak discharge

## 2.6.2 What happens in case of shortcutting?

### Time duration of shortcutting

When considering the conceptual case again and especially the case where polder C floods due to a breach at C.I (the dike at River 1), the polder fills up, with the amount of inflow being dependant on the characteristics of the breach and the water level imposed on the dike. When the polder has filled up to a certain 'critical' volume, the C.II dike is loaded from the inside (and the outside if the water level at River 2 is still high). Then different things can happen: C.II can stay intact and C.II can overtop or breach. There is also a possibility that C.II has already failed due to high loads from River 2. In the case that C.II is not overloaded nor overtopped no shortcutting occurs. In the case that C.II overflows, which is very likely to happen, at least before it fails, this can be described in the following way: At a certain moment after the breach at C.I water starts flowing over the dike into River 2, increasing the discharges and thus the water levels. The time between the initiation of the breach at C.I and flowing over of C.II at River 2 is called  $T_{through}$ . This parameter is also distributed and is dependent on the breach flow and the critical volume for overflow. These values are governed by the dimensions and topography of the polder and the dikes. In formula this gives:

$$T_{through} = f(Q_{breach}, V_{crit})$$

Assuming that the outflow at  $t+T_{through}$  equals the inflow at  $t$  gives for the downstream discharge in river 2:

$$Q_2(t) = Q_{2,normal}(t) + Q_{breach}(t - T_{through})$$

This is an assumption based upon the idea that the water in the polder will travel like a discharge wave. With advanced modelling techniques such as 2D hydrodynamic modelling this is automatically dealt with.

### Dike failure due to polder side loading

Another possibility next to overtopping is that, at a certain moment dike C.II starts eroding or becomes unstable and a breach occurs. This depends on the strength parameters of the dike and

the water level and high water duration on both sides. In the Delft Cluster approach the dike was considered symmetrical but it is doubtful whether this is true, as was also mentioned in the conclusions and recommendations of that report (Vrouwenvelder et al., 2010). For a common Dutch river dike the outer slope is relatively steep compared to the inner slope, a typical profile is shown in Figure 2-18.

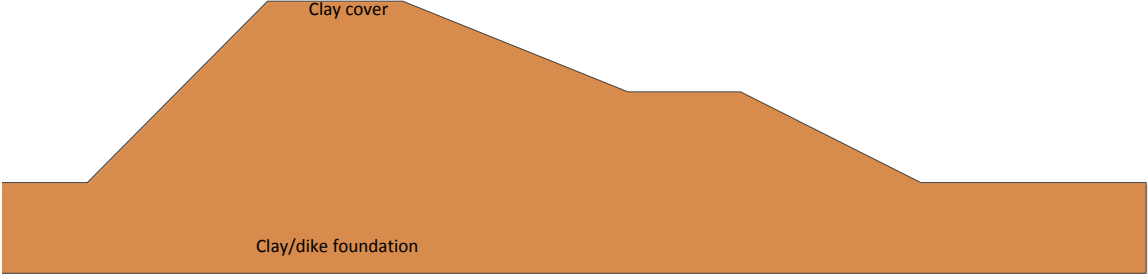


Figure 2-18 General cross section of Dutch river dike.

When the dike is loaded from the river, the common failure mechanisms are failure due to overtopping, piping and instability of the inner slope as shown in Figure 2-19.

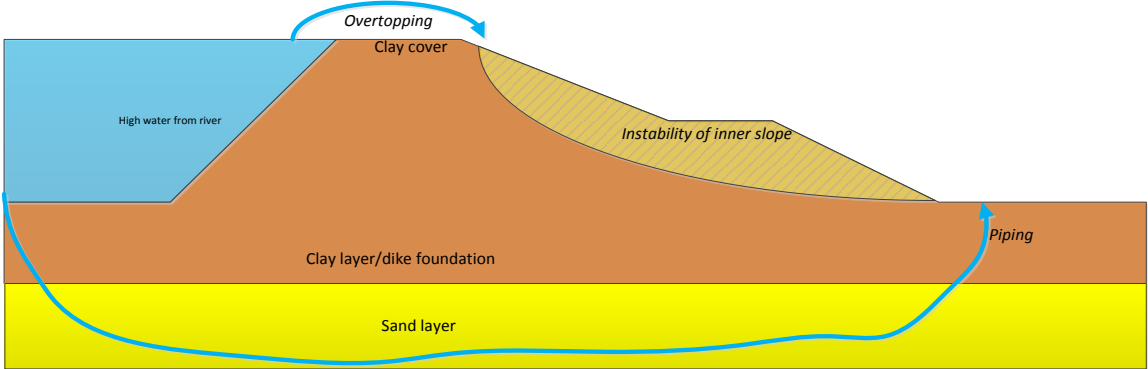


Figure 2-19 Failure mechanisms for load from river side

However, as the outer slope is much steeper than the inner slope in a situation with an inundated polder and a lower river level the dominant failure conditions of the dike will be different. Since not much research has been done on failure of dikes under loading from the inner slope, some assumptions would have to be made in order to give a realistic representation of its behaviour. Two cases are considered to illustrate the failure mechanisms of these dikes. The first case is when the river is at its highest level and the polder is also completely filled up as shown in Figure 2-20.

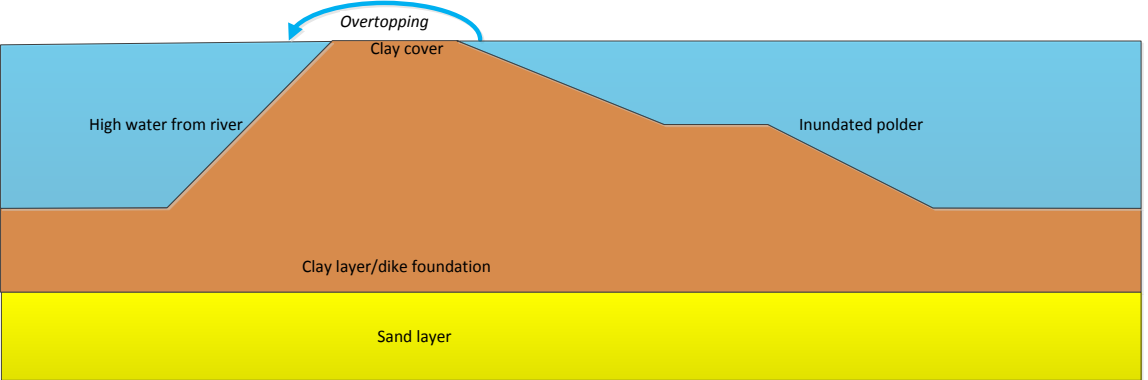


Figure 2-20 Loads on dike when polder is inundated

In this case the dike is completely soaked with water and will thus most likely become very unstable. Therefore it seems realistic to assume that after some time the dike will erode away and breach. As there is no water head over the dike there will be no piping. It thus seems realistic to assume that for extreme water levels at both sides, the dike fails when it overtops from the inside.

The second situation is when the water level at the river is relatively low, for instance when the peak discharge has already passed, hasn't arrived yet, or, in the case of two rivers there is no high water at the river. This case is shown in Figure 2-21.

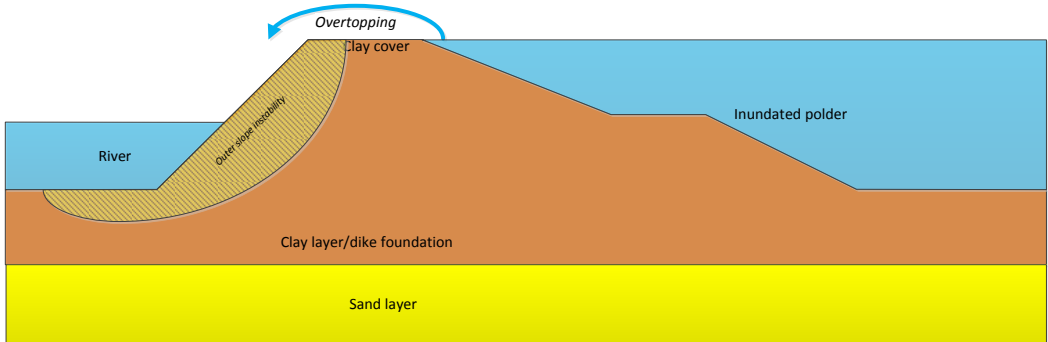


Figure 2-21 Loads on dike when polder is inundated and river at lower level

In this case overtopping could cause erosion of the outer slope of the dike. This will happen more rapidly than in cases with erosion at the inner slope, due to the steeper slope and thus lower critical overflow discharge. As there is usually a clay cover layer at the inner side of the dike the water will be unable to enter the porous sand layer so piping will most likely not be an issue. Only when there are gaps in the clay cover this could cause internal erosion or piping, but as the point of this study is not to give a detailed geotechnical description of dikes, this will not be considered. Instability might be the biggest issue with this type of dikes, as the outer slope of river dikes is usually quite steep and thus not very stable. The situation is in that sense comparable to outer slope failure due to rapid drawdown of river water levels where the phreatic level in the dike core cannot react to the changing conditions fast enough. The importance of instability in this type of cases can also be observed from the geotechnical analysis in Appendix B. In this appendix a dike cross section at dike ring 48 was considered, based on the data used by VNK2 (Ministerie van Infrastructuur en Milieu, 2005). When doing a stability analysis using the Bishop method (for background see paragraph 3.3.2), this resulted in the Factor of Safety<sup>2</sup> for slope instability, as shown in Table 2-2, for a typical cross section at dike ring 48. This shows that indeed for polder side loads the dike is less stable.

	Water level at polder	Water level at river	Safety coefficient
Case 1	low	high	1.75
Case 2	medium	high	2.13
Case 3	high	low	0.84
Case 4	high	medium	1.75

Table 2-2 Bishop Factor of Safety for a dike at dike ring 48 under inner and/or outer slope loading

<sup>2</sup> The Factor of Safety is a result of a Bishop stability calculation. It is calculated by dividing the strength of the dike under a certain loading by the loading itself. This results in a safety factor. More details can be found in paragraph 3.3.2

When considering failures from the inner slope in a risk analysis, this can be done by using fragility curves (see paragraph 3.3.4) based on the fragility curves for ‘normal’ failures. For overtopping these curves can be assumed the same, although it is debatable whether the breach will develop as fast as for normal failures. As piping can most likely be neglected this fragility curve will have a very high mean. In the appendix it was shown that for instability the safety for outer slopes is less than for inner slopes, the fragility curves can thus be shifted towards a lower failure level. This will lead to a lower resistance against instability, the same resistance for overtopping and no piping for failures due to inner slope loading. In the future it might be worthy to further investigate this behaviour for dikes, as it can be quite essential in giving good estimates for the consequences of negative load interdependencies.

**2.6.3 What happens when water flows from River 1 into River 2?**

*Timing of the discharge waves*

The first step to be taken in analysing this situation is to investigate the boundary conditions. Assuming that extreme discharges at River 1 and River 2 are correlated the timing of these discharge waves can be very important for the extent of the interactions. For instance: if the high water at River 2 is already gone, the probability of a dike breach due to shortcutting at River 2 is much lower than for a case where the additional discharge enters the river at the highest water level. Assuming two standard shaped discharge waves this relation can be described by a standard normal distribution with mean 0 and a standard deviation governed by the correlation of the two rivers as shown in Figure 2-22.

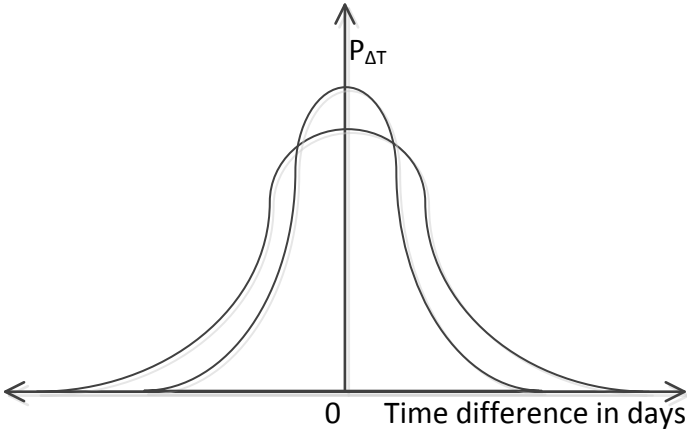


**Figure 2-22 Time difference of discharge peak arrival between River 1 and 2 for two different correlation values**

In this figure the more narrow distribution is for two rivers with a stronger correlation. In that case the value for  $P_{\Delta T} = f(\rho_{River\ 1, River\ 2})$  has less spread due to the higher probability that two high discharge waves occur at the same time. When doing a risk assessment this time difference can be accounted for in the boundary conditions if a Monte Carlo simulation is used.

*Additional breaches at other dike rings*

In the approach suggested by Vrouwenvelder et al. (2010) the problem was modelled by using an extended inundation model which also modelled the dike rings along the Meuse. This gave quite reasonable results but the additional breaches at D and E were not considered, these dikes could only overtop. For the conceptual case this would result in the following (schematized) inundation pattern:

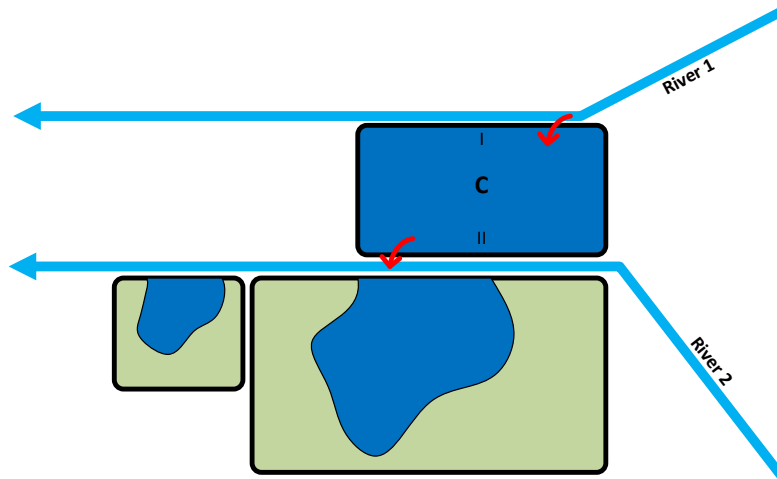


**Figure 2-23 Conceptual inundation pattern when not considering additional dike breaches along River 2**

It can be seen from the figure that the polders are only partially inundated, most likely the same would happen for the other polders further downstream. This has a large influence on the consequences, as the inundation depths will, although they might be more wide spread, also be smaller, causing less damage in certain areas. When considering additional dike breaches the inundation pattern could look like the following:

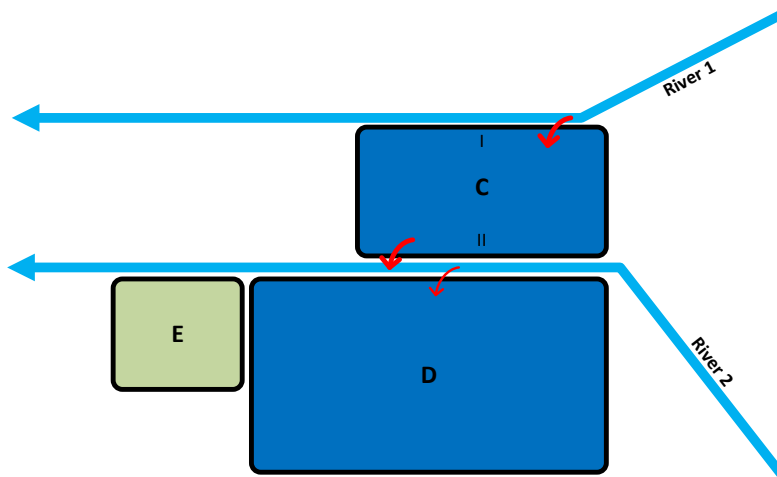


**Figure 2-24 Inundation pattern when considering additional dike breaches**

The conceptual case and the effects identified in this chapter will be used and analysed in Chapter 4, in order to define the new methodology for incorporating load interdependencies in risk analysis.

### 3. General framework for flood risk analysis

In this chapter the, for this research relevant, theoretical basics of flood risk analysis and how they are used in practice are discussed as well as the computational methods and techniques available for doing a proper risk analysis.

#### 3.1 Risk and its use in quantitative flood risk analysis

Risk is an often used quantity to assess the potential damage of undesired events. In the Oxford dictionary risk is defined as:

- 1) Exposure to danger or loss
- 2) The possibility that something unpleasant will happen

These are two very common definitions, however one of the main definitions in quantitative risk analysis is that risk is the function of probability of an event and the consequences of the same event (Jonkman, 2007). When doing a quantitative analysis considering many flood events this results in the risk being the summation of the risk for all possible flood events, given by the following formula (van Mierlo et al., 2008):

$$R = E[D] = \int D(\underline{x}) * f(\underline{x})d\underline{x}$$

with:  $E[.] =$  *expectation operator*  
 $D =$  *damage resulting from  $\underline{x}$*   
 $\underline{x} =$  *vector of random variables describing the flood event*  
 $f(\underline{x}) =$  *probability density of  $\underline{x}$*

Given the basic form of the formula above there are many different strategies for assessing damage and the corresponding event probabilities, however in all risk analysis probabilities of events or failures and consequences are used. These elements are standard in risk analysis in the Netherlands (Jongejan et al., 2011; VNK2 project office, 2012), Germany (Vorogushyn et al., 2010), the UK (Dawson and Hall, 2006; Dawson et al., 2005) and the USA (Kalyanapu et al., 2012) although they might consider and model them in a different way. The for this research most important elements and differences will be discussed in the following paragraphs.

#### 3.2 Methods for risk analysis in the Netherlands and abroad

##### 3.2.1 Introduction

In the Netherlands there are and have been several different methods for assessing flood risks. The two main types of analysis are VNK2 (Veiligheid Nederland in Kaart 2) and WV21 (Waterveiligheid 21e eeuw). Their approach is briefly introduced here as well as how it is done in the United Kingdom.

##### 3.2.2 VNK2: How safe are we?

The VNK2-project is the follow up of the VNK1-project, and it aims to quantify flood risks in the Netherlands with the current flood defence conditions, and enable prioritization of interventions based on its risk reduction. It is based upon a detailed analysis of dike failure probabilities using PC-ring and on a quantitative analysis of the consequences of different flood scenarios. The general framework for assessing the consequences is shown in Figure 3-1.

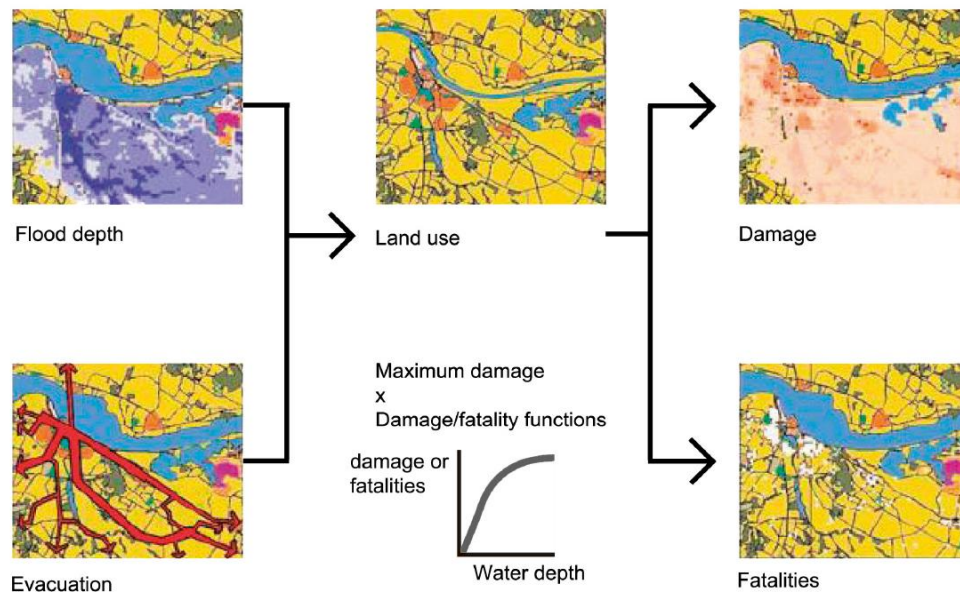


Figure 3-1 Methodology used in VNK2 to assess the consequences of different flood scenarios (Jongejan et al., 2011)

The estimation of failure probabilities is done by a detailed geotechnical and statistical analysis of the strength of different dike sections, and a failure probability calculation using the first order reliability method. Damages are estimated by using inundation maps for floods of different levels using the decimation height<sup>3</sup> as interval. There are thus for instance scenarios for 1/100, 1/1.000, 1/10.000, 1/100.000-year conditions for all selected breach locations. These scenarios and the evacuation plans are input for the HIS-SSM module which is the commonly used tool for estimating flood damages(see paragraph 3.5.3). This results in a combination of damage and fatalities and their probability of occurrence, thus resulting in the total risk of flooding in a dike ring.

The VNK2-project is a systematic approach for flood risk analysis, and in most cases, a very good methodology to identify weak spots, prioritize interventions and assess the safety of different dike rings and locations. However, a disadvantage of the VNK2-approach is that it does not consider load interdependencies and large scale effects in its general framework, only the effects by relief due to other breaches at the same dike ring are taken into account. To assess the consequences of cascade effects in the Randstad area, a separate study was executed by Ter Horst (2012), but in the cases of for instance the Waal and Maas (for more detail see paragraph 2.4.1) the lack of assessing shortcutting underestimates the risk for failure of the Waal dike. This is a potentially dangerous situation, because specifically in this case, but also in some other cases, it could underestimate (or overestimate) consequences of dike breaches, as was shown in different studies on load interdependencies. This can cause the use of unrealistic data for making decisions on dike reinforcement project for these cases.

<sup>3</sup> The decimation height, or in Dutch: 'decimeringshoogte', is the water level difference between design water levels for 1/10, 1/100, 1/1000-year return frequencies. For an exponential distribution, which is usually the case in water systems, this value is a constant, however the behavior of the system can cause the decimation height to not be a constant, e.g. in the case of shortcutting.

### 3.2.3 WV21: How safe should we be?

WV21 or 'Waterveiligheid 21e eeuw' is a project with as aim to assess economically optimal safety standards in the Netherlands and investigate the risk of mortality and casualties in different flood scenarios (de Bruijn and van der Doef, 2011). The goal is that the information obtained can be used as input in the discussion on new flood protection standards. Besides the difference with VNK2 in project goal, one of the main differences is that WV21 considers safety and risk of dike reaches instead of dike rings. These dike reaches are different from the sections used in VNK2 to calculate the safety of the dike ring. The WV21 analysis takes load interdependencies into account in some cases but this is done in a simplified manner. In the case of the Waal and Maas for instance, where the water from the Waal can cause an increase of the water levels in the Maas by approximately 1 meter the damage is increased by using damages from all downstream dike rings, and weighing them proportionally on the length of their dikes or using correlation factors for different dike rings (Beckers and de Bruijn, 2011). This is a simplified representation of reality, and it could well be that in some cases the damage is much higher, while in some cases only a dike in a relatively unhabitated area fails so the damage is much lower. In the case of the Randstad, which has proven to be an area with a quite significant influence of cascade effects, it is not taken into account due to the assumption that all dikes are working as designed and no system behaviour is allowed then (de Bruijn and van der Doef, 2011). However, even with the quite simplified manner in which load interdependencies is dealt with in WV21, it can still be seen that it has a significant influence on the economically optimal safety standards of different dike reaches. In Figure 3-2 it can be seen that dike reach 40-2 has a much higher standard than the surrounding dike reaches. This is caused by the fact that the damage for breaches at that location is almost entirely determined by damage at the Maas. The differentiation in the WV21 calculations clearly shows the importance of interactions between dike rings and different rivers.

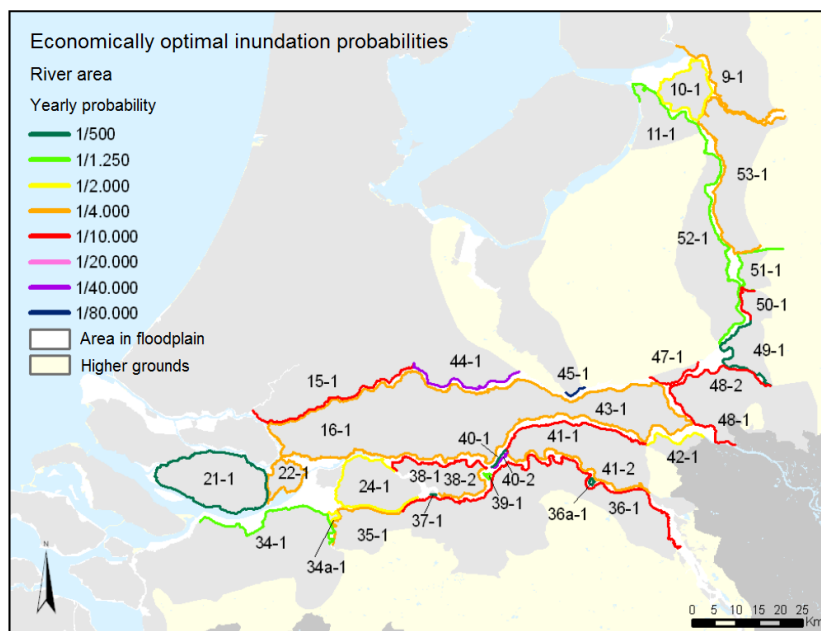


Figure 3-2 Economically optimal inundation probabilities for different dike reaches found from WV21 (Deltares, 2011)

### 3.2.4 Risk analysis in the UK

As a comparison for the Dutch methodologies mentioned in the preceding paragraph a short comparison is made to compare this to risk assessments in the UK.

In the United Kingdom flood risk assessments are slightly different from the Netherlands. The RASP-project suggested a methodology based on different approaches with different hierarchical levels. These levels then determine the accuracy with which different parameters have to be known and modelled (Sayers and Meadowcroft, 2005). The different detail levels in the analysis determine the method with which for instance the reliability of the flood defences is modelled, however the higher detail level analyses use fragility curves and Monte Carlo simulation to simulate the reliability of the flood defence system, which is different from the Netherlands where FORM is used (see 2.4.6). For the hydraulic modelling the low level analysis use empirical estimates for flood extent, higher level methods use the storage cell model LISFLOOD-FP. However it has to be noted that LISFLOOD-FP usually needs calibrated inundation data to give a realistic approach of the flood extent (Horritt and Bates, 2002) although Apel et al. (2009b) showed that the LISFLOOD-FP model gave very reasonable results for a case at the Elbe. It has to be noted that the typology of floods in England is different from the Netherlands as there are no large polder systems like the Netherlands and there is more relief in the terrain causing more rainfall runoff problems and smaller flood extents.

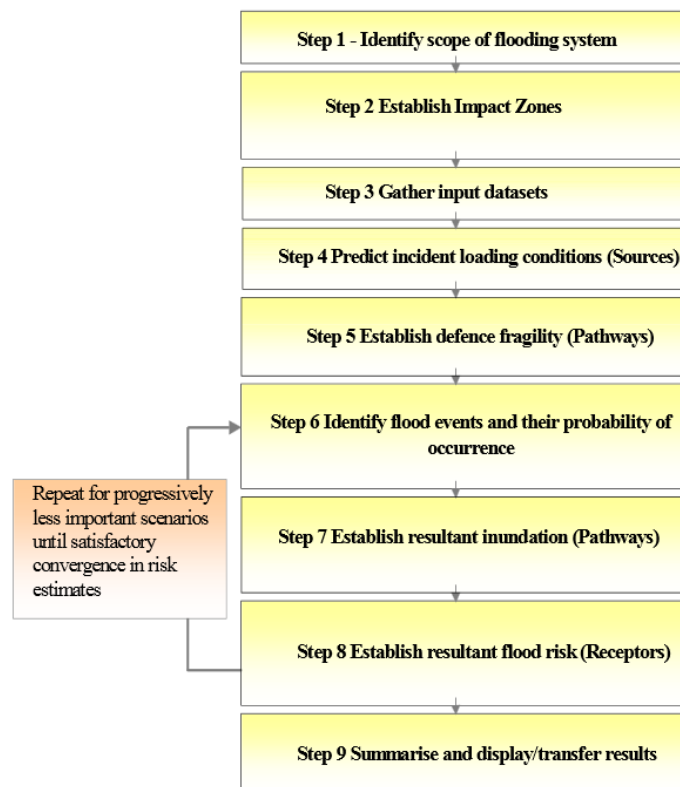


Figure 3-3 Generic process of the RASP methodology (Sayers and Meadowcroft, 2005)

### 3.3 Flood defences in risk analysis

For assessments of flood risks a proper analysis of the reliability of flood defences has a pivotal role. During the last decades, flood protection design has developed from building dikes with crests one meter above the highest known water level, to designing dikes to resist a certain statistically obtained design water level. In the Netherlands the design water levels which the dike has to be able to resist are defined by law. These levels are based on economic optimization, aimed at balancing investments and risk reduction (Jonkman et al., 2008). In the Netherlands dikes are often considered as dike ring areas, and the VNK2-method which is now used to assess the safety considers the safety and consequences of a whole dike ring and the contribution of different parts of the ring to the risk (VNK2 project office, 2012).

At first the design of flood defences was solely based on failures caused by overtopping, other failure mechanisms such as piping were dealt with by general guidelines on dike design, see for instance TAW (1985). During recent years other failure mechanisms such as instability of the inner slope and piping have also been taken into account in more detail, since they have shown to play a significant role in the safety of dikes and hydraulic structures. The failure mechanisms overtopping, piping and slope instability are nowadays considered in flood risk analysis, the other failure mechanisms usually are not, although for hydraulic structures this is different. Research on breaches in Hungary and Germany has shown that the major part of failures in river dikes is caused by the aforementioned three failure mechanisms (Vorogushyn et al., 2009).

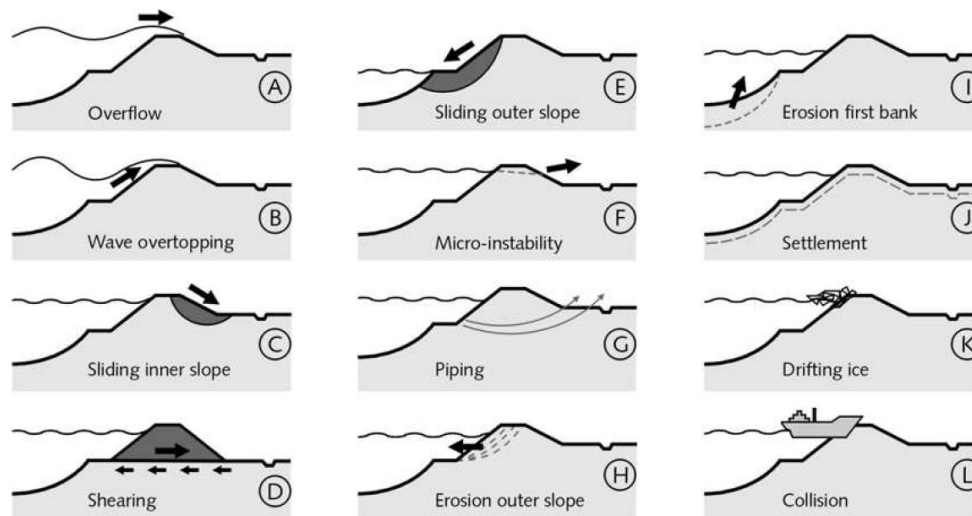


Figure 3-4 An overview of failure mechanisms (TAW, 1998)

#### 3.3.1 Failure probabilities of dikes

To determine the failure probability of a dike (or hydraulic structure but these are not specifically considered here) usually a probabilistic approach is used. The basis of most reliability calculations is the limit state function with the following form (CUR Publicatie 190, 1997):

$$Z = R - S$$

In which  $R$  is the strength of the element and  $S$  the solicitation or load on the element. For  $Z < 0$  the element fails. This can be different for different failure mechanisms, as for instance for overtopping the limit state is reached when the overflow over the crest equals the critical

overtopping flow (TAW, 1998), while for piping this is governed by a certain water level combined with a certain load duration. Classically the deterministic approach for designing structures uses a safety factor; only recently the probabilistic approach was adopted, mainly due to the increasing capacity of computers which enabled the use of first-order reliability methods and Monte Carlo simulations. The main disadvantage of the deterministic approach is that it does not consider uncertainties in any parameter. It can thus be that a probabilistic design, based on a certain desired failure probability is a lot safer than a design using one design level multiplied by a safety factor; even if the safety factor is relatively high the uncertainty can cause failure in specific cases. In most deterministic designs the safety factor has been based upon experience and expert judgment. The methodology of calculating element reliability is split up in three levels, the deterministic approach is classified as the level I approach.

Reliability methods which consider two values (e.g. mean and standard deviation) for each uncertain parameter as well as the correlation between different parameters are classified as level II methods. The most common amongst these is the first order reliability method (FORM) which is also used in the VNK2-method.

The more advanced level III methods are fully probabilistic and based on Monte Carlo simulations of all uncertain parameters. By using a large set of combinations the probability density function is reconstructed from the distribution and can be used for the reliability analysis. More details on the different probabilistic methods that are available can be found in paragraph 0.

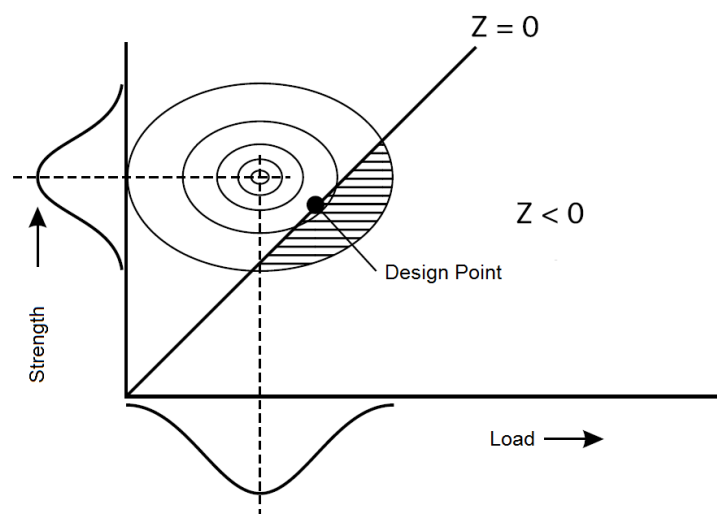


Figure 3-5 2D probability distribution for strength and loading of an element (TAW, 1998)

### 3.3.2 Failure mechanisms

As mentioned before, dikes can fail in many ways. The different failure mechanisms of dikes have different sources, which can be distinguished in three clusters based on the factor that induces them (Vorogushyn et al., 2009):

- Hydraulic failure: mainly overtopping and overflow. These mechanisms are governed by extreme hydraulic loads causing erosion.
- Geohydraulic failures: piping and instability caused by seepage. These mechanisms are governed by a combination of geotechnical properties of the dike and hydraulic loads.

- Global static failures: instability due to high loads. These mechanisms are triggered by high pressure forces.

The three main failure mechanisms are briefly discussed below.

### Overtopping

Overtopping is the most commonly considered failure mechanism and was the basis for all dike designs in the Netherlands until a few years ago. It is dependent on one main load which is the water level on the outer slope of the dike. Failure occurs when the flow over the dike crest is at a level where the grass cover of the dike starts to erode and subsequent erosion of the dike crest causes a dike breach. The limit state for overtopping is thus described by the following formula (Vrouwenvelder et al., 1999):

$$Z = m_{qc} * q_{qc} - m_{q0} * q_0$$

In which  $m_{qc}$  and  $m_{q0}$  represent factors for the uncertainty of the overflow erosion models and  $q_{qc}$  and  $q_0$  are the critical discharges for erosion.

### Piping

Until a few years ago, in the Netherlands, failure due to piping was accounted for in the design rules by TAW (TAW, 1985). Due to lack of knowledge and computational restrictions it was not possible to include piping failures in the reliability analysis of flood defences. In recent years this has changed and piping failure probabilities have shown to be heavily underestimated in previous analysis. Several parts of the Dutch flood defences were disapproved based on piping calculations. This caused some discussion on whether this was realistic but Vrijling et al. (2010) concluded that it was indeed necessary to take piping into account in the way it was done.

Piping is a failure mechanism in which, due to a high difference in water pressure on two sides of the flood defence, water flows through or underneath the dike with a sufficient velocity to cause erosion of sand particles from the foundation. This can cause the structure or dike to become unstable and eventually, when the erosion has developed far enough, structural failure follows. Piping can be considered a geohydraulic failure mechanism: it is both dependent on the load and the geotechnical stability of the flood defence. When considering a dike, the soil usually has a quite a large variation, making the soil properties and thus the geotechnical strength of dikes uncertain. When considering piping safety usually the rule of Bligh or Sellmeijer is used (TAW, 1999). Bligh is a relatively simple rule which relates the water level difference at both sides, the total width of the dike  $L$ , and the soil properties of the dike, by using a factor  $C_{Bligh}$ , to each other using the following formula:

$$\Delta H \leq \Delta H_C = \frac{C_{Bligh}}{L}$$

This gives relatively conservative estimates for the critical head ( $\Delta H_C$ ). Sellmeijer also includes models for groundwater flow in his formula, making it a more accurate but also a more complex formula which needs more data than the Bligh formula. When considering failure of a dike reach due to piping, it is important to take into account the effect of the length of the reach. This will be further discussed in paragraph 3.3.3.

### Instability of the inner slope

The third major failure mechanism in river dike failures is instability of the inner slope. At a certain moment when the water level is high and the phreatic level in the dike has risen to a certain critical level the dike can become unstable and slide off due to a reduction of the frictional forces in the soil.

An often used method to analyse such mechanisms is the Bishop method. Bishops method slices up a certain sliding circle in small pieces and calculates the resultant forces and thus a Factor of safety. The value for this Factor of safety represents the safety factor used for the macrostability of the dike slope and depends on the safety requirements. An important requirement for applying Bishop is that the soil has to be fully drained and no water overstressing is allowed (Zwanenburg et al., 2013). Another requirement is that the sliding circles have to be circular.

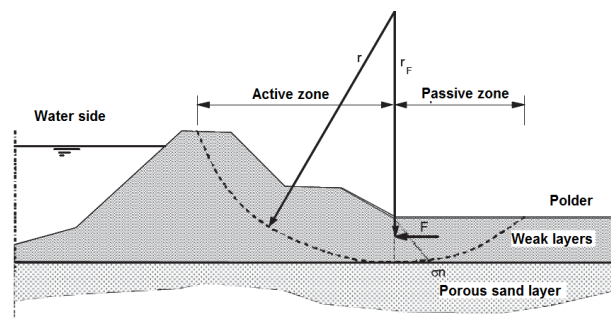


Figure 3-6 Bishop sliding circle (Zwanenburg et al., 2013)

The Bishop Method uses the following equation for calculating the Factor of Safety:

$$FS = \frac{1}{\sum W * \sin \alpha} * \sum [c' * l + W(\cos \alpha - r_u * \sec \alpha) * \tan \phi']$$

With:	FS:	Factor of safety	[-]
	W:	Weight of slice of soil	[kN]
	c':	Cohesion of the soil	[kPa]
	l:	length of base of slice	[m]
	$\alpha$ :	angle of base of slice compared to horizontal	[°]
	$r_u$ :	pore pressure ratio (typically 0.5)	[-]
	$\phi'$ :	angle of internal friction of the soil	[°]

In cases where the soil is not fully drained or where the most important sliding circles are not circular other methods such as finite element methods might provide a solution. In current practice in the Netherlands nearly all stability analysis are executed assuming fully drained circumstances.

#### 3.3.3 Spatial effects in flood defence reliability

As was mentioned in the preceding paragraph, the reliability of flood defences for especially geohydraulic failures is dependent on the amount of information and the length of the defence. Due to the uncertainties in soil parameters, the length of the reach increases the uncertainty. This causes the strength of long reaches with for instance only one known cross section to have a higher uncertainty, as the correlation of the soil parameters decreases with the distance to the

known location. In Figure 3-7 this uncertainty can also be observed: even when there are several measurements it can still be the case that the weakest spot is lower than expected.

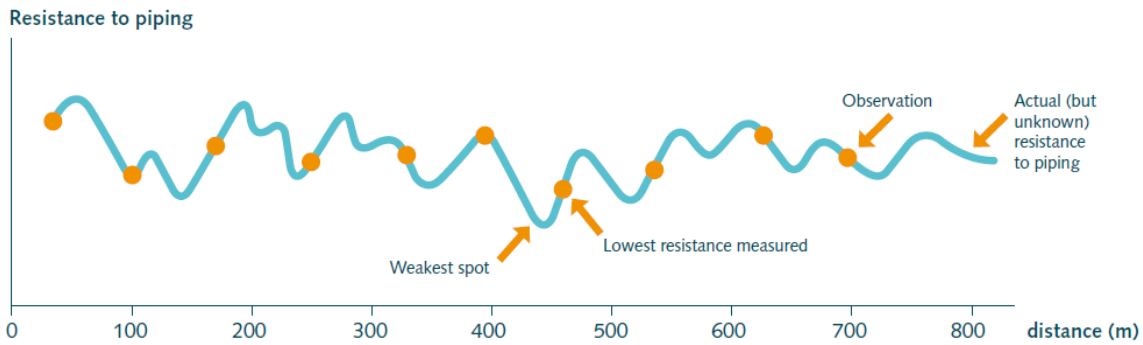


Figure 3-7 Piping resistance: reality and observations (VNK2 project office, 2012)

Kanning (2012) studied the effect of spatial variability on failure probabilities for piping. In Figure 3-7 the principle of spatial variability is shown in relation to the safety of the elements:

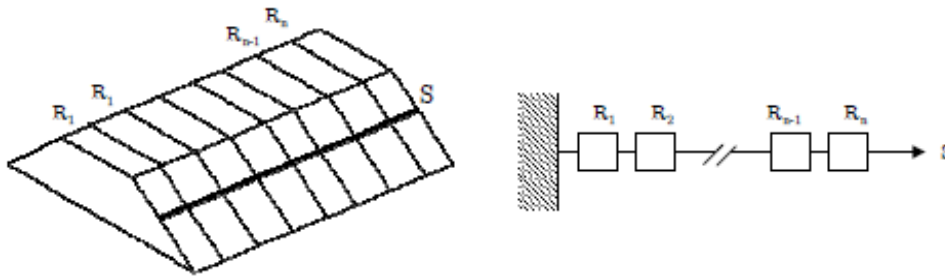


Figure 3-8 Principle of the length effect for a dike consisting of n elements (Kanning, 2012)

The flood defence behaves as a serial system: when accounting for a longer reach or larger elements (for instance due to lack of data), the uncertainty and thus the failure probability increases. The length effect is also strongly determined by the correlation of the strength of the various elements, this is shown in Figure 3-9.

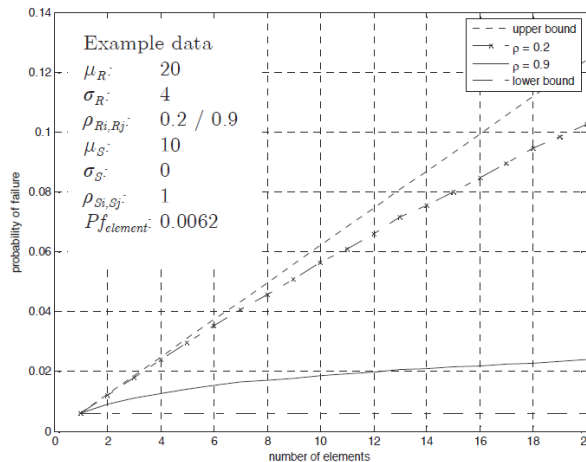


Figure 3-9 Failure probability for a dike of n elements with various correlation coefficients (Kanning, 2012)

From this figure it appears that, to obtain a reasonable estimate for the failure probability it is necessary to have a decent amount of data, otherwise the uncertainty becomes large. When incorporating these spatial effects in a flood risk analysis, it thus means that to determine the resistance against piping, it is not sufficient to consider only 1 or 2 cross sections for a dike section (of a certain length). For overtopping this is of less importance as crest heights are the governing strength parameter and these usually have a strong correlation and lower uncertainty.

### 3.3.4 Fragility curves

The fragility curve is a structural reliability method which is quite common in mechanical and earthquake engineering. Fragility functions were first applied by the United States Army Corps of Engineers (USACE) to assess failure probabilities of flood defences, although they use a slightly different method (Buijs et al., 2007). There are different ways to construct fragility curves, for instance the USACE uses curves mainly based on expert judgement, whereas for instance mechanical and earthquake engineering use curves based on empirical data. A third method is by using structural reliability models as a basis. This is also the approach recommended by Buijs et al.(2007), and it has become increasingly popular in flood defence assessments during recent years, and is now used in for instance the VNK2-method.

The fragility curve relates the failure probability of a structure to a certain loading. The definition for the failure probability of a dike section is:

$$P_f = P(Z \leq 0) = P(R \leq S) = \iint_{Z \leq 0} f_{RS}(r, s) dr ds$$

With  $f_{RS}$  the joint probability function of load and strength. If R and S are independent which is often the case for flood defences this can be written as:

$$\begin{aligned} P_f &= \int_{S=-\infty}^{S=\infty} \int_{R=-\infty}^S f_S(s) * f_R(r) dr ds \\ &= \int_{S=-\infty}^{S=\infty} f_S(s) * \int_{R=-\infty}^S f_R(r) dr ds \\ &= \int_{S=-\infty}^{S=\infty} f_S(s) * F_R(r) ds \end{aligned}$$

$f_S(s)$  is then the probability density function for random variables of load  $S$ , and  $F_R(r)$  is the cumulative density function which gives the failure probability for a given value of the strength  $R$  (van der Meer et al., 2008).

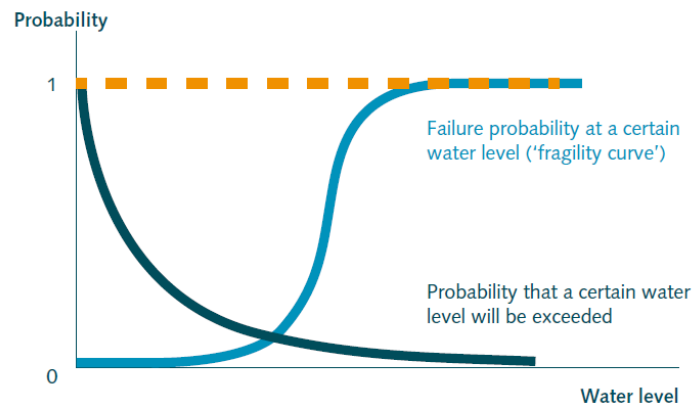


Figure 3-10 Representation of a failure probability calculation using a water level distribution and a fragility curve (VNK2 project office, 2012)

### Fragility curves: difference between failure modes

For overtopping the determination of a fragility curve is relatively easy, as overtopping failure is almost fully determined by the water level imposed on the structure, as was shown by ter Horst (2005). This can also be observed in Figure 3-11 where the fragility curve for overtopping is very narrow, representing a normal distribution with a low standard deviation for the crest height.

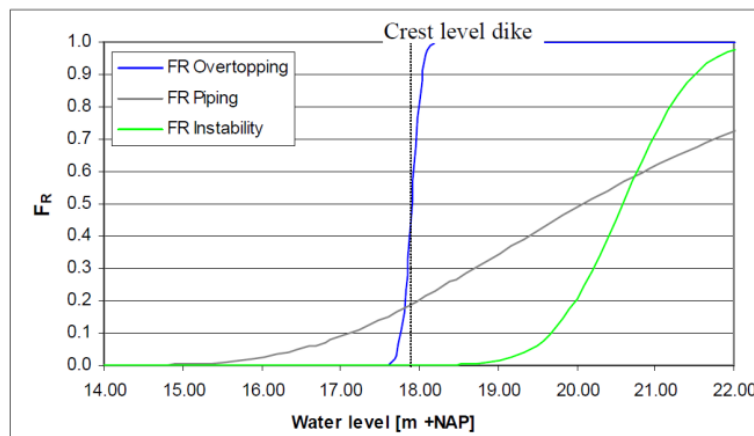


Figure 3-11 Fragility curves as found by Ter Horst (2005)

This research also showed that fragility curves for piping (and instability) show a lot more spreading, mainly because piping is not solely governed by the water level, but also by different geotechnical parameters and the duration of the flood wave. In this case the failure probability for piping was 0,2 at crest level and 0,1 at 1 meter below crest level. For water levels more than 0,5 meters (depending on the amount of wave run-up) below the crest of the dike, piping is thus the governing failure mechanism. For water levels around and above the crest level overtopping quickly becomes the governing failure mode. Vorogushyn et al. (2009) demonstrated that based on experimental data the piping and instability curves are indeed a lot wider. They also showed the influence of different parameters on the fragility curves, and especially that the hydraulic conductivity values of the sand layer have an enormous influence on the fragility curves. This certainly shows that the fragility curves for geohydraulic failure modes have to be handled with care as there is usually quite some uncertainty in the different parameters. This also emphasizes the importance of a correct representation of length effects. Another element quantified in the

study by Vorogushyn et al. (2009) is the time dependence for piping failure. Different results for different time durations of loads are presented, and it is clearly shown that time is of significant influence on piping failures. It is also shown from the graphs that water levels below the crest level of a dike can still have a significant contribution to the failure probability. However, to construct fragility planes such as the ones in Figure 3-12 a lot of data is necessary, which is not always available.

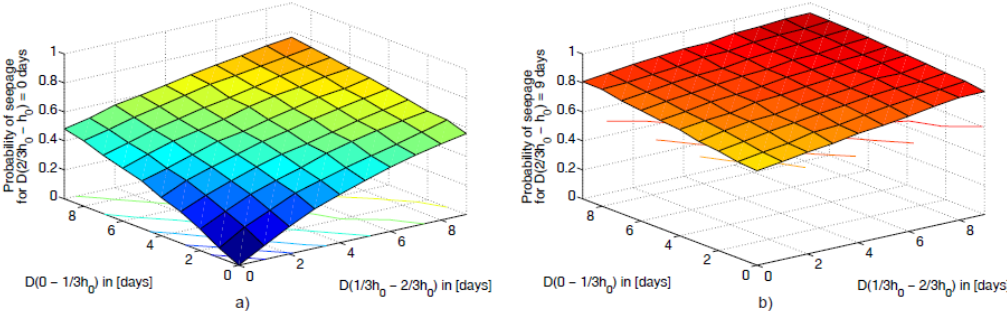


Figure 3-12 3-dimensional seepage fragility curves for different durations in different water level intervals. The intervals represent portions of the total dike height and  $D(h)$  is the duration of the loading at a certain interval (Vorogushyn et al., 2009)

### 3.4 Methods for probabilistic analysis of flood defences

#### 3.4.1 Type II: First-order reliability method (FORM)

This method is used in the VNK2-approach (Jongejan et al., 2011) since it gives accurate results for large numbers of cases and is relatively efficient in terms of computing time. In the FORM approach the limit state function is linearized at the design point, which is the point at  $Z=0$  for which the failure probability is the highest. In the FORM approach this point is determined iteratively until it no further converges. First the distributions of the uncertain variables are transformed to standard normal distributions and are normalized using the method shown in CUR Publicatie 190 (1997). This results in the reliability index  $\beta$  being equal to the distance between the design point and the origin as shown in Figure 3-13. The linearized reliability function has the following form:

$$Z = \beta - \alpha_R * u_R - \alpha_S * u_S$$

With:

- $\beta$  = Hasofer-Lind reliability index
- $\alpha_R$  = influence coefficient of strength
- $u_R$  = strength
- $\alpha_S$  = influence coefficient of load
- $u_S$  = load

Since the values for  $u_R$  and  $u_S$  are 0 due to the normalization of the random variables the expected value of  $Z(\mu_Z) = \beta$ . Since both  $\alpha_R$  and  $\alpha_S$  are equal to 1 and  $\sigma_Z = \sqrt{\alpha_R^2 + \alpha_S^2}$  this gives:

$$P_f = P(Z \leq 0) = \Phi(\beta)$$

In which  $\Phi(\beta)$  is the cumulative standard normal distribution.

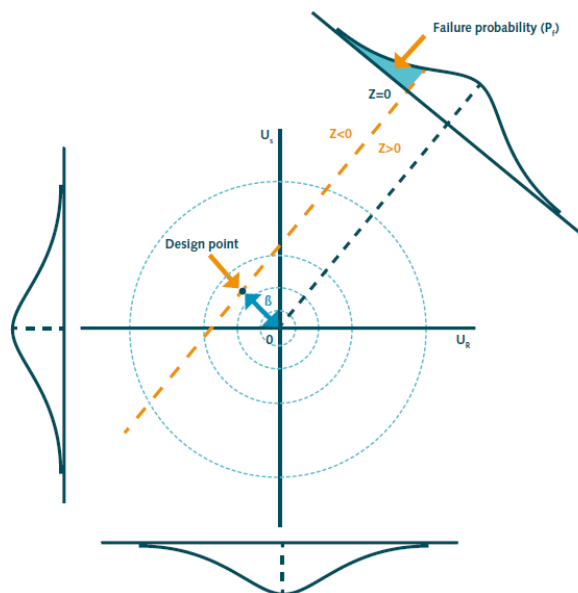


Figure 3-13 Overview of the different parameters in a FORM analysis after normalization of the uncertain variables (VNK2 project office, 2012)

### 3.4.2 Type III: Monte Carlo simulation

Monte Carlo methods are very accurate and are for instance used in risk analysis in the UK (Dawson et al., 2005). They are accurate as long as the distributions are known but their main disadvantage is that they have a longer computation time, especially for rare events when large numbers of simulations are needed. However, this can be dealt with by for instance importance sampling (Dawson and Hall, 2006).

The principle of a Monte Carlo simulation is not very complicated: from a given set of stochastic variables a large amount of deterministic simulations of events is simulated. Due to the stochastic nature of the input the output will also have a random nature, and will represent the statistical distribution originated from all the uncertainties in the input parameters. In the case of flood risk analysis usually the goal is to determine under which circumstances and parameter values a dike fails. The output of the MC simulation is then a set of positive and negative Z-values, for which negative values represent load/strength combinations leading to failure of the system. Counting the number of failures then leads to the probability of failure, as can be seen in Figure 3-14.

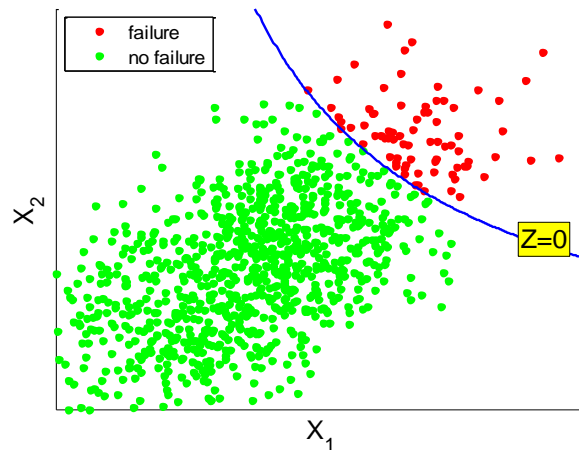


Figure 3-14 Set of Monte Carlo simulations with their Z-values

The probability of failure  $P_f$  is then:

$$\hat{P}_f = \frac{N_f}{N} = \frac{\sum_{i=1}^N I(Z(\mathbf{X}))}{N}$$

With  $\hat{P}_f$  an estimate of  $P_f$  and  $I$  an indicator function indicating failure (for  $Z < 0$   $I=1$ , otherwise  $I=0$ ).

A possible disadvantage of standard Monte Carlo simulations (or ‘Crude Monte Carlo’), is that for events with a very small frequency of occurrence, a large amount of simulations is necessary as, when considering data of a too small number of simulations, the variation in results for different simulations will be very large. Therefore a large amount of simulations has to be executed to obtain a sufficient accuracy in the results. The amount of samples necessary can be estimated by comparing the result for the failure probability with the expected failure probability. If the difference is too big either the expectation was wrong or the amount of samples has to be

increased. This can also be done by using a convergence plot. A convergence plot plots the failure probability against the number of simulations. When the failure probability has converged to a stable level, set by a desired accuracy, the number of samples is sufficient.

### Importance sampling

Another solution to solve the problem of large datasets in case of extremely rare events is Importance sampling. Importance Sampling can increase the effectivity of a Monte Carlo simulation by giving the same or a better accuracy with less samples. This is done by replacing the actual failure probabilities  $f$ , by a more efficient probability distribution  $h$ . Efficient means, in this case, that it gives more failures for the same sample size. This brings along that the failure probabilities are different and these have to be adapted using the following formula:

$$\hat{P}_f = \frac{\sum_{i=1}^N I(Z(\mathbf{X})) \frac{f(\mathbf{X})}{h(\mathbf{X})}}{N}$$

The  $h$ -function can take any form, although the choice for this function determines the efficiency of the sampling. The efficiency of the sampling procedure can be quantified by looking at the difference between bias and standard deviation. For a bias close to zero the following formula is applicable:

$$P[|\hat{P}_f - P_f| < \varepsilon_1] < \varepsilon_2$$

For the bias to be zero, for any combination of small positive values  $\varepsilon_1$  and  $\varepsilon_2$ , there is a minimum number of samples  $N^*$ . The number of samples thus has to be chosen large enough to meet this criterion. For the societal risk tool project it was found that, for the case considered, the uniform sampling of river discharges gave very good results in terms of bias and standard deviation. Figure 3-15 shows the sampling method and Figure 3-16 shows the results for bias and standard deviations for different return periods.

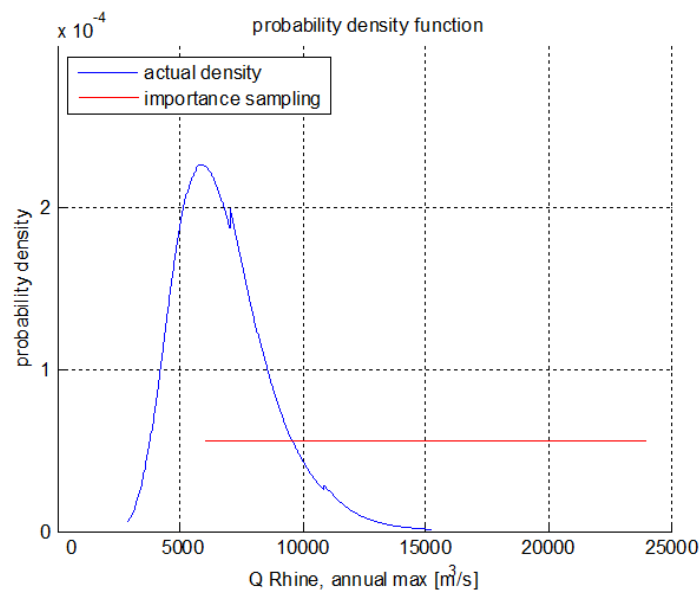


Figure 3-15 Sampling strategy used in the societal risk tool (De Bruijn et al., 2013)

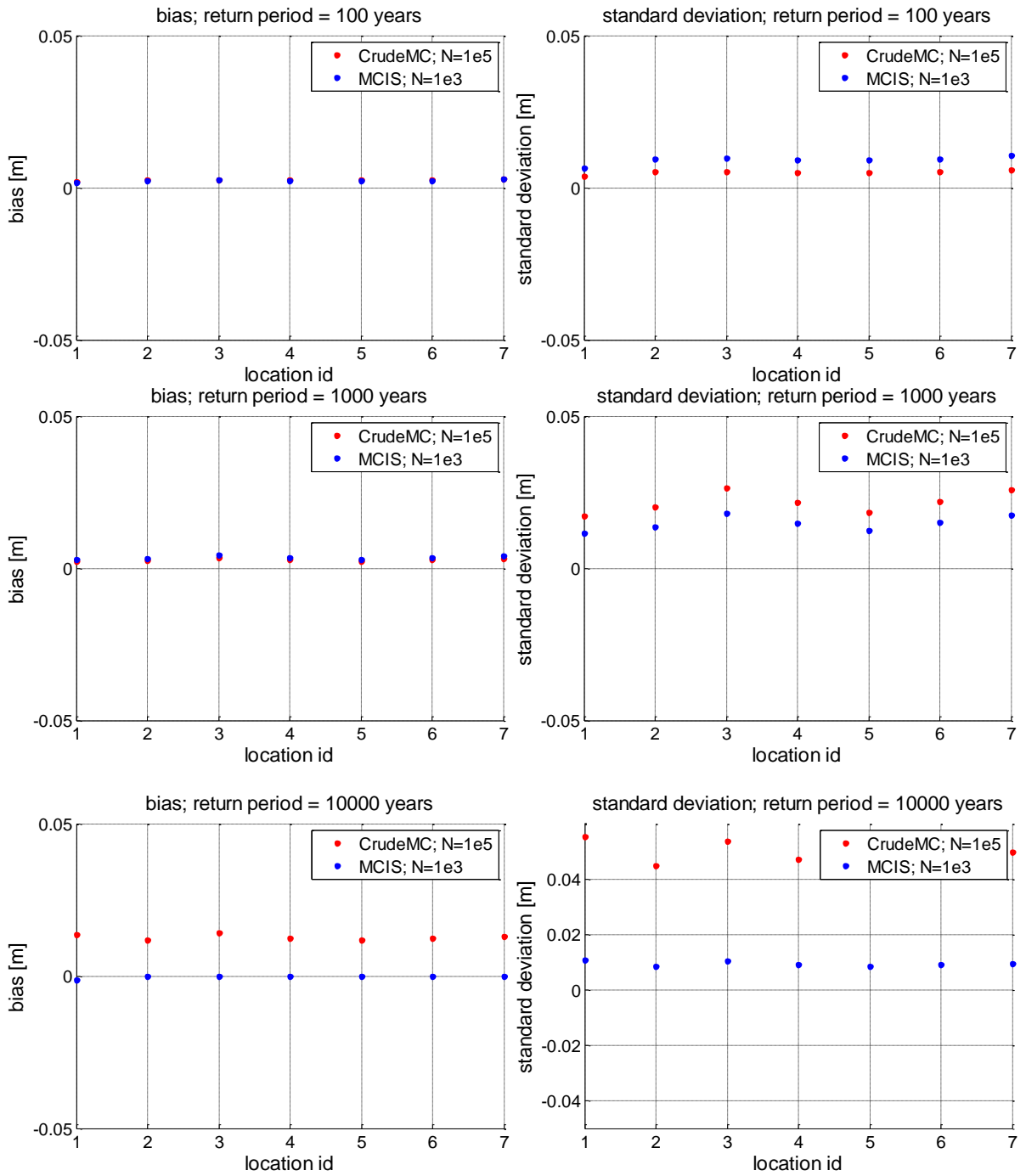


Figure 3-16 Bias and standard deviation for Crude Monte Carlo and Monte Carlo with uniform Importance Sampling of river discharges at Lobith for the societal risk tool project at Deltares (De Bruijn et al., 2013)

### Comparison of methods

In this chapter the first-order reliability method (FORM) and Monte Carlo with or without Importance Sampling were introduced. These are not the only methods, for instance numerical integration is also available. However, for cases with many variables numerical integration becomes very time consuming and it is therefore not suitable for this research. FORM is a method that requires relatively little computation time, however as it linearizes the Z-function accuracy is lost when the Z-function becomes non-linear. Also the function sometimes converges to a 'local' design point instead of the real design point. Lastly FORM calculates the failure probability for one location, when calculating it for many more locations the efficiency is easily lost as it also has to calculate the combinations of failures. In cases of event based analysis with many breaches this is not feasible. The last option is to use Monte Carlo techniques. Crude Monte Carlo has one main disadvantage which is that, for low probability failures it needs a lot of simulations to give a reliable estimate of the failure probability. However, this problem can be solved by applying Importance Sampling.

### 3.5 Quantifying flood risk

The second important parameter in the formula for risk is the damage of a flood scenario. In flood risk management there are two main indicators used for hazard indication and quantification:

- Loss of life risk
- Economic risk

Loss of life risk is usually quantified in either Local Individual Risk or societal risk, however since LIR is not relevant for this thesis it is not further considered here. There are also some other types of damages, such as environmental damage and psychological damage, these are however very difficult to quantify and therefore seldom considered in flood risk analysis. The consequences of a flood are determined using inundation depths, damage functions relating inundation depths to damage and for casualties the fraction of evacuated people. In the Netherlands the standard set of functions used for this are the functions from HIS-SSM, this will be further discussed in paragraph 3.5.3.

#### 3.5.1 Societal risk

Societal risk (or group risk) is the probability that a certain amount of people dies in a disaster. Usually events with large numbers of fatalities but a small probability of occurrence, are found to be less acceptable than small numbers of fatalities with a higher frequency of occurrence (De Bruijn et al., 2013). By quantifying societal risk an expected value of loss of life per year can be defined and the events with the largest number of casualties can be identified. A common way to represent societal risk is by the use of a FN-curve, a curve which shows the number of casualties and the probability of an event exceeding that number of casualties. The area under a FN-curve represents the expected number of fatalities per year  $E(N)$ .

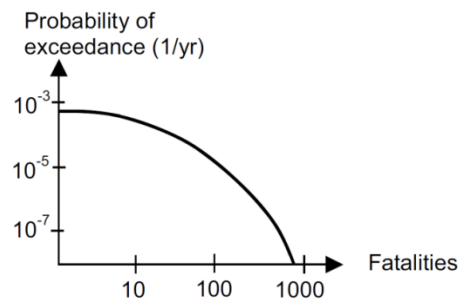


Figure 3-17 Example of an FN curve (Jonkman, 2007)

### 3.5.2 Economic damage

Economic damage consists of both direct and indirect damage of a flood disaster. Calculating economic damage, enables a comparison of cost and risk/damage reduction of preventive measures, thus giving a good guide in assessing the cost effectiveness of for instance dike improvements. Economic damage is closely related to casualties: In areas with a high societal risk there is often a lot of economic activity and thus economic risk and vice versa. A common way to represent economic damage is by use of a FD-curve, which is similar to the FN-curve. The area under the FD-curve is, just as with the FN-curve, the expected damage per year  $E(D)$ .

In the Netherlands as well as in the UK dike design is based upon economic optimization. Limits for economic damage are less common although there is an example for dam design in the US (Jonkman et al., 2003). The dike design in the Netherlands is, although based upon economic optimization, not completely founded on it, mainly due to lack of computational capacity in the fifties and sixties when the standards were defined. During that time it was decided to give South Holland a standard below the calculated economic optimum, 1/10.000 year instead of 1/125.000 year. Slijkhuis et al. (1997) showed that for a risk-averse situation in which uncertainty is taken into account, the crest level for the Hoek van Holland sea dike should be much higher than the current level. The WV21-project shows similar results for dikes all over the Netherlands (Deltares, 2011).

Although it is ethically open for discussion the value of a statistical life can also be expressed in a monetary value. The value of life has estimates between 1 and 11 million euros but recent research on this topic suggests a value of 6.8 million euros per lost statistical life (Bockarjova et al., 2012). Putting economic value to casualties enables a better comparison between damages thus enhancing a cost-benefit analysis.

### 3.5.3 HIS-SSM

In the Netherlands the Dutch Standard Damage and Casualty Model (HIS-SSM) is used to assess flood impacts in the Netherlands (Kok et al., 2005). It calculates direct damage and damage due to business interruption in the flooded area, provides the number of inhabitants of the flood-area and estimates the number of potential fatalities. The model contains detailed data on land use, objects (houses, cars, companies) and the number of inhabitants. It also contains damage and mortality functions which relate the land use and objects present and the flood depth to damage and casualty assessments. By providing flood data such as water depths, and if available rise rates and flow velocities damage and casualties can be estimated.

### 3.6 Flood modelling

Modelling flood patterns is an essential part of flood risk analysis as the flooding depth, water level rise rate and flow velocities are needed as input for HIS-SSM, in order to be able to determine the number of casualties and damage. For modelling floods there are several possible techniques. However, the most accurate ones have one thing in common: they are computationally very expensive. The increase in computer capacity has led to a more wide application of inundation models, but especially in a probabilistic context they still have to be handled with care. Another difficulty with inundation models is that it is very hard to calibrate the model, as there are usually not many properly measured examples of inundation that can be used. However, despite all uncertainties flood modelling fulfils a pivotal role in estimation of flood extent and consequences. A couple of different types of models used in flood risk assessments, which are interesting for this research are discussed in the following paragraphs.

#### 3.6.1 Storage cell models

Storage cell models are used in flood risk assessments in the UK and Germany, and are useful for fast estimation of flood damages (Dawson et al., 2005; Vorogushyn et al., 2012). The main application of this type of models is floodplain inundation. One of the most commonly used storage cell models is LISFLOOD-FP. The model is based on a raster Digital Elevation Map and the river channel flow is modelled by the one-dimensional linear kinematic Saint-Venant equations (Bates and De Roo, 2000). When the bankful capacity of the river channel is exceeded or a dike breaches, the flood wave propagation is simulated by solving the discretized momentum and continuity equations over the grid. The continuity equation is then:

$$\frac{\partial h^{i,j}}{\partial t} = \frac{Q_x^{i-1,j} - Q_x^{i,j} + Q_y^{i,j-1} - Q_y^{i,j}}{\Delta x \Delta y}$$

Where  $h$  is the water surface elevation,  $i,j$  denotes the location of the cell and  $Q$  is the discharge in  $m^3/s$  in  $x$ - or  $y$ -direction (Dawson et al., 2005). The second equation is the momentum equation, also discretized over the grid:

$$Q_x^{i,j} = \frac{h_{flow}^{5/3}}{n} \left( \frac{h^{i-1,j} - h^{i,j}}{\Delta x} \right)^{1/2} \Delta y$$

Where  $n$  denotes the roughness coefficient by Manning, and  $h_{flow}$  is the water depth in the adjacent cells in meters.

The calibration of storage cell models is quite difficult, but reasonable results can be obtained by using land cover maps and deriving corresponding roughness coefficients. A disadvantage is that this type of models is not suitable for urban areas as they cannot represent flow conditions there, due to the inertia dominated flow (Apel et al., 2009b), as this causes inaccuracies and large computation times. For larger areas with a relatively small discharge through the floodplain (mainly storage), the storage cell approach is quite useful (Asselman, 2009).

#### 3.6.2 2D hydrodynamic modelling

In the Netherlands the use of 2D inundation models has been quite common in flood risk analysis during recent years. For instance both VNK2 and WV21 use 2D inundation models to obtain the flood extent and related damage of flood scenario's (Beckers and de Bruijn, 2011; VNK2 project office, 2012). One of the most commonly used versions in the Netherlands is the

2D Overland flow module in Sobek 2.12/2.13, which is capable of hydrodynamically modelling 2D flow in a grid based on a Digital Elevation Map. The Sobek 2D module is based on solving the Saint-Venant equations for momentum and continuity for a finite difference staggered grid. The continuity equation is:

$$\frac{\partial(uh)}{\partial x} + \frac{\partial(vh)}{\partial y} + \frac{\partial\zeta}{\partial t} = 0$$

The momentum equations are for respectively x and y direction:

$$\frac{\partial u}{\partial t} + u \frac{\partial u}{\partial x} + v \frac{\partial u}{\partial y} + g \frac{\partial h}{\partial x} + g \frac{u|\bar{u}|}{C^2 h} + au|u| = 0$$

$$\frac{\partial v}{\partial t} + u \frac{\partial v}{\partial x} + v \frac{\partial v}{\partial y} + g \frac{\partial h}{\partial y} + g \frac{v|\bar{u}|}{C^2 h} + av|v| = 0$$

with:

- $u$  = velocity in x-direction [m/s]
- $v$  = velocity in y-direction [m/s]
- $|\bar{u}|$  = velocity magnitude ( $=\sqrt{u^2+v^2}$ ) [m/s]
- $\zeta$  = water level above plane of reference [m]
- $h$  = total water depth ( $=\zeta+d$ ) [m]
- $d$  = total water depth [m]
- $C$  = Chezy coefficient [ $\sqrt{\text{m/s}}$ ]
- $a$  = wall friction coefficient [1/m]

These equations are then solved numerically, resulting in flow velocities, water levels and discharges for all cells.

2D models are often coupled with 1D models for river flow; Sobek for instance is able to model rivers as 1D and switch to 2D in case water flows out of the 1D reach. This is computationally much more efficient than also modelling the river as 2D. The principle of this is shown in Figure 3-18.

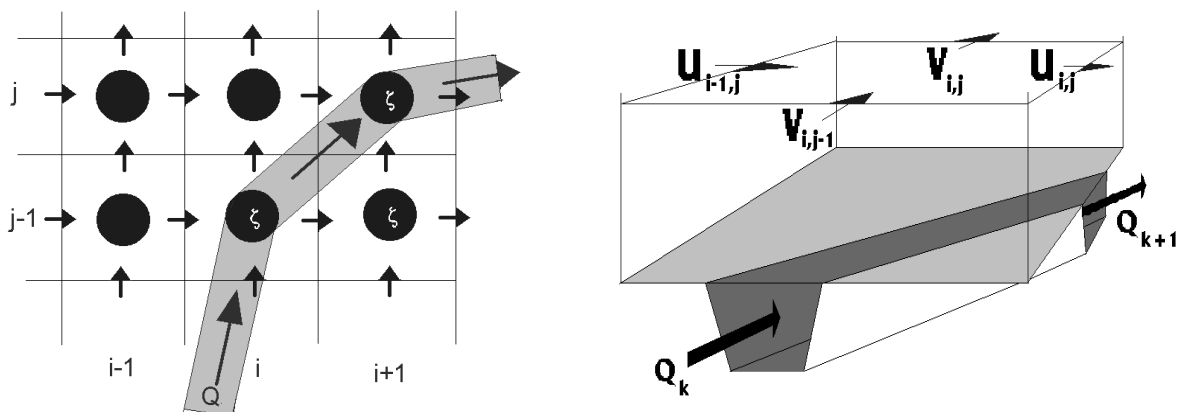


Figure 3-18 Principle of water flow through a 1D2D model

### 3.6.3 3Di modelling

A new development in the field of hydrodynamic modelling is the so called 3Di modelling. 3Di modelling is very similar to 2D modelling, except that it can be more accurate due to the use of quadtrees (Stelling, 2012). The principle of a quadtree is shown in Figure 3-19.

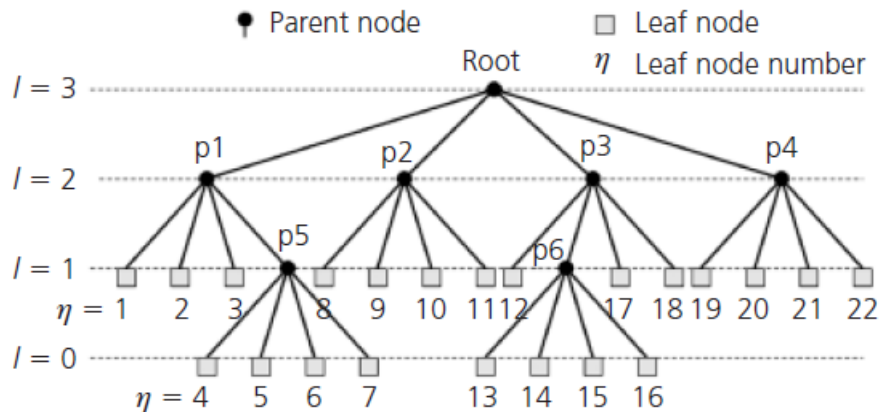


Figure 3-19 Hierarchical quadtree ordering (Stelling, 2012)

Using a quadtree enables the model to switch between different sub-grid scale levels, enabling more accurate modelling at locations with high variation in elevation and more rapid calculation of large homogenous planes. This technique seems to be very promising, as it is capable of combining detailed modelling where necessary, with at least the same calculation speed as regular 2D models. In the future it will also be possible to build '1D3Di-models', however this is one of the many things still in development.

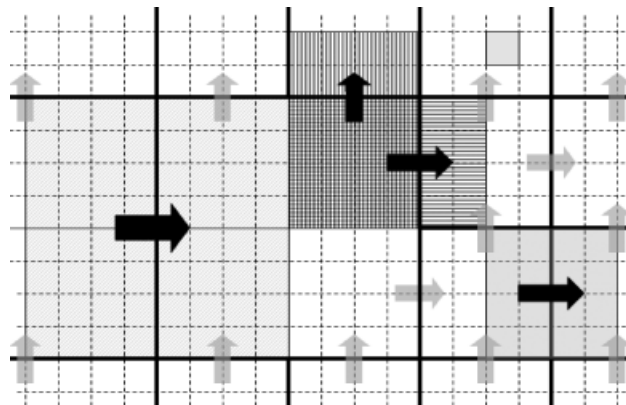


Figure 3-20 Example of the use of different grid scales in 1 model (Stelling, 2012)

### 3.6.4 0D-models

Another possibility for modelling inundations is by use of a so called 0D model. In this type of models a polder is split up in different parts with a certain storage capacity, which are all linked to each other. This type of model was applied for the case of Zuid-Beveland and gave reasonable results in terms of inundation depths (Deltares, 2009). The advantage of this type of model is that, in the study considered, it was 240 times faster than the 1D2D-model with which it was compared. The 0D schematization can thus be very useful for modelling effects of negative interdependencies, as a fast schematization is necessary to consider such effects in a probabilistic context.

### 3.6.5 Calculation speed

In terms of calculation speed, hydrodynamic modelling, especially in 2D, is very time consuming. For instance the inundation simulations done by Delft Cluster, took 2 to 6 days per run for only 1 dike ring (Vrouwenvelder et al., 2010). However due to the increasing computing speed and use of parallel processing this can of course be decreased significantly. Kalyanapu et al. (2011) have shown that using GPU for 2D simulations can speed up calculations by a factor 30. This has to be kept in mind if 2D models are applied on large scale. However for large scale, e.g. national scale, analysis 2D models are not that useful for aforementioned reasons.

### 3.6.6 Conclusion

When considering the methodologies discussed above, it appears that two factors are most important in making a choice between one of the many available methods: calculation speed and accuracy. 2D is the most accurate while 0D is probably the least accurate. On the other hand, when looking at calculation time 0D is a lot faster than 2D. When making a choice between the methods, these factors are the most important ones for making a choice.

## 3.7 Dike breach modelling

To link the flood defence reliability with the hydrodynamic situation when a dike breaches, it is important to properly model the effects of the dike breach on the hydraulic situation in the system. Dike breach modelling is especially important in this study, as it not only determines the damage in the polder behind the breach, but the breach discharge also influences the situation downstream, and can also determine whether other dikes are relieved or also overloaded causing failures.

### 3.7.1 Van der Knaap and Verheij-van der Knaap formulas

Van der Knaap (2000) proposed a formula to estimate breach growth in both sand and clay dikes in time. For sand dikes this van der Knaap formula is given by:

$$B_{sand}(t) = 67 * \log\left(\frac{t}{522}\right)$$
$$B_{clay}(t) = 20 * \log\left(\frac{t}{288}\right)$$

These formulas are useful as they are quite simple and not much data is known to estimate dike breaches. However, this is of course also their disadvantage as they are not that accurate. Therefore Verheij (2003) proposed a new formula which is much more accurate. This formula for instance takes the head difference over the dike into consideration as well as parameters for critical flow velocity. It is thus much more detailed but it also needs more input data. There are two versions of the Verheij – van der Knaap formula, a very detailed one and the following one, which is more compact:

$$B = 1,3 * \frac{g^{0,5} H^{1,5}}{u_c} * \log\left(1 + 0,04 * \frac{g}{u_c} t\right)$$

In this formula  $u_c$  is the critical flow velocity in m/s for the cover material of the dike. H is the head over the dike in meters.

### 3.7.2 Use of statistical data on dike breaches

In the research by Vorogushyn et al. (2010) the dike breach width was not calculated by use of formulas, but by fitting a probability distribution on data obtained from the 2002 Elbe floods. This was a good solution in that case, as the case study was also on the 2002 Elbe floods the same situation was considered. The statistical data on breach widths showed a large amount of breaches with a width below 100 meters, most likely caused by the fact that most dikes were quite clayey.

#### 4. New methodology for assessing load interdependencies of flood defences

In this chapter a new methodology is presented, which enables accounting for load interdependencies in flood risk analysis. First of all, the probabilistic effect of dike breaches on water levels and discharges is explained using a conceptual method. After that, by using the knowledge from that model and the literature in Chapter 2, a probabilistic framework is defined which enables accounting for load interdependencies in risk analysis.

##### 4.1 Analysis of effects of load interdependencies

To further explain the effects of load interdependencies on water levels and failure probabilities, a simple model was made in Matlab, which is used to explain the different relations in the system. Figure 4-1 shows the hypothetical example case used in this paragraph, which is the same as the one used in paragraph 2.6.

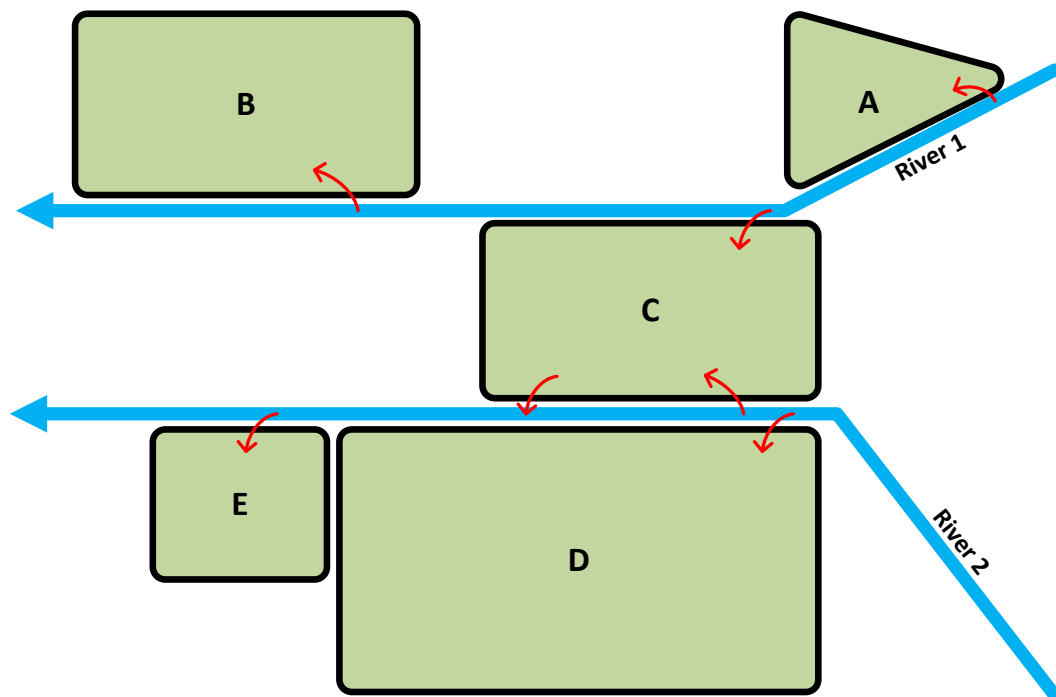


Figure 4-1 Hypothetical water system with load interdependencies

In this fictive situation all kinds of interactions between the different areas are possible, these are shown by the red arrows in the figure. For simplicity sake the definition of dike rings is used. The above schematization was modelled in Matlab. In this case only overtopping was considered and it was assumed that an exceedence of the dike crest level resulted in dike failure. The breach discharge was assumed to be  $1/10^{\text{th}}$  of the river discharge. For simplicity sake, time was not considered, so it was assumed that breaches always reduced the maximum discharge downstream by 10%, while in reality this can show an enormous variation. Backwater effects of breaches were not considered so breaches only have influence downstream. A similar analysis where time and backwater effects are considered can be found in van der Wiel (2004). The boundary condition and dike strength were considered using probabilistic distributions. For the discharge, an exponential distribution with a mean of  $1.600 \text{ m}^3/\text{s}$  was assumed. The dike levels were determined by taking the 1/100-year water level as design level and assuming a normal

distribution with as mean the design level and a coefficient of variation  $V$  of 10%. Furthermore the rivers were assumed to have the dimensions shown in Table 4-1.

River 1			
<b>i</b>	Bottom slope	$10^{-4}$	$[-]$
<b>L<sub>1,0</sub></b>	Length upstream of A	10	$[km]$
<b>L<sub>1,1</sub></b>	Length of A	10	$[km]$
<b>L<sub>1,2</sub></b>	Length of C	15	$[km]$
<b>L<sub>1,3</sub></b>	Length of B	15	$[km]$
<b>C</b>	Chezy coefficient	45	$[m^{\frac{1}{2}}/s]$
<b>h<sub>0</sub></b>	Bottom level at beginning of reach	10	$[m]$
<b>B</b>	Width of river	400	$[m]$
River 2			
<b>i</b>	Bottom slope	$10^{-4}$	$[-]$
<b>L<sub>2,0</sub></b>	Length upstream of D	35	$[km]$
<b>L<sub>2,1</sub></b>	Length of D	25	$[km]$
<b>L<sub>2,2</sub></b>	Length of E	5	$[km]$
<b>C</b>	Chezy coefficient	45	$[m^{\frac{1}{2}}/s]$
<b>h<sub>0</sub></b>	Bottom level at beginning of reach	10	$[m]$
<b>B</b>	Width of river	250	$[m]$

Table 4-1 Dimensions of rivers 1 & 2

#### 4.1.1 Positive load interdependencies in the conceptual model

When a dike fails, the water level in the river lowers, as part of the discharge is diverted into the polder behind the failed dike. This is a case of positive load interdependencies: the failure of a dike has a positive effect on the safety of other dikes. When considering the case in Figure 4-2, the hydraulic conditions at the dikes protecting B are influenced by the conditions at dikes A and C and vice versa. This can be illustrated by a simple example.

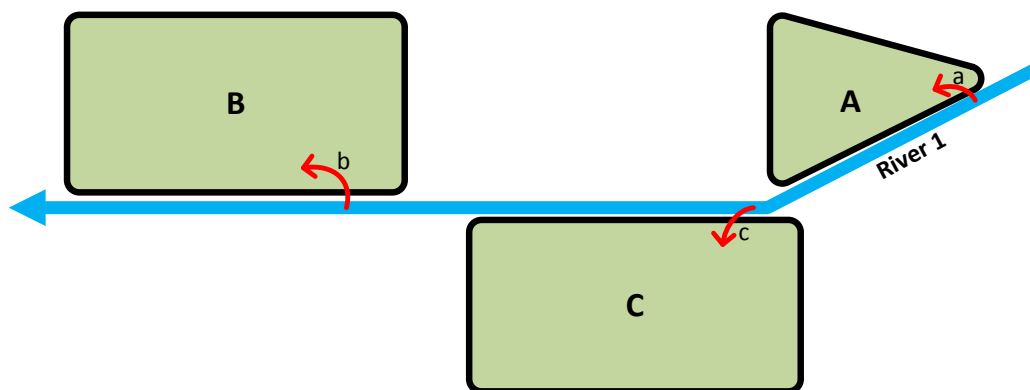


Figure 4-2 Case of positive load interdependence

This part of the model was modelled in Matlab in order to investigate the positive load interdependencies. It can be expected, based on the findings by Apel et al. (2009a), that the frequency of high discharges at breach b will be smaller than at breach a. When executing a Monte Carlo simulation with  $n=250.000$  this gives the graphs for the non-exceedence probabilities of discharges shown in Figure 4-3.

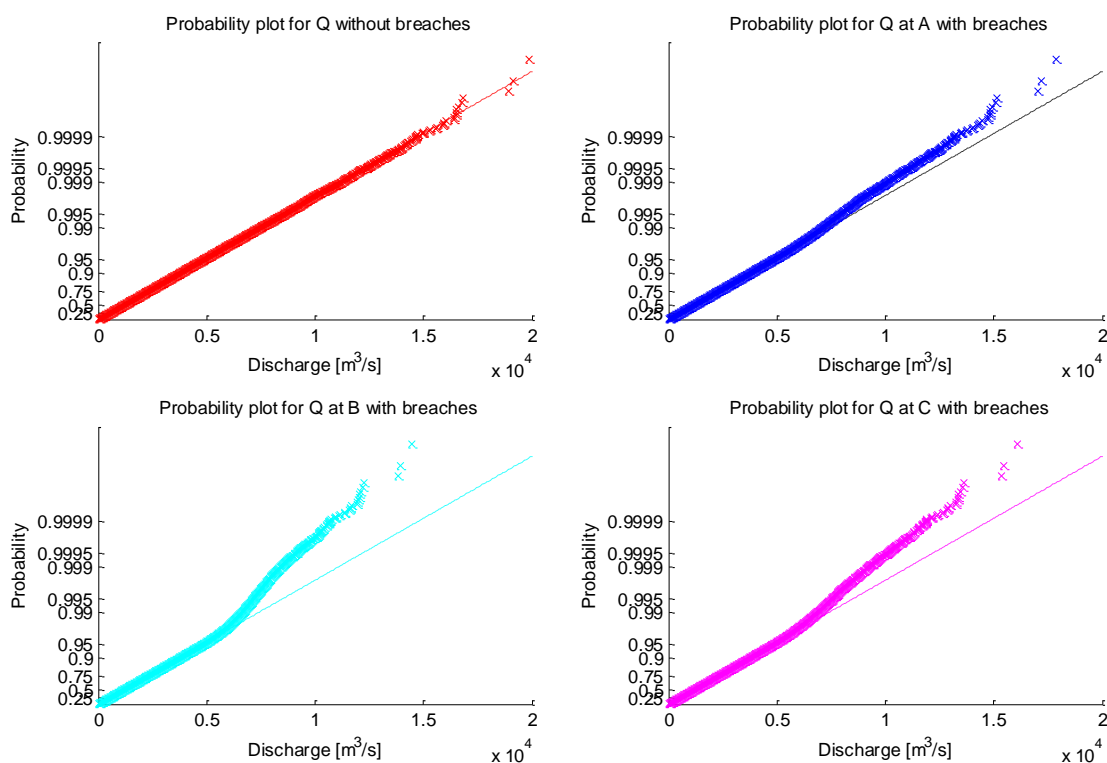


Figure 4-3 Non-exceedence probabilities of the river discharge at different locations

From these figures it can indeed be concluded that for an increasing amount of breaches the probability of high discharges decreases: breaches at one location cause load relief at other locations. For B, the effect of relief is the largest, for A the smallest, as could be expected given the amount of possible breaches upstream of the location. When comparing the discharges for a return period of 1/1.000 years this gives the values from Table 4-2.

Location	No breaches	Location A	Location C	Location B
<b>Discharge [m³/s]</b>	11.000	10.050	9.100	8.300

Table 4-2 Discharges for 1/1.000 year return frequencies for all locations in the conceptual system

The fact that the return period for a certain discharge decreases, entails the principle of load relief and thus lower failure probabilities, especially for downstream dikes. The adaptation of exceedence probabilities thus seems a very convenient way to cope with this effect in risk analysis. The relief effect is also visible in the water level probabilities. In Figure 4-4 the water levels with and without breaches for the most downstream location are shown, it can be observed that for higher water levels, the probabilities decrease when considering breaches upstream. In the figure, three lines can be observed, these are caused by the occurrence of 1, 2 or 3 breaches, each causing a 10% decrease in discharge.

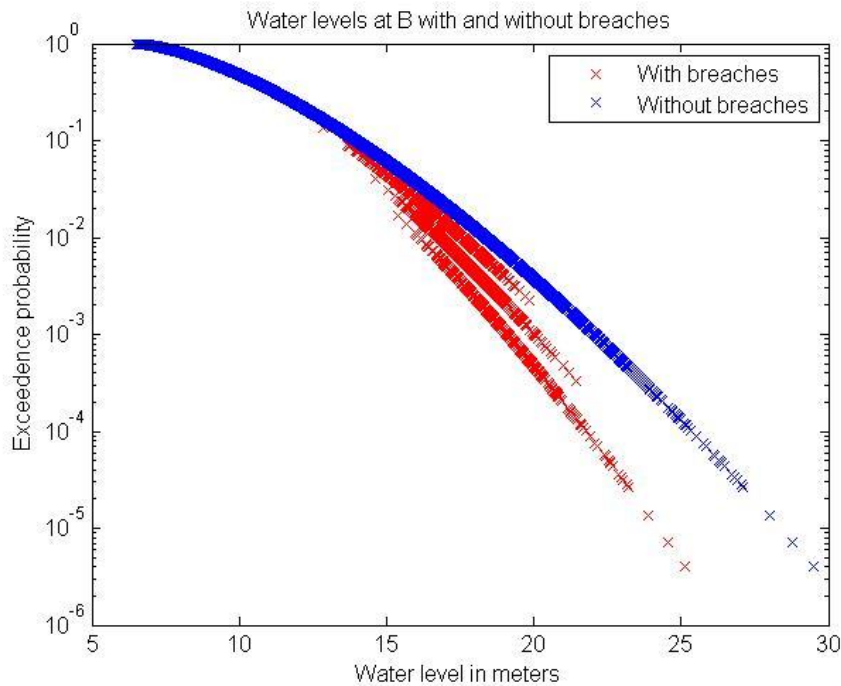


**Figure 4-4 Water levels and their exceedence probabilities with and without load interdependencies**

This example shows that in order to incorporate these positive effects in a risk analysis, the most important parameters that need to be changed, are the hydraulic loads and their corresponding return periods. This can be accomplished by using a hydrodynamic model of the entire water system and then executing a Monte Carlo analysis with multiple breaches. From the maximum water levels in the scenarios and their exceedence probabilities, the new exceedence probability graph can be determined. This can then, for instance, be used as a boundary condition for risk assessments. However regarding the calculation, the following things have to be kept in mind:

- The storage of the polders in this example is assumed to be infinitely large, in reality polders could fill up, reducing their effect on the discharge.
- Time is not considered: the time of breach initiation can have a large influence on the maximum discharge, especially if the storage in the polders is not that large.
- The breach flow is set at 10% of the maximum discharge, in reality this might show large variations.

Above issues can be addressed by using a Monte Carlo simulation and a hydrodynamic model including breach growth and modelling of the polders as was done in De Bruijn et al. (2013).

#### 4.1.2 Negative load interdependencies in the conceptual model

As was shown in the study by Van Mierlo and van Buren (2006b), dike breaches can also have a negative effect on water levels at other locations. These effects are called negative load interdependencies and are usually caused by shortcutting between two rivers or two branches of a river.

Negative load interdependencies are a lot more complex to incorporate in risk analysis, as they interact between different river reaches and are not restricted to just one river. In paragraph 2.6 a set of important factors in this type of cases was already identified. The principle and the way these interactions can be accounted for in risk analysis are again discussed using the basic case from paragraph 4.1, in Figure 4-5 the relevant parts are shown.

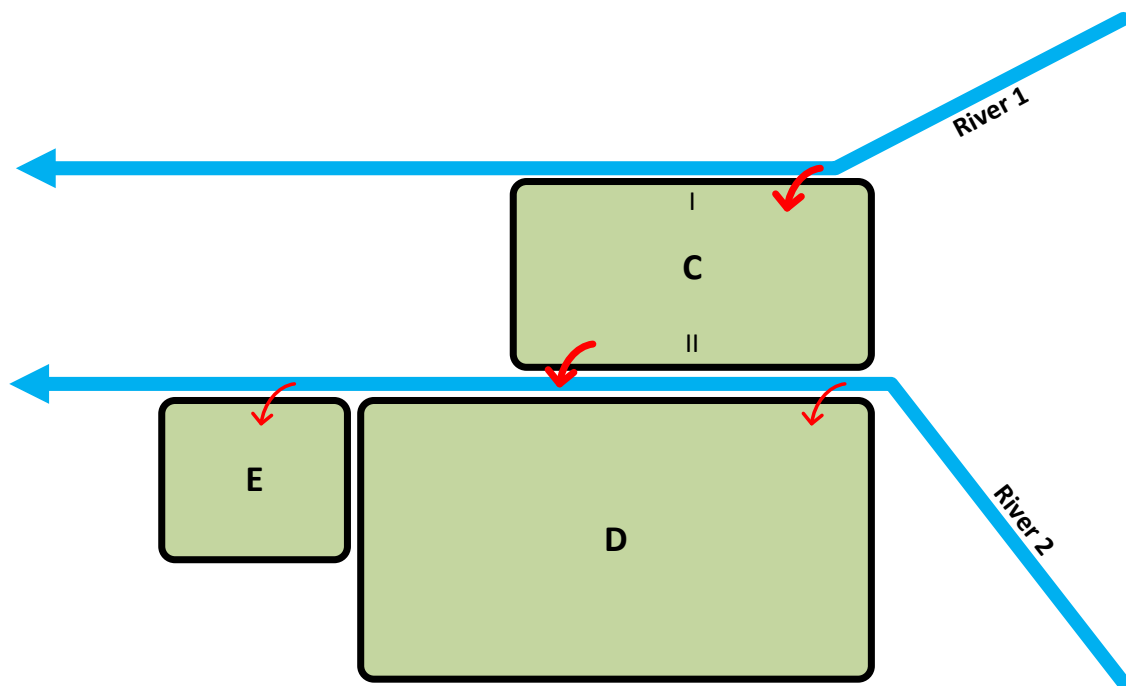


Figure 4-5 Schematization of the mechanism of negative system behaviour

The goal of this chapter is not to fully elaborate what happens, but more to give a conceptual idea of what happens when shortcutting between two rivers occurs. Therefore the case from Figure 4-5 was modelled using the following assumptions:

- When C breaches at River 1, the breach flow is added to the maximum discharge at River 2. This is not exactly how it works in practice, as it takes time for the water to reach River 2, but it gives a good principle idea of the effect shortcutting could have.
- The discharge in River 2 is 2/3<sup>rd</sup> of the discharge of River 1, so they are fully correlated.
- Only shortcutting is considered, so there are no positive interdependencies accounted for at River 2.

The other assumptions are the same as in the base case. When doing a Monte Carlo simulation with  $n=250,000$  this results in the non-exceedence probability plots from Figure 4-6.

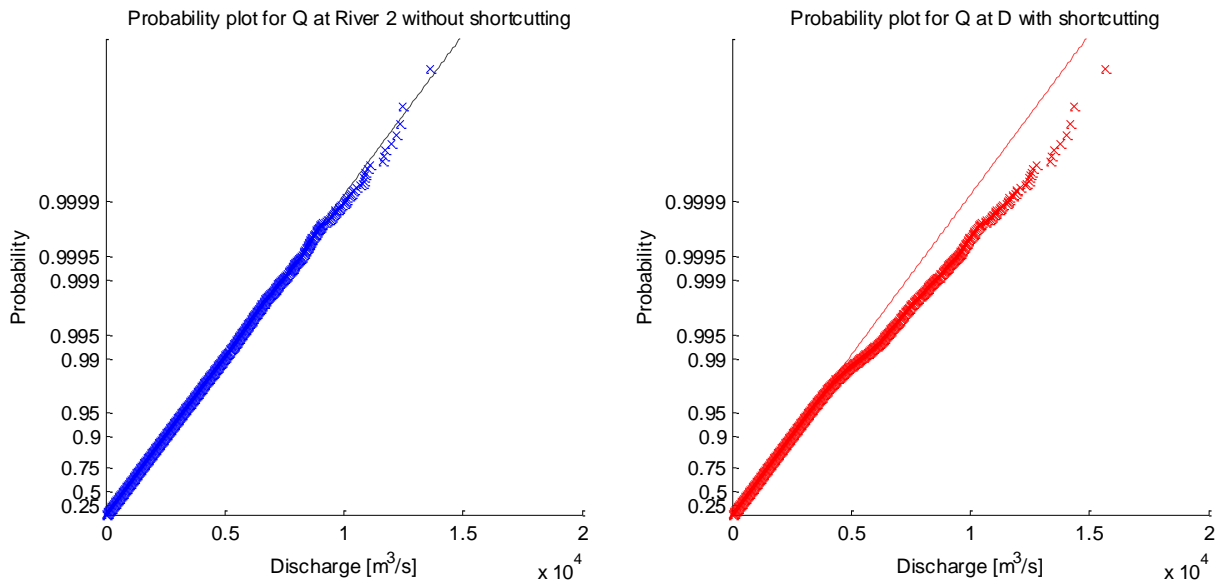


Figure 4-6 Non-exceedence probabilities with and without shortcutting from River 1

What can be seen is the opposite from what was found for positive interdependencies. When shortcutting occurs, the probability of a higher discharge increases. Therefore, due to the higher water levels and discharges at River 1, also the failure probabilities of dikes along River 2 increase due to the increased load. The 1/1000 year discharge increases from 7.600 m<sup>3</sup>/s to 8.800 m<sup>3</sup>/s.

When looking at the scenarios for dike ring C, the (negative) load interdependencies do not change anything, however for dike ring D an extra scenario type occurs. For dike ring C, when assuming full independence of the two sides of the dike ring, the failure probability can be described by:

$$P_{f,C} = P_f(C_{River\ 1}) + P_f(C_{River\ 2}) - P_f(C_{River\ 2} \cap C_{River\ 1})$$

For dike ring D this gives:

$$P_{f,D} = P_f(D|C\ does\ not\ fail) + P_f(D|C\ fails\ from\ River\ 1)$$

Or when generalizing:

$$P_{f,D} = P_f(D|no\ influence\ River\ 1\ at\ River\ 2) + P_f(D|interaction\ of\ River\ 1\ and\ River\ 2)$$

It can thus be seen that the failure probability for D is composed of two components: one caused by a high discharge from River 2 and one conditional failure caused by failure of C and consequential failure of D. When reconsidering the probability plot for cases with shortcutting this leads to the effects shown in Figure 4-7.

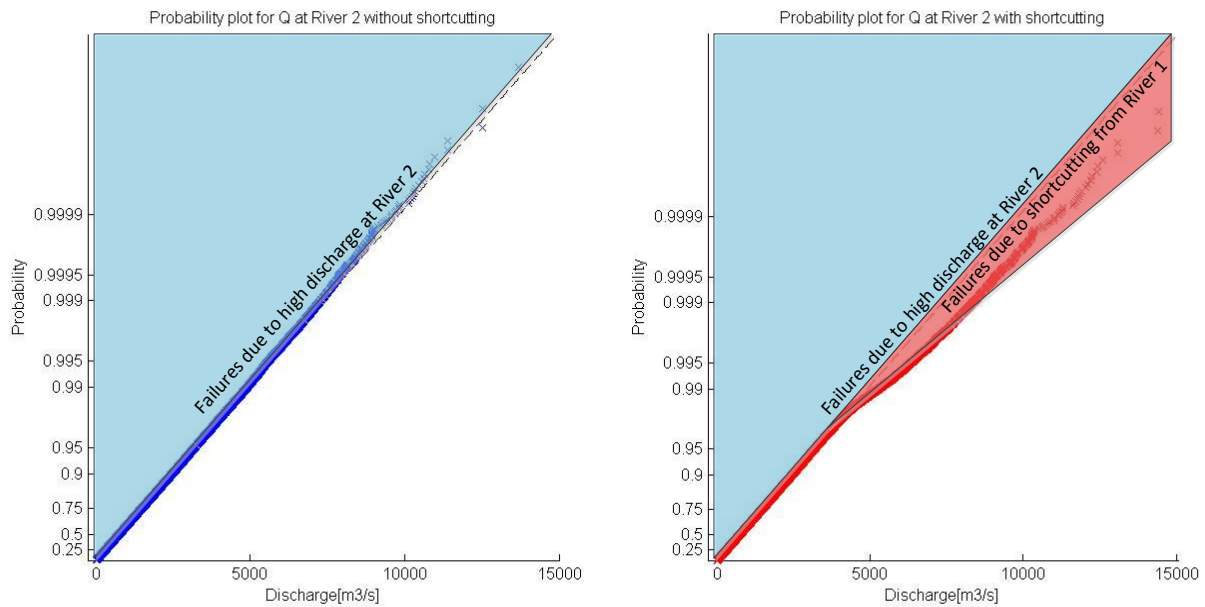


**Figure 4-7 Non-exceedence probability plot for shortcutting with distinction between failures due to shortcutting and 'normal' failures**

It can be clearly observed that a part of the failures is 'new' and not considered in risk analysis neglecting load interdependencies. The first term is in normal situations not the same as the failure probability when not considering load interdependencies, as it is conditional to the non-failure of C. Especially when there is a strong correlation between high discharges in River 1 and River 2 the first term can become relatively small, as in most cases where D fails, also a failure of C occurs. Describing this in terms of failure probabilities and conditional failure probabilities is quite difficult, as there are many dependencies and factors of influence. This can be dealt with by using a (fast) hydrodynamic model and a Monte Carlo simulation.

A convenient way to describe the different scenario's possible, is by using an event tree to describe all possible scenarios. For this event tree only areas C and D are considered, as addition of E or other areas along River 2 would make it a very unclear figure. The event tree is shown in Figure 4-8. In the event tree the situation discussed using the conceptual model is marked in grey.

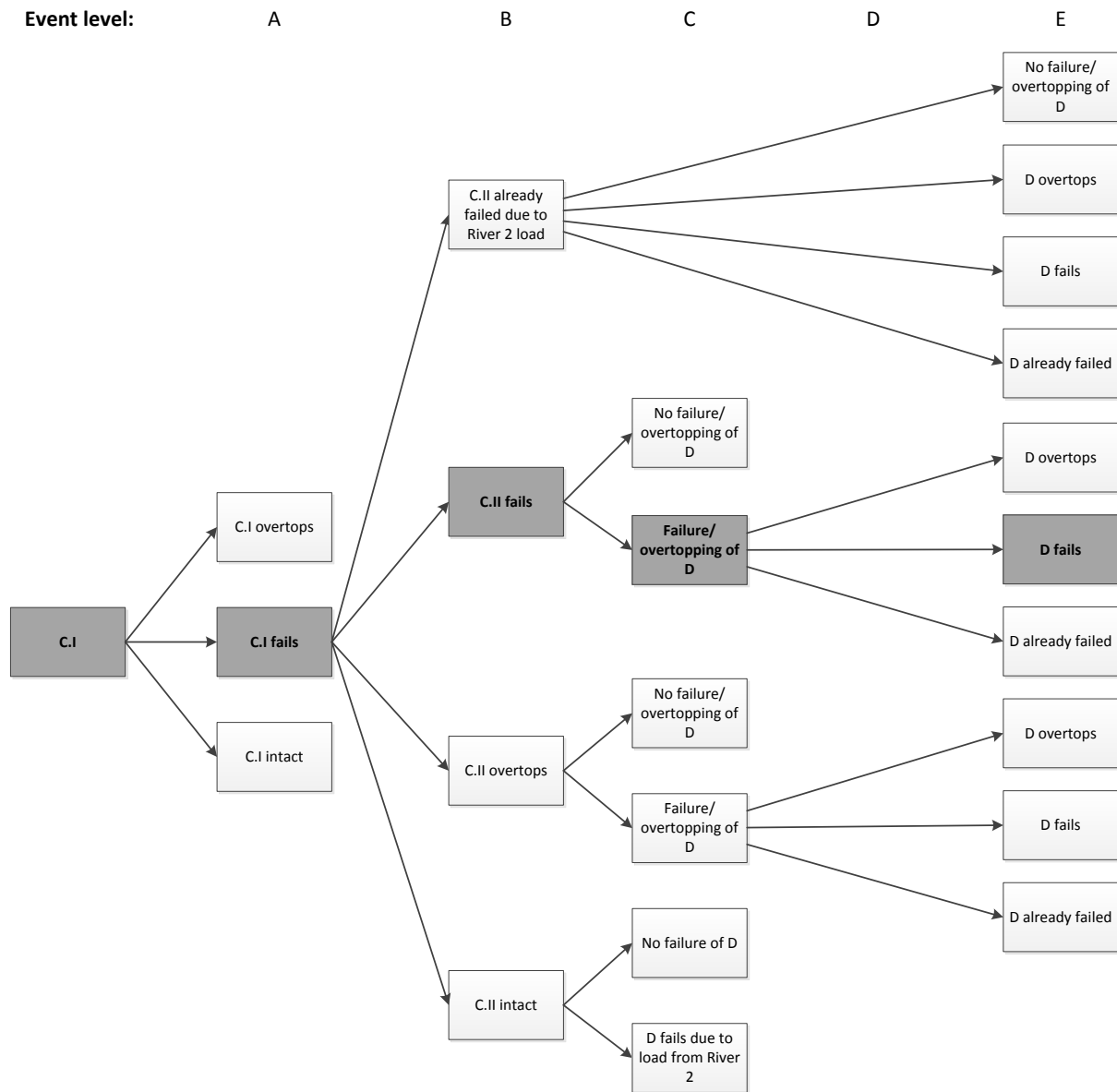


Figure 4-8 Event tree for failures at C and D

In the event tree it can be seen that there are already many possibilities when only considering 2 dike areas. When considering even more dike rings, the number of possible scenario's will become enormous. Therefore, when developing a new framework, it is important to have a calculation method which can automatically handle many different scenario's.

## 4.2 New methodology for incorporating load interdependencies in flood risk analysis

In this chapter a new method for incorporating load interdependencies in risk analysis will be introduced. First a general outline is presented, then the methodology for adding positive load interdependencies is discussed, and at last a methodology capable of dealing with all load interdependencies is presented. The new method will be further tested and applied on the case in Chapter 5.

### 4.2.1 Possible outline of risk analysis

For cases where load interdependencies are of importance, a system approach to flood risk is most logical, as many different scenarios with different breach locations are considered. Based upon the different risk analyses discussed in paragraph 3.2, one could define an outline for flood risk analysis which is shown in Figure 4-9.

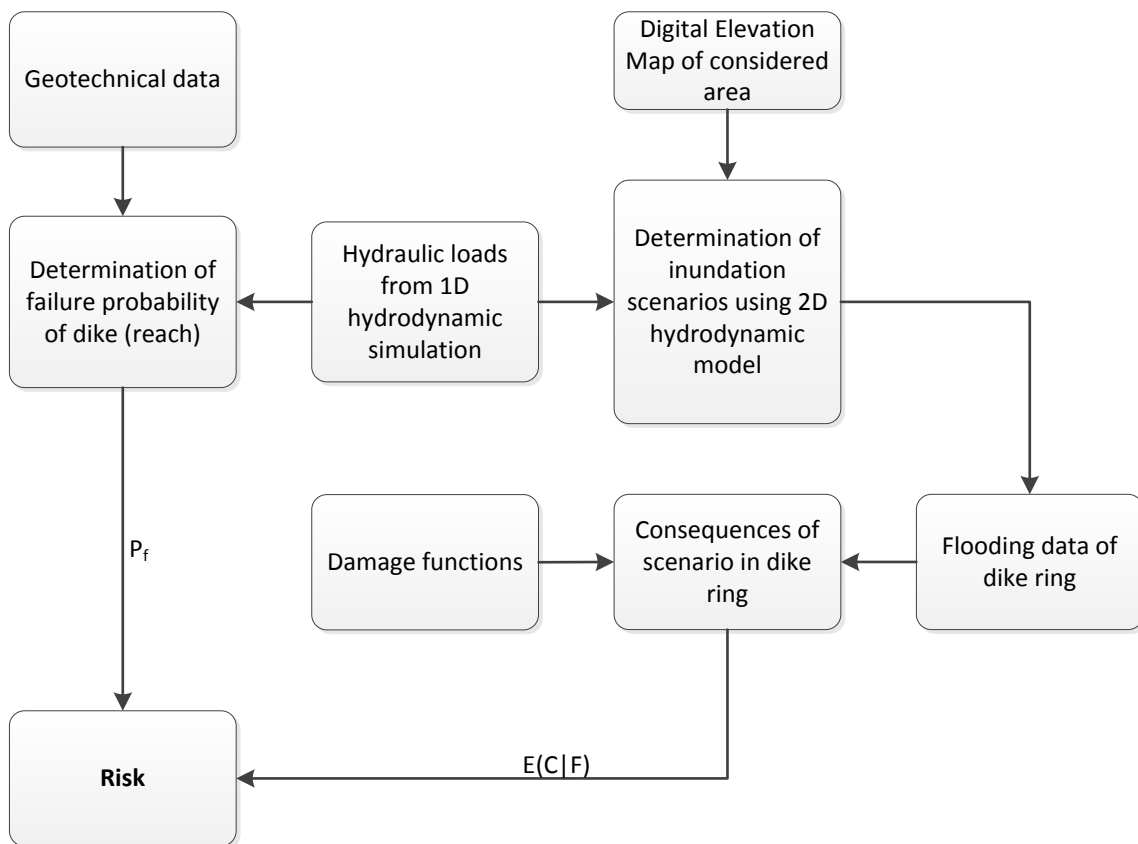


Figure 4-9 General outline of risk analysis

In this methodology, which is very comparable to the VNK2-method, the failure probability is determined based upon the hydrodynamic loads from a 1D simulation, the effect of breaches at other dike rings is not taken into account and, as the failure probability is calculated separately from the hydraulic conditions in the hydrodynamic model, it is also not possible to do so using the above method.

### 4.2.2 Computations with positive load interdependencies

In the context of the above suggested methodology, accounting for positive load interdependencies does not need many changes. When considering the factors of importance identified in the preceding paragraphs, the main and in fact only adaptation is that, while in the

original analysis the water levels and return periods used are based upon situations where no dike breaches occur, they are now dependent on the situation upstream of the considered location. These water levels can be derived from a 1D hydrodynamic model where dike breaches are considered, using a methodology similar to the one used by Apel et al. (2009a) or for the societal risk tool (De Bruijn et al., 2013). Therefore the only change needed is found in the calculation of the hydraulic loads, as can be observed in Figure 4-10 where it is marked gray.

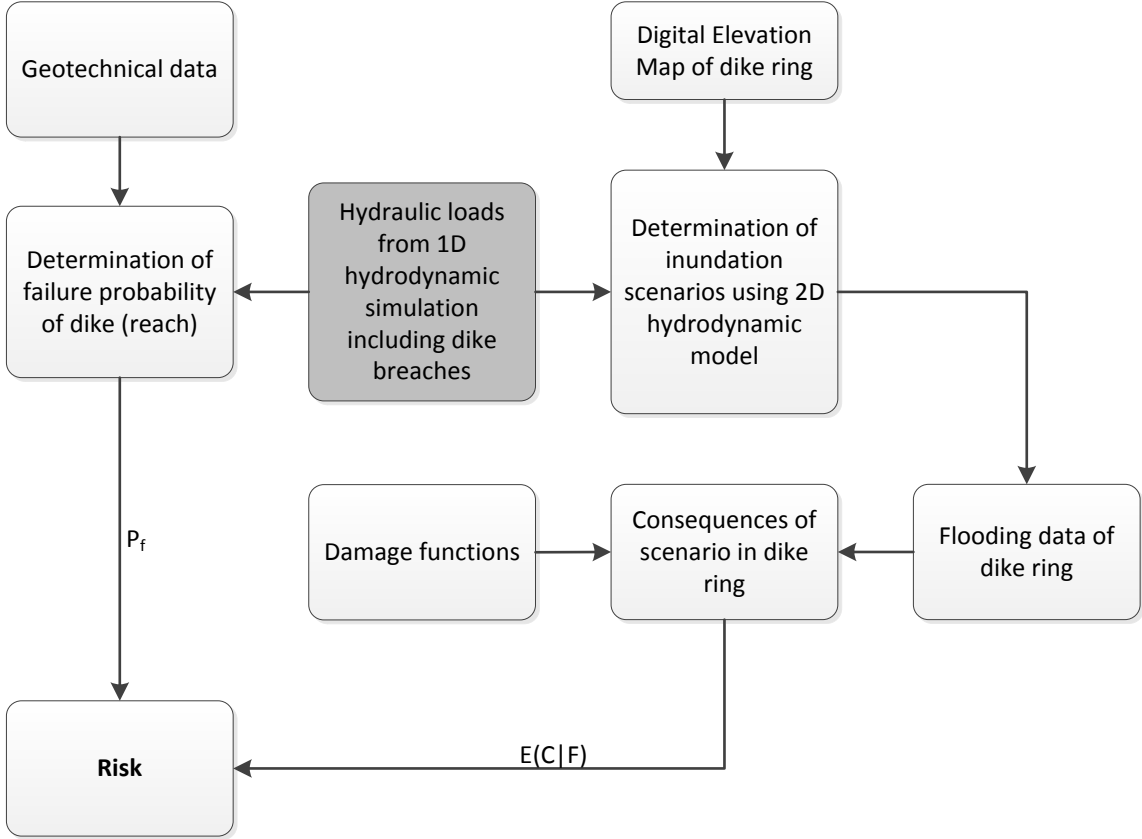


Figure 4-10 General outline of risk analysis including positive load interdependencies

Thus, if for instance there is a situation where there are no negative load interdependencies, it is possible to use this methodology, which is very similar to for instance the VNK2-method. However, when negative load interdependencies are to be accounted for, a different methodology is necessary as the effects of negative interdependencies are a lot more complicated, and cannot be accounted for by just changing the boundary conditions.

**4.2.3 Negative load interdependencies: modelling the interaction between land and river**

Thus, for incorporating negative load interdependencies a new approach is needed. In Chapter 2.6 several complicating factors when considering the effects of negative load interdependencies were discussed, such as timing of discharge waves, shortcutting time and failure of dikes when loaded from the inner slope. To account for these factors more computational additions are necessary than just adapting the water level return frequencies.

An important part of this is that the interaction between the flooding land and the river has to be modelled, which means that a correct representation of the inundation pattern is required. However, given the probabilistic context and the amount of variables, it is also important that

the model has a relatively low computation time. There are several options available, four of them are discussed here:

- Using 1D2D-hydrodynamic modelling as suggested by Vrouwenvelder et al. (2010)
- Using a 1D model coupled with a 2D storage cell inundation model. This is more or less the approach used by Vorogushyn et al. (2010)
- Using a 0D schematization coupled with parameterized 2D inundation scenarios
- Using a 3Di inundation model coupled with a 1D model

The first option is an integrated 1D2D approach, which was also used in the Delft Cluster study. This is quite accurate, but also computationally very demanding, especially in combination with a Monte Carlo analysis.

The second option was used in the Elbe study by Vorogushyn et al. (2010), and is a trade-off between accuracy and computation time. Storage cell models are usually quite fast for larger areas and are thus a good option for this type of problems.

The third option is to use a 0D schematization and couple this with parameterized 2D inundation data from existing sources or new scenarios. This enables a relatively accurate simulation since 2D models are used but also a decrease in computation time as the inundation simulations have to be run only once. A parameterization could be used in the line of calculating 2D scenarios for 1/100, 1/1.000 and 1/10.000 year conditions, with breaches at different moments in time. Then the most probable scenarios are also calculated in 2D, which makes it possible to calibrate the 0D model and calculate damages more accurately. A possible problem could be the tuning of the 0D schematization, but Asselman (2009) showed that for a simple flat polder this can still give quite accurate results. For the more sloping parts 1D branches can provide a solution. Another disadvantage is that deterministic inundation scenarios are used in a probabilistic setting, this has to be handled with care.

The fourth option is to use a 3Di inundation model combined with a 1D hydrodynamic model of the river. 3Di seems very useful for quick simulations of inundations as the raster size can be varied, making it possible to save calculation time on large flat areas and still have a reasonable resolution at areas with a more varied topography. However 3Di is still in development and especially the combination with 1D is still in its early stages. Also it is not exactly known how fast 3Di is going to be.

In Table 4-3 an overview is given of the different methods and their advantages and disadvantages at computation time, accuracy, background data and model availability and the programmability.

Method	Computation time	Accuracy	Availability of models & data	Programmability
<b>1D2D</b>	-- Very demanding due to many 2D simulations	++ Very accurate due to 'exact' modelling of flood	+ 2D models and calibrated 1D models are available	-- Difficult to program especially when efficiency is required
<b>1D with storage cell</b>	<b>0</b> storage cell is faster than 2D for large polders	+ Accurate when inertia doesn't play a big role which is the case	-- No storage cell models available for the required areas	<b>0</b> Unknown
<b>0D with parameterized 2D inundation scenarios</b>	+ Relatively quick since inundation scenarios have to be calculated only once	<b>0</b> Parameterization can give inaccuracies, scenarios have to be chosen carefully	++ 2D model, 1D model and dike data are available	+ Main difficulty is tuning the 0D schematization
<b>1D with 3Di inundation</b>	<b>0/+</b> Depending on accuracy found when using large raster sizes it is quicker than storage cell but not as quick as 0D	<b>0</b> Not known but pilots are promising	- No 3Di models available yet, but might be possible to base this on 2D model	- Development of 1D/3Di modelling is still in early stages, bugs are to be expected

Table 4-3 Different methods and their advantages and disadvantages (ratings at scale between -- and ++)

Based upon the available models for the case study in Chapter 5, the current practice in risk analysis and the trade-off between computation time and accuracy, the choice is made to use a 0D schematization and parameterized 2D inundation simulations. This also fits the suggested methodology for positive load interdependencies.

#### 4.2.4 Methodology for incorporating load interdependencies in flood risk analysis

When incorporating negative load interdependencies, the simple change in boundary conditions is not sufficient anymore. Therefore also the inundations have to be modelled in a probabilistic context. As this is quite time consuming a fast model is necessary, in paragraph 4.2.3 0D modelling was found to be very suitable for this case. In Figure 4-11 an overview of the new methodology is shown, the fast inundation model is a model using 0D and 1D techniques to simulate floods. There are in fact two cores in the computation: the Hydrodynamic modelling core and the 2D hydrodynamic modelling. The 2D model has to be run for a set of scenarios covering the most probable scenarios in terms of return period and time of breaching during the discharge wave. The 2D model is used to set-up and calibrate the fast inundation model and determine the consequences per flood zone. A flood zone is in this case an area which is characterized by having more or less the same water level during a flood. More explanation on this can be found in paragraph 5.5.4, where it is discussed using the case study as example. The consequences per scenario give relations between water levels and damage for all different flood zones defined. This makes it possible to determine the damage using the 2D model and then calculate it using water level data from the fast inundation model.

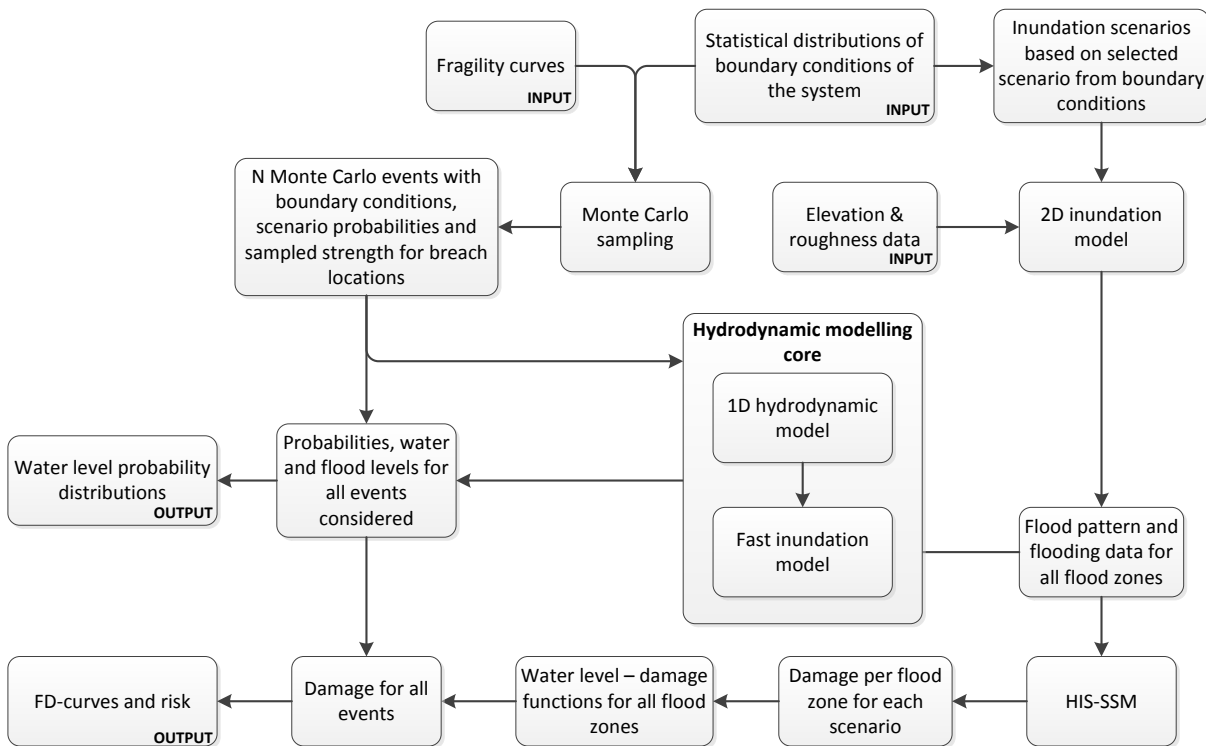


Figure 4-11 Methodology for risk analysis accounting for both positive and negative load interdependencies

The main core of this method is the 1D hydrodynamic model and the fast inundation model. After these are tuned using the data from the 2D model it is run probabilistically using input for dike heights and boundary conditions. These are sampled using Monte Carlo with Importance Sampling, to avoid an excessive number of simulations. The probabilistic calculation using this model, gives breach discharges, breach locations and maximum water levels in the system as output. When this is combined with the water level – damage relationships from the 2D model, this enables a fast calculation of the total damage in the system as well as probabilistic distributions for water levels in the system.



## 5.2 Shortcutting at the Bovenrijn/IJssel area

Van Mierlo (2005a) showed that in the Bovenrijn/IJssel area the water level in the IJssel can increase due to dike breaches at the Bovenrijn at for instance Rees (in Germany) or Lobith. This is caused by the fact that at Pannerden and the IJsselkop the discharge distribution is (assumed) to be the same as usual but at the IJssel the discharge is increased by additional water flowing over land and back into the river. An essential factor in this, is the fact that the river valley is sloping downwards, thus enabling a relatively large flow over land towards the more downstream areas. This flow is enlarged due to the presence of the Oude IJssel. This river has a controlled water level and can be shut off from the IJssel, but the land is more or less shaped like a downsloping river bed. When dike ring 48 is flooded this increases the amount of water flowing towards the IJssel and the downstream dike ring areas. A schematization of the process for this case is shown in Figure 5-2, for a random river discharge  $Q$ . It has to be noted that in this case the time factor is ignored, it does not necessarily mean that the maximum discharge at the IJssel is increased by  $8/9 \Delta Q$ , only that the breach influences the discharge distribution at the river branches, which might cause an increase in discharge and thus higher water levels at the IJssel. This principle was also shown in paragraph 4.1.2 using the conceptual model.

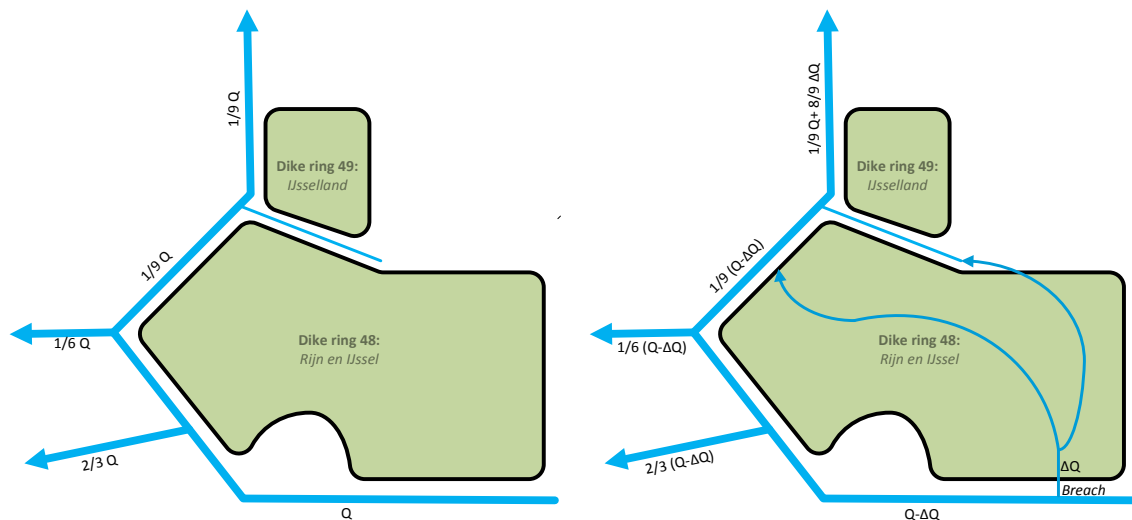


**Figure 5-2 Effect of dike breaches at dike ring 48 on the discharges in the different river branches. Left: normal situation. Right: situation with a breach at the Bovenrijn. Please note that the time influence is ignored!**

When the discharge at the IJssel increases, the water levels will also rise. This does not solely have consequences for dike rings 48 and 49, also the dike rings further downstream (50, 51, 52 and 53) will be influenced. However, aside from the increased flooding probability due to the higher water levels, the flooding of these dike rings is not that different for cases with shortcutting when compared to normal cases.

However, it is not always the case that shortcutting occurs. The IJssel has as a characteristic that, due to the typology of the river and its dikes the dike rings behave like a cascade. This means that if the downstream dike ring, in this case 49 (or 48 or a German dike) fails, as a consequence also 50, 51 and 53 flood due to the relatively low and weak separating flood defences between the dike rings and the sloping nature of the river valley.



Figure 5-3 Separating canal and dikes between dike ring 49 and 50

The separation between the dike rings is usually a river or canal with relatively low dikes. The separation between 48 and 49 is the Oude IJssel, and between 49 and 50 the dike ring areas are separated by the dikes and drainage canal shown in Figure 5-3. As the river valley slopes down, the water will easily flow over the separating dike into the next polder causing the cascade effect. Figure 5-4 shows a cross section of the dike rings along the IJssel; from this figure the sloping nature of the dike rings is well visible.

Another important aspect at the IJssel area is that the whole area can flood due to dike breaches in Germany. This makes the problem even more complex as also a part of Germany has to be considered.

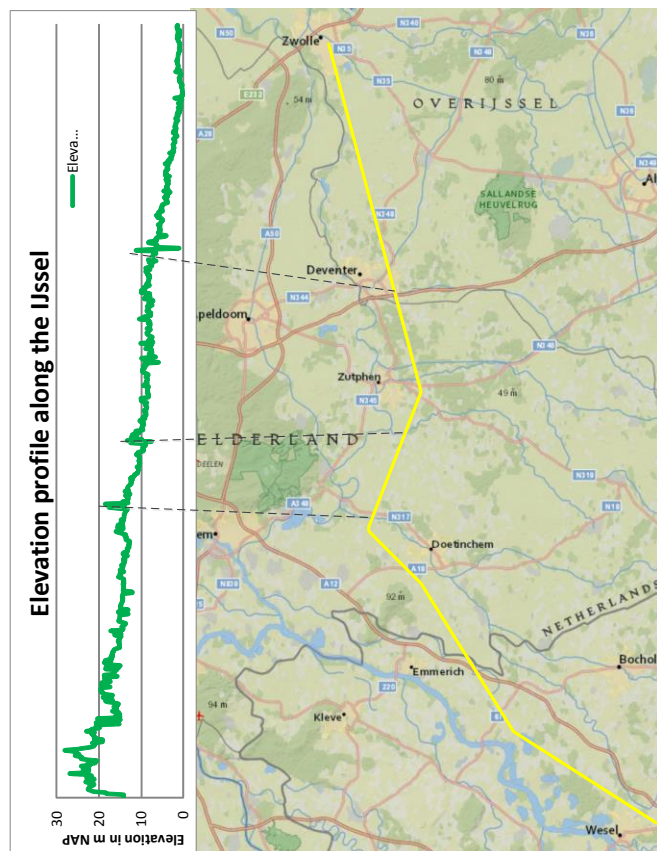


Figure 5-4 Elevations at the polders on the right bank of the IJssel

### 5.3 Qualitative analysis of floods in the case study area

In order to have a good idea of how floods propagate in the studied area, a few cases were investigated in the 2D model. In Figure 5-5 the flood depths for Spijk are shown for 5 points in time after the breach. In the pattern the behaviour of the dike rings as a cascade can be clearly observed, the flood propagates downstream over land and overflows the category-c flood defences separating the dike rings. What can also be observed is that there is very little flooding upstream of Spijk, this emphasizes the characteristic of the area as being a sloping river valley. The breach flow is very high in this case: 4.000 m<sup>3</sup>/s.

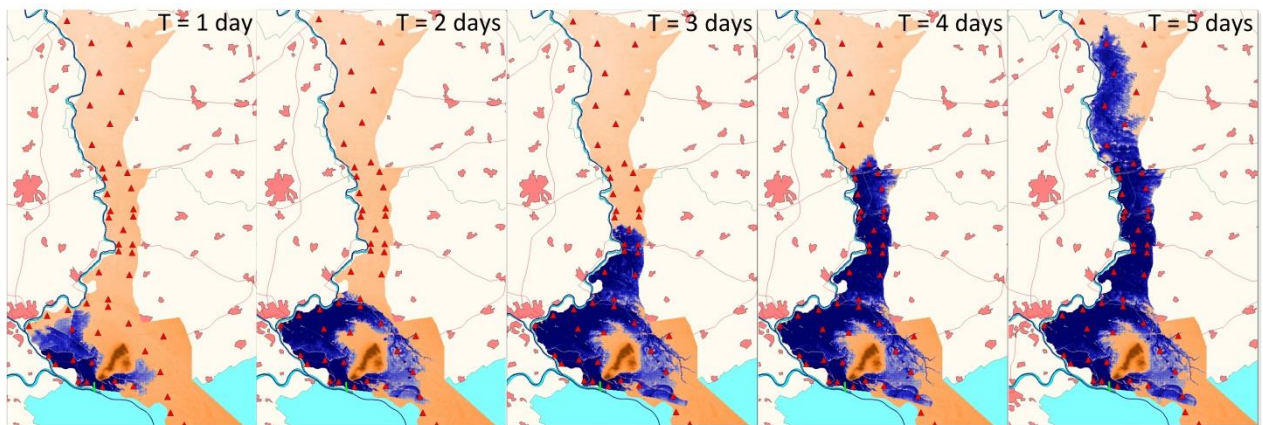


Figure 5-5 Flood depths for a breach at Spijk for a 1/10.000 year discharge from the 2D model

## 5.4 Set up of the models for inundation modelling

### 5.4.1 Available and used models

To be able to properly model the consequences of dike breaches in the area it is necessary to use suitable models for the case study area. In this case two 1D models for the rivers were available, a 1D hydrodynamic model in Sobek 2.12 and the 1D hydrodynamic Sobek-RE model used in the societal risk tool. As only Sobek 2.12/2.13 is compatible with 1D2D modelling this model is used for the rivers. The model had one important part missing, namely the Niederrhein part between Wesel and Lobith in Germany. This part was obtained from the Bundesanstalt für Gewässerkunde and added to the model. As 2D model a Delft FLS model provided by the Provincie Gelderland was used, this model contained elevation data for the entire province of Gelderland. However, since part of the dike rings along the IJssel are located in Overijssel and part of the area of interest along the Bovenrijn is located in Germany near Wesel, other models were also needed. These were obtained using AHN data, land use maps and a Nikuradse roughness – land use table obtained from van Mierlo et al. (2003). A more detailed description on how the models were put together can be found in Appendix D.

### 5.4.2 Boundary conditions

The boundary conditions in the modelled area are:

- Discharge at Wesel ( $Q_{\text{Wesel}}$ )
- Q-h relation at the IJssel at Kampen
- Q-h relation at the Lek at Ameide
- Q-h relation at the Waal at Gorinchem

The Q-h relations are obtained from the Delft-FLS model provided by the Provincie Gelderland, this model was also used for the VNK2-analysis in this area. It has to be noted that especially the Q-h relation at the IJssel is a bit uncertain, as it largely depends on the water level of the IJsselmeer and the h could also increase in time compared to Q. This is not taken into account, to avoid too much complexity, but the results seem to be in line with the design levels at the IJssel. The Q-h relations at the Lek and Waal are in the transitional area but the effect of sea water levels at these locations is negligible. Also, they are quite far downstream from the relevant areas along the IJssel, so their influence on the results will be of minor importance.

The discharge at Wesel is assumed to have the same statistical distribution as the discharge at Lobith. As there are no major tributaries between Wesel and Lobith this is a realistic assumption, however, due to peak attenuation the discharges at Lobith are now slightly lower. However, the difference is small, especially when considered relative to the total discharge of for instance 18,000 m<sup>3</sup>/s. Therefore the boundary condition is moved, but not adapted. In the next paragraph the results of the model will be compared with the design water levels, here it can also be observed that the differences with reality are only minor and are caused by the model inaccuracy and not the change in boundary location.

### 5.4.3 Comparison of hydraulic results of the model with the design water levels

When considering only the 1D-model it is important to have a good overview of the inaccuracies. Therefore the model was run with a standard discharge wave from Ministerie van Verkeer en Waterstaat (2007) with a maximum discharge of 16,000 m<sup>3</sup>/s. When considering the difference in water levels at different locations it can be seen that the difference is usually between 0 and

30 centimetres, which is accurate enough for this research. An overview of the differences is given in the map in Figure 5-6, from which it can be observed that only for a small part of the IJssel the water levels show some deviation.

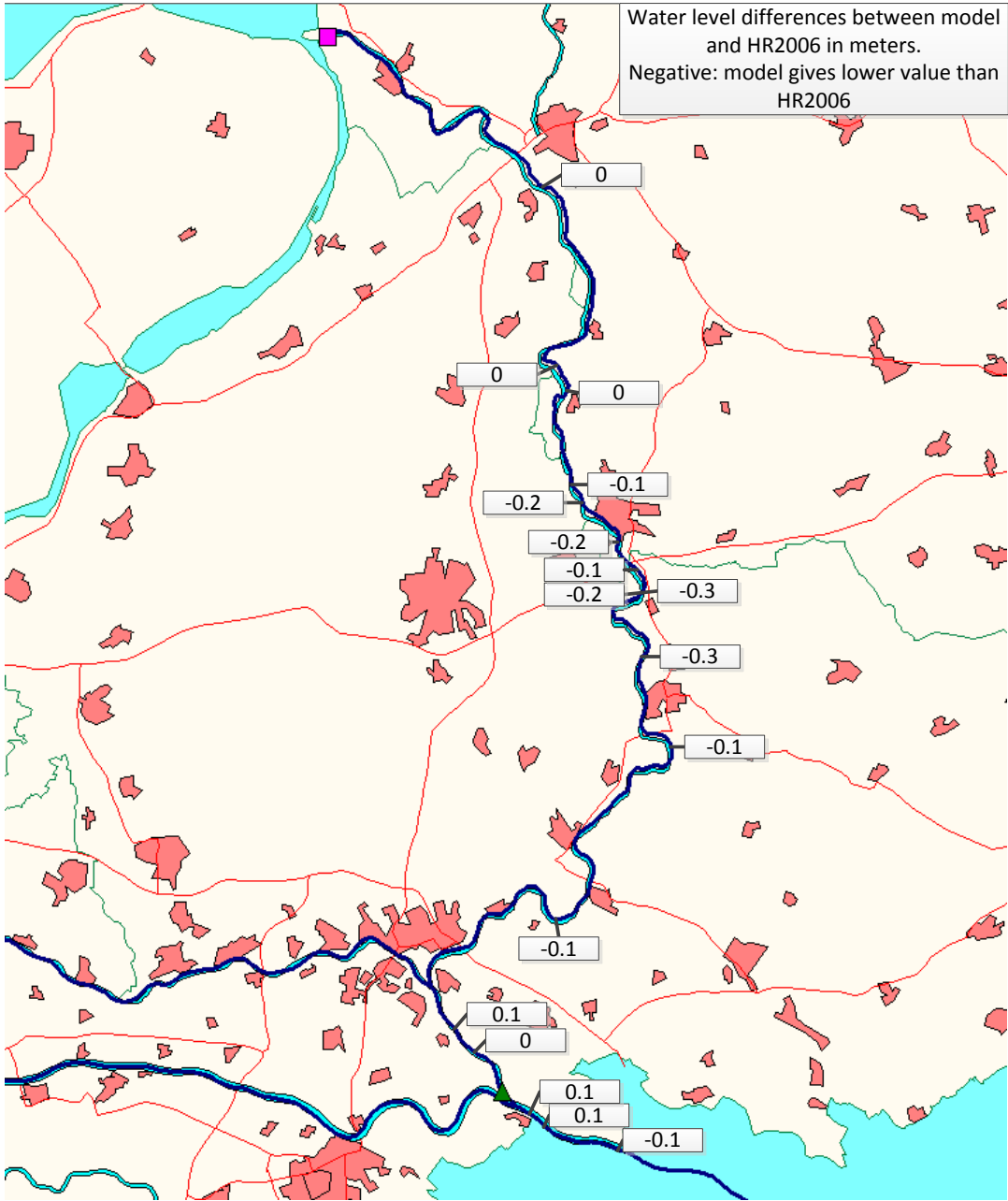


Figure 5-6 Water level differences between model and HR2006 for design discharge wave

## 5.5 Applying the method to the case study area

### 5.5.1 General outline

The next step is to apply the methodology from the previous chapter to the case study area. In this paragraph the outline of the used method will be discussed and applied to the case. The methodology is again shown in Figure 5-7. In the figure three 'phases' of the model are identified: pre-processing, hydrodynamic calculations and post-processing. This is also the way the method is further discussed in the following paragraphs.

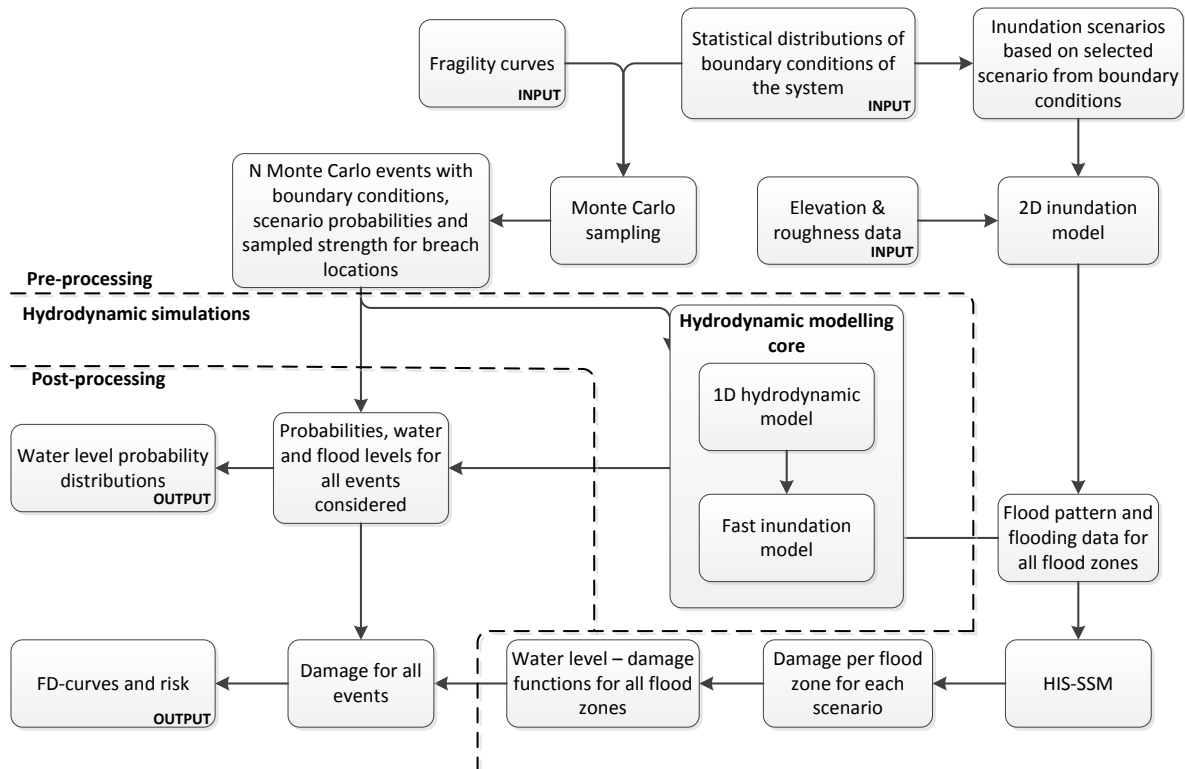


Figure 5-7 Methodology as applied in the case study

### Breach locations

The breach locations used are the same as in WV21 and for the societal risk tool. These are shown in Figure 5-8. Additionally, because for this situation breaches in Germany can flood dike ring 48, a set of breaches at the German part of the river is selected, these are also shown in the figure.

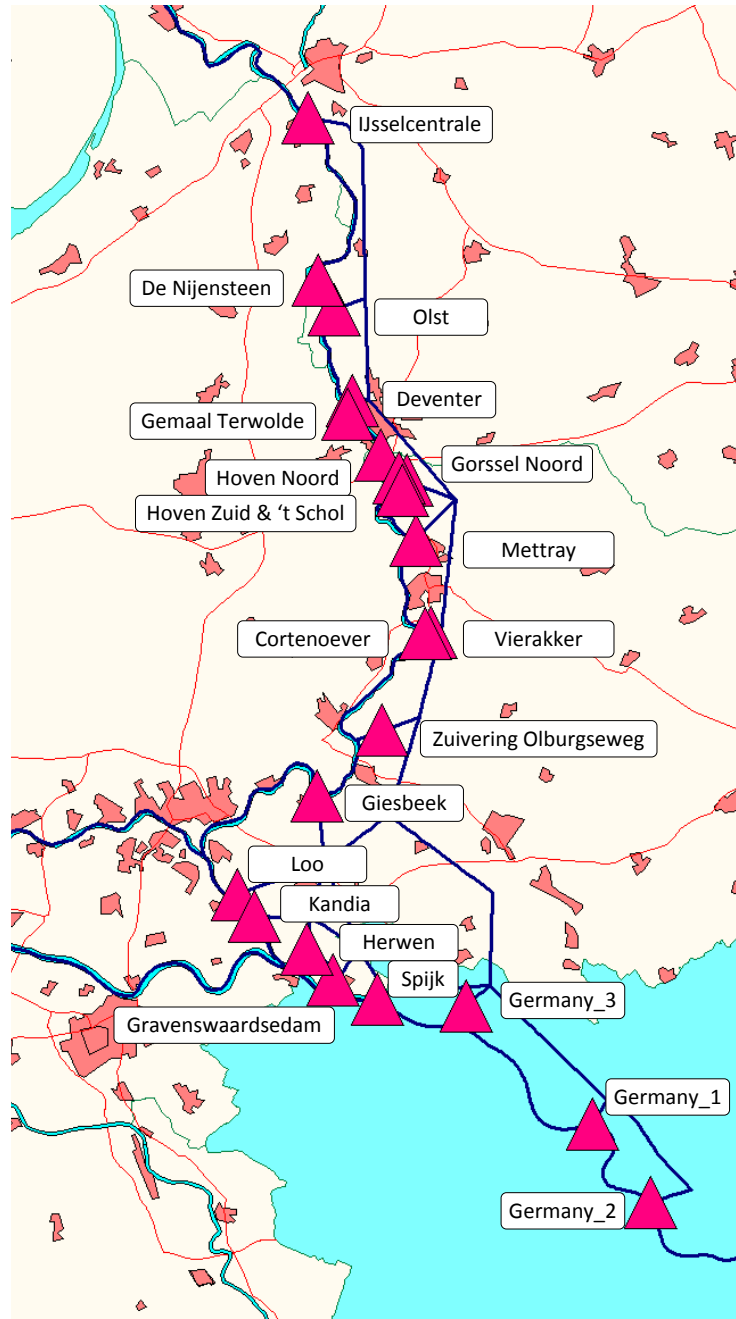


Figure 5-8 Breach locations as used in the case study, all breach locations are at the right bank of the river except De Nijenstein, Terwolde, Hoven, 't Schol and Cortenoever

Regarding the breach locations it has to be noted that the influence of the choice of breach locations on results for damage can be quite significant, especially when length effects for for instance piping failures are not taken into account properly. For the case of 'Land van Maas en Waal' Vrouwenvelder et al. (2010) found that for cases with different numbers of scenarios results for damage and casualties showed variations of up to 200%. This emphasizes the

importance of the number of breaches and a correct representation of the spatial effects of failure mechanisms such as the length effect in piping, especially when considering the actual strength of the dikes, which was done in the study on the ‘Land van Maas en Waal’. However, for this case the design level of the dike was set to have an exceedence frequency of 1/1.250 per year, in those cases the length effects are of less importance as it is assumed that a dike reach fails once in 1.250 years. For this case the different breaches are based on the ones from the societal risk tool, so the same fragility curves for the dike reaches can be used. As exceedence probabilities and not probabilities of flooding were used, the length effect is of less importance, although, in reality, even if a dike would be up to the 1/1.250 year standard, the standard deviation would be higher, especially for longer dike reaches.

The effect of the choice of the breach locations is not just important for the failure probabilities, but also for the consequences of the different scenarios: the bottom levels of the land behind the breach and the presence of secondary flood defences can have a large influence on the breach discharge. For instance, for a 1/10.000 year discharge and a failure at the top of the wave the breach at Germany\_1 gives a discharge of approximately 1.500 m<sup>3</sup>/s, while the breach at Germany\_2 gives a discharge of 2.800 m<sup>3</sup>/s, even though the breaches are similar and at the same river branch.

**5.5.2 Pre-processing**

*Boundary conditions*

The first step in pre-processing is defining the hydraulic boundary conditions. The model has 4 boundaries which were already discussed before. Three of the boundary conditions are Q-h relationships for the downstream boundaries, the fourth boundary is the river discharge at Wesel, Germany. For the river discharge probability distribution the statistical distribution for Lobith is used. This gives a slightly lower discharge in the system due to peak attenuation, however the difference is small, in the order of 200 m<sup>3</sup>/s for the most extreme situations with discharges over 20.000 m<sup>3</sup>/s. The probability distribution used is the same as was used in the societal risk tool project at Deltares (De Bruijn et al., 2013). The statistics of the Rhine discharge at Lobith are described by the values in Table 5-1.

Return Period (year)	a	b
<b>0&lt;RP&lt;2</b>	1621,156	5893,3
<b>2&lt;RP&lt;25</b>	1517,582	5965,092
<b>RP&gt;25</b>	1316,454	6612,497

**Table 5-1 Statistical description of discharge at Lobith (De Bruijn et al., 2013)**

The a and b values can then be used in the following formula which describes the exceedence probability for an annual maximum q higher than Q:

$$P(q > Q) = e^{-e^{-\frac{q-b}{a}}}$$

For each Monte Carlo run in the model a discharge is sampled from this distribution. These are then transformed into discharge waves, by using standard shaped discharge waves and a lower limit of 6.000 m<sup>3</sup>/s. The lower limit prevents stability problems caused by river branches running dry in Sobek. The discharge waves used for the 1/100, 1/1.000 and 1/10.000 year discharges used in the 2D model are shown in Figure 5-9. For the fast inundation model the

discharge waves are scaled. The discharge waves are then constructed by multiplying the normalized discharge wave with the peak discharge. A minimum discharge of 6.000 m<sup>3</sup>/s is used, in case the normalized discharge wave gives a lower discharge. The tables used for the discharge waves can be found in Appendix E.

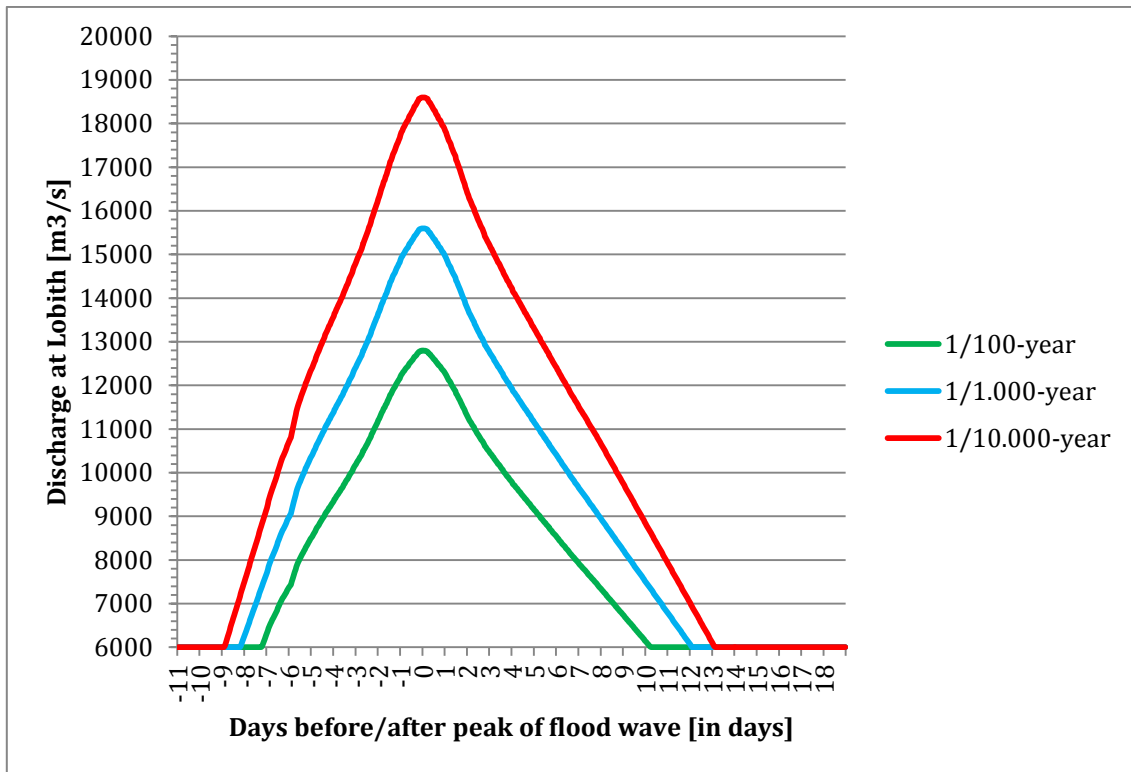


Figure 5-9 Discharge waves for the 2D simulations, the same discharge shape is used for the fast inundation model

### Fragility curves

The second input parameter for the hydrodynamic model is the dike strength for all 22 breach locations in the model. The fragility curves are also the same as used in the societal risk tool project, and these are derived using the Dike Analysis Module (DAM) for the WV21 dataset (De Bruijn et al., 2013). For the breach locations in Germany the fragility curves for Spijk are used.

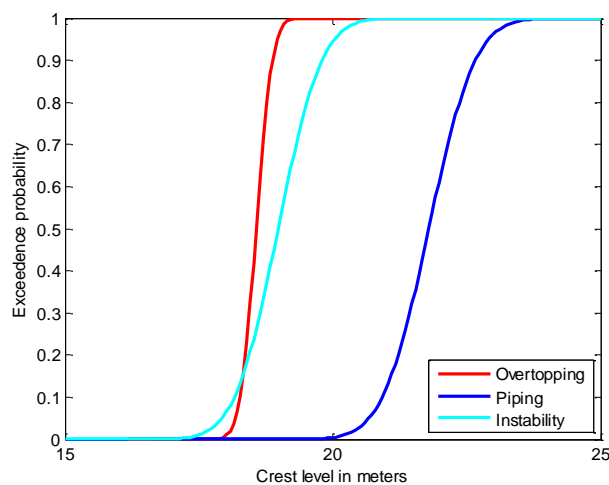


Figure 5-10 Fragility curves for three failure mechanisms for Spijk

This results in fragility curves for three failure mechanisms: overtopping, piping and macrostability. It has to be noticed that the DAM curves for piping are based on 500 meter sections of dikes, length effects are thus not considered. If one wants to account for these effects, the fragility curves thus will have to be adapted, in order to account for the additional uncertainty for longer dike reaches. However, as in this case only design levels are considered this is not taken into account, it is assumed that all dikes considered are up to standard. Given this assumption, all the fragility curves have to be combined and shifted towards the desired level. However as in this case the dikes can also fail from the polder side, this brings along some complications. As was shown in paragraph 2.6.2 the dike can be considerably weaker for loading from the inner slope, especially for macrostability failures. On the other hand, piping failures will most likely not play a role and these are thus neglected. The fragility curves for failure from the polder side have to be adapted compared to the fragility curves for 'normal' failures, as the mean of the distribution will be different. Compared to the original fragility curves the curves for overtopping are identical, the curves for piping are not considered and the mean for the macrostability curves is lowered by 1 meter. The value of 1 meter is picked quite arbitrarily, it is recommended to further investigate this behaviour of dikes.

The next step is to shift the fragility curves to the design level, however as the dike has a different strength for polder side failures, it cannot be simply shifted to the design level for those curves; another approach is needed. An outline of how this is dealt with is shown in Figure 5-11, the used Matlab script and resulting fragility curves can be found in Appendix F. The differences between polder and river side strength are generally found to be within the order of decimetres, however it could well be that with further research, it will appear that the macrostability curves will have to be shifted to an even lower level.

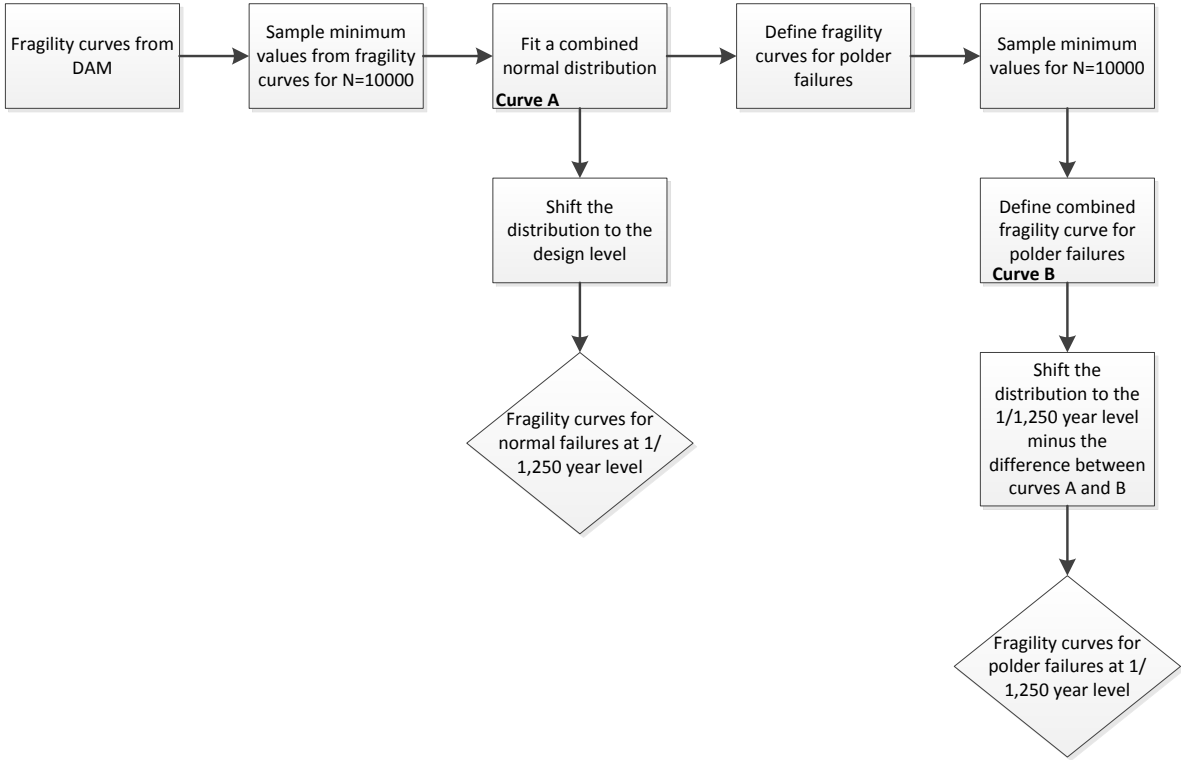


Figure 5-11 Method for shifting the fragility curves

### Monte Carlo with importance sampling

The next step in generating the right input for the hydrodynamic model, is generating enough samples for a converging Monte Carlo simulation. As the failure probabilities are quite small, it is necessary to have a considerable amount of runs for the simulation to give stable results. Therefore is advisable to use Importance Sampling techniques, in order to reduce the required number of samples. The importance sampling techniques available were already discussed in paragraph 3.4.2. Considering the fact that uniform sampling including the extreme discharges in the tail of the distribution showed the best results for the societal risk tool (De Bruijn et al., 2013) and that the dataset in that case was the same, this sampling technique is also applied here.

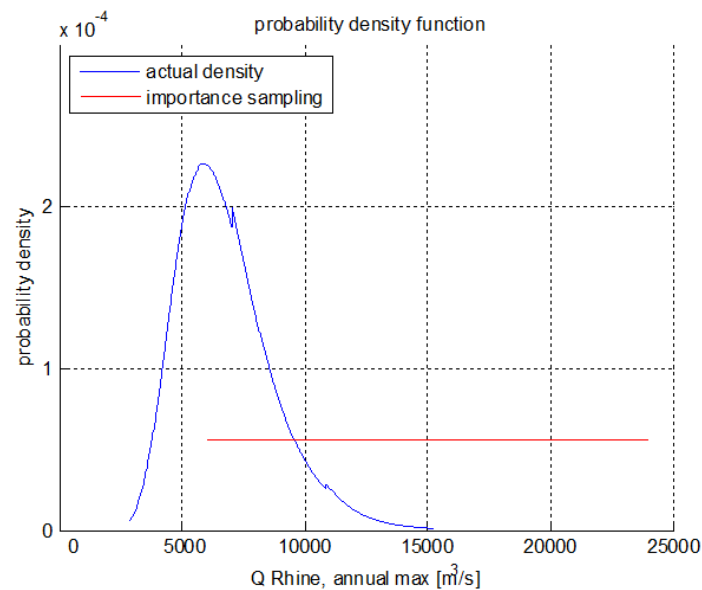


Figure 5-12 Uniform importance sampling for Rhine discharges

When applying Importance sampling it is necessary to handle the event probabilities with care: as these are changed in the sampling process these have to be transformed back to their original values.

The sampled discharges for the Rhine, combined with the values sampled from the fragility curves for the dike strengths at all breach locations, are used as input for the hydrodynamic model. The input sheet is shown in Appendix G.

### Flood scenarios

In order to be able to calibrate the fast inundation model a set of 2D scenarios has to be run. This is done using a 2D model with the elevation and friction data discussed in paragraph 5.4.1 as well as the Sobek 1D model for the river system, which is also the basis for the fast inundation model. In order to cover the whole array of important scenarios for the total risk, the scenarios have to be chosen wisely. As the most interesting breaches are located at dike ring 48 and in Germany these locations have to be simulated in order to get a good view of the flood patterns in the area. As not only the water level, but also the time of the breach during the discharge wave is of importance for the flood extent, the simulations are done for 9 different scenarios which are presented in Table 5-2. The scenarios are defined by using 3 different discharges for different return periods, as well as different times of breaching during the wave. For instance the 10.000

year -4 day scenario is a scenario with a 1/10.000 year flood wave and a breach 4 days before the peak of the flood wave.

Scenario	Return period [in years]	$\Delta T_{\text{relative to peak}}$ (in days)
1	100	0
2	1.000	0
3	1.000	-1
4	1.000	-2
5	10.000	0
6	10.000	-1
7	10.000	-2
8	10.000	-3
9	10.000	-4

Table 5-2 Inundation scenarios with their return period and time of breaching

As the breaches at dike ring 49 and further downstream are of less importance for studying the behaviour of the system, these were not simulated in order to save time.

In the scenarios considered the breach is set to fail at a certain point in time. After this the breach grows to a width of 200 meters according to the van der Knaap formula for breach growth (see also paragraph 3.7.1) as shown in Figure 5-13.

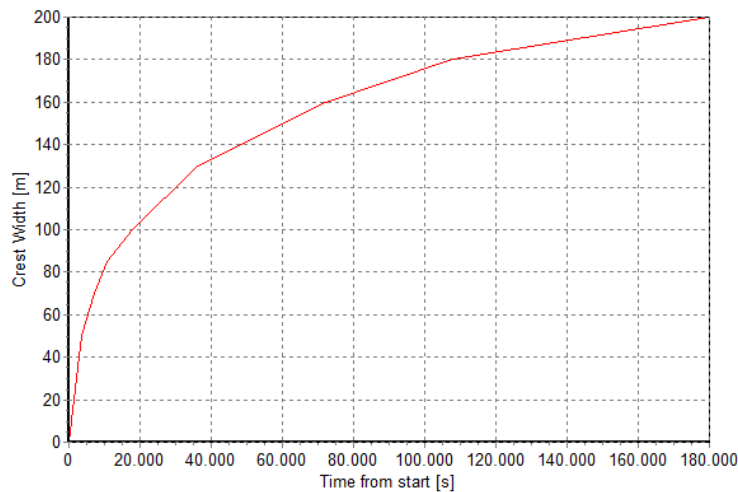


Figure 5-13 Standard breach growth as used in both models

In both the 2D simulations and the fast inundation model, the breaches are always assumed to grow according to the above shown time – width relation.

With the above scenarios it is possible to calculate flood patterns for all scenarios defined. These can then be used for calibrating the fast inundation model and deriving water level – damage relations for the flood zones in the case study area.

### 5.5.3 Hydrodynamic modelling

#### Setup of 0D/fast inundation model

Next to the 1D model used for modelling the rivers, a fast inundation model is to be constructed in order to calculate the different flood scenarios fast enough to enable a Monte Carlo simulation. This will go at the expense of some of the accuracy, which can be obtained with 2D modelling but is not achievable with 1D or 0D modelling.

To correctly schematize the fast inundation model, the first step is to analyse the flood patterns and roughly define the main routes flood water follows during a flood. This is a relatively easy step as it is quite easy to observe this from the 2D inundation depths over time as is shown in Figure 5-14.

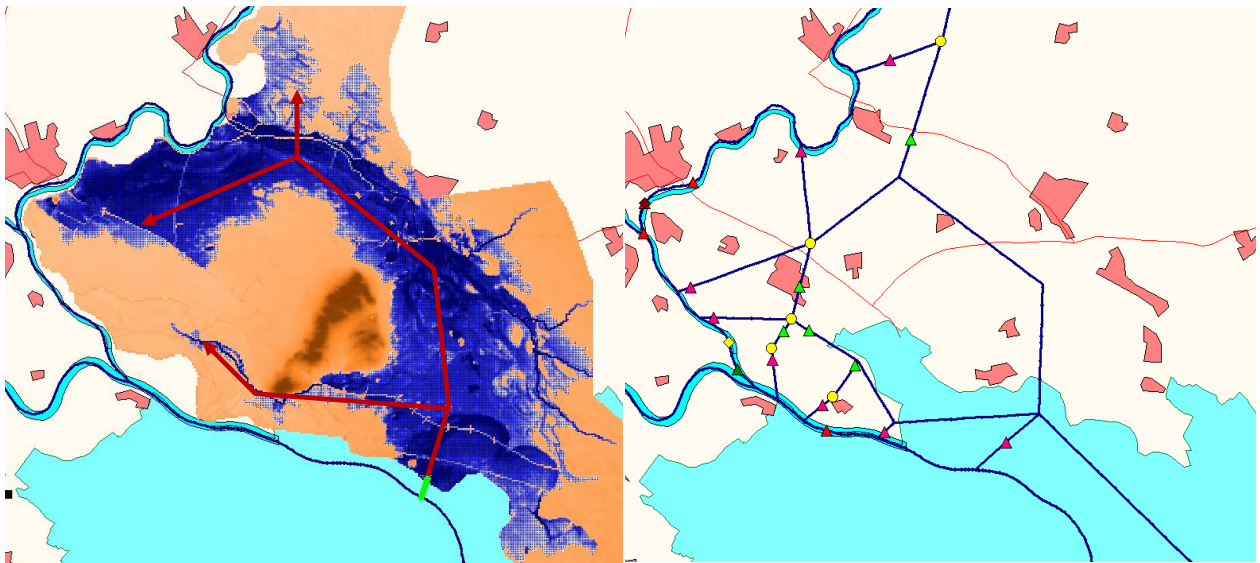


Figure 5-14 Comparison between 2D flood pattern and set up of the 0D model

In schematizing the flood plain, two methods were used in Sobek: branches with Y-Z profiles obtained from the altitude data and nodes with storage, also based on the altitude data of a certain area. To link these nodes to the network a standard type of profile was used as a 'dummy branch'. The storage nodes were used for lower parts of the model, the parts not behaving like a 'river' during a flood. The cross sections were used for the areas where there was not that much storage but which behave as a river. An overview of the model and the profiles used is shown in Figure 5-15, more data on the profiles is given in Appendix H. As strictly speaking the fast inundation model is not a 0D model due to the presence of 1D branches with storage, the term 'fast inundation model' is a better description.

When all these branches are defined and the connections with the different breaches are established the next step is to put the bottom levels, branch lengths and friction at values comparable to the real values as a start for tuning the model. By doing so the behavior of the network will be as close to the real situation as it can possibly be without further calibration.

The breaches are simulated by using a General Structure node in Sobek. This node grows in width according to the van der Knaap formula and has a crest level of approximately the land elevation at the breach location. However, the crest level can be changed in order to calibrate the breach discharges.

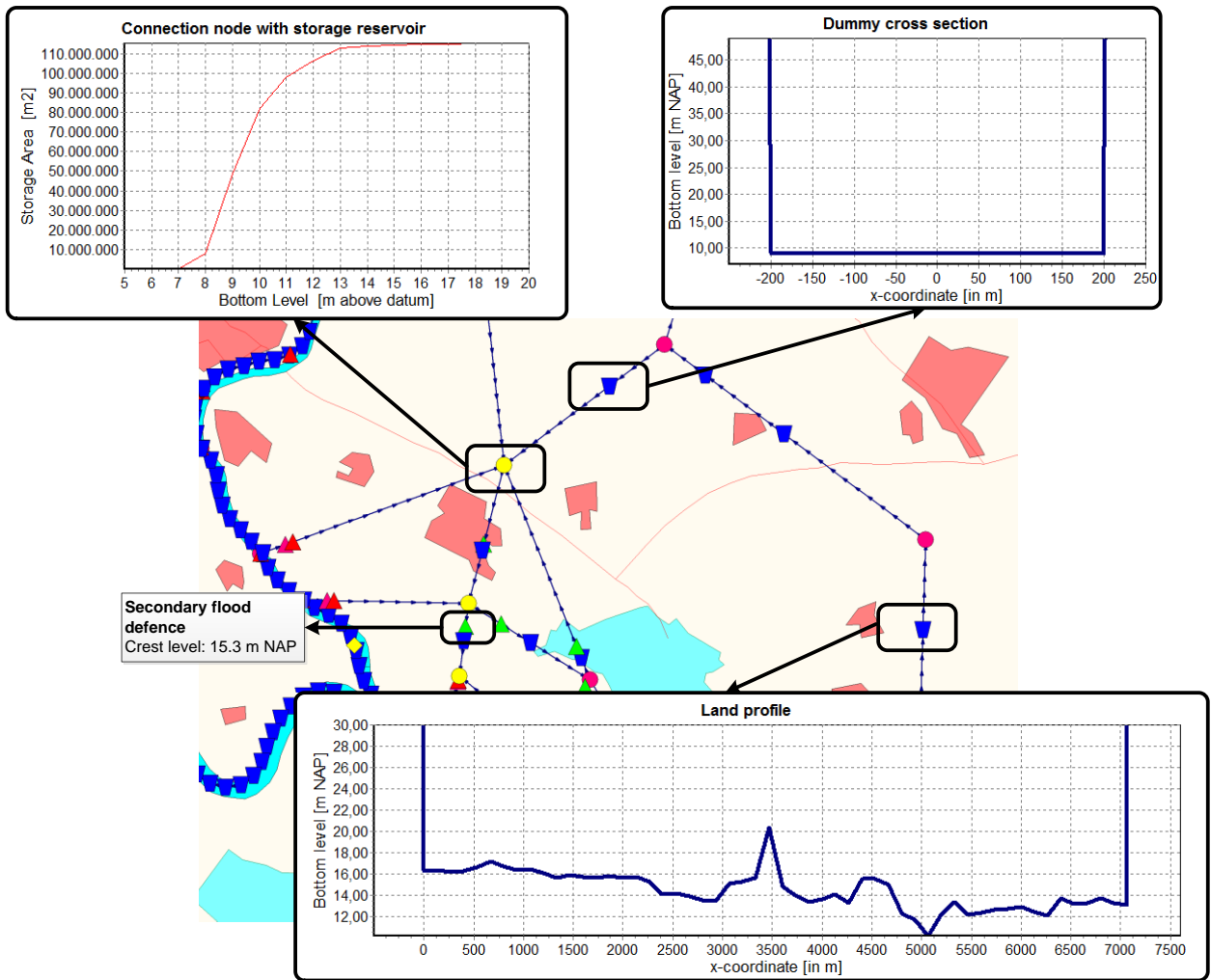


Figure 5-15 Profiles and data for different types of nodes for the western part of dike ring 48 as used in the model

### Time step and calculation grid

To determine the time step and calculation grid density for the 1D model, the Courant number is the governing parameter. The Courant number is given by the following formula, in which  $v$  is the estimated flow velocity,  $\Delta t$  the time step in seconds and  $\Delta l$  the distance between two calculation points:

$$C = \frac{\bar{v}\Delta t}{\Delta l}$$

For a good numerical model  $C$  should be around or below 1 in order to obtain stable results (Deltares, 2013). The time step in the original model was 10 minutes and the velocity is usually between 1 and 2 m/s. This gives a  $\Delta l$  of approximately 1000 meters for a Courant number of 1 and a velocity of 2 m/s, and 500 meters for a velocity of 1 m/s. Therefore it is decided to use a calculation grid distance of 500 meters with a time step of 10 minutes.

### Tuning of fast inundation model using 2D flood scenarios

The next step is to calibrate the fast inundation model using the 2D flood scenarios. The first parameter that is calibrated is the breach discharge. For all breach locations, the model is adapted in order to get the breach discharge in 4 scenarios as close to reality as possible, the procentual differences for the different scenarios are shown in Table 5-3.

Breach location	Absolute differences [in %]			
	1/100 year	1/1,000 year	1/10,000 year	1/10,000 year t=-4d
<b>Germany_2</b>	39%	7%	4%	8%
<b>Germany_1</b>	60%	13%	4%	-
<b>Germany_3</b>	4%	0%	1%	
<b>Spijk</b>	7%	0%	4%	5%
<b>Gravenswaardsedam</b>	23%	53%	2%	0%
<b>Herwen</b>	9%	13%	2%	13%
<b>Kandia</b>	15%	1%	6%	31%
<b>Loo</b>	18%	2%	0%	13%
<b>Giesbeek</b>	-	7%	2%	6%

Table 5-3 Differences in breach discharges of 0D and 2D model

For most breaches some tuning was necessary, and it was also observed that in some cases the discharge did not show the expected pattern for breach discharge. This was mainly caused by secondary dikes, which caused the water level right behind the breach to build up quickly before the secondary dike was overtopped. This caused differences in breach discharges between the 0D and 2D model, especially for events with a lower return period. A big difference could for instance be observed for the breach at Gravenswaardsedam, which is shown in Figure 5-16. In this figure it can be seen that the shape of the breach discharge is similar, but the total inflow is quite different. However, in this case it was not an improvement to further try calibrating the breach for lower discharges, as it behaved perfectly for the 1/10.000 year scenarios and further calibrating caused a loss of accuracy at the higher discharges. As the scenarios with higher return periods will have a much larger effect on the total risk, given the limited flood extent of the 1/1.000 year scenarios in this case, it is more important to obtain accurate results for the scenarios with a higher return period and larger flood extent.

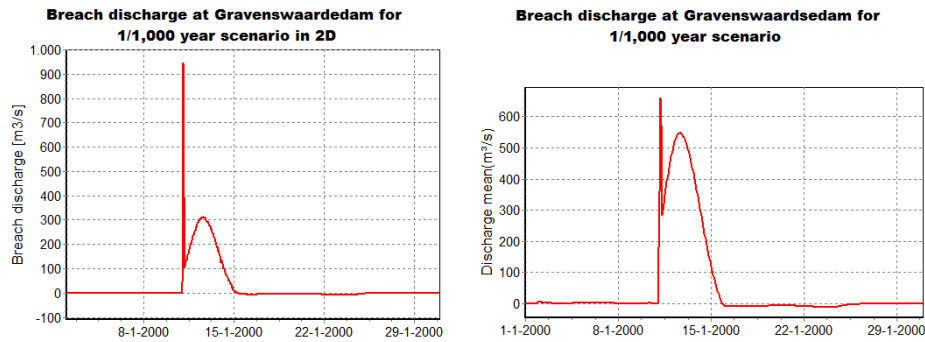


Figure 5-16 Breach discharges for 1,1000 year scenario at Gravenswaardesdam

After the breach discharges are tuned the next step is to tune the model in such a way that the water levels in the polder in the 2D model are close to the levels in the fast inundation model. This is checked for a set of scenarios and it appeared that for most cases the water levels are within half a meter of the 2D model. By making some additional changes to the friction in the branches, it is possible to increase the accuracy even more. The differences found for two scenarios are shown in Table 5-4. For all 13 scenarios which are compared the differences can be found in Appendix I. From the table it appears that for both scenarios, although they start at a different side the behaviour of the model is quite similar. The water levels only show a large difference in deviation for the zones 53\_2 and 53\_3. Also, both scenarios have an area which is dry in 2D but wet in the fast inundation model, this has to do with the locations of the measurement stations used, and it only happens in cases where the water depth is very low and thus not spread across the whole flood zone.

Flood zone	Loo 10.000 year			Germany_2 10.000 year		
	H <sub>2D</sub> [m NAP]	H <sub>0D</sub> [m NAP]	Difference [m]	H <sub>2D</sub> [m NAP]	H <sub>0D</sub> [m NAP]	Difference [m]
48_1	Dry	12,62		15,1	14,6	0,5
48_2	13,1	12,6	0,5	13,4	12,8	0,6
48_3	13,2	12,6	0,6	13,1	12,7	0,4
48_4	Dry	Dry		Dry	Dry	
48_5	Dry	Dry		Dry	Dry	
48_6	Dry	Dry		Dry	Dry	
48_7	Dry	Dry		Dry	11,25	
49	11,1	10,8	0,3	11	10,9	0,1
50	11	10,3	0,7	10,8	10,3	0,5
51	10,2	9,9	0,3	10,2	9,9	0,3
53_1	6,2	4,9	1,3	6,2	4,6	1,6
53_2	5	4,8	0,2	4	4,5	-0,5
53_3	5	4,8	0,2	4	4,5	-0,5
53_4	5	4,6	0,4	4	3,4	0,6

Table 5-4 Water level differences between 0D and 2D for two scenarios

Another aspect is the propagation velocity of the flood wave, in order to determine at which moment the water flows back into the river. This is especially important in cases with shortcutting. However, due to the structure of the fast inundation model, it is very difficult to resemble this behaviour. Due to the use of for instance storage nodes the system does not fill up in the same way as the 2D model. However, by setting the frictions in the 'dummy branches' to a

very low level it is possible to get the arrival of the flood waves to approximately the same point in time, although this is definitely one of the weaker points of the 0D/1D modelling technique. In Figure 5-17 the water levels for the western part are shown for both the fast inundation model and the 2D simulations, for the case Germany\_2 10,000 year t = 0 days. What can be seen is that the difference between peak arrival is around 2 days, with the water levels in the inundation model dropping slightly faster than in 2D.

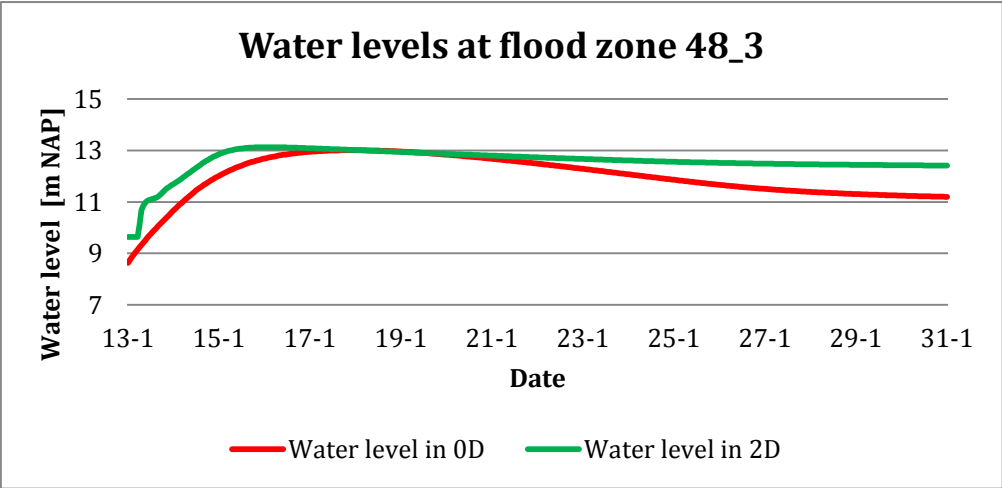


Figure 5-17 Water level at flood zone 48\_3 for both models in the case Germany\_2 10,000 year t = 0 days

**Defining controllers and triggers in Sobek**

In order to correctly simulate the breaches for all possible breach locations, two controllers are defined. The first controller is used to close the breach at the first second of the simulation. This is necessary as it is not possible to define a General Structure with a crest width of 0. If an initial crest width of a value just above 0 is used, this causes very low water depths behind the structure, making the calculation unstable and very slow, as the time step has to be decreased in order to calculate the water depths. Therefore the choice is made to close the breach at the first time step. The second controller is used to control the dike breach, and increases the crest width according to the standard relation from the van der Knaap formula. This controller is triggered by 2 different triggers. The first trigger is based on the sampling from the fragility curves and consists of a hydraulic trigger for the water level, which starts after 3 days into the simulation in order to prevent interference with the first controller. The second trigger consists of a hydraulic trigger based on the flow through the breach. This trigger is necessary as in some cases the first trigger stops, causing the breach growth to stop for a few time steps until the water level is back at the trigger level. The trigger based on the breach discharge prevents this behaviour. At the breach locations where dikes can fail from both the polder and river side 4 triggers are used: the two triggers mentioned above for the water levels at both sides, and the discharges in both directions.

**Setting up a Monte Carlo simulation using the fast inundation model with multiple triggers**

In order to be able to run a Monte Carlo simulation in Sobek, it is necessary to have an additional tool which is able to generate a set of N Sobek schematizations based on the sampled variables, run all those cases and then sample the results in a single spreadsheet. In order to do so, an input spreadsheet containing all data is read into a small tool, which is then able to run Sobek 1.000 times. The values that are changed are the input discharge wave and the strength for all possible breach locations. As output 4 different sheets were generated with the following data:

breach discharges, polder water levels, maximum water levels at different locations in the river and data on whether breaches were activated or not. However, during the analysis of the data it appeared that the last sheet did not show the correct values. This was caused by the fact that in some cases, although the breach was activated, this was not shown in the output sheet. At the time step before the breach Sobek calculates that during the next time step the trigger will be activated and starts opening the breach. However due to the dropped water level at the breach location the water level never really activates the trigger so the trigger is registered as off.

#### 5.5.4 Post-processing

##### *Data from hydrodynamic model*

In order to analyse the output from the hydrodynamic simulations 4 different output files with different parameters were generated. These parameters and their use are discussed below:

- Data for water levels at different locations in the river: The water levels at the different breach locations were generated as output, in order to be able to analyse the water level distributions with or without considering the different types of breaches.
- Data for water levels in polders: In order to calculate the economic damage and risk, a set of locations in the polder was selected, representing different areas. When combining this with water level - damage relationships, it is possible to calculate the total damage for each scenario
- Data on whether the dike failed: In case one of the triggers of a breach was activated, this was also shown in the output. This enables investigating which breaches occur when and which breaches occur at the same time. However, as was mentioned before this data was not generated correctly.
- Breach discharges: In order to analyse the water flowing in and out of the river, and in order to assess whether these discharges were realistic, also the breach discharges were generated as output. However these were mainly useful for verifying the model and to see if no excessive breach discharges occurred.

The most important output parameters are thus the water levels in the polders, for calculating the risk, and the water levels in the river, for calculating the effects of load interdependencies on the loads on flood defences. Especially for the risk calculation there are some important calculation steps which need to be done, these are discussed below.

##### *Deriving water level – damage relationships for different flood zones*

In order to calculate economic damage for a scenario it is necessary to be able to link the polder water levels in the model to the damage calculated from the 2D scenarios. This is done by deriving water level – discharge relationships for different flood zones in the area. In order to do so water level – discharge relationships are derived from a set of 13 2D simulations. The first step is to define the different flood zones for which the damage had to be calculated, these are shown in Figure 5-18. The presence of secondary flood defences provides a good idea on how to divide the area, and also from the flood simulations the general pattern of floods is quite clear. For the areas surrounded by primary and secondary dikes a flood zone is defined, while for the more sloping parts the area is split up in a few zones.

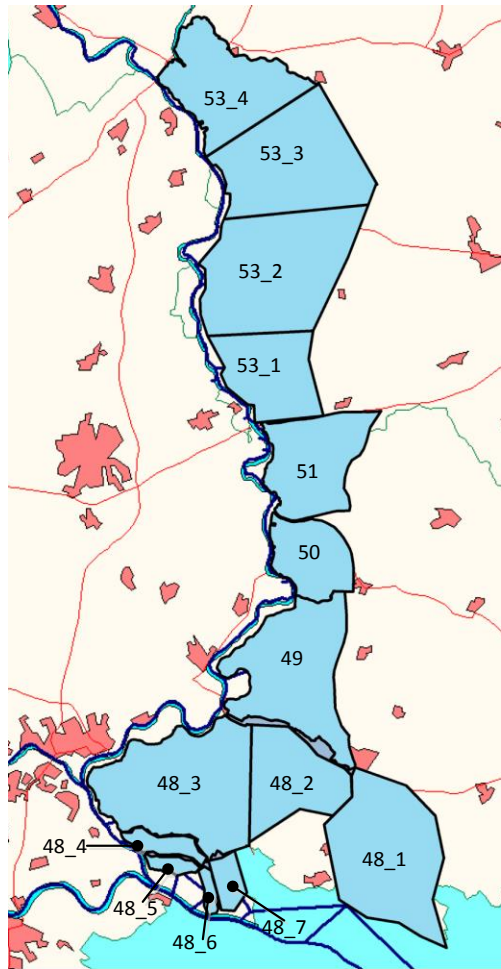


**Figure 5-18 Flood zones used for determining the damage per area**

After these areas are defined the economic damage for the 15 scenarios can be calculated in HIS-SSM, using the Standaardmethode2008 and SSM100NL2006 dataset. This results in damages for the different zones, which can be linked to the water level in the area in the same scenario. Then scatter plots are made for all areas and a logarithmic trend line is fitted to the data. The choice is made to fit a logarithmic function as the shape of a logarithmic function is closest to the normal shape of damage functions, as is for instance shown in Figure 5-19.

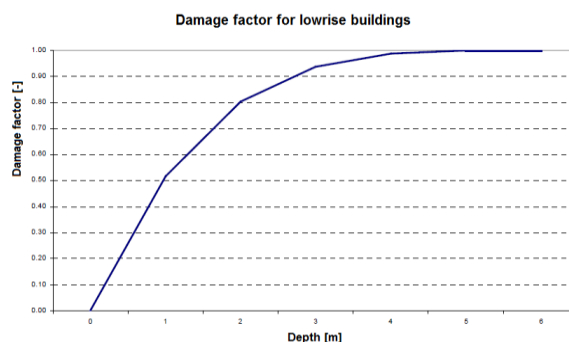


**Figure 5-19 HIS-SSM function for damage at low-rise buildings**

Linear functions for instance would result in overestimated damages for extreme flood depths, as damage has a physical maximum which is now represented by the asymptotic behaviour of the logarithmic function. Polynomial curves would have the disadvantage that for a very high

depth the curve might slope down, giving a decrease in damage for an increase in water depth. Therefore a logarithmic curve is most logical. Figure 5-20 shows the relation and results for flood zone 48\_3.

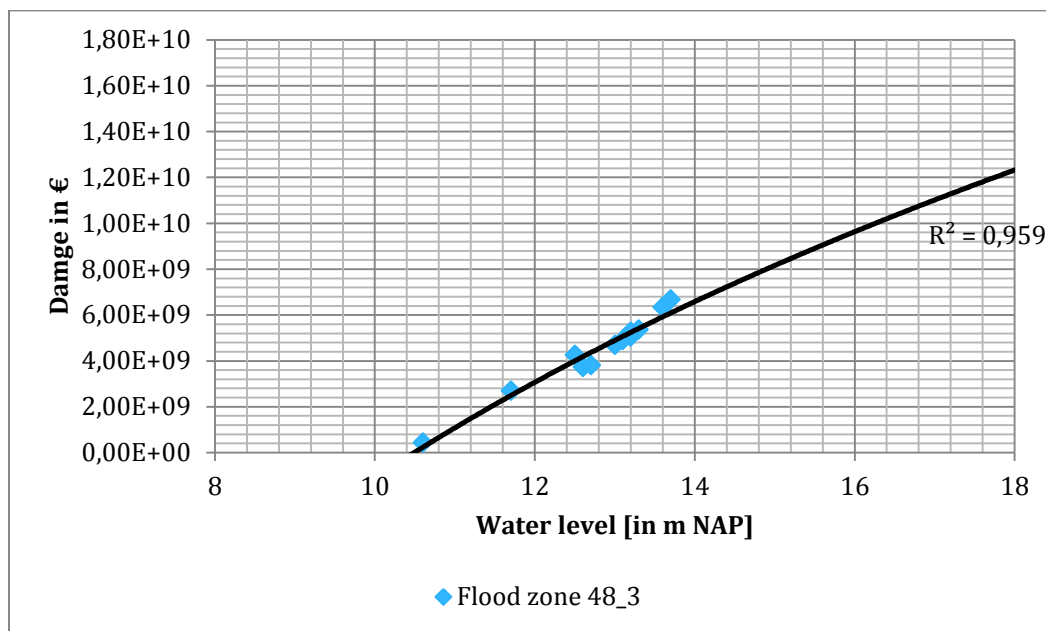


Figure 5-20 Logarithmic water level - damage curve for flood zone 48\_3 based on 13 water levels and damages for 13 2D scenarios

In most cases the trend lines shows a very good fit with  $R^2$ -values between 0,9 and 1. When comparing the damages calculated from the 2D water level data and the water level – damage curves to the damage from HIS-SSM, the difference is typically within 10%, mainly caused by the fact that only 1 point is used in order to calculate the damage in a whole flood zone. In order to also derive the damage from the fast inundation model, it is important to analyse the water level differences between the fast inundation model and the 2D model for the same scenarios. As is shown in Table 5-4 and Appendix I, the differences between the inundation model and 2D scenarios are generally in the same order of magnitude for most scenarios. Therefore for 13 scenarios the water level differences between the fast inundation model and the 2D scenarios are averaged and used to shift the water level – damage relationships. On average this doesn't really improve the performance of the curves, as there are a few very dominant scenarios with a relatively low damage, which have a very large deviation. However, when weighing the differences upon the risk contribution the shifted 0D curves give a considerably better estimate for the damage, it gives the same performance as the calculations based on the measurement stations in 2D, for the considered set of scenarios. The differences are shown in Table 5-5 and Table 5-6. The first column shows the detailed damage calculation from HIS-SSM, the other columns show the damage obtained from the water level –damage relationships, using one measurement point per flood zone.

Scenario	HIS SSM damage in €	Damage for 2D in €	Difference to HIS-SSM in %	Damage for 0D with regular functions in €	Difference to HIS-SSM in %	Damage for 0D with shifted functions in €	Difference to HIS-SSM in %
Gravensw 10000	3,6E+09	3,5E+09	1%	2,8E+09	21%	3,7E+09	4%
Gravensw 100	1,5E+08	2,6E+08	73%	5,8E+08	283%	5,8E+08	283%
Gravensw 1000	2,8E+08	4,6E+08	69%	5,6E+08	105%	4,2E+08	51%
Herwen 10000	6,0E+09	6,3E+09	5%	2,5E+09	58%	3,4E+09	43%
Herwen 100	7,6E+09	7,3E+09	4%	8,0E+08	89%	8,0E+08	89%
Loo 10000	5,7E+09	5,8E+09	2%	5,0E+09	12%	5,9E+09	3%
Loo 100	2,5E+10	2,6E+10	4%	2,5E+10	1%	2,8E+10	11%
Spijk 10000	1,5E+10	1,3E+10	8%	1,3E+10	10%	1,6E+10	12%
Spijk 1000	3,7E+10	3,5E+10	6%	2,5E+10	34%	2,8E+10	25%
Spijk 100	2,0E+10	2,4E+10	16%	2,1E+10	5%	2,4E+10	20%
Germany_2 10000	6,9E+09	7,1E+09	2%	7,0E+09	1%	8,0E+09	15%
Germany_2 1000	2,0E+10	2,4E+10	17%	2,4E+10	18%	2,7E+10	34%
Germany_2 100	3,8E+09	3,0E+09	20%	4,9E+09	31%	7,6E+09	99%
<b>Average non-weighted difference</b>			<b>17,48%</b>		<b>51,33%</b>		<b>53,07%</b>

Table 5-5 Performance of water level – damage relations for 13 scenarios

Method	Total risk difference in %
HIS-SSM	0%
2D	5%
Fast inundation model with regular curves	9%
Fast inundation model with shifted curves	6%

Table 5-6 Performance of methods in calculation of risk for the 13 scenarios

### Calculating the total risk

A very convenient way of showing the output for economic damages for different exceedence probabilities, is by means of a FD curve. This curve shows the exceedence probabilities and damages. A very useful property of the FD curve, is that the area below the curve is the total risk or expected yearly value of damage for the area. The FD curve can be constructed by summing up the risk contributions of all scenarios. Numerical integration of the curve then gives the total risk for the considered area. The total area of the bins in the graph is given by:

$$E(D) = \sum_1^N \frac{1}{2} (P_N + P_{N+1}) (D_N - D_{N-1})$$

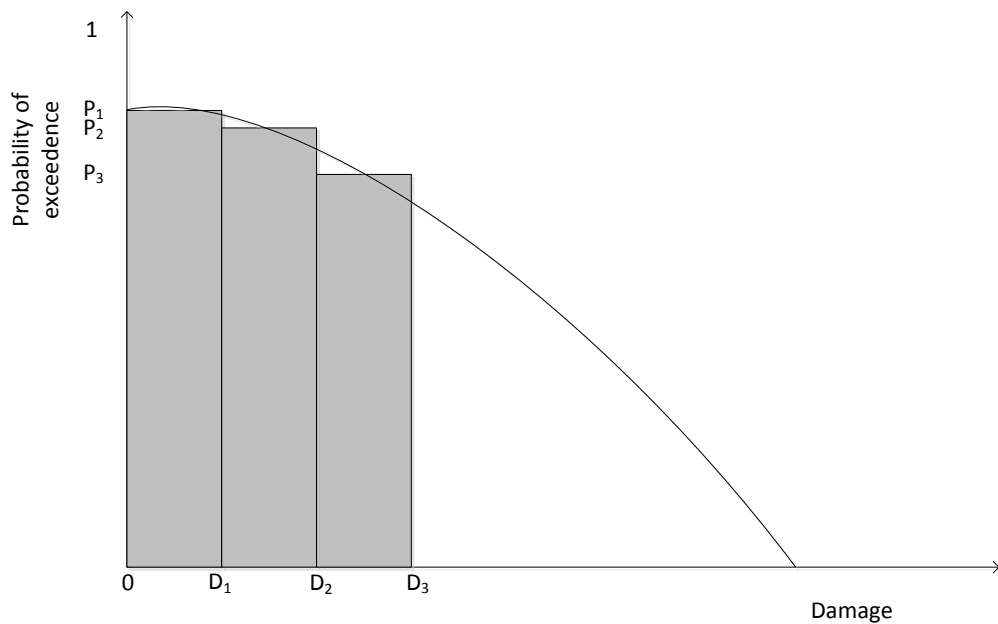


Figure 5-21 Procedure for calculation of the total risk

### 5.5.5 Other important assumptions in the model

In this paragraph some assumptions in the analysis are further explained.

- **Category-c flood defences only overtop**

In the IJssel catchment the dike ring areas are separated by primary flood defences, which are often not reliable and not as well maintained as the river dikes. However, as the complexity of the model will be increased if breaches at these locations are taken into account, the secondary dikes are assumed to stay intact. In reality this is debatable, as most of the category-c defences are not up to strength and will most likely breach, however, the exact strength is not known. In the future it would be advisable to further look into this, and investigate the influence of breaches of secondary dikes (and other higher elements such as elevated (rail)roads).

- **Dikes are up to strength, failures are only dependent on water level**

In this case study two assumptions regarding the strength of the dikes are made. The first is that they are up to the set safety standard. This means that the mean for their strength is always at the 1/1,250 year design level. Also, time dependence of failure mechanisms is not considered, for instance piping failures also occur at a certain water height. As was shown by Vorogushyn et al. (2009) this is not how it works in reality, but due to the available data on dike strengths it is assumed that failures are independent of time. Also, when a dike breaches from the polder side, there is no trigger defined to account for the water level head over the dike. In cases with breaches from the inside these are generally caused by macrostability, however, as was shown in Appendix B these failures are dependent on the head over the dike, not solely on the water level. This is not accounted for as there was no data on the strength of the dikes in those cases.

## 5.6 Results for the Bovenrijn/IJssel case study

In this section the results of the model for the case of the Bovenrijn/IJssel are presented. The results were analysed using three different indicators to quantify the effects: the influence of load interdependencies on water levels, number of breaches and on economic damage. In order to get a good view of the effects of load interdependencies, five different scenarios were considered. The first scenario is a case where dikes can breach from both polder and river side, and thus covers all possible effects of shortcutting, cascade effects and load relief. The second scenario does not consider dike breaches from the polder side, there is thus less shortcutting and the aim of this scenario is to quantify the effect of dike breaches from the polder side, however, shortcutting can occur but only if a dike already breached from the outside. The third scenario is a case where no flow from polder to river is possible: water that flows out of the river will stay in the polder. The fourth scenario is the same as the first, except that cascade effects between the dike rings at the right bank are now not considered. The fifth and last scenario is a reference scenario where no breaches occur.

Scenario	Breaches from river	Shortcutting possible?	Breaches from polder	Cascade possible
<b>With breaches</b>	<b>Yes</b>	<b>Yes</b>	<b>Yes</b>	<b>Yes</b>
<b>No polder breaches</b>	<b>Yes</b>	<b>Yes</b>	No	<b>Yes</b>
<b>No shortcutting</b>	<b>Yes</b>	No	No	<b>Yes</b>
<b>No cascade</b>	<b>Yes</b>	<b>Yes</b>	<b>Yes</b>	No
<b>No breaches</b>	No	No	No	No

Table 5-7 Scenarios used for comparing effects of load interdependencies

The breach locations considered in the model are shown in Figure 5-22.

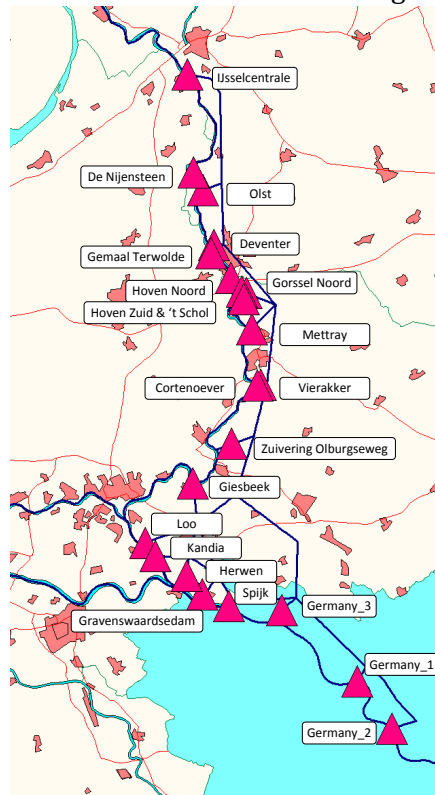


Figure 5-22 Breach locations in the model

### 5.6.1 Effects of load interdependencies on water levels

The first indicator used to identify the effects of interdependencies, is the effect of breaches on water levels. From the conceptual model studied in Chapter 4.1 it was shown that, in case of water flowing out of the river due to dike breaches, the return periods for high water levels increase. From the findings by Apel et al. (2009a) it was found that this effect was especially large for discharge waves much higher than the design level of the river dikes. In the case of shortcutting, the effect can be compensated or even negative, with much higher water levels than expected. From the model built for the Bovenrijn/IJssel case, similar behaviour was found as can be seen from Figure 5-23, Figure 5-24 and Figure 5-25, which show water levels and their exceedence probabilities for three locations along the IJssel: Giesbeek, Deventer and IJsselcentrale. In these graphs trendlines for the scenarios with breaches, without shortcutting and without cascade effect are shown. The scenario without polder breaches is left out of the graphs, as it behaves almost the same as the scenario with breaches for all cases. From the graph for Giesbeek it can be seen that in the case of the scenario with breaches, where water can flow back into the IJssel, the water levels found are slightly higher than in cases without breaches. This is most likely caused by breaches at Giesbeek where water from the flooded dike ring 48 flows into the IJssel. At Deventer the positive effects caused by upstream breaches outweigh the negative effects caused by shortcutting: the scenario with breaches gives lower water levels than cases without breaches. At IJsselcentrale similar results are found although the reduction of the return frequencies is not as much as at Deventer. Based on the figures it can be concluded that the effects of shortcutting are very variable between different locations at one river: at Deventer the positive load interdependencies dominate while at Giesbeek the negative effects are dominating. In the case of Deventer this is most likely caused by a set of breaches just downstream, which can cause relief at Deventer. In Appendix K the same figures can be found for the other breach locations in the model.

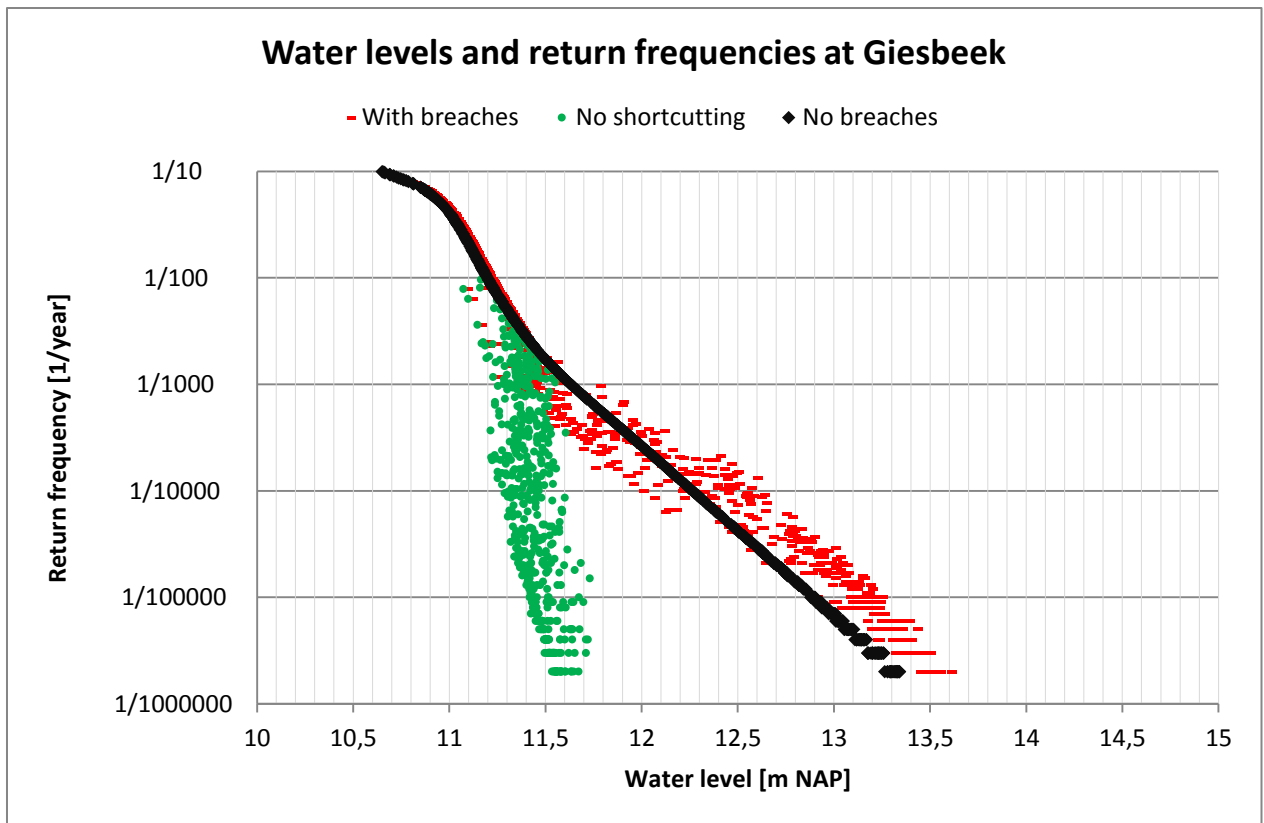


Figure 5-23 Water levels and return frequencies at Giesbeek

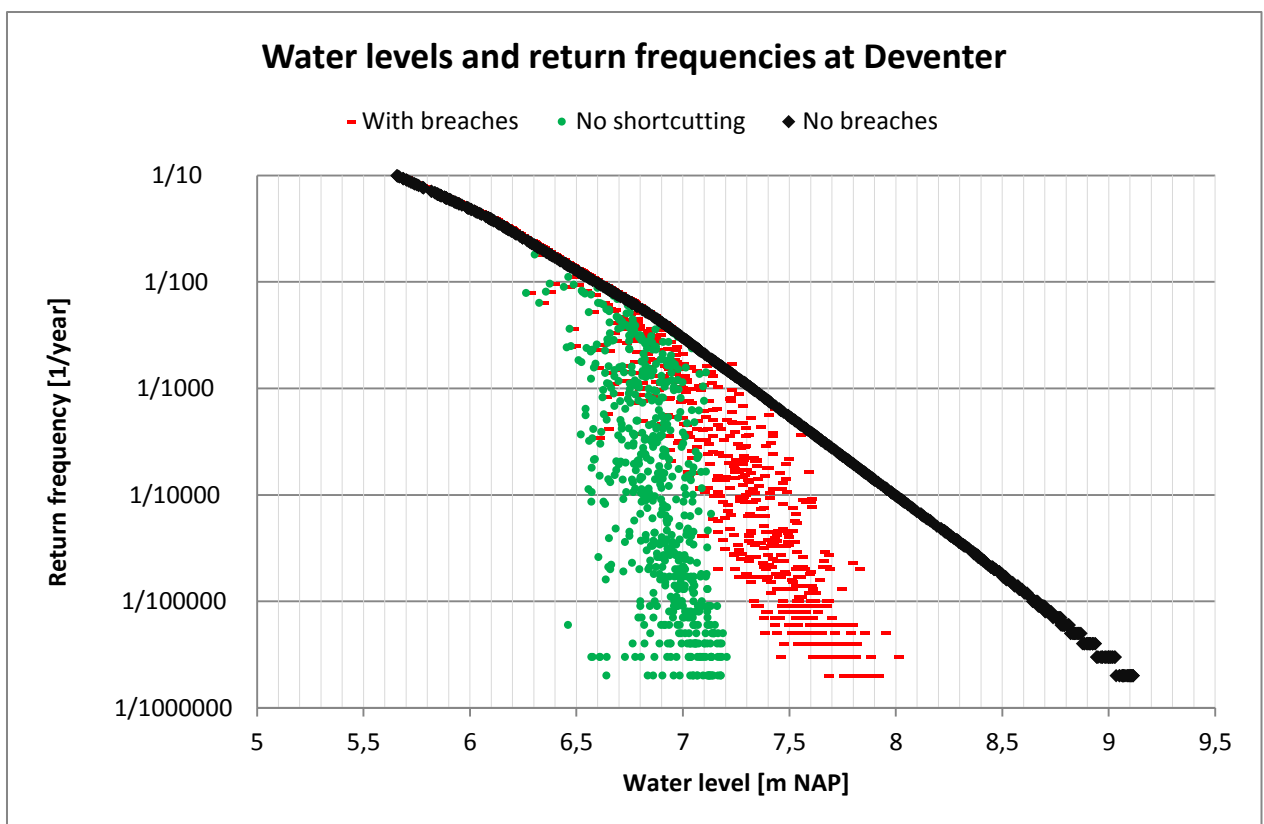


Figure 5-24 Water levels and return frequencies at Deventer

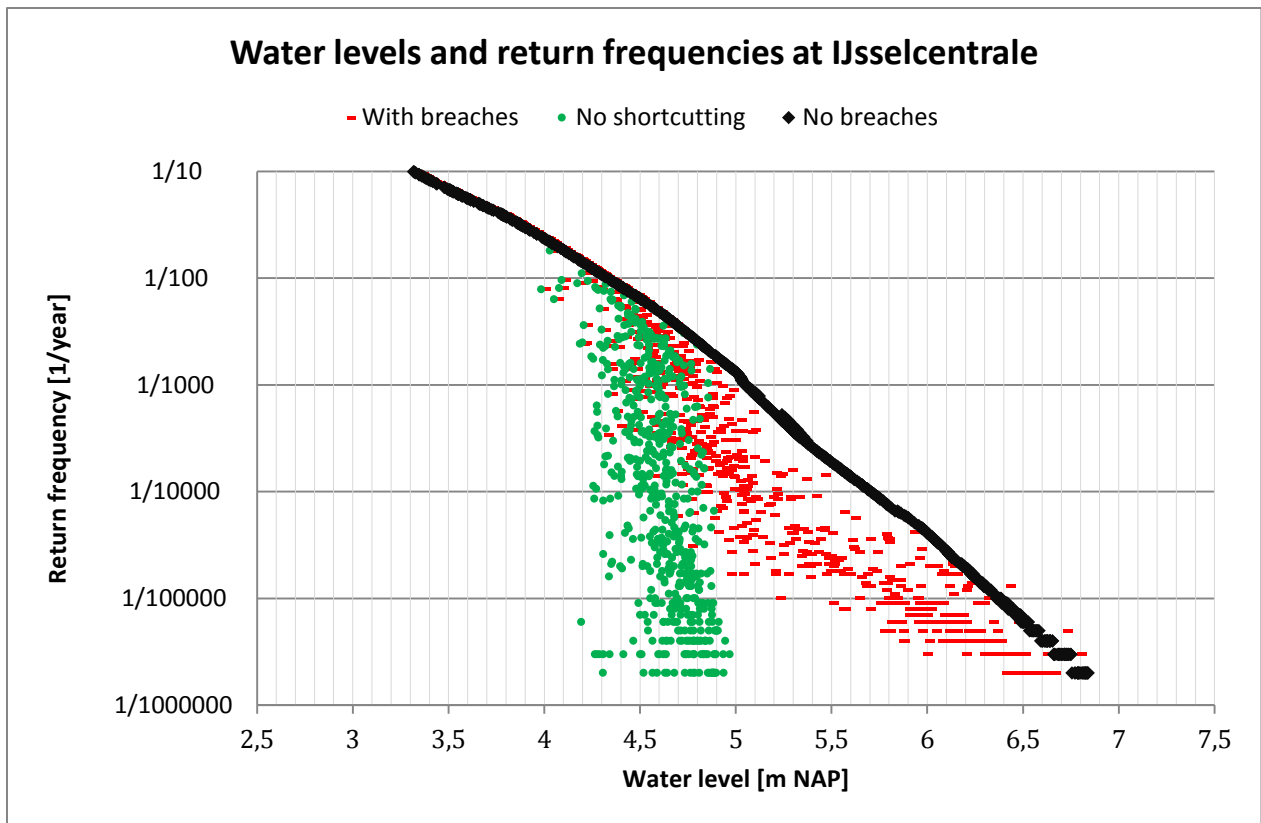


Figure 5-25 Water levels and return frequencies at IJcentrale

When considering these graphs it is also very important to notice that for cases in scenario 3, the water levels seem to approach an asymptote: the water levels are limited. This shows that for very high discharges and cases with pure positive load interdependencies water levels approach an asymptotic level, as was also shown in De Bruijn et al. (2013). In reality this is not the case for the IJssel, as in that case the results will be closest to the case with breaches, but as negative effects do not occur in all cases, for many other areas in the Netherlands this might be reality.

As the scenario without breaches resembles the water levels currently used in flood risk analysis and dike design, it is interesting to compare these with the findings for the case with breaches, Table 5-8 shows a comparison of the design levels and the maximum water levels for 1/1.250 year scenarios for 8 breach locations in the system. The results for the scenario with breaches are given by means of an upper and lower bound. It is impossible to use a standard exponential trend line to derive the new level, as the water levels do not follow an exponential distribution anymore. What can be seen from the table is that for the locations at the Bovenrijn the return periods are significantly lower than before, which is clearly caused by positive load interdependencies. On the other hand, even though positive effects seem to be dominating at the IJssel, there are still quite some cases where the lower bound for cases with breaches gives return periods below the design level. Therefore in cases with shortcutting, it can be concluded that the resulting water level is extremely case dependant.

Breach location:	1/1.250 level [m NAP]	design	Return period in Scenario 1 lower bound [in years]	Return period in Scenario 1 upper bound [in years]
IJsselcentrale	5,0		2.000	70.000
Deventer	7,4		4.000	300.000
't Schol	8,2		1.100	9.000
Vierakker	9,8		900	4.000
Giesbeek	11,7		1.000	9.000
Loo	15,3		4.000	300.000
Herwen	17,3		6.000	900.000
Spijk	18,4		2.000	900.00

Table 5-8 Design water levels and actual return periods from the model

When further looking into a location with purely positive load interdependencies, it is interesting to see how the current design level compares to the water levels found from the model. For the breach at Herwen the realizations for the cases with and without shortcutting are nearly similar, so the conditions at that location are almost completely determined by positive load interdependencies, the results for the scenarios with and without breaches at Herwen are shown in Figure 5-26, as well as the current design level. What can be seen is that the new return period for the design level is much higher than 1.250 years. Although there are a few simulations where the design level is exceeded at a 1/4.000 event, it is not until the 1/10.000 year discharge that the design level is seriously exceeded.

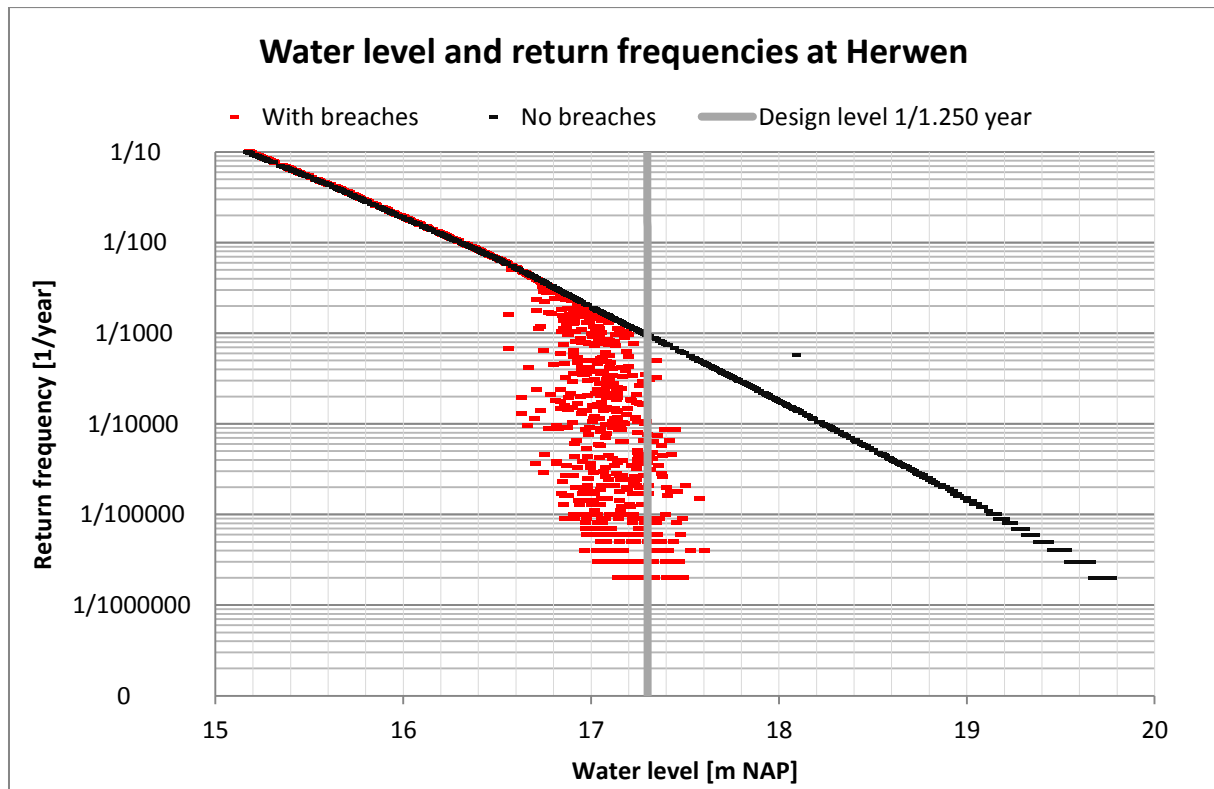


Figure 5-26 Water level and return frequencies at Herwen

When considering the figures found for the water levels, aside from the change in water level for each return frequency, one of the main observations is that the water levels, for each return frequency, show considerable spreading. This is shown in Figure 5-27. This spread is caused by the fact that the water levels are dependent on breaches at other locations. As the strength of the dikes, and thus the occurrence of breaches, is uncertain, also the water levels become uncertain. The fact that the water levels are spread for events with the same return frequency, emphasizes the presence of load interdependencies.

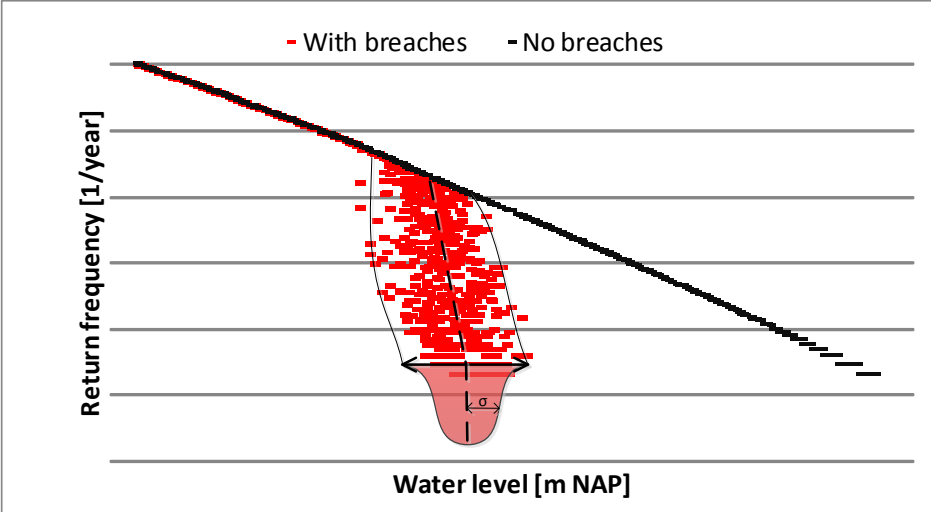


Figure 5-27 Uncertainty in water levels caused by interdependencies

### 5.6.2 Effects of load interdependencies on number of breaches

When considering the different scenarios, it is also interesting to see at which breach locations the influence of both positive and negative load interdependencies is the largest. As was mentioned, the output of the number of breaches was not generated completely correctly. However, it is still possible to see the influence of different scenarios on the different numbers of breaches. In Table 5-9 the breaches for a set of locations for both polder and river side failures are shown.

Breach location	With breaches		No polder breaches		No shortcutting		No breaches	
	<i>River</i>	<i>Polder</i>	<i>River</i>	<i>Polder</i>	<i>River</i>	<i>Polder</i>	<i>River</i>	<i>Polder</i>
<b>IJsselcentrale</b>	112	222	228	0	39	0	86	137
<b>Olst</b>	113	55	162	0	16	0	45	6
<b>Gemaal Terwolde</b>	306	0	275	0	15	0	209	0
<b>Deventer</b>	219	4	203	0	15	0	112	0
<b>Giesbeek</b>	158	326	325	0	121	0	156	337
<b>Loo</b>	132	82	168	0	57	0	164	151
<b>Spijk</b>	83	71	95	0	91	0	86	74
<b>Germany_2</b>	352	0	352	0	352	0	352	0

Table 5-9 Number of times breaches were triggered for different locations in the system

What can be seen is that for Germany\_2 the scenario does not have influence, which is quite logical as it is close to the upstream boundary. The dike reach at Giesbeek frequently fails from the polder side and is thus very important for shortcutting effects. This could also be observed in the water level probabilities in the previous paragraph. The same holds for the dike reach at IJsselcentrale, this shows that dike reaches at the lowest point of a dike ring area, which is the case with Giesbeek and IJsselcentrale frequently fail from the polder side due to the accumulating water at the lowest point of such an area. In the scenario without outflow, it can be seen that the number of breaches at dike ring 52, in the table at Gemaal Terwolde, is enormously reduced, which is in line with what could be expected for a case without shortcutting effects.

### 5.6.3 Effects of load interdependencies on economic risk

The second main indicator for the influence of load interdependencies is the influence on the economic risk. First the damages for all separate flood zones are calculated, summed up and then plotted in an FD-curve. The potential damage at dike ring 52, at the left bank of the IJssel, is relatively low, compared to the damages on the right bank. Therefore it is to be expected that, for the total area, the case where there is no outflow of the polders will give the highest damage, as there is no mitigating effect of water flowing back into the river. When considering the FD curve in Figure 5-28 this can indeed be observed: the outflow of the right bank mitigates the flood damage, although it increases the number of failures at the left bank, as was already observed in the number of breaches shown in the previous paragraph. However, due to the relatively low possible damage at the left bank, accounting for breaches lowers the total damage, even though in most cases a larger area will be inundated. It can also be observed that the cascade effects at the right bank have no influence on the total damage: the curve for the case without cascade effects is exactly the same as for the case with breaches.

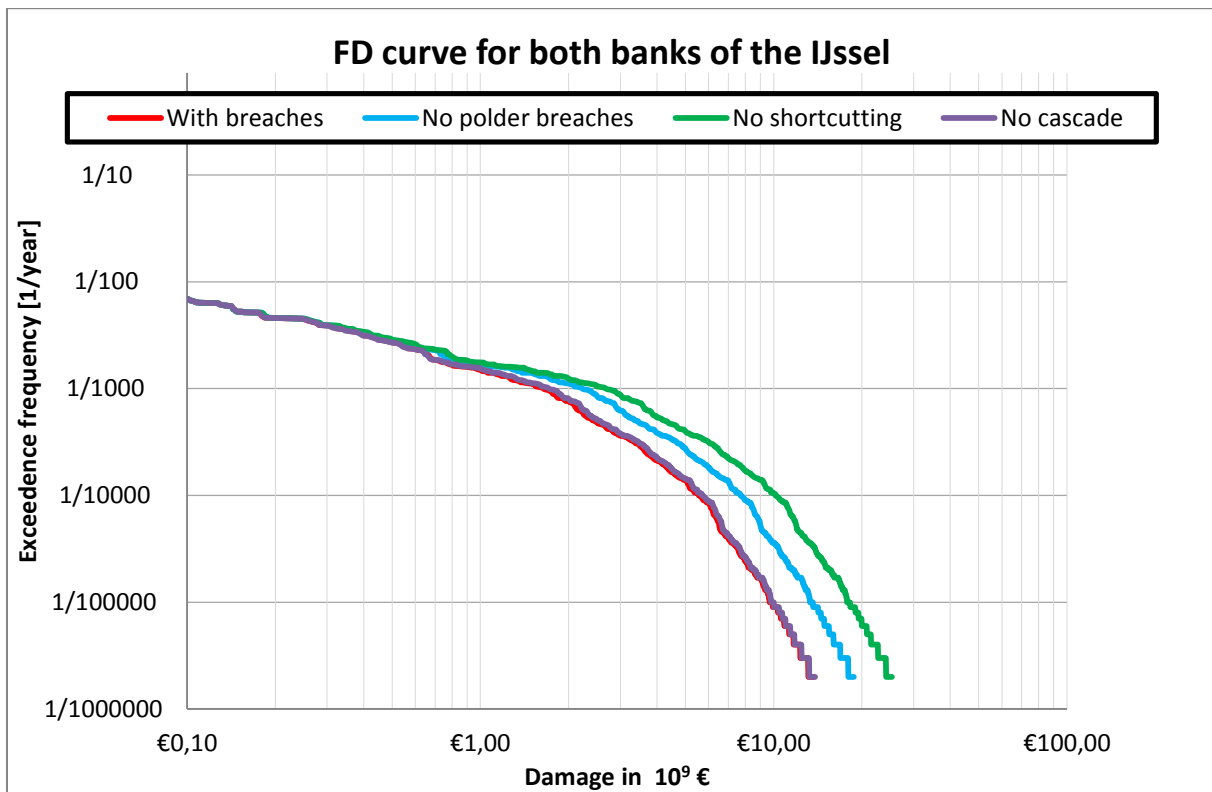


Figure 5-28 FD curve total case study area

When considering the FD curve for dike ring 52 this behaviour can be observed even clearer: the curve in Figure 5-29 shows that for the case without shortcutting there is a much lower risk than for cases where outflow of the polders on the right bank is possible. The cascade effect at the right bank does not have a significant influence on the damage at the left bank, it is almost the same as for the case with breaches.

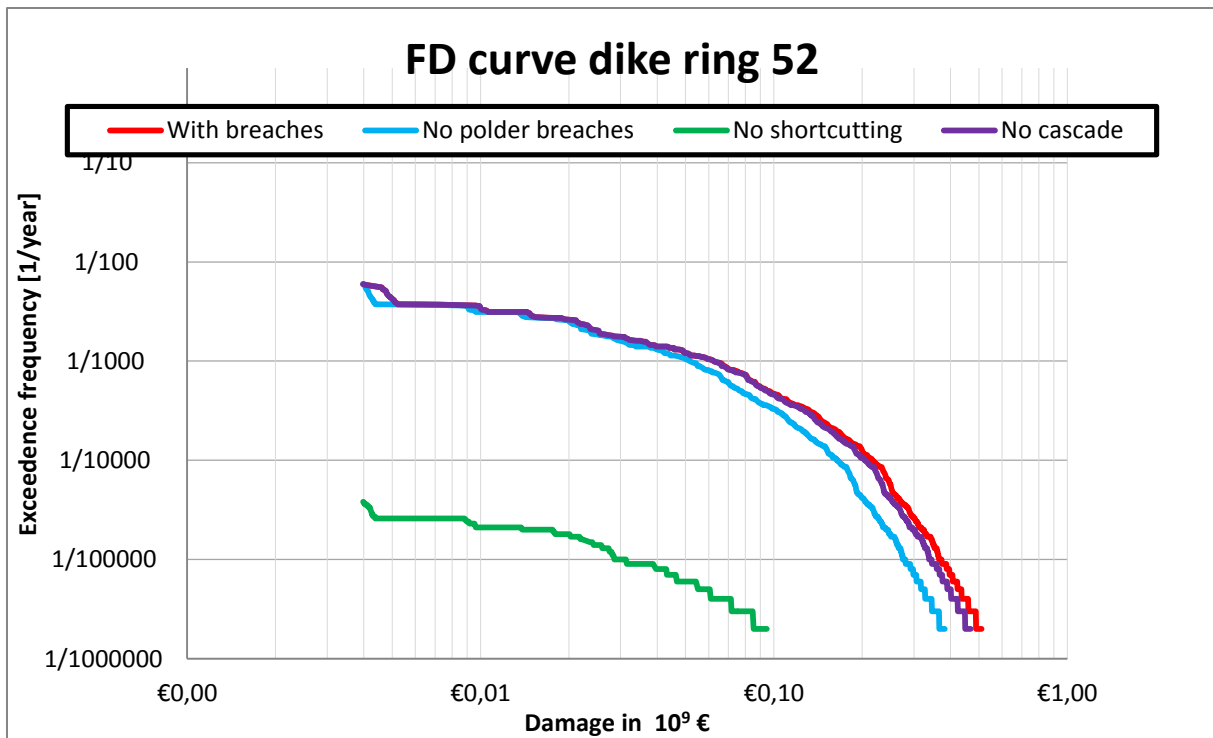


Figure 5-29 FD curve for dike ring 52

The FD-curve for dike ring 52 clearly shows that in cases without outflow there is a large influence of positive load interdependencies at dike ring 52: the loads on the dikes are significantly lower, resulting in a much lower number of failures. This also clearly shows that shortcutting plays a significant role in the risk calculation for the IJssel area. As the cascade effects have so little influence on the total damage there has to be some kind of redistribution. This can indeed be observed when considering the FD-curve for dike ring 48 (Figure 5-30): Lower damages are found for Scenario 1, caused by outflow to dike ring 49.

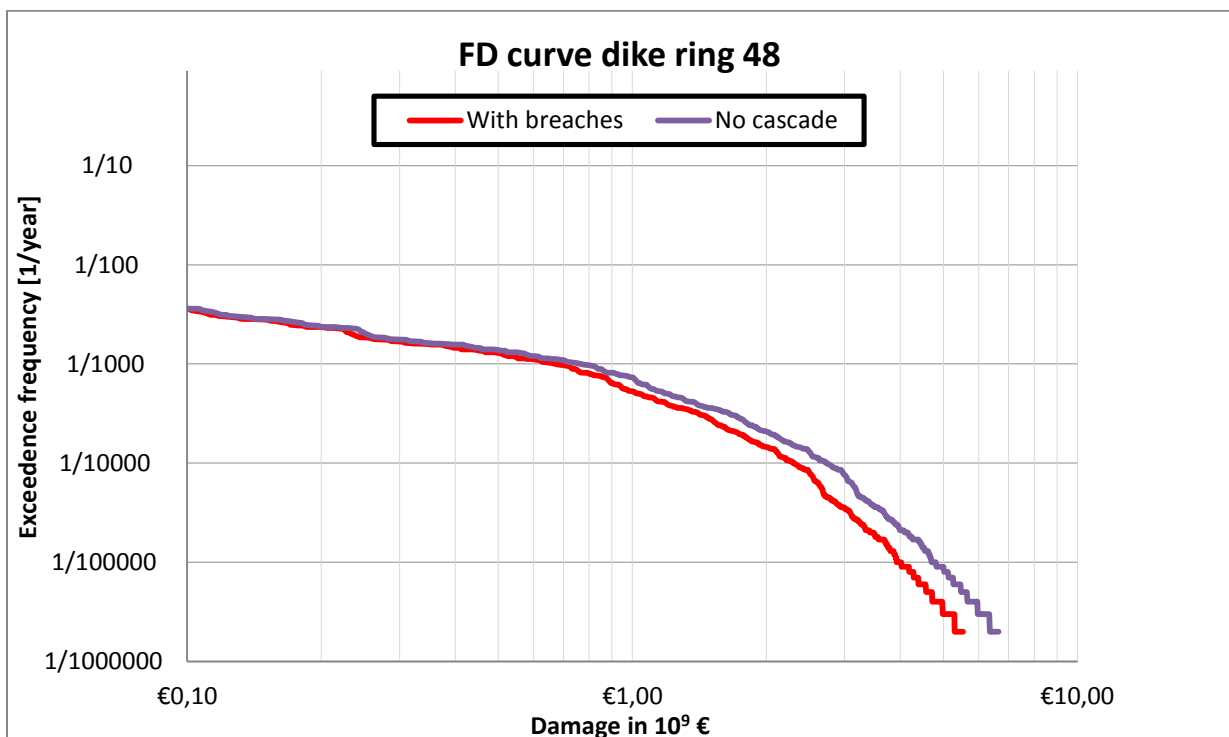


Figure 5-30 FD curve for right bank of the IJssel

In order to get a better view of the distribution of the risks in the area, the total risk is a good indicator. The total risk of the different areas can be calculated by numerical integration of the FD-curves in the above figures. This is done for different parts of the area. The total risk for the considered areas is shown in Table 5-10 for the cases with and without cascade effects, in the last columns the difference in risk caused by the cascade effect is shown.

Area	Economic risk [10 <sup>6</sup> €/year]	Economic risk without cascade [10 <sup>6</sup> €/year]	Difference in risk caused by cascade effect [10 <sup>6</sup> €/year]	Procentual difference when considering cascade effects
<b>Total area</b>	27,4	27,3	+0,1	+0,4%
<b>Right bank</b>	26,4	26,4	-	-
<b>Dike ring 48</b>	10,8	13,1	-2,3	-17,6%
<b>Dike ring 49</b>	1,4	1,0	+0,4	+40%
<b>Dike ring 50</b>	3,5	2,4	+1,1	+45,8%
<b>Dike ring 51</b>	0,3	0,046	+0,25	+543%
<b>Dike ring 52</b>	0,98	0,88	+0,1	+11.4%
<b>Dike ring 53</b>	10,4	9,8	+0,6	+6.12%

Table 5-10 Total risk for different areas in the case study

The remarkable thing is that for the total risk it doesn't matter whether cascade effects are taken into account: the total risk is the same. However, the distribution of the risk over the area changes, as can be expected: dike ring 48 has a higher risk when not taking into account cascade effects. This is caused by the increased flood depths due to the absence of outflow to dike ring 49. As the water now also flows out of the breaches at the Pannerdens kanaal there is less discharge through the IJssel, thus for the rest of the areas the risk is reduced. This compensates the increased risk at dike ring 48.

### Influence of load interdependencies on duration of the load

As was seen from the preceding results, the maximum water levels at the IJssel change significantly when taking into account load interdependencies. In general the water levels are observed to be lower. However, the water is still in the system and has to run off. By studying a single case this behavior was further investigated. The case considered has a discharge of 17.278 m<sup>3</sup>/s at Wesel. The amount of breaches is significant, there are about 5 breaches at the IJssel, as the breach at Giesbeek fails from the polder side, thus increasing the discharge through the IJssel. Figure 5-31 shows the discharge at a point approximately 3 kilometers downstream of IJsselcentrale for a time period of 2 months.

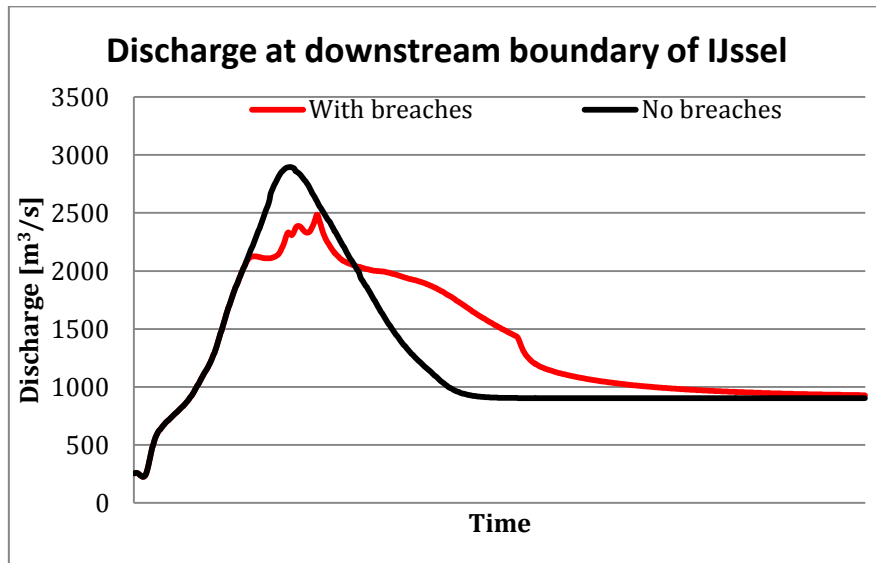


Figure 5-31 Discharge wave for a location near the downstream boundary of the IJssel. The time period is 2 months

What can be observed is that indeed the peak of the discharge wave is significantly lower, but what is the most remarkable is the different shape. The peak is more irregular, due to the breaches, but the high discharge also lasts a lot longer. The discharge for Scenario 1 is above 1.500 m<sup>3</sup>/s until 20 days after the peak of the discharge at Wesel, for Scenario 5 this is only 12 days. This emphasizes the importance of time duration of loads in these cases, as longer loads might induce more failures caused by time-dependent mechanisms such as piping.

#### 5.6.4 Computational performance of the new model

One of the main reasons for using a fast inundation model was that in terms of computational capacity it is almost impossible to do a Monte Carlo simulation for 1.000 cases with 2D modelling. The computer used for the calculations had an quad core Intel Core i7-2600(3.40 GHz) processor with 8 logical processors and 16 GB of RAM. For the 2D cases run, which were relatively simple as they only consisted of 1 breach at a time, typical calculation times were between 3 and 10 hours on one thread at once. With the Monte Carlo simulation in the fast inundation model it was possible to run at all cores simultaneously, enabling an analysis of 1000 simulations to run within 6 hours, including pre- and post- processing. If it is assumed that when using 2D it would also be possible to run 8 calculations at a time this would still take around 900 hours for 1 analysis, which is approximately 150 times slower. The computational performance of the used inundation model is thus very good.

## 5.7 Conclusions and recommendations on the case study results

### Conclusions

In previous risk analysis for the IJssel area, the effects of load interdependencies have been neglected or only dealt with in a very simplified manner. By using the methodology from Chapter 4, it is possible to execute a Monte Carlo analysis simulating the effects of load interdependencies in the area. From the results it can be concluded that the influence of load interdependencies is quite significant; both negative and positive load interdependencies can be clearly observed to have a significant effect on both flood risk and water levels. Positive interdependencies, i.e. load reductions, were mainly observed for the Bovenrijn and Pannerdens kanaal, while in the IJssel branch both negative and positive interdependencies were visible. Whether negative or positive interdependencies are dominant is very dependent on the location and type of the breaches. A polder side failure with a large outflow nearby can cause large negative effects, while a series of smaller normal breaches can compensate this effect or cause large positive effects. This could for instance be observed for the breach location at Deventer, for which the water levels were dominated by positive effects, while upstream at Giesbeek negative effects were much more dominant. Furthermore it can be concluded that, based on the data found for cases without polder outflow, positive interdependencies have a significant influence on the loads on flood defences. Although not that important for the IJssel, at the Bovenrijn the influence was quite significant, causing the dikes to have a lower actual exceedence probability than the design level: safety levels increase to a level above the design level due to load relief. Also it was observed that for purely positive effects, water levels tend to behave asymptotically for low return frequencies.

From the risk calculations it can be concluded that in this specific area, it is necessary to account for load interdependencies in flood risk analysis. From the results it was shown that for the left bank of the IJssel, the risk was significantly increased by the outflow from the different breach locations at the right bank. For the whole area, the risk is lowered by the outflow of the right bank, as it decreases the flood depths at the right bank compared to the case considered in scenario 3, where no outflow is possible. The area is also characterized by an imbalance in potential damage at the right and left bank. The potential damage at the left bank is much lower, which causes the damage, in cases where water can flow out of the polders at the right bank, to have a lower maximum than for cases without outflow. In cases where the potential damage at the left bank would be higher, the cases with outflow could result in higher damages than without outflow. Regarding cascade effects it can be concluded that the cascade effects do not have an influence on the total damage in this area. The effects of the cascade interactions are mainly observed in the redistribution of the risk over the dike ring areas at the right bank of the river. When ignoring the cascade effects it can be observed that the risk for dike ring area 48 increases, while for the other dike rings it decreases.

When considering the duration of the load, it is observed that while loads are generally lower, they last a lot longer. This shows that it is important to also consider time-dependence of failure mechanisms. If loads are a lot longer but lower, for instance piping failures will become much more dominant due to their time-dependence.

## Recommendations

In order to improve the model, several improvements are recommended, these are discussed below:

- Calibrate outflow of breaches

As was seen above the results for the new methodology are in line with what could be expected. However there are also a few quite large uncertainties in the analysis, especially in the fast inundation model. First of all the outflow of the breaches plays an important role in the results. As was seen in the comparison of scenarios 1, 2 and 3 the outflow at the breach locations has a large influence on the damage and resulting water levels. However, the outflow rate of the breach locations was not specifically calibrated and is thus uncertain.

- Investigate bias for specific scenarios

Secondly the hydraulic behaviour of the model is similar but not identical to the 2D simulations. This means that the model might have some bias in specific cases due to for instance an under- or overestimation of the propagation velocity of the flood water. If the model is to be used in further flood risk analysis for this area this should be investigated.

- Take length effects into account

The fragility curves used now originate from DAM and in this case length effects are not taken into account. This is for this case not too much of a problem and it is actually quite convenient as lower standard deviations yield more clear results in terms of dike breaches: more breaches are occurring at the same water levels and there are less 'outliers', thus resulting in a clearer view on the effects of load interdependencies. However, the fact that the length effect was not taken into account has to be kept in mind when considering the results for the case study, even though for the bigger picture the difference will most likely be marginal, considering the fact that exceedence probabilities were defined, and the calculations are not based upon real dike strengths. However, in further analysis of this area it is advisable to take length effects into account.

- Investigate polder side failures

Another uncertainty can be found in the definition of the fragility curves for polder side failures: it is now dealt with by shifting the fragility curves with a quite random value, not based on solid research. However, as could be seen from the results, in most cases the results for scenarios 1 and 2, where polder failures were and weren't considered are similar, so the influence is most likely not that big. In further analysis it might be worthwhile to investigate the behaviour of more dike cross sections for polder side failures. Also, in the model it was assumed that polder side failures completely depend on the water level in the polder. This might cause polder side failures for cases where the water level in the river is higher than in the polder. Therefore new failure definitions for polder failures should be based on a water level and a minimum head over the flood defence, in order to deal with this problem.

- Use more advanced triggers for failure mechanisms

Given the available data it was not feasible to use more advanced failure mechanisms in this case. However, as was seen in for instance paragraph 3.3.4 on fragility curves for piping failures, time has a significant influence on these failures. Given the results found on the change in duration of the discharge waves, in further research it is advisable to account for this in the model. Although water levels might be lower at some locations, they can have a much longer duration due to polder outflow. In order to correctly represent the effects of breaches on loads it is necessary to also account for load duration, as a long-lasting relatively low load might also lead to failure. This type of triggers cannot be defined in Sobek-1D Flow, therefore the use of the RTC (Real Time Control) module is advisable.

- Improve water level – damage curves

As was seen the water level – damage curves performed quite well for the selected scenarios. However, it is doubtful whether the same results would have been obtained if 13 other scenarios would have been used for calibration. Therefore it is advisable to investigate these curves and base them on more data from more scenarios.

- Include mitigating measures in cases with negative effects

In cases with negative effects in the model, the consequences were determined by the probabilistic distributions for the dike strength. However, in order to mitigate the effects, it might for instance be advisable to deliberately breach a dike at the Pannerdens Kanaal, in order to discharge more flood water through the Nederrijn/Lek and less through the IJssel. It seems worthwhile to investigate the implementation of such measures in the methodology.

## 5.8 Applications of the method on flood risk management in the IJssel area

As was shown in the case, both positive and negative interdependencies can have significant effects on flood risk calculations. However, the question is whether it is wise to consider these effects in all cases. Therefore in this paragraph a few applications on the case study area are discussed where positive and/or negative interdependencies should or should not be considered.

### Dike design

In case of dike design it is very important to consider negative load interdependencies. As was observed in for instance the study on dike ring 41 “Land van Maas en Waal” (Vrouwenvelder et al., 2010), the effect of negative load interdependencies can have a large influence on the total risk. In order to keep the risk at an acceptable level it is important that negative interdependencies are taken into account in the total risk calculation. Not taking them into account could result in a higher actual risk than acceptable, which could for instance be observed in the case study for water levels at Giesbeek. In the WV21 calculation of economic optimal safety standards negative effects were taken into account. This was visible in for instance a higher safety standard for the southern Waal dike, which prevents shortcutting to the Meuse. The same can be seen for the dike protecting dike ring 48, which, as was seen from the case study, can prevent cascade effects in the IJssel area if it is reinforced (Deltares, 2011). From the damage calculations it was shown that cascade and shortcutting effects have a significant contribution to the risk. Therefore in the case study area the dike at dike ring 48 should be reinforced.

When considering dike design it is very difficult to consider positive load interdependencies. When considering positive interdependencies and relief of downstream dikes in dike design, this can lead to a very complex situation, especially when a dike reach needs reinforcement. For instance, if we consider the conceptual case from Chapter 4, for which water levels at B, the most downstream location in the considered river, are shown in Figure 5-32, this can be shown by a simple example.

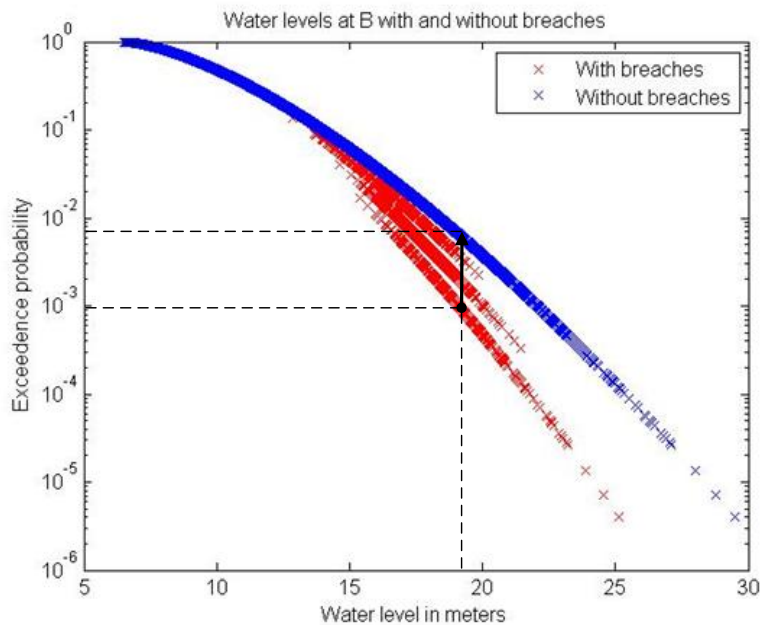


**Figure 5-32 Water levels in the conceptual case and the change in safety level in case upstream dikes are reinforced**

If we consider a situation where the dike at B has been designed with a safety standard of 1/1.000 year, it would have a crest level of approximately 18 meters, if positive load interdependencies are taken into account in the design. But, if at both upstream dikes the dikes are changed to for instance an unbreakable delta dike, suddenly the safety level at B drops to around 1/300 year. This shows that, if for dike design positive load interdependencies are taken into account, reinforcing one dike changes the safety level at all other dikes. If positive effects would be considered, it would thus be necessary to either raise all other dikes at the same time, or accept a lower safety level at all other areas. However, this does not seem a very workable situation. For instance, if in the case study the dike opposite to Spijk, at the other side of the river would be reinforced, the dike at Spijk would be less safe. Considering the enormous damage in case of breaching at Spijk, it is doubtful whether this reinforcement would have a positive effect on the total risk.

Another aspect when considering positive load interdependencies, is that for certain dike rings it is assumed that others fail first, thus providing relief. This has two difficult aspects. The first aspect is that it is assumed that another dike fails, while it is not supposed to fail, at least not in public opinion. However, a probably bigger problem is that dikes are designed for a certain time period. This implies that, for instance on weak soils, extra height to compensate settlements is applied. However, in flood risk analysis this is not taken into account and it is also not constant in time. When considering positive load interdependencies this would have as a consequence

that the load relief effect downstream would change (increase) over time, due to settlements upstream.

Considering the above examples and arguments it is not advisable to account for positive load interdependencies in dike design, negative load interdependencies have to be considered, as they can have a large influence on the consequences when a certain dike reach fails. This holds for both the case study area and in general.

**Prioritization of reinforcement projects**

When considering dike reinforcement projects it can be very useful to take load interdependencies into account. An example in Vietnam showed that load interdependencies can have a significant influence on the risk reduction of different dike reinforcement projects (Diermanse et al., 2007). It was even observed that some dike reinforcements would have a negative effect on the total risk. If load interdependencies and their effect on risk are considered in prioritizing dike reinforcement projects, it gives a better insight in the total effect of a certain measure. This enables better prioritization, as risk reduction is calculated more accurately when considering the whole system. Regarding the IJssel area, if we assume that the dike safety levels are changed to the WV21 levels shown in Figure 5-33, it can be seen that both dike reaches 48-1 and 50-1 have to be improved. However, from the results in the case study, it was shown that breaches at 48-1 have significant influence on the risk behind dike reach 50-1. Therefore it is better to first reinforce reach 48-1, as this provides a much bigger risk reduction.

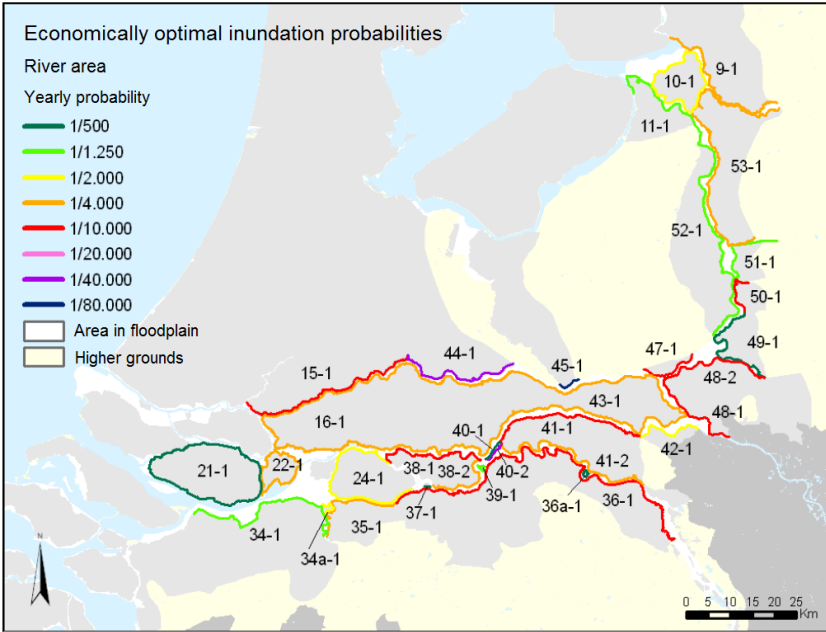


**Figure 5-33 Economically optimal inundation probabilities from WV21**

**Safety assessment**

In the Netherlands the safety of dikes is currently assessed using the VNK2-method. This method considers dike rings, but not the system around it. However, for safety assessments, is it useful to consider load interdependencies in this context? When checking whether a dike is strong enough it should be compared to how it was designed. For safety assessments it is thus not necessary to consider positive interdependencies. However, this changes when a dike is not up to standard at several locations. In those cases the different reinforcement projects need to be

prioritized. Thus, when doing a safety assessment the same assumptions as in the design have to be made. When the dikes need improvement however, this can be done more accurately by considering load interdependencies.

#### Calculations of Maximum Probable Damage

Insurance companies insuring flood risk are usually very interested in the Maximum Probable Damage: the maximum amount of money they would have to pay out in one realistically probable event. This determines the amount of re-insurance they need to take, in order to be able to pay out. If no load interdependencies, both positive and negative, would be taken into account, this would result in an overestimation of the Maximum Probable Damage. Therefore, it can be very rewarding to account for load interdependencies, as the Maximum Probable Damage will, in the case of the Netherlands, be significantly lower. When considering positive load interdependencies, for instance the amount of casualties will be significantly lower, the same will hold for the damage (De Bruijn et al., 2013). This was also observed for the case study area, where, although negative effects increased the risk at some locations, effects of positive interdependencies reduced the damage. Therefore insurance companies should account for load interdependencies.

#### Estimating loss of life

For loss of life estimation negative load interdependencies are not relevant, mainly due to the large time horizon of this type of floods. This causes the evacuation fractions to be high in those cases, so large numbers of extra casualties due to negative effects are not likely. Therefore the method is, aside from that it is not suitable for calculation of loss of life, also not needed. For the cases mentioned in the preceding paragraph, casualties should be considered in the same way as the economic damage, except for effects of negative load interdependencies with large time horizons. For instance in the case study, breaches at dike ring 48 might flood the whole IJssel catchment, but it would take at least a week before the flood would reach the downstream end. In those cases there is enough time to inform and evacuate people.

## 6. Conclusions and recommendations on the new methodology

The objective of this thesis, which was presented in Chapter 1 was:

*Develop a framework for flood risk analysis which enables accounting for load interdependencies of flood defences.*

From the literature studied, the general conclusion could be drawn that load interdependencies of flood defences can have a significant effect on flood risk. It can be concluded that positive load interdependencies are universal for lowland rivers, while negative load interdependencies are case specific. It was concluded that it is very important to consider these interdependencies in further flood risk analysis, but it was also concluded that there is no general method to do so. Based on previous research and a simple conceptual case model, it was concluded that there are two main indicators for assessing the effects of load interdependencies in flood risk analysis: the influence on the risk, and the influence of flood defence failures on water levels at other locations in the system. Also a set of main factors of influence on the effects of load interdependencies were defined, the most important and general ones are:

- Dike strength for polder side failures
- Timing of failures during a discharge wave
- Retention volume of polder

Other factors of influence are more case specific and/or not by definition characteristic for cases with load interdependencies, but generally important for assessing floods, the most important ones are:

- Breach size
- Locations of secondary dikes and elevation of land behind breaches
- Timing of discharge waves in cases of two rivers
- Width of discharge wave

In order to deal with the effects of load interdependencies in a probabilistic context, a fast calculation method was needed; as the commonly used methods in the Netherlands were not suitable for this type of problems. Therefore a combination of Monte Carlo with Importance Sampling and a fast inundation model were chosen.

In the case study the methodology defined in Chapter 4 has shown promising results. The results for the case study were in line with the basic principles found in literature and the conceptual case: depending on parameters and system properties, load interdependencies can have both positive and negative effects on flood defence loads. These effects are mainly observed in a change in water level probability distributions and also in a change of the risk distribution.

The results found from the case study were in line with what could be expected, although there are still quite some uncertainties in the case study model. However, it can be concluded that the new methodology shows promising results and copes with the many scenarios causing positive and negative load interdependencies quite well.

### *Conclusions on the performance of the methodology*

- The methodology used, deals with the problems risk analysis for large areas have in terms of computational efficiency. Commonly used methods in the Netherlands are not

suitable for large areas with many different scenarios, the new methodology deals with this problem: it is fast, mainly due to the use of Monte Carlo with Importance Sampling in combination with a fast inundation model. The results are found to be realistic although more analyses and more case studies are necessary, to be able to fully assess the value of the results found and the general performance of the methodology.

- The methodology of simulating floods with a fast inundation model, calibrated by a set of 2D flood scenarios works, although it is quite complex to calibrate the model, especially if this has to be done manually.
- The fast inundation model should not be used to investigate flood damage in specific scenarios: it is not accurate enough and in those cases 2D modelling is preferable.
- The performance of the water level – damage functions is in line with the expectations and yields realistic estimates for the economic risk. However, to obtain a more accurate risk estimation, it might be necessary to further calibrate these functions using more scenarios.

#### *Conclusions on the application of the methodology*

- As was shown in the results of the case study, the influence of load interdependencies is significant for the case study area. It can therefore be concluded that in calculations of flood risks, these effects need to be accounted for properly.
- Before using the method with the fast inundation model, it should be assessed qualitatively whether negative load interdependencies are of relevance for the case considered. If not, building a fast inundation model is a waste of time and current methods such as the VNK2-method with, if desired, adapted boundary conditions to account for positive load interdependencies, are more suitable for a proper estimation of flood risks.
- Positive load interdependencies are very useful for prioritizing dike reinforcement projects. When accounting for load interdependencies the estimates for risk reduction due to a certain dike improvement are more accurate, which enables a better use of the available money.
- For dike design it is not advisable to account for positive load interdependencies: any change in strength at a section might cause the rest of the dikes to become of insufficient strength. It is however necessary to account for negative interdependencies: the load increase caused by flood water flowing back into the river can be quite significant and can cause large increases in loads at certain locations.
- When studying negative interdependencies it is important to consider mitigating measures, such as controlled dike breaches, in order to reduce the negative effects.
- The nature of the fast inundation model is most likely not suitable for estimating casualties. As the hydrodynamic behaviour of the model is different from reality, it will be very difficult to correctly calculate flow velocities and rise rates, which are important for loss of life estimations. However, due to the fact that negative interactions such as shortcutting take place over longer time periods, the methodology is most likely not relevant for loss of life calculations.

#### *Subjects for further study*

Further study on methodologies accounting for load interdependencies should compare the use of different modelling techniques and their performance: in Germany and the United Kingdom for instance the use of storage cell models is quite wide spread. It would be interesting to

compare computational performance and accuracy with 2D modelling and the fast inundation model used in this research, in order to get a better view on the computational performance of the methods for cases at lowland rivers. Also it can be investigated what the effect of more advanced breach formulas and different breach widths is on the results.

Another improvement would be to optimize the fast inundation model. Currently there are quite some inaccuracies in flood propagation and flood levels: by using more data and an optimization algorithm the inaccuracy in the model could be decreased. This would also make it possible to use these models in a more general context: by using data from existing 2D simulations and a simple schematization of an area, it would be possible to build a relatively accurate fast inundation model.

The magnitude of the consequences of load interdependencies is quite case dependent. In some cases it might for instance be possible to mitigate consequences by controlled dike breaches, in order to avoid uncontrolled breaches at other locations. Especially given the relatively long time available before for instance shortcutting occurs, it is very well possible that there are options to mitigate effects during a crisis. To further improve the study on the effects of load interdependencies, this type of measures should be investigated and if possible included in the computational method.



## 7. References

- Apel, H., Merz, B., and Thielen, A.H. (2009a). Influence of dike breaches on flood frequency estimation. *Computers & Geosciences* 35, 907–923.
- Apel, H., Aronica, G.T., Kreibich, H., and Thielen, A.H. (2009b). Flood risk analyses—how detailed do we need to be? *Nat Hazards* 49, 79–98.
- Asselman, N. (2009). Flood modelling: model choice and proper application (Deltares).
- Bates, P., and De Roo, A.P.. (2000). A simple raster-based model for flood inundation simulation. *Journal of Hydrology* 236, 54–77.
- Beckers, J., and de Bruijn, K. (2011). Analyse van slachtofferrisico's Waterveiligheid 21e eeuw (Deltares).
- Bockarjova, M., Rietveld, P., and Verhoef, E. (2012). Composite Valuation of Immaterial Damage in Flooding: Value of Statistical Life, Value of Statistical Evacuation and Value of Statistical Injury (Rochester, NY: Social Science Research Network).
- De Bruijn, K., and van der Doef, M. (2011). Gevolgen van overstromingen - Informatie ten behoeve van het project Waterveiligheid in de 21e eeuw (Delft: Deltares).
- De Bruijn, K.M., Diermanse, F., van Zandvoort, E., and Kramer, N. (2013). A new method to assess societal flood risk (Delft: Deltares).
- Buijs, F., Simm, J., Wallis, M., and Sayers, P. (2007). Performance and reliability of flood and coastal defences (London: DEFRA/Environment Agency Flood and Coastal Erosion Risk Management R&D Programme (Great Britain)).
- CUR Publicatie 190 (1997). Probabilities in civil engineering, Part 1: Probabilistic design in theory (Gouda: Stichting CUR).
- Van Dantzig, D. (1956). Economic decision problems for flood prevention. *Econometrica* 24, 276–287.
- Dawson, R., and Hall, J. (2006). Adaptive importance sampling for risk analysis of complex infrastructure systems. *Proc. R. Soc. A* 462, 3343–3362.
- Dawson, R., Hall, J., Sayers, P., Bates, P., and Rosu, C. (2005). Sampling-based flood risk analysis for fluvial dike systems. *Stoch Environ Res Ris Assess* 19, 388–402.
- Deltacommissie (1961). Rapport Deltacommissie. Deel 1. Eindverslag en interimadviezen (SDU).
- Deltares (2009). LTV-O&M thema Veiligheid deelproject 2: Vergelijking Nederlandse en Vlaamse (maatgevende) waterstandsverlopen en modelleringswijzen voor de bepaling van overstromingskarakteristieken bij een doorbraak langs het Schelde-estuarium.
- Deltares (2011). Maatschappelijke kosten-batenanalyse Waterveiligheid 21e eeuw (Delft: Deltares).
- Deltares (2013). SOBEK User Manual.
- Diermanse, F., Sloff, K., and Ogink, H. (2007). Flood risk analysis for the Bac Hung Hai polder, Vietnam (WL|Delft Hydraulics).

- Engel, H. (2002). *Das Augusthochwasser 2002 im Elbegebiet* (Koblenz: Bundesanstalt für Gewässerkunde).
- Van der Ham, W., and van de Ven, G.P. (2004). *Afleiden of opruimen : de strijd om de beste aanpak tegen het rivierbederf : een beschouwing van 300 jaar rivierverbetering in het kader van de spankrachtstudie* (RWS, RIZA).
- Hesselink, A.W., Stelling, G.S., Kwadijk, J.C.J., and Middelkoop, H. (2003). Inundation of a Dutch river polder, sensitivity analysis of a physically based inundation model using historic data. *Water Resources Research* 39, n/a–n/a.
- Horritt, M.S., and Bates, P.D. (2002). Evaluation of 1D and 2D numerical models for predicting river flood inundation. *Journal of Hydrology* 268, 87–99.
- Ter Horst, W.L.A. (2005). *How safe are Dikes during Flood Waves? Analysis of the Failure Probability of Dike Ring Areas in Flood Wave Situations.*
- Ter Horst, W.L.A. (2012). *Veiligheid Nederland in Kaart 2 Overstromingsrisico van dijkringgebieden 14, 15 en 44.*
- Infrastructure Development Institute (2002). *Report on Preliminary Study of the Elbe River Floods.*
- Jongejan, R.B., Stefess, R., Roode, N., ter Horst, W.L.A., and Maaskant, B. (2011). *The VNK2 project: a detailed, large-scale quantitative flood risk analysis for the Netherlands. (Tokyo-Japan),.*
- Jonkman, S.N. (2007). *Loss of life estimation in flood risk assessment; theory and applications. Civil Engineering and Geosciences.*
- Jonkman, S.N., van Gelder, P.H.A.J.M., and Vrijling, J.K. (2003). An overview of quantitative risk measures for loss of life and economic damage. *J. Hazard. Mater.* 99, 1–30.
- Jonkman, S.N., Kok, M., and Vrijling, J.K. (2008). Flood risk assessment in The Netherlands: a case study for dike ring South Holland. *Risk Anal.* 28, 1357–1374.
- Kalyanapu, A.J., Shankar, S., Pardyjak, E.R., Judi, D.R., and Burian, S.J. (2011). Assessment of GPU computational enhancement to a 2D flood model. *Environmental Modelling & Software* 26, 1009–1016.
- Kalyanapu, A.J., Judi, D.R., McPherson, T.N., and Burian, S.J. (2012). Monte Carlo-based flood modelling framework for estimating probability weighted flood risk. *Journal of Flood Risk Management* 5, 37–48.
- Kanning, W. (2012). *The Weakest Link: Spatial Variability in the Piping Failure Mechanism of Dikes.* Dissertation. TU Delft.
- Van der Knaap, F. (2000). *Breach growth as a function of time* (Delft: WL|Delft Hydraulics).
- Kok, M., Huizinga, H.J., Vrouwenfelder, A.C.W.M., and van den Braak, W.E.W. (2005). *Standaardmethode 2005 Schade en Slachtoffers als gevolg van overstromingen.*
- Van der Meer, J., ter Horst, W., and van Velzen, E. (2008). Calculation of fragility curves for flood defence assets. In *Flood Risk Management: Research and Practice*, W. Allsop, P. Samuels, J. Harrop, and S. Huntington, eds. (CRC Press),.

- Van Mierlo, M., Schweckendiek, T., and Courage, W. (2008). Importance of river system behaviour in assessing flood risk. In *Flood Risk Management: Research and Practice*, W. Allsop, P. Samuels, J. Harrop, and S. Huntington, eds. (CRC Press),.
- Van Mierlo, M.C.L.M., Gudden, J.J., and Overmars, J.M.S. (2003). Calibratie DelftFLS model, Noordrijn-Westfalen en Gelderland (WL|Delft Hydraulics).
- Van Mierlo, M.C.L.M. (2005a). Verkenning van systeemwerking in het bovenriviereengebied van de Rijntakken (WL|Delft Hydraulics).
- Van Mierlo, M.C.L.M. (2005b). Reductie overstromingsschade door systeemwerking (veiligheidsdiscussie) (WL|Delft Hydraulics).
- Van Mierlo, M.C.L.M., and van Buren, R. (2006a). Uitwerking systeemwerking Maas (WL|Delft Hydraulics).
- Van Mierlo, M.C.L.M., and van Buren, R. (2006b). Verkenning systeemwerking in Nederland (WL|Delft Hydraulics).
- Van Mierlo, M.C.L.M., and Vrouwenfelder, A.C.W.M. (2007). Assessment of flood risk accounting for river system behaviour. *International Journal of River Basin Management* 5, 93–104.
- Van Mierlo, M.C.L.M., Vrouwenfelder, A.C.W.M., Calle, E.O.F., Vrijling, J.K., Jonkman, S.N., de Bruijn, K., and Weerts, A.H. (2003). Effects of River System Behaviour on Flood Risk (Delft: Delft Cluster).
- Mierzwa, M. (2005). Methodology for Flow and Salinity Estimates in the Sacramento-San Joaquin Delta and Suisun Marsh Chapter 3: Jones Tract 2004 Levee Break DSM2 Simulation.
- Ministerie van Infrastructuur en Milieu (2005). Veiligheid Nederland in Kaart: overstromingsrisico dijkkring 48 Rijn en IJssel.
- Ministerie van Verkeer en Waterstaat (2007). Hydraulische Randvoorwaarden primaire waterkeringen voor de derde toetsronde 2006-2011.
- Olson, K.R., and Morton, L.W. (2012a). The impacts of 2011 induced levee breaches on agricultural lands of Mississippi River Valley. *Journal of Soil and Water Conservation* 67, 5A–10A.
- Olson, K.R., and Morton, L.W. (2012b). The effects of 2011 Ohio and Mississippi river valley flooding on Cairo, Illinois, area. *Journal of Soil and Water Conservation* 67, 42A–46A.
- Sayers, P., and Meadowcroft, I. (2005). RASP: A hierarchy of risk-based methods and their application. (University of York),.
- Slijkhuis, K.A., van Gelder, P.H.A.J.M., and Vrijling, J.K. (1997). Optimal dike height under statistical-, damage- and construction-uncertainty. *Structural Safety and Reliability* vol. 7, 1137–1140.
- Stelling, G.S. (2012). Quadtree flood simulations with sub-grid digital elevation models. *Proceedings of the ICE - Water Management* 165, 567–580.
- TAW (1985). Leidraad voor het ontwerpen van rivierdijken: Deel 1: Bovenriviereengebied (Rijkswaterstaat, DWW).

- TAW (1998). Grondslagen voor waterkeren (Technische Adviescommissie voor de Waterkeringen).
- TAW (1999). Technisch rapport zandmeevoerende wellen (Delft: Technische Adviescommissie voor de Waterkeringen).
- TAW (2000). Van overschrijdingskans naar overstromingskans (Den Haag: Rijkswaterstaat, DWW).
- Verheij, H. (2003). Aanpassen van het bresgroeimodel in HIS-OM (WL|Delft Hydraulics).
- Ververs, M., and Klijn, F. (2004). Werken noodoverloopgebieden? Lessen uit de overstromingen van 1926. Geografie.
- VNK2 project office (2012). Flood Risk in the Netherlands VNK2: The method in brief.
- Vorogushyn, S., Merz, B., and Apel, H. (2009). Development of dike fragility curves for piping and micro-instability breach mechanisms. *Nat. Hazards Earth Syst. Sci.* 9, 1383–1401.
- Vorogushyn, S., Merz, B., Lindenschmidt, K.-E., and Apel, H. (2010). A new methodology for flood hazard assessment considering dike breaches. *Water Resources Research* 46.
- Vorogushyn, S., Lindenschmidt, K.-E., Kreibich, H., Apel, H., and Merz, B. (2012). Analysis of a detention basin impact on dike failure probabilities and flood risk for a channel-dike-floodplain system along the river Elbe, Germany. *Journal of Hydrology* 436–437, 120–131.
- Vrijling, J.K., Kok, M., Calle, E.O.F., Epema, W.G., Van der Meer, M.T., Van den Berg, P., and Schweckendiek, T. (2010). Piping: Realiteit of Rekenfout? (Rijkswaterstaat, Waterdienst).
- Vrouwenvelder, A.C.W.M., Steenbergen, H.M.G.M., and Slijkhuis, K.A.. (1999). Theoriehandleiding PC-ring Deel A: Mechanismebeschrijvingen (Delft: TNO Bouw).
- Vrouwenvelder, A.C.W.M., Van Mierlo, M.C.L.M., Calle, E.O.F., Markus, A.A., Schweckendiek, T., and Courage, W.M.G. (2010). Risk analysis for flood protection systems (Delft Cluster).
- Waterwet (2009). Waterwet.
- Van der Wiel, W.D. (2004). Probabilistic risk assessment of a system of dike ring areas (TU Delft, Faculty of Civil Engineering and Geosciences, Hydraulic Engineering).
- Zwanenburg, C., van Duinen, A., and Rozing, A. (2013). Technisch rapport Macrostabieliteit (Deltares).





# Appendix

---

## List of figures in Appendix

Figure A-1 Set up of the societal risk tool .....	118
Figure A-2 Sampling functions used in the societal risk tool.....	119
Figure A-3 Sobek-RE Deltarijn model.....	120
Figure A-4 FN-curve results from societal risk tool .....	120
Figure A-5 Number of breaches found from societal risk tool.....	121
Figure B-6 Schematic representation of overtopping for both sides of a dike.....	122
Figure B-7 Dike cross section from VNK2 study on dike ring 48.....	123
Figure B-8 Critical sliding circle for the most critical case considered .....	124
Figure H-9 Overview of which profiles were used where in the model.....	139
Figure H-10 Dummy branch profile .....	140
Figure H-11 Profile A.....	141
Figure H-12 Profile B.....	141
Figure H-13 Profile L .....	142
Figure H-14 Profile O.....	142
Figure H-15 Storage of area a .....	143
Figure H-16 Storage of area b .....	143
Figure H-17 Storage of area c.....	144
Figure H-18 Storage of area d .....	144
Figure H-19 Storage of area e .....	145
Figure H-20 Storage of area f .....	145
Figure H-21 Storage of area g .....	146
Figure H-22 Storage of area i .....	146
Figure J-23 Water level - damage curve for Flood zone 48_1.....	149
Figure J-24 Water level - damage curve for Flood zone 48_2.....	149
Figure J-25 Water level - damage curve for Flood zone 48_3.....	149
Figure J-26 Water level - damage curve for Flood zone 48_4.....	150
Figure J-27 Water level - damage curve for Flood zone 48_5.....	150
Figure J-28 Water level - damage curve for Flood zone 48_6.....	150
Figure J-29 Water level - damage curve for Flood zone 48_7.....	151
Figure J-30 Water level - damage curve for Flood zone 49 .....	151
Figure J-31 Water level - damage curve for Flood zone 50 .....	151
Figure J-32 Water level - damage curve for Flood zone 51 .....	152
Figure J-33 Water level - damage curve for Flood zone 53_1.....	152
Figure J-34 Water level - damage curve for Flood zone 53_2.....	152
Figure J-35 Water level - damage curve for Flood zone 53_3.....	153
Figure J-36 Water level - damage curve for Flood zone 53_4.....	153
Figure K-37 Water level and return frequencies at Germany_1.....	154
Figure K-38 Water level and return frequencies at Spijk.....	154
Figure K-39 Water level and return frequencies at Loo .....	155
Figure K-40 Water level and return frequencies at Giesbeek .....	155
Figure K-41 Water level and return frequencies at Vierakker.....	156
Figure K-42 Water level and return frequencies at 't Schol .....	156
Figure K-43 Water level and return frequencies at Deventer .....	157
Figure K-44 Water level and return frequencies at Olst.....	157
Figure K-45 Water level and return frequencies at De Nijenstein .....	158
Figure K-46 Water level and return frequencies at IJcentrale .....	158

Figure L-47 FD curve for dike ring 49 .....	159
Figure L-48 FD curve for dike ring 50 .....	159
Figure L-49 FD curve for dike ring 51 .....	160
Figure L-50 FD curve for dike ring 53 .....	160

### List of tables in Appendix

Table E-1 Standard discharge waves at Lobith .....	130
Table F-2 Combined fragility curves .....	133
Table G-3 Layout of Sobek input sheets .....	136
Table I-4 Water levels for 2D and the fast inundation model for dike ring area 48 .....	147
Table I-5 Water levels for 2D and the fast inundation model for other locations .....	148

## A The societal risk assessment tool by Deltares

### A.1 Tool for assessing societal risks

At Deltares a new type of tool has been developed in order to calculate societal risks for the Netherlands as a whole. The aim is to calculate the FN-curve in the Netherlands while taking positive load interdependencies into consideration. This is done by combining a hydrodynamic model with a probabilistic framework including dike strength, boundary conditions and evacuation scenarios. The considered area consists of both the tidal and non-tidal area of the Dutch water system. This Appendix aims to give a short summary of the set-up of the project and especially the for this research important aspects. More details can be found in De Bruijn et al. (2013).

### A.2 Set up of the tool

The tool made consists of 2 main components: the probabilistic framework consisting of sampling load and strength variables as well as the evacuation fractions and the hydrodynamic model. A set-up is shown in Figure A-1.

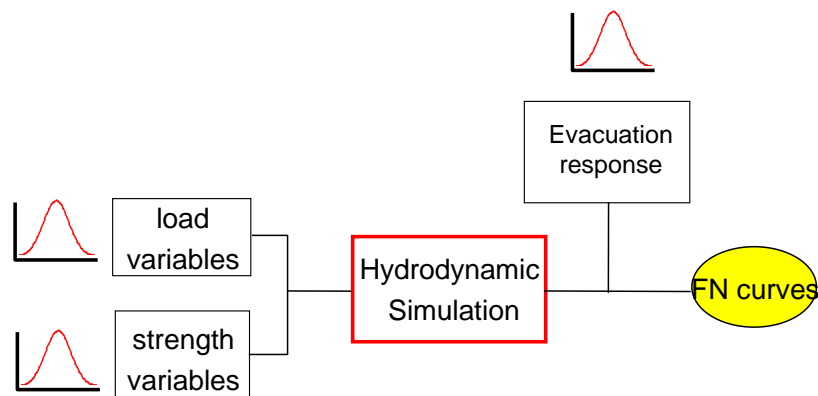


Figure A-1 Set up of the societal risk tool

First the load and strength variables are sampled using Monte Carlo with Importance Sampling. After that a set of Sobek scenarios is generated and run in a 1D Sobek-RE model. During post-processing the evacuation fractions are used to calculate the number of fatalities for each scenario. This results in an FN curve for the Netherlands.

### A.3 Probabilistic framework

The main part of the probabilistic framework deals with the sampling of load and strength variables. Another part deals with evacuation scenarios, these are not considered in this research so they are not elaborated further. The main point of this is that different scenarios for 3 areas in the system (upper river, transition and tidal river area) are considered with different evacuation fractions.

#### Sampling of load variables

In this case, 4 relevant load variables are identified: the discharge of the river Rhine at Lobith, the discharge of the river Meuse at Lith, the sea water level at Hoek van Holland and the functioning of the storm surge barrier near Hoek van Holland. These river discharges are sampled from their respective statistical distributions for peak discharges, using uniform importance sampling. By using a scaled discharge wave these are then converted to time series

for the discharge. The sea water levels are also derived using the statistical distribution for tidal peak levels at the Maasmond. By using a standard hydrograph for the length of the high water a time series for the sea level can be generated. Two types of scenarios are considered: scenarios with high sea water levels and moderate discharges and scenarios without storm surge but with extreme discharges. The barrier is a third factor: it can fail in cases with high sea water levels. The timing of both upstream and downstream boundary conditions is taken care of by assuming that the discharges at Meuse and Rhine occur at the same time. Also the Meuse discharge is correlated to the Rhine discharge with  $\rho = 0.6$ . for the sea water level it is assumed that, in cases where there are high sea water levels the peak sea water level is 2 days after the high river discharge. Due to this assumption the high waters arrive approximately at the same time in the transitional area.

**Sampling of resistance variables**

For the resistance values from the fragility curves for the different breach locations are used. Fragility curves of 3 failure mechanisms, overtopping, piping and macrostability, were sampled and combined in order to get one fragility curve for each location.

**Monte Carlo with Importance Sampling**

In order to do a Monte Carlo simulation it was necessary to apply Importance Sampling in order to reduce the number of required runs for a stable calculation. This was done using the functions in Figure A-. These functions were used after testing a variety of sampling density functions for their bias and standard deviations. The two shown in the figure are the best for the respective boundary conditions.

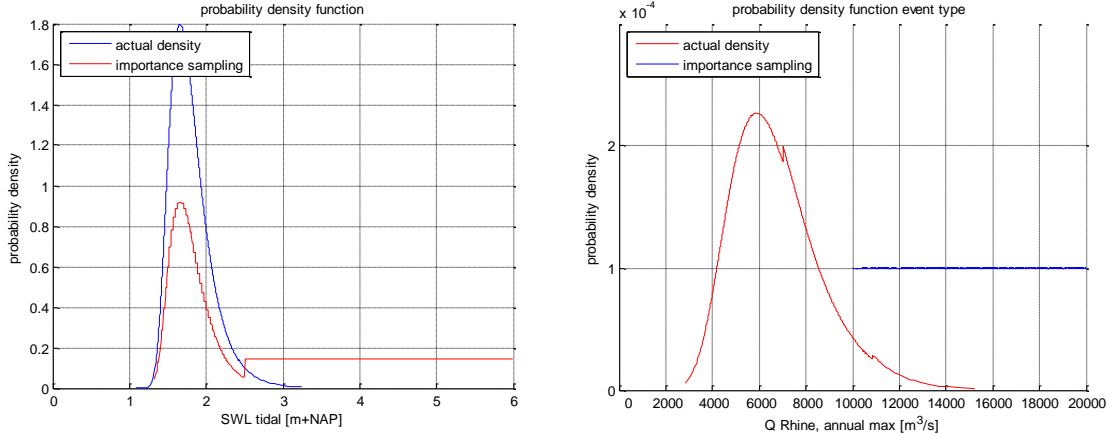


**Figure A-2 Sampling functions used in the societal risk tool**

In addition to the sampled boundary conditions for each scenario a dike strength was sampled for the strength distribution for all dike breach locations.

#### A.4 Hydrodynamic model simulation

The scenarios with the sampled values are then converted to Sobek input which was then used in the Deltarijn model in Sobek-RE, which is shown in Figure A-3.

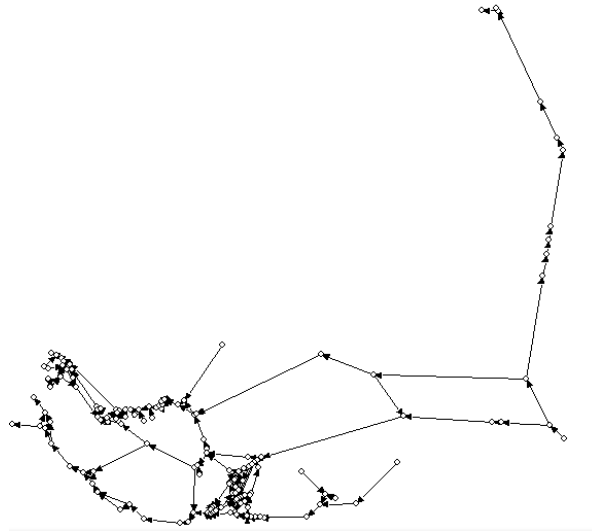


Figure A-3 Sobek-RE Deltarijn model

The breaches in the model are described by a simple standard breach growth based on the formula by Verheij - van der Knaap (2003). The simulation time was 1 month with a 10 minute time step.

#### A.5 Results

The results from this tool for assessing societal risk showed that the influence of positive load interdependencies and relief is quite significant as can be seen from the FN-curve in Figure 5.8-4. This case used the probabilities from WV21.

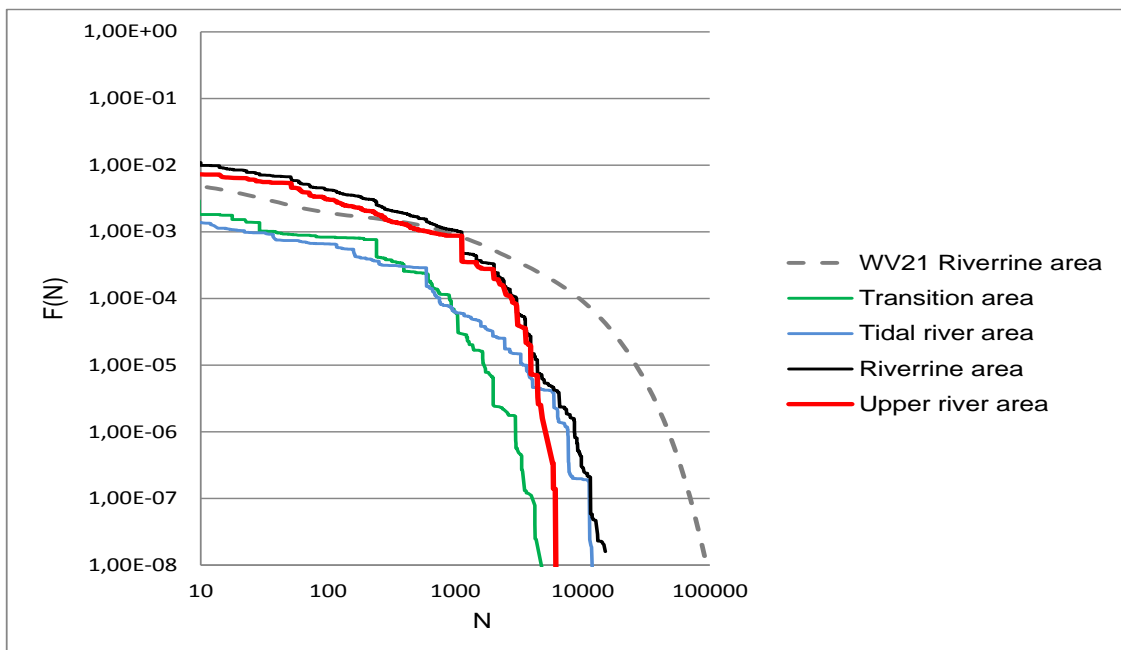


Figure 5.8-4 FN-curve results from societal risk tool

This shows that by the new method of incorporating positive load interdependencies the expected number of fatality is much lower, especially for extreme scenarios. It was also observed that when accounting for load interdependencies the number of breaches decreased significantly, as is shown in Figure 5.8-5.

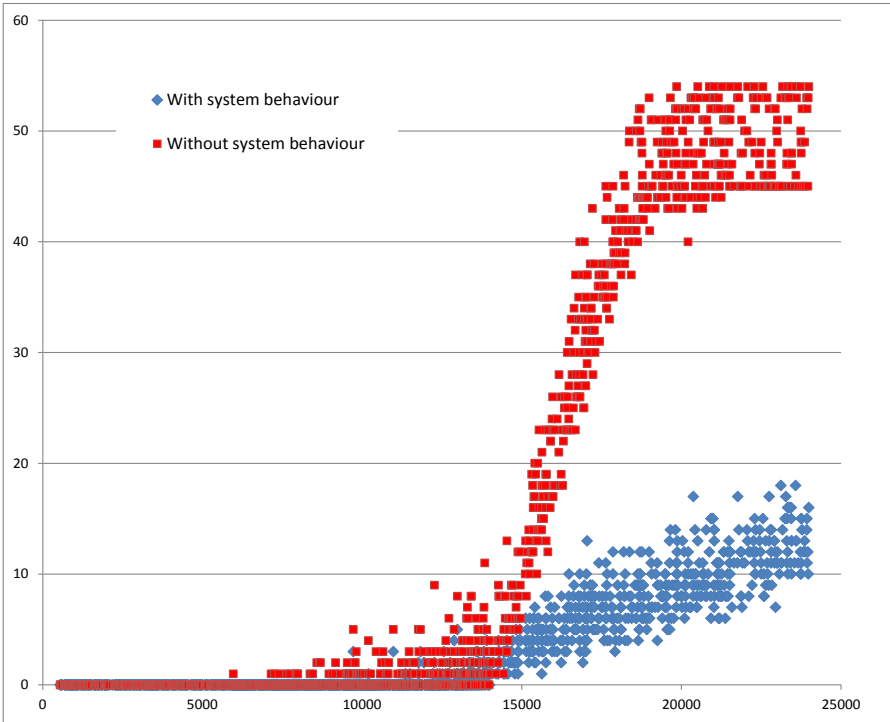


Figure 5.8-5 Number of breaches found from societal risk tool

All in all the societal risk assessment tool showed that the influence of load interdependencies is large, although the uncertainty in the model is also large. It also has to be noted that negative interdependencies are not taken into account. More details can be found in the report by De Bruijn et al. (2013).

## B Dike stability in case of inner slope loading

In case of a loading from the polder side of the dike it was suggested that the dikes behave differently. When negative interactions such as shortcutting occur a strange situation occurs: the dike, protecting the land from the river is loaded from the polder side. As dikes are designed for resisting loads on the outer slope of the dike this is not the situation they were designed for. As the failure of the dike determines the extent of the negative interactions it is very important to at least have an idea of what happens. Therefore the three main failure mechanisms are compared for outer and inner slope loading under a set of circumstances.

### B.1 Overtopping

The effect of overtopping from the inside of the dike is difficult to determine. What happens is shown in Figure B-6.

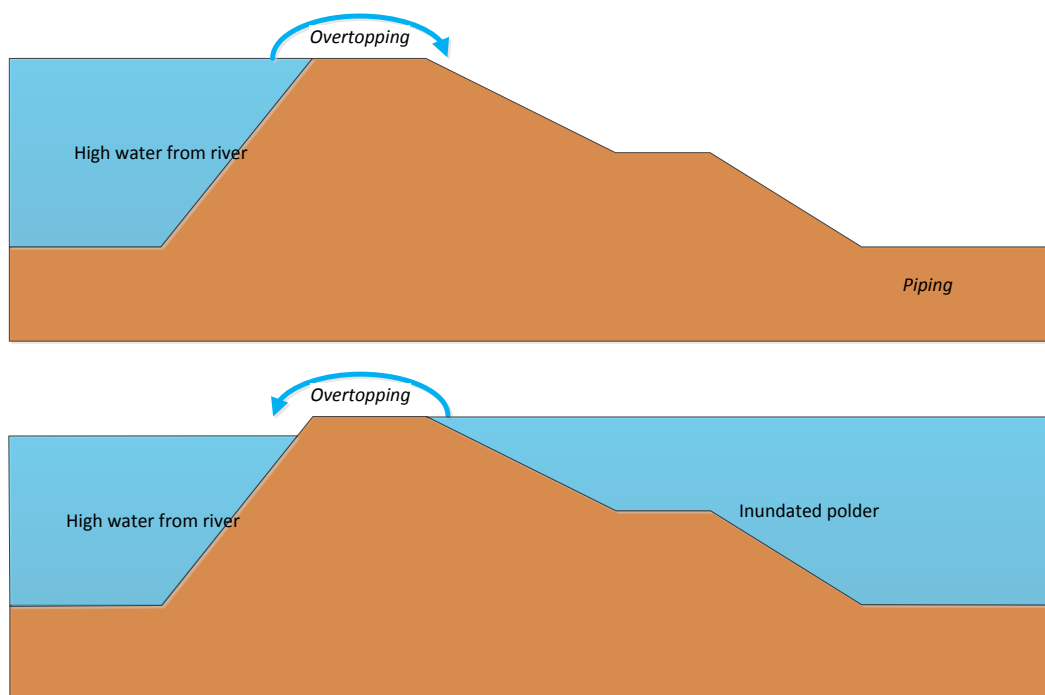


Figure B-6 Schematic representation of overtopping for both sides of a dike

What can be seen in Figure B-6, is that when the water in the river is high and the dike overtops from the inside, the flow velocity of the overtopping water will be relatively low due to the small head. Therefore the grass cover will most likely stay intact. On the other hand, the dike is completely soaked with water and thus potentially quite weak, especially if the water level in the river lowers, instability will be quite plausible.

If there is a high water level at both sides of the dike, it doesn't matter too much whether the dike fails or not, when it overtops as the head over the dike is relatively small so the breaching will not influence the discharge too much. Therefore it is assumed that, when overtopping starts, regardless of the water level at the outer side of the dike, breaching will initiate and grow according to the normal process.

## B.2 Piping

Due to the build-up of dikes, with a steep outer slope and a relatively flat inner slope, and the fact that there is water on both sides, failure due to piping will be very unlikely. Especially instability will have occurred long before the pipes are sufficiently developed to let the dike fail. Therefore, given the small head and relative importance of piping compared to other mechanisms, piping is not considered for inverse dike failures.

## B.3 Instability of the outer slope

Due to the design of most dikes, dikes are quite stable when loaded from the river, but once the load is imposed on the other side this is not the case anymore. As most dikes have a steep outer slope and a flatter inner slope the stability when loads are imposed from the river side is quite good. When the loads are imposed from the polder side however, there is a lot less stability. Using D-GeoStability, a program provided by Deltares a simple investigation was done on a set of dikes. The dikes considered are not real in terms of exact geotechnical properties, only the geometries as used in the VNK study of dike ring 48 were used (Ministerie van Infrastructuur en Milieu, 2005). The calculation method is the method by Bishop which was introduced in Chapter 2. The choice of the dikes is based on the most common structure of Dutch river dikes and the geometry used is a cross section at dike ring 48.

## B.4 Instability of the outer slope of a cross section in dike ring 48 when assuming a complete clay dike

The dike considered consists of soft clay ( $\rho=14 \text{ kN/m}^3$ ,  $c=8 \text{ kN/m}^2$ ,  $\varphi=20^\circ$ ) and has the following geometry, derived from the VNK2 study on dike ring 48 'Rijn en IJssel':

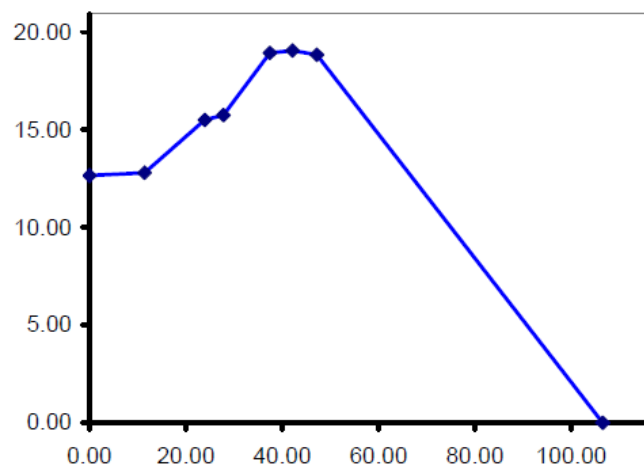


Figure B-7 Dike cross section from VNK2 study on dike ring 48

To check the influence of the direction of the load and the water levels on both sides of the dike on the safety coefficient 4 different cases are considered:

- Case 1: high water at the river, piezometric level at the polder 1.5 meters below ground level
- Case 2: high water at the river, polder slightly inundated with 3.4 meters of water above ground level
- Case 3: high water at polder, water level at river 13.5 meters below crest level
- Case 4: high water at polder, water level at river 3 meters below crest level

When calculating the stability for these situations this gives the following safety coefficients:

	Water level at polder	Water level at river	Safety coefficient
Case 1	low	high	1.75
Case 2	medium	high	2.13
Case 3	high	low	0.84
Case 4	high	medium	1.75

It has to be noted that the phreatic level inside the dike is assumed to be linear, this is not a completely correct representation of reality but it is sufficient for the goal of this short investigation. Given the results it can be concluded that indeed for high water levels at polders and lower levels at the river the dike quickly becomes unstable. In Case 3 the safety coefficient is not even half of the design situation in Case 1. Figure B-8 shows the critical slip circle for Case 3.

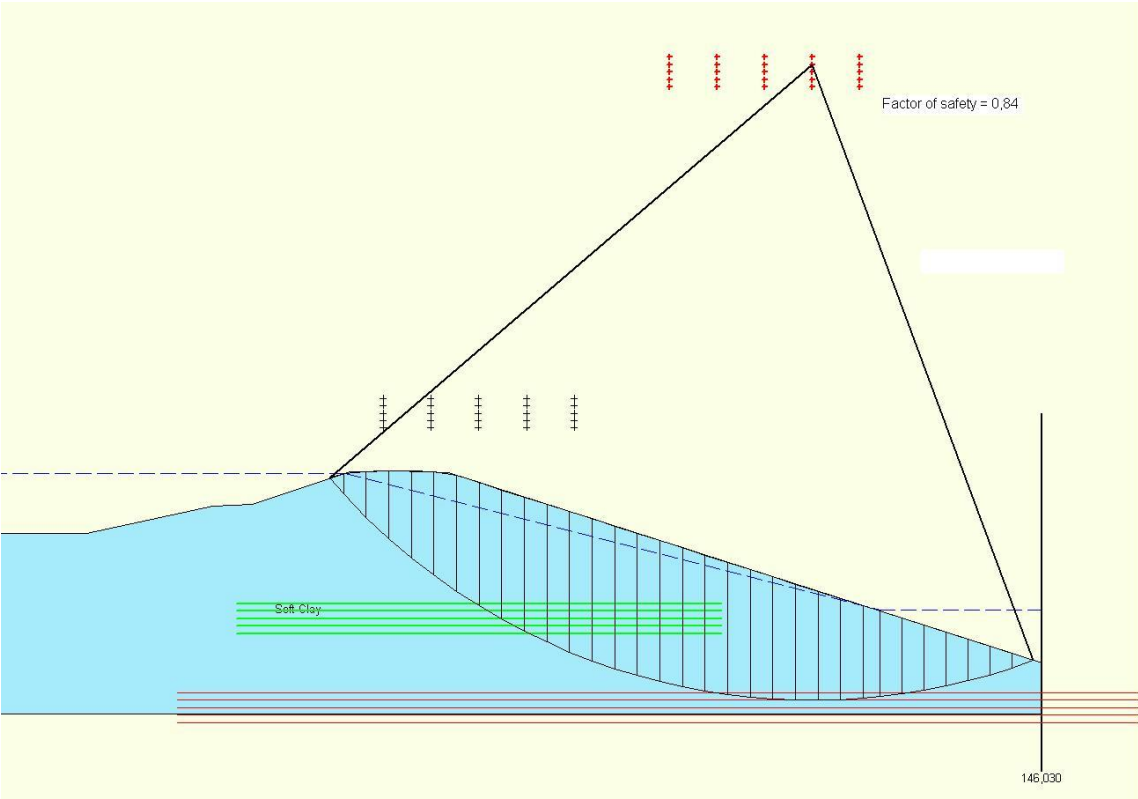


Figure B-8 Critical sliding circle for the most critical case considered

Based on the found factors of safety for the different cases it can be concluded that in terms of stability dikes are significantly weaker when loaded from the polder side.

## C MATLAB script used for the conceptual case

This appendix shows the script used for the conceptual case in Chapter 4. The script shown is for the case with negative effects, however by changing the comment markers to the right lines in the code it is also useable for the positive effects.

```
clear all
close all
%%PARAMETERS
%RIVER 1
L1_0=10000; L1_1=10000; L1_2=15000; L1_3=15000; L1_4=50000;
C1=45; i1=10^-4; h0_1=10; B1=400;
%RIVER 2
L2_0=35000; L2_1=25000; L2_2=5000; L2_3=50000;
C2=45; i2=10^-4; h0_2=10; B2=250;
%BOUNDARY CONDITIONS
%River 1
X=linspace(0,20000,1000);
P1=1-expcdf(X,1600);
Q1=X;
%River 2
X=linspace(0,20000,1000);
P2=1-expcdf(X,1200);
Q2=X;
Q1_100=expinv((1-(1/100)),1600)
Q2_100=expinv((1-(1/100)),1200)
H1_100=((Q1_100/B1).^2)/(C1.^(2)*i1).^(1/3); %Dike design level
H2_100=((Q2_100/B2).^2)/(C2.^(2)*i2).^(1/3); %Dike design level
%%Monte Carlo Simulation
V=0.1;
n=250000;
for i=1:n,
Q1(i)=exprnd(1600);
Q2(i)=Q1(i)*(2/3);
P_Q1(i)=1-expcdf(Q1(i),1600);
P_Q2(i)=1-expcdf(Q2(i),1600);
%Ha_dike(i)=normrnd(H1_100,V*H1_100);
%Hb_dike(i)=normrnd(H1_100,V*H1_100);
Hc_dike(i)=normrnd(H1_100,V*H1_100);
Hd_dike(i)=normrnd(H2_100,V*H2_100);
He_dike(i)=normrnd(H2_100,V*H2_100);
Hw1(i)=(((Q1(i)/B1).^2)/(C1.^(2)*i1)).^(1/3);
Hw2(i)=(((Q2(i)/B2).^2)/(C2.^(2)*i2)).^(1/3);
end
%BREACHES
%Here the breach parameters are written. These are fragility curves
%from a normal distribution
%Breach discharge
C_b=0.1;
C_bthrough=3;
%Breach a
%Hb_a=h0_1-i1*L1_0; %Bottom level
%Hd_a=Hb_a+Ha_dike; %Dike crest level
% %Breach b
%Hb_b=h0_1-i1*(L1_0+L1_1+L1_2);
%Hd_b=Hb_b+Hb_dike; %Dike crest level
% %Breach c
Hb_c=h0_1-i1*(L1_0+L1_1);
Hd_c=Hb_c+Hc_dike; %Dike crest level
% %Breach d
Hb_d=h0_2-i2*(L2_0+0.5*L2_1);
Hd_d=Hb_d+Hd_dike;
% %Breach e
Hb_e=h0_2-i2*(L2_0+L2_1);
Hd_e=Hb_e+He_dike;
% %Breach f
% Hb_f=h0_2-i2*(L2_0+L2_1+0.5*L2_2);
```

```

%Water levels
%Ha0=Hb_a+Hw1;
%Hb0=Hb_b+Hw1;
Hc0=Hb_c+Hw1;
Hd0=Hb_d+Hw2;
He0=Hb_e+Hw2;
%Ha0_nobreaches=Ha0;
%Hb0_nobreaches=Hb0;
Hc0_nobreaches=Hc0;
Hd0_nobreaches=Hd0;
He0_nobreaches=He0;
%Za0=Hd_a-Ha0;
%Zb0=Hd_b-Hb0;
Zc0=Hd_c-Hc0;
Zd0=Hd_d-Hd0;
Ze0=Hd_e-He0;
%Za0_nobreaches=Hd_a-Ha0;
%Zb0_nobreaches=Hd_b-Hb0;
Zc0_nobreaches=Hd_c-Hc0;
Zd0_nobreaches=Hd_d-Hd0;
Ze0_nobreaches=Hd_e-He0;
Z0=zeros(n,3);
Zmin=zeros(n,1);
Zmin1=zeros(n,1);
%Qa=Q1;
%Qb=Q1;
Qc=Q1;
Qd=Q2;
Qe=Q2;
%Breach 1
for i=1:n,
    %First loop, let first dike breach
    if Zc0(i)<0 | Zd0(i)<0 | Ze0(i)<0,
        Zmin1(i)=min(Zc0(i),Zd0(i));
        Zmin(i)=min(Ze0(i),Zmin1(i));
        if Zmin(i)==Zc0(i)
            Z0(i,1)=1;
        elseif Zmin(i)==Zd0(i)
            Z0(i,2)=1;
        elseif Zmin(i)==Ze0(i)
            Z0(i,3)=1;
        end
        %Qa(i)=Q1(i)-Z0(i,1)*C_b*Q1(i);
        Qc(i)=Q1(i)-Z0(i,1)*C_b*Q1(i);
        %Qb(i)=Q1(i)-Z0(i,1)*C_b*Q1(i)-Z0(i,2)*C_b*Qa(i)-Z0(i,3)*C_b*Qb(i);
        Qd(i)=Q2(i)-Z0(i,2)*C_b*Q2(i)+Z0(i,1)*C_b*Q1(i)*C_bthrough;
        Qe(i)=Q2(i)-Z0(i,2)*C_b*Q2(i)-Z0(i,3)*Qd(i)+Z0(i,1)*C_b*Q1(i)*C_bthrough;
        %Ha_proc(i)=(((Qa(i)/B1).^2)/(C1.^2*i1)).^(1/3);
        %Hb_proc(i)=(((Qb(i)/B1).^2)/(C1.^2*i1)).^(1/3);
        Hc_proc(i)=(((Qc(i)/B1).^2)/(C1.^2*i1)).^(1/3);
        Hd_proc(i)=(((Qd(i)/B2).^2)/(C2.^2*i2)).^(1/3);
        He_proc(i)=(((Qe(i)/B2).^2)/(C2.^2*i2)).^(1/3);
        %Ha0(i)=Hb_a+Ha_proc(i);
        %Hb0(i)=Hb_b+Hb_proc(i);
        Hc0(i)=Hb_c+Hc_proc(i);
        Hd0(i)=Hb_d+Hd_proc(i);
        He0(i)=Hb_e+He_proc(i);
        %Za0(i)=Hd_a(i)-Ha0(i);
        %Zb0(i)=Hd_b(i)-Hb0(i);
        Zc0(i)=Hd_c(i)-Hc0(i);
        Zd0(i)=Hd_d(i)-Hd0(i);
        Ze0(i)=Hd_e(i)-He0(i);
    end
    %set Z-values to very high
    if Zc0(i)<0 && Z0(i,1)==1
        Zc0(i)=99;
    end
    if Zd0(i)<0 && Z0(i,2)==1
        Zd0(i)=99;
    end
    if Ze0(i)<0 && Z0(i,3)==1
        Ze0(i)=99;
    end
end

```

```

%second breach
if Zc0(i)<0 | Zd0(i)<0 | Ze0(i)<0,
    Zmin1(i)=min(Zc0(i),Zd0(i));
    Zmin(i)=min(Ze0(i),Zmin1(i));
    if Zmin(i)==Zc0(i)
        Z0(i,1)=1;
    elseif Zmin(i)==Zd0(i)
        Z0(i,2)=1;
    elseif Zmin(i)==Ze0(i)
        Z0(i,3)=1;
    end
    %Qa(i)=Q1(i)-Z0(i,1)*C_b*Q1(i);
    Qc(i)=Q1(i)-Z0(i,1)*C_b*Q1(i);
    %Qb(i)=Q1(i)-Z0(i,1)*C_b*Q1(i)-Z0(i,2)*C_b*Qa(i)-Z0(i,3)*C_b*Qb(i);
    Qd(i)=Q2(i)-Z0(i,2)*C_b*Q2(i)+Z0(i,1)*C_b*Q1(i)*C_bthrough;
    Qe(i)=Q2(i)-Z0(i,2)*C_b*Q2(i)-Z0(i,3)*C_b*Qd(i)+Z0(i,1)*C_b*Q1(i)*C_bthrough;
    %Ha_proc(i)=(((Qa(i)/B1).^2)/(C1.^2*i1)).^(1/3);
    %Hb_proc(i)=(((Qb(i)/B1).^2)/(C1.^2*i1)).^(1/3);
    %Hc_proc(i)=(((Qc(i)/B1).^2)/(C1.^2*i1)).^(1/3);
    %Hd_proc(i)=(((Qd(i)/B2).^2)/(C2.^2*i2)).^(1/3);
    %He_proc(i)=(((Qe(i)/B2).^2)/(C2.^2*i2)).^(1/3);
    %Ha0(i)=Hb_a+Ha_proc(i);
    %Hb0(i)=Hb_b+Hb_proc(i);
    %Hc0(i)=Hb_c+Hc_proc(i);
    %Hd0(i)=Hb_d+Hd_proc(i);
    %He0(i)=Hb_e+He_proc(i);
    %Za0(i)=Hd_a(i)-Ha0(i);
    %Zb0(i)=Hd_b(i)-Hb0(i);
    %Zc0(i)=Hd_c(i)-Hc0(i);
    %Zd0(i)=Hd_d(i)-Hd0(i);
    %Ze0(i)=Hd_e(i)-He0(i);
end
%set Z-values to very high
if Zc0(i)<0 && Z0(i,1)==1
    Zc0(i)=99;
end
if Zd0(i)<0 && Z0(i,2)==1
    Zd0(i)=99;
end
if Ze0(i)<0 && Z0(i,3)==1
    Ze0(i)=99;
end

%third breach
if Zc0(i)<0 | Zd0(i)<0 | Ze0(i)<0,
    Zmin1(i)=min(Zc0(i),Zd0(i));
    Zmin(i)=min(Ze0(i),Zmin1(i));
    if Zmin(i)==Zc0(i)
        Z0(i,1)=1;
    elseif Zmin(i)==Zd0(i)
        Z0(i,2)=1;
    elseif Zmin(i)==Ze0(i)
        Z0(i,3)=1;
    end
    %Qa(i)=Q1(i)-Z0(i,1)*C_b*Q1(i);
    Qc(i)=Q1(i)-Z0(i,1)*C_b*Q1(i);
    %Qb(i)=Q1(i)-Z0(i,1)*C_b*Q1(i)-Z0(i,2)*C_b*Qa(i)-Z0(i,3)*C_b*Qb(i);
    Qd(i)=Q2(i)-Z0(i,2)*C_b*Q2(i)+Z0(i,1)*C_b*Q1(i)*C_bthrough;
    Qe(i)=Q2(i)-Z0(i,2)*C_b*Q2(i)-Z0(i,3)*C_b*Qd(i)+Z0(i,1)*C_b*Q1(i)*C_bthrough;
    %Ha_proc(i)=(((Qa(i)/B1).^2)/(C1.^2*i1)).^(1/3);
    %Hb_proc(i)=(((Qb(i)/B1).^2)/(C1.^2*i1)).^(1/3);
    %Hc_proc(i)=(((Qc(i)/B1).^2)/(C1.^2*i1)).^(1/3);
    %Hd_proc(i)=(((Qd(i)/B2).^2)/(C2.^2*i2)).^(1/3);
    %He_proc(i)=(((Qe(i)/B2).^2)/(C2.^2*i2)).^(1/3);
    %Ha0(i)=Hb_a+Ha_proc(i);
    %Hb0(i)=Hb_b+Hb_proc(i);
    %Hc0(i)=Hb_c+Hc_proc(i);
    %Hd0(i)=Hb_d+Hd_proc(i);
    %He0(i)=Hb_e+He_proc(i);
    %Za0(i)=Hd_a(i)-Ha0(i);
    %Zb0(i)=Hd_b(i)-Hb0(i);
    %Zc0(i)=Hd_c(i)-Hc0(i);
    %Zd0(i)=Hd_d(i)-Hd0(i);
    %Ze0(i)=Hd_e(i)-He0(i);
end
end

```

```
%set Z-values to very high
if Zc0(i)<0 && Z0(i,1)==1
    Zc0(i)=99;
end
if Zd0(i)<0 && Z0(i,2)==1
    Zd0(i)=99;
end
if Ze0(i)<0 && Z0(i,3)==1
    Ze0(i)=99;
end
end
```

## **D Building of the fast inundation model**

In this Appendix, in addition to the comments made in the Main Report regarding the build-up of the models, a few additional remarks are made regarding some behaviour of the models encountered in this research.

### **D.1 Making of the 1D model**

In order to combine the two models for the German part of the Rhine and the Netherlands the models were bot cut to their desired size. The original German part of the model stretched from Andernach to Pannerden, but was cut to the part from Wesel to Pannerden, while the part of the Dutch model used stretched from Lobith to the three downstream boundaries. The original model consisted of all main rivers and canals in the Netherlands. All irrelevant branches were deleted.

In combining the models a problem was encountered. Due to problems in Sobek the friction layer files were not copied correctly, causing wrong errors in the friction of all branches in the model. By cleaning up the model using the Clean-up tool in Sobek 2.13.002 and by correcting the wrongly copied lines in the friction file, this was solved.

### **D.2 Making of the 2D model**

To be able to do the 2D simulations necessary for gathering knowledge on the flood patterns in the area a 2D model was added. The model used was a Delft FLS model, the same as was used in VNK2. However, as this model did not include the most downstream part of the banks of the IJssel these had to be obtained differently. This was done by using AHN data and land use data. The two elevation and friction grids were then merged in ArcGIS.

The breaches used in the 2D model were 1D dam breach branches. The formula used was the van der Knaap formula for which the maximum breach width was set to 200 meters. The initial width was set to be 25 meters. The breaking depth was set to the approximate land level behind the breach and the discharge coefficient to 1. Other possibilities such as a general structure as was used in the fast inundation model were also considered but the use of the 1D Dam Break branch is very easy and convenient.

### **D.3 Building the fast inundation model**

The fast inundation model was built based upon the flood patterns found from the 2D model. By investigating the flood patterns of the different scenarios it was possible to derive a general flow pattern which was then used. In order to get the water levels as close to the level in the 2D model as possible, the model was calibrated using the data from elevation and friction data. After that, in order to get better results, the frictions and some of the elevations and widths of the dummy branches were changed. Eventually nearly all dummy branches, except the ones connecting the inundation model to the river were given a very low friction. It was found to be very important to start with the real values such as the height of the secondary flood defences in order to avoid strange behavior, as changing the height of for instance an inner dike might improve performance for one scenario but might also decrease the performance for the other scenarios.

## E Discharge waves

The discharge waves used are shown in the table below. The first column shows the time, the second column the value for the scaled discharge wave, the last columns show the resulting values for the 1/100, 1/1.000 and 1/10.000 year discharge waves. The values are not given for every time step but for every 6 hours.

Table E-1 Standard discharge waves at Lobith

Time before or after peak [days]	Normalized value [-]	1/100-year discharge [m <sup>3</sup> /s]	1/1,000-year discharge [m <sup>3</sup> /s]	1/10,000-year discharge [m <sup>3</sup> /s]
-11	0,146644	6000	6000	6000
-10,75	0,168446	6000	6000	6000
-10,50	0,190249	6000	6000	6000
-10,25	0,212052	6000	6000	6000
-10,00	0,233855	6000	6000	6000
-9,75	0,255657	6000	6000	6000
-9,50	0,27746	6000	6000	6000
-9,25	0,299263	6000	6000	6000
-9,00	0,321066	6000	6000	6000
-8,75	0,342868	6000	6000	6377,35
-8,50	0,364671	6000	6000	6782,881
-8,25	0,386474	6000	6028,991	7188,412
-8,00	0,408277	6000	6369,114	7593,943
-7,75	0,430079	6000	6709,236	7999,474
-7,50	0,451882	6000	7049,359	8405,005
-7,25	0,473685	6063,165	7389,482	8810,536
-7,00	0,494063	6324	7707,375	9189,563
-6,75	0,518125	6632	8082,75	9637,125
-6,50	0,538938	6898,4	8407,425	10024,24
-6,25	0,558875	7153,6	8718,45	10395,08
-6,00	0,575938	7372	8984,625	10712,44
-5,75	0,603438	7724	9413,625	11223,94
-5,50	0,628125	8040	9798,75	11683,13
-5,25	0,6475	8288	10101	12043,5
-5,00	0,665	8512	10374	12369
-4,75	0,6825	8736	10647	12694,5
-4,50	0,699375	8952	10910,25	13008,38
-4,25	0,715	9152	11154	13299
-4,00	0,730625	9352	11397,75	13589,63
-3,75	0,74625	9552	11641,5	13880,25
-3,50	0,761875	9752	11885,25	14170,88
-3,25	0,779375	9976	12158,25	14496,38
-3,00	0,79625	10192	12421,5	14810,25
-2,75	0,813125	10408	12684,75	15124,13
-2,50	0,8325	10656	12987	15484,5
-2,25	0,853125	10920	13308,75	15868,13
-2,00	0,875	11200	13650	16275
-1,75	0,89625	11472	13981,5	16670,25
-1,50	0,916875	11736	14303,25	17053,88

-1,25	0,935	11968	14586	17391
-1,00	0,953125	12200	14868,75	17728,13
-0,75	0,96875	12400	15112,5	18018,75
-0,50	0,98125	12560	15307,5	18251,25
-0,25	0,994375	12728	15512,25	18495,38
0,00	1	12800	15600	18600
0,25	0,99625	12752	15541,5	18530,25
0,50	0,984375	12600	15356,25	18309,38
0,75	0,9725	12448	15171	18088,5
1,00	0,95875	12272	14956,5	17832,75
1,25	0,9425	12064	14703	17530,5
1,50	0,923125	11816	14400,75	17170,13
1,75	0,903125	11560	14088,75	16798,13
2,00	0,8825	11296	13767	16414,5
2,25	0,865	11072	13494	16089
2,50	0,848125	10856	13230,75	15775,13
2,75	0,831875	10648	12977,25	15472,88
3,00	0,8175	10464	12753	15205,5
3,25	0,804375	10296	12548,25	14961,38
3,50	0,790625	10120	12333,75	14705,63
3,75	0,776875	9944	12119,25	14449,88
4,00	0,764375	9784	11924,25	14217,38
4,25	0,751875	9624	11729,25	13984,88
4,50	0,739375	9464	11534,25	13752,38
4,75	0,726875	9304	11339,25	13519,88
5,00	0,715	9152	11154	13299
5,25	0,703125	9000	10968,75	13078,13
5,50	0,69125	8848	10783,5	12857,25
5,75	0,67875	8688	10588,5	12624,75
6,00	0,666875	8536	10403,25	12403,88
6,25	0,654375	8376	10208,25	12171,38
6,50	0,6425	8224	10023	11950,5
6,75	0,630625	8072	9837,75	11729,63
7,00	0,618875	7921,6	9654,45	11511,08
7,25	0,607688	7778,4	9479,925	11302,99
7,50	0,596063	7629,6	9298,575	11086,76
7,75	0,584688	7484	9121,125	10875,19
8,00	0,573308	7338,346	8943,609	10663,53
8,25	0,561872	7191,963	8765,205	10450,82
8,50	0,550436	7045,58	8586,801	10238,11
8,75	0,539	6899,197	8408,397	10025,4
9,00	0,527564	6752,814	8229,992	9812,683
9,25	0,516127	6606,431	8051,588	9599,971
9,50	0,504691	6460,049	7873,184	9387,258
9,75	0,493255	6313,666	7694,78	9174,545
10,00	0,481819	6167,283	7516,376	8961,833
10,25	0,470383	6020,9	7337,972	8749,12
10,50	0,458947	6000	7159,568	8536,408
10,75	0,44751	6000	6981,164	8323,695
11,00	0,436074	6000	6802,76	8110,983

11,25	0,424638	6000	6624,355	7898,27
11,50	0,413202	6000	6445,951	7685,557
11,75	0,401766	6000	6267,547	7472,845
12,00	0,39033	6000	6089,143	7260,132
12,25	0,378894	6000	6000	7047,42
12,50	0,367457	6000	6000	6834,707
12,75	0,356021	6000	6000	6621,994
13,00	0,344585	6000	6000	6409,282
13,25	0,333149	6000	6000	6196,569
13,50	0,321713	6000	6000	6000
13,75	0,310277	6000	6000	6000
14,00	0,29884	6000	6000	6000
14,25	0,287404	6000	6000	6000
14,50	0,275968	6000	6000	6000
14,75	0,264532	6000	6000	6000
15,00	0,253096	6000	6000	6000
15,25	0,24166	6000	6000	6000
15,50	0,230223	6000	6000	6000
15,75	0,218787	6000	6000	6000
16,00	0,207351	6000	6000	6000
16,25	0,195915	6000	6000	6000
16,50	0,184479	6000	6000	6000
16,75	0,173043	6000	6000	6000
17,00	0,161606	6000	6000	6000
17,25	0,15017	6000	6000	6000
17,50	0,138734	6000	6000	6000
17,75	0,127298	6000	6000	6000
18,00	0,115862	6000	6000	6000
18,25	0,104426	6000	6000	6000
18,50	0,09299	6000	6000	6000
18,75	0,081553	6000	6000	6000
19,00	0,072023	6000	6000	6000

## F Fragility curves

In the table below the values for the fragility curve of all 22 breach locations for both river and polder side failures are shown. All values are in meters. These values are based upon the original fragility curves for overtopping, piping and macrostability. The curves are shifted to the design level.

Table F-2 Combined fragility curves

Breach location	River side		Polder side	
	$\mu$	$\sigma$	$\mu$	$\sigma$
Olst	6,90	0,24	6,89	0,24
IJcentrale	5,00	0,24	4,79	0,28
Deventer	7,40	0,24	7,40	0,24
DeNijenstein	6,60	0,24	6,38	0,35
Gemaal Terwolde	7,40	0,24	7,19	0,36
't Schol	8,20	0,24	7,98	0,36
Cortenoever	11,10	0,24	11,10	0,24
Gorssel Noord	8,10	0,23	8,08	0,25
Mettray	8,50	0,24	8,50	0,24
Vierakker	9,80	0,24	9,73	0,25
Zuivering Olburgseweg	11,10	0,24	11,09	0,24
Giesbeek	11,60	0,24	11,57	0,24
Loo	15,30	0,27	15,10	0,47
Kandia	15,60	0,24	15,60	0,24
Herwen	17,30	0,29	17,09	0,48
Gravenswaardsedam	17,80	0,28	17,59	0,49
Spijk	18,40	0,30	17,85	0,54
Hoven-Zuid	8,20	0,24	7,99	0,36
Hoven-Noord	8,10	0,24	7,89	0,36
Germany_1	19,20	0,30	18,64	0,54
Germany_2	22,90	0,30	22,35	0,55
Germany_3	21,50	0,31	20,95	0,54

## F.1 Script for shifting and combining fragility curves

This script shows how the fragility curves were combined and how the fragility curves for the polder side were derived.

```
clear all
close all
BreachInfo = readBreachInfos('all', []);
nlocs=22;
Breachfile = 'Boven_benedenrivierengebied_breslocatieoverzicht.xls';
DesignLevel = xlsread(Breachfile, 'SobekuitvoerStatistiek_154som', 'D:D');
FragilityCurves=BreachInfo.FragilityCurves;
FragCurv=zeros(22,2);
BreachLocNames = BreachInfo.BreachLocNames;
n=10000;
for j=1:nlocs
    i=1;
    for i=1:n
        FC1(i)=normrnd(FragilityCurves(j,1,1),FragilityCurves(j,2,1));
        FC2(i)=normrnd(FragilityCurves(j,1,2),FragilityCurves(j,2,2));
        FC3(i)=normrnd(FragilityCurves(j,1,3),FragilityCurves(j,2,3));
    end
    FCtotal=[FC1; FC2; FC3]';
    FCmin=min(FCtotal, [],2);
    [mu1,sigma1,muci1,sigmaci1] = normfit(FCmin);

    FragCurv(j,1)=mu1;
    MU_1(j,1)=mu1;
    FragCurv(j,2)=sigma1;
end
FragCurv(:,1)=DesignLevel;
%% Now, define the fragility curves for the polder side
j=1;
F_instab=1; %height with which the instability fragility curve is decreased
FragCurvInside(:,1,1)=FragilityCurves(:,1,1);
FragCurvInside(:,1,2)=65000*ones(1,22);
FragCurvInside(:,1,3)=FragilityCurves(:,1,3)-F_instab;
FragCurvInside(:,2,:)=FragilityCurves(:,2,:);

FragCurvIn=zeros(22,2);
for j=1:nlocs
    i=1;
    for i=1:n
        FC1in(i)=normrnd(FragCurvInside(j,1,1),FragCurvInside(j,2,1));
        FC2in(i)=normrnd(FragCurvInside(j,1,2),FragCurvInside(j,2,2));
        FC3in(i)=normrnd(FragCurvInside(j,1,3),FragCurvInside(j,2,3));
    end

    FCtotalin=[FC1in; FC2in; FC3in]';
    FCminin=min(FCtotalin, [],2);
    %
    [mu2,sigma2,muci2,sigmaci2] = normfit(FCminin);

    FragCurvIn(j,1)=mu2;
    MU_2(j,1)=mu2;
    FragCurvIn(j,2)=sigma2;
    dFragCurvIn(j,1)=DesignLevel(j)-MU_1(j);
end
%%Shift curves to norm level
FragCurvIn(:,1)=FragCurvIn(:,1)+dFragCurvIn(:,1);
%% write resulting fragility curves to excel file
ncurves = size(FragCurv,2);
FCurves = NaN(nlocs,2*ncurves);
for j=1:nlocs
    FCurves(j,1:2) = FragCurv(j,:);
    FCurves(j,3:4) = FragCurvIn(j,:);
end
% prevent annoying warning
warning('OFF','MATLAB:xlswrite:AddSheet');
% open excel-file
outputfile='intermediate\CombFrag.xls';
if exist(outputfile,'file')>0
    delete(outputfile);
end
end
```

```

% values
M = cell(nlocs+1, ncurves);
M{1,1} = 'Bresnaam';
for j=1
    M{1,j+1} = ['mu' num2str(j)];
    M{1,j+2} = ['sd' num2str(j)];
    M{1,j+3} = ['mu' num2str(j+1)];
    M{1,j+4} = ['sd' num2str(j+1)];
end
M(2:end,1) = BreachLocNames;
M(2:end,2) = num2cell(FCurves(:,1));
M(2:end,3) = num2cell(FCurves(:,2));
M(2:end,4) = num2cell(FCurves(:,3));
M(2:end,5) = num2cell(FCurves(:,4));
xlswrite(outputfile, M, 'sheet1');

% delete empty excel sheets
deleteEmptyExcelSheets([pwd filesep outputfile]);

```

## G Sobek input sheets

The input sheets used for the Monte Carlo simulation in Sobek have the structure shown in Table G-3. The first column gives the scenario number, the second the peak discharge for the Rhine at Wesel, the third column gives the annual non-exceedence probability for the scenario. Then there are columns with trigger levels for the triggers for both polder side and river side failures for all breaches. These values as well as the discharge are read by a tool in order to make N Sobek schematizations with various parameters.

**Table G-3 Layout of Sobek input sheets**

			“Breach name”		“Breach name”	
Scenario	Q_Rhine [m <sup>3</sup> /s]	P [-]	H_riv [m]	H_land [m]	H_riv [m]	H_land [m]
1	22777,2	0,999995	7,147	7,205	4,957	4,811
2	7605,56	0,712294	7,172	6,598	5,082	5,134
3	8111,2	0,784171	6,774	7,129	5,196	4,544
4	23064,01	0,999996	6,529	6,917	5,167	4,43
5	8373,68	0,815044	7,218	6,562	5,066	5,129
...						
N						

## G.1 Script for generating Sobek input sheets

This script shows how the input sheets for the Monte Carlo simulation in Sobek were generated. The script uses functions from Open Earth Tools and some other smaller scripts which are not shown here.

```
N=1000; %Number of simulations
% copy original fragility curves to other location
copyfile('input_new\Fragility_initial.xls', 'intermediate\Fragility.xls');
% link paths
if isempty(which('readStochasts.m'))
    addpath(genpath_exclude(pwd, {'output'}));
end
% read structure with breach information
BreachInfo = readBreachInfos('all', []);
FragCurvFile = 'intermediate/CombFrag.xls';
FragCurves = xlsread(FragCurvFile, 'sheet1');
nlocs=length(FragCurves);
stochast = struct('Name', [], 'Distr', [], 'Params', []);
    stochast.Distr = @werklijn_inv;
    XP = xlsread('input_new\StatisticsRHineMeuse.xls', 'QRAM');
    stochast.Params = num2cell(XP);
    stochast.Params = {XP};
    stochast.Name = 'QRAM';
%% SAMPLING OF DISCHARGE
%%Importance Sampling
ind=0;
ind=ind+1;
IS(ind).Name = 'QRAM';
[dummy, idd] = ismember(IS(ind).Name, {'QRAM'});
ISR=[];
%importance sampling through X-values
IS(ind).Method = @prob_is_x;
ISR(1).Distr = @unif; % uniform
ISR(1).Params = {6000 24000}; % boundaries
ISR(2).Distr = str2func(strrep(func2str(stochast.Distr), '_inv', '')); % actual
distribution function
ISR(2).Params = stochast(idd).Params; % parameters of actual distribution function
IS(ind).Params =ISR;

%%Sample discharges
result=MC( ...
    'stochast', stochast, ...
    'NrSamples', N, ...
    'x2zVariables', {'BreachInfo', BreachInfo}, ...
    'x2zFunction', @x2zMHWP2 ...
    'IS', IS ...
);
%% SAMPLING OF FRAGILITY CURVES
for i=1:N
    for j=1:nlocs
        H_out(i,j)=normrnd(FragCurves(j,1), FragCurves(j,2));
        H_in(i,j)=normrnd(FragCurves(j,3), FragCurves(j,4));
    end
end
end
%% GENERATE OUTPUT FILE
MCOutPutDir = MakeDateDir('output');

Q=result.Output.x;
P=result.Output.P;

outputfile=[MCOutPutDir filesep 'inputsheetSobek.xls'];
if exist(outputfile, 'file')>0
    delete(outputfile);
end
M= cell(N,nlocs+2);
M(2,1)={'Scenario'};
M(2,2)={'Q_Rhine [m3/s]'};
M(2,3)={'P [-]'};
M(3:N+2,2)=num2cell(roundoff(Q,2));
M(3:N+2,3)=num2cell(P);
```

```
for i=1:nlocs
M(1,2+2*i)=BreachInfo.BreachLocNames(i);
M(2,2+2*i)={'H_riv [m]'};
M(2,3+2*i)={'H_land [m]'};
M(3:N+2,2+2*i)=num2cell(roundoff(H_out(:,i),3));
M(3:N+2,3+2*i)=num2cell(roundoff(H_in(:,i),3));
end
i=1
ScNr=zeros(1000,1);
for i=1:N
    ScNr(i)=i;
end
M(3:N+2)=num2cell(ScNr(:));
xlswrite(outputfile, M, 'InvoerFile');
```

## H Profiles in the fast inundation model

In the map below the different types of profiles are shown. The profiles based on GIS data are also shown on the following pages.

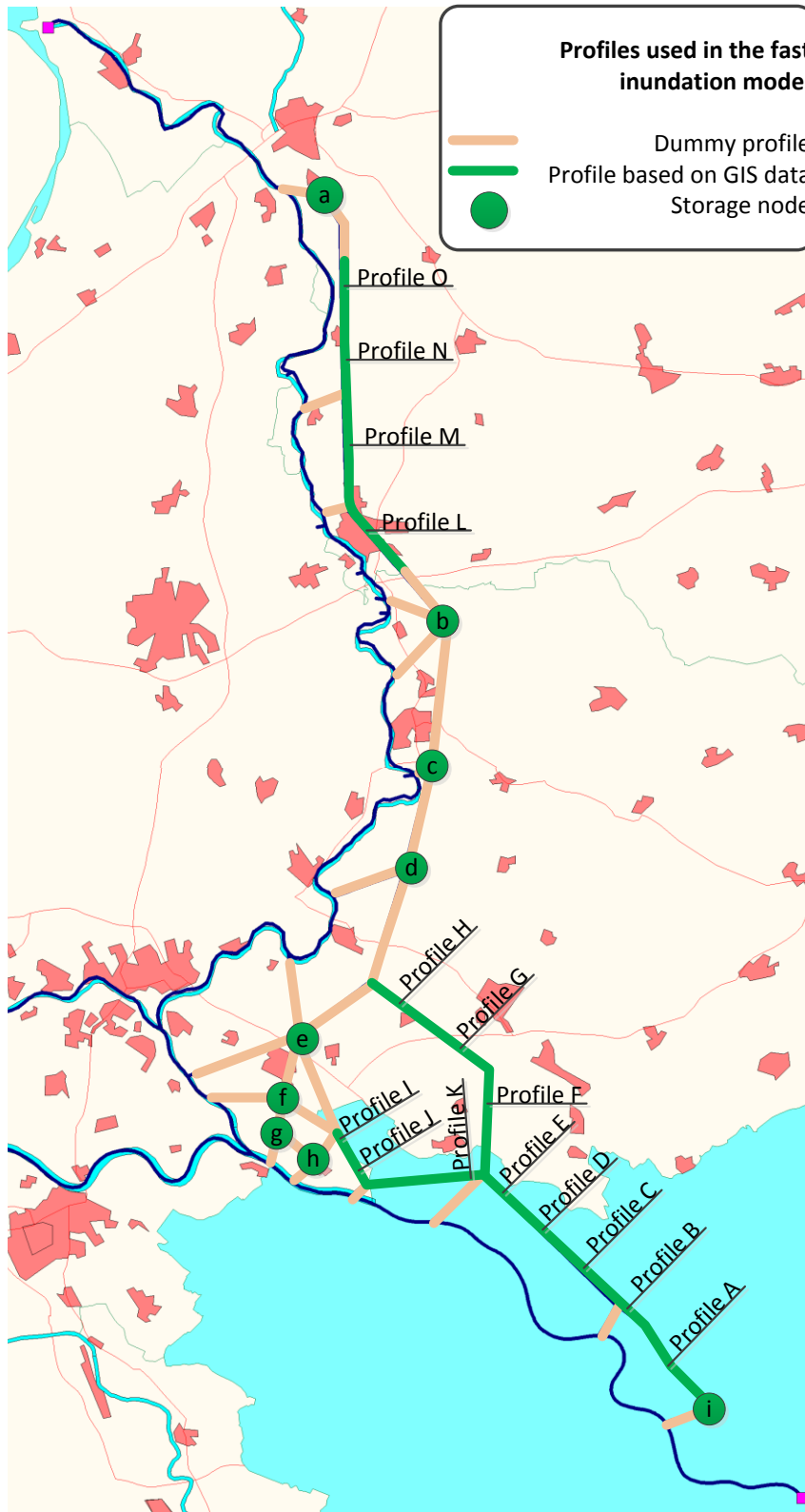


Figure H-9 Overview of which profiles were used where in the model

### H.1 Dummy branch

Below a typical profile for a dummy branch is shown. Please note that the dummy branches can vary in width and in bottom level depending on the location. The one shown is the most commonly used profile for dummy branches.

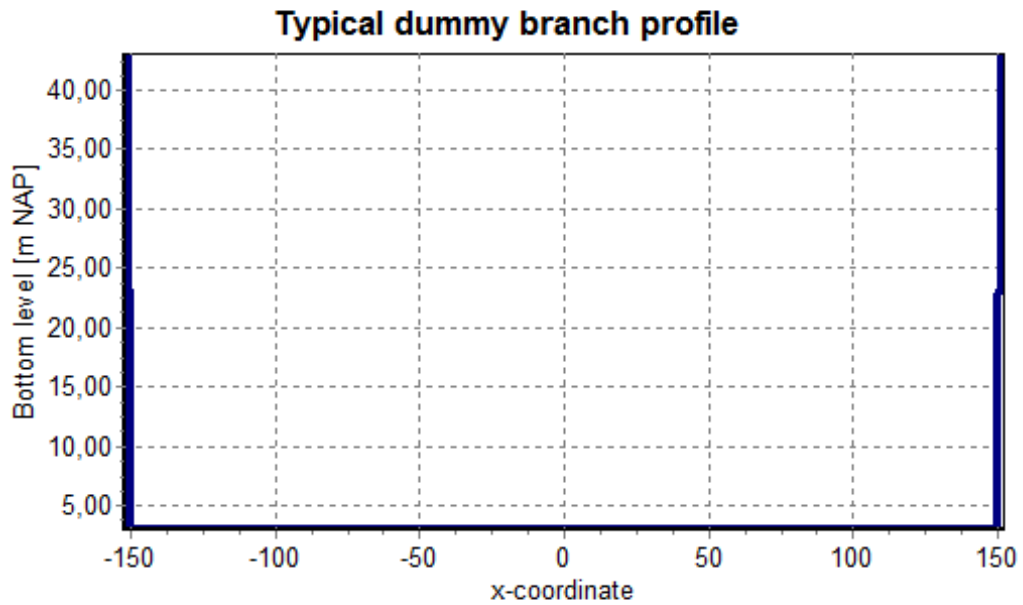


Figure H-10 Dummy branch profile

## H.2 GIS based profiles

In this paragraph a few of the GIS based profiles used in the model are shown.

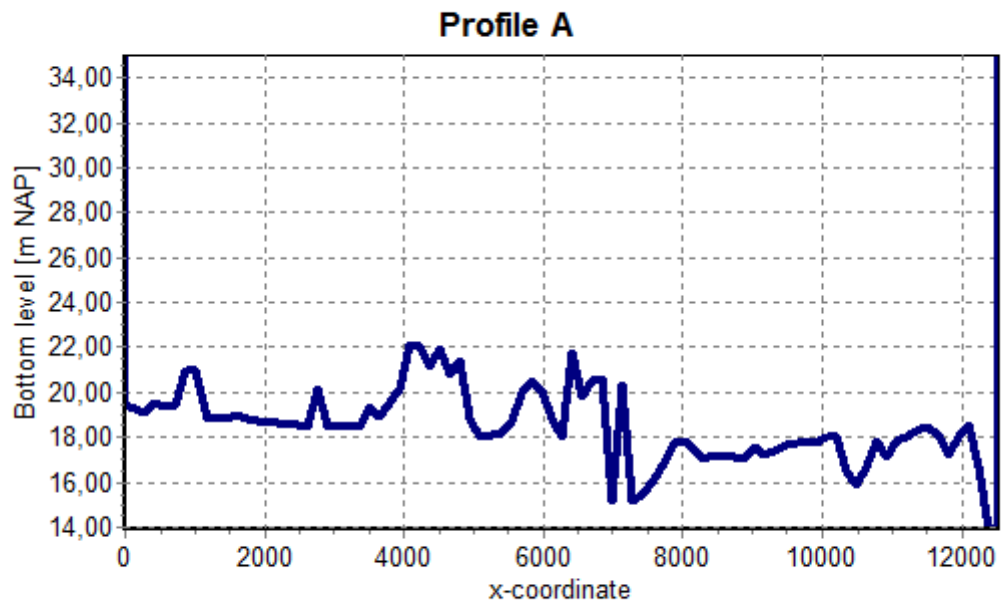


Figure H-11 Profile A

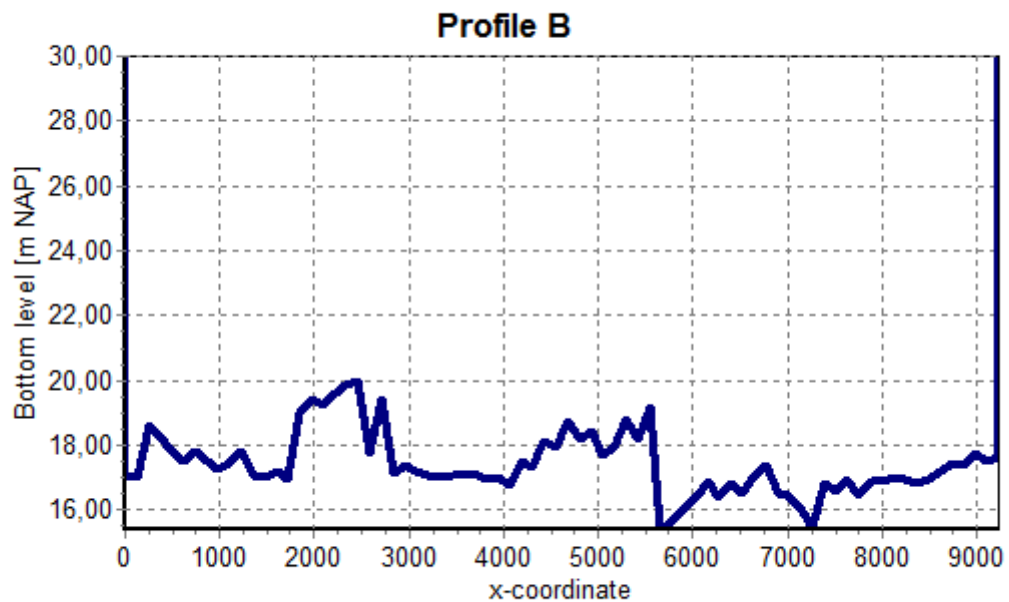


Figure H-12 Profile B

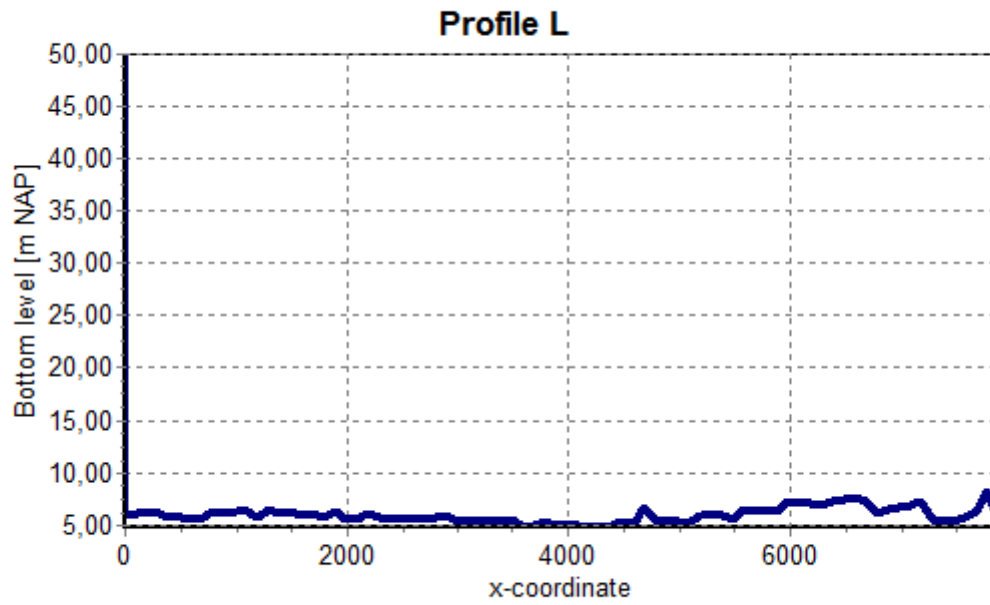


Figure H-13 Profile L

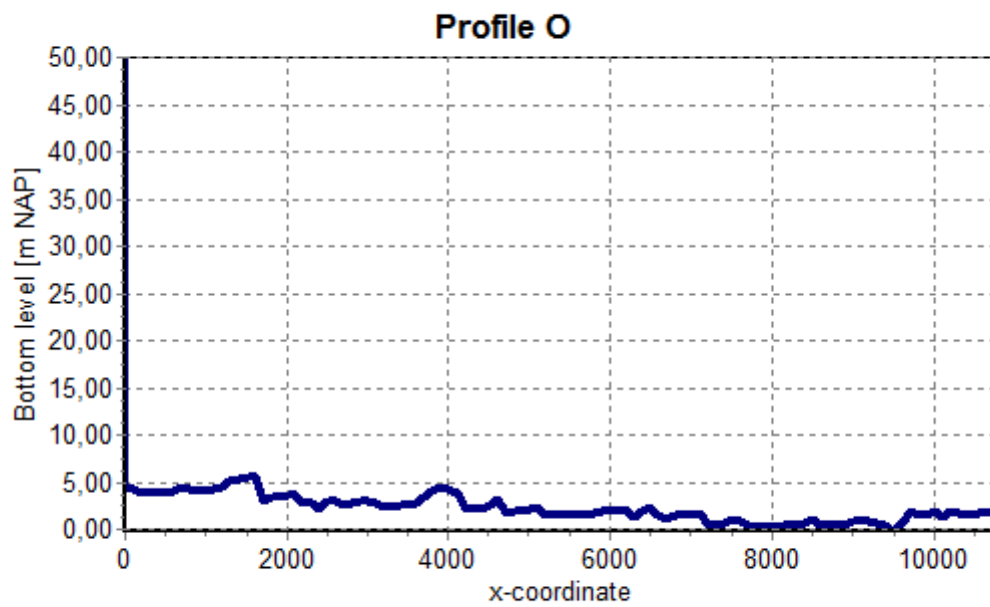


Figure H-14 Profile O

### H.3 Reservoir storage areas

This paragraph shows all the reservoir nodes and their storage areas at different bottom levels. Storage area h was assumed to have a 100.000 m<sup>2</sup> storage area at a bottom level of 10 m NAP. This could be done as the polder it represents is very small and flat.

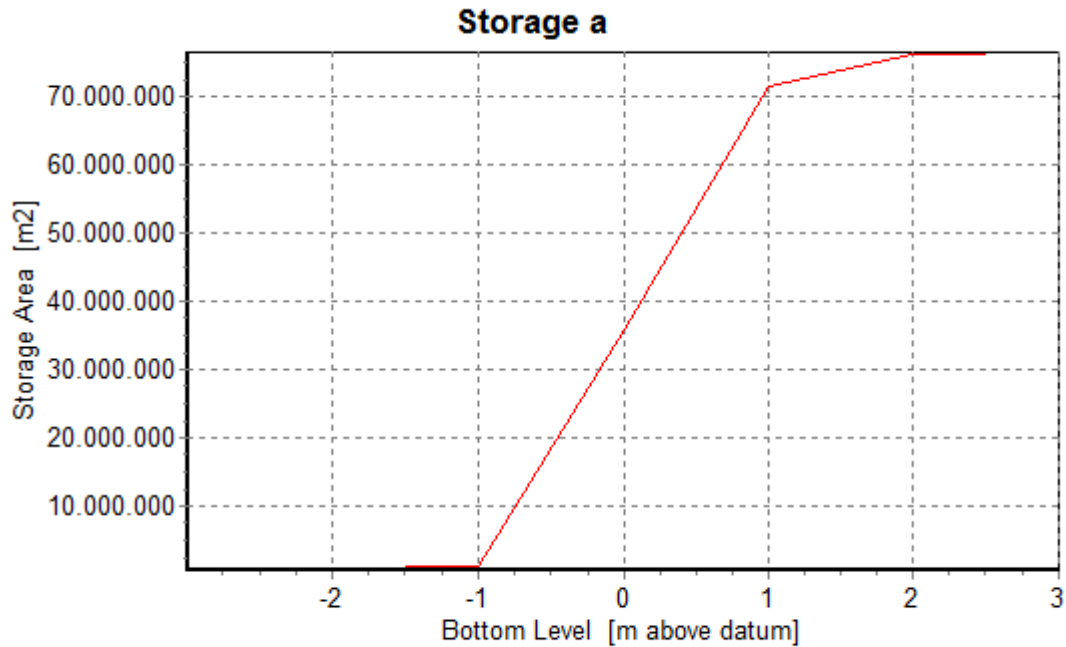


Figure H-15 Storage of area a

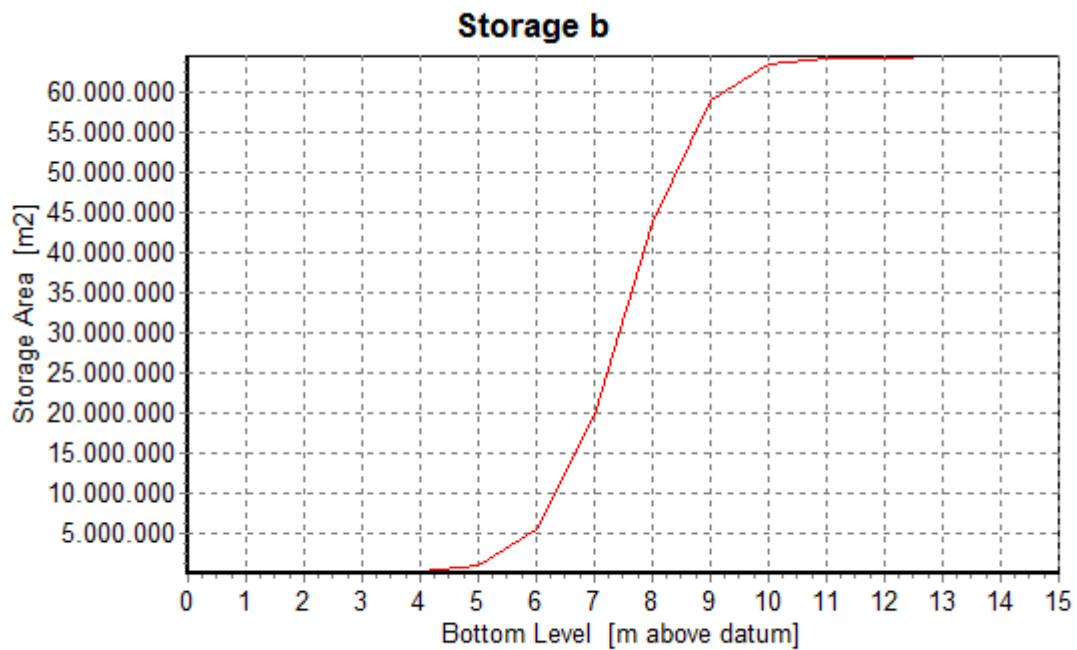


Figure H-16 Storage of area b

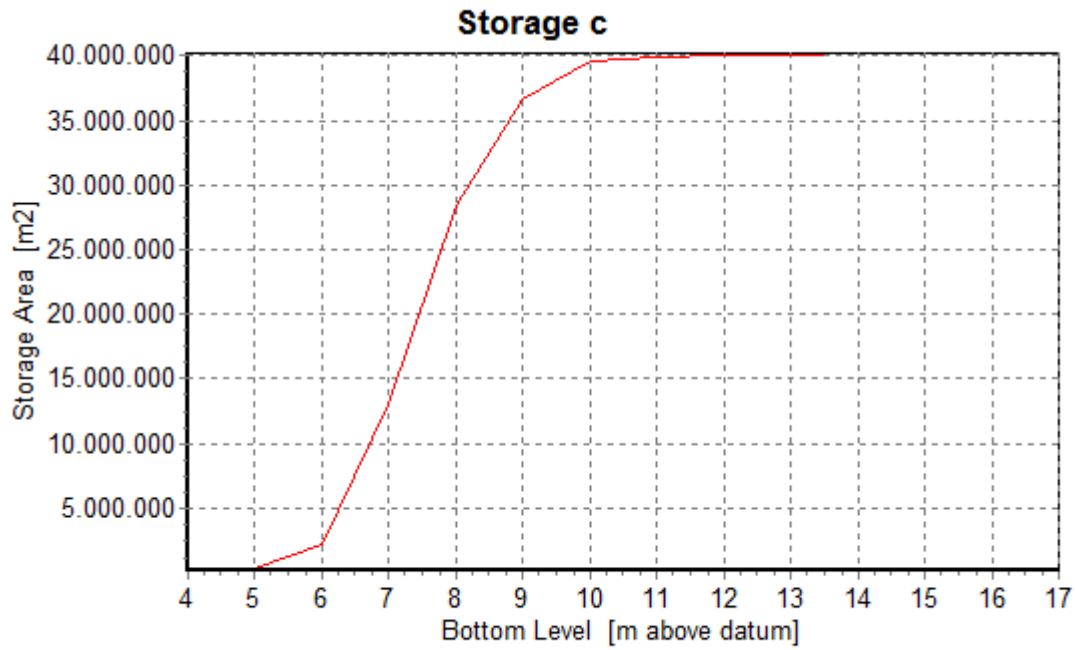


Figure H-17 Storage of area c

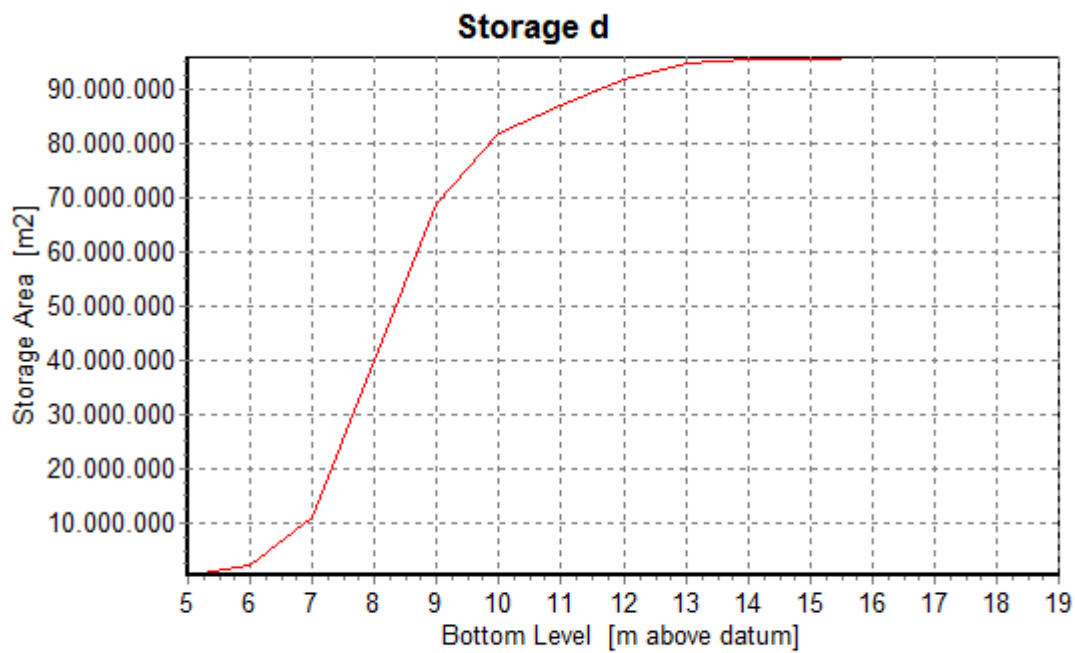


Figure H-18 Storage of area d

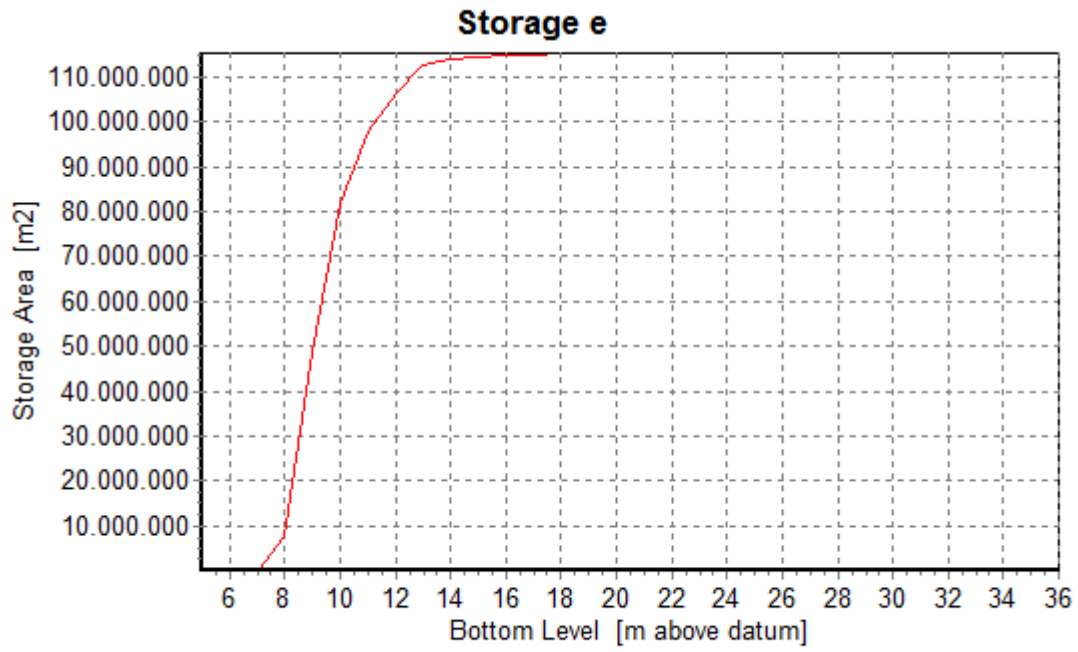


Figure H-19 Storage of area e

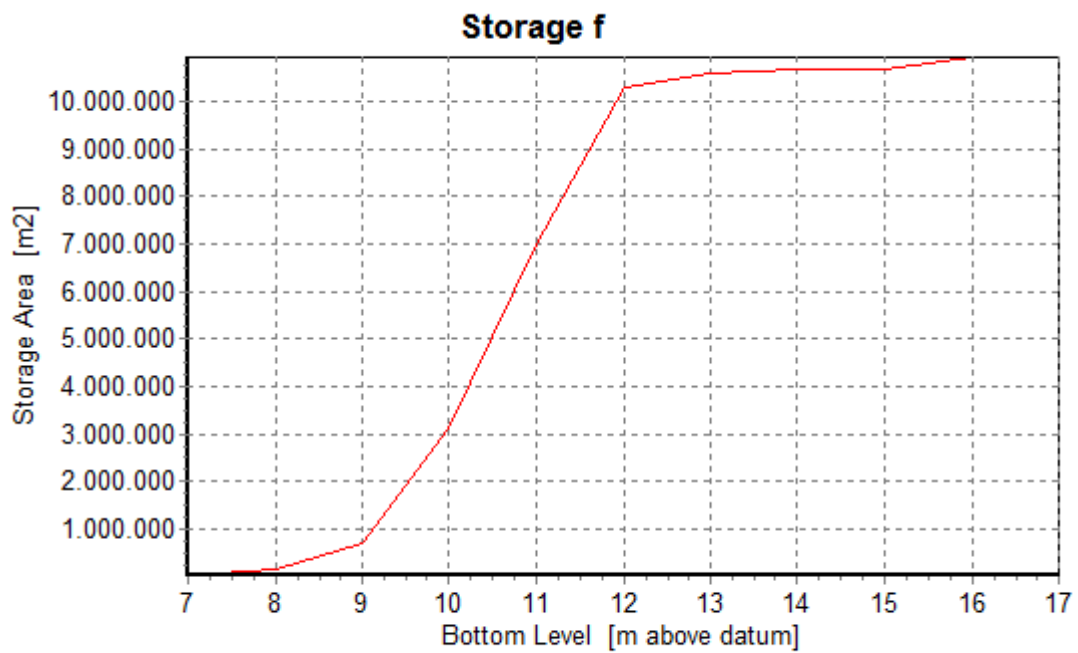


Figure H-20 Storage of area f

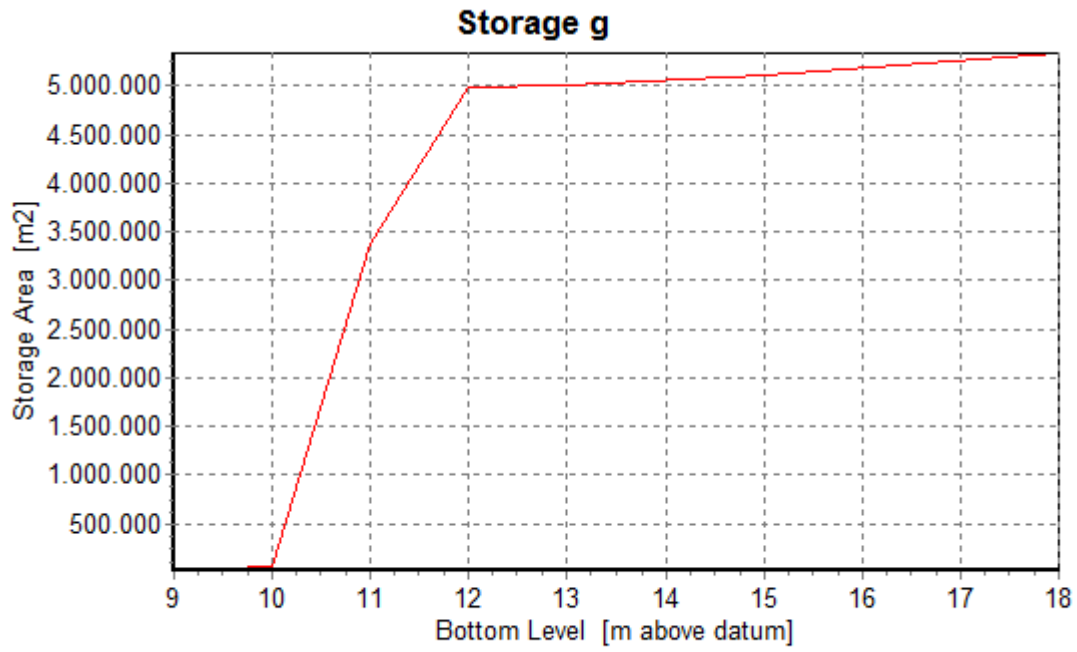


Figure H-21 Storage of area g

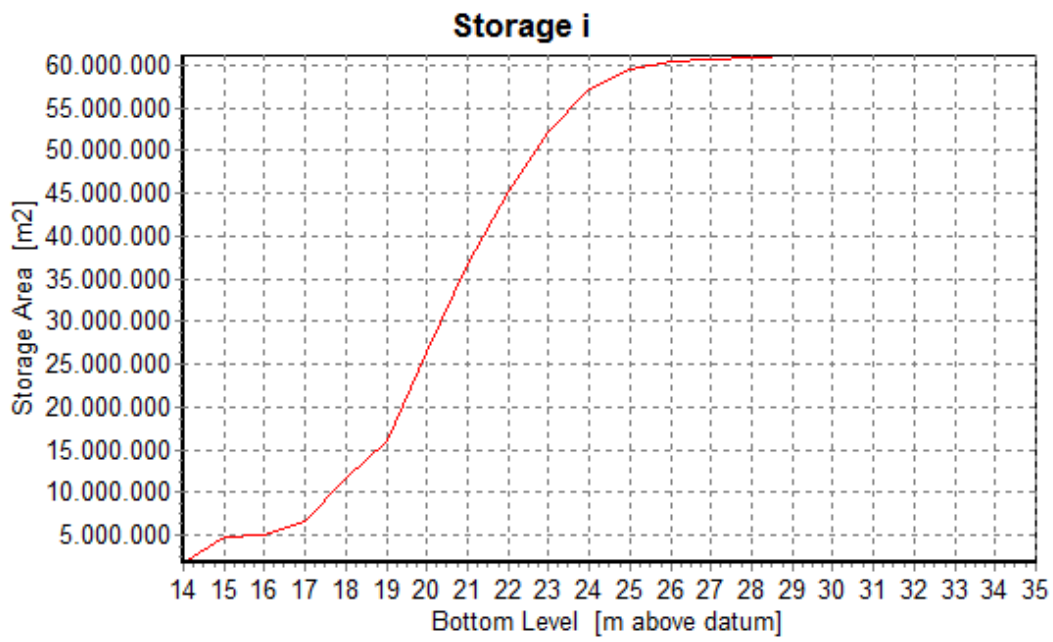


Figure H-22 Storage of area i

## I Differences between 2D and 0D for different scenarios

These tables show the water levels for both 2D and 0D for the same locations for all the flood zones. What can be observed is that for some cases the 2D is dry but the 0D has a (relatively low) water level, this is caused by the fact that for 2D the water level is measured at 1 location which can just stay dry while there is water at other places in the flood zone.

Table I-4 Water levels for 2D and the fast inundation model for dike ring area 48

	48_1		48_2		48_3		48_4		48_5		48_6		48_7	
Scenario	H_2D	H_0D												
<b>Gravensw 10000</b>	Dry	12,1	11,7	11,4	11,7	11,4	16,5	16,4	16,5	16,4	17,7	18,0	16,5	16,4
<b>Gravensw 100</b>	Dry		16,3	16,8	Dry	10,0								
<b>Gravensw 1000</b>	Dry	11,7	Dry	9,1	Dry	7,3	14,2	15,5	Dry	13,0	17,2	17,5	14,2	15,5
<b>Herwen 10000</b>	Dry	12,1	13,0	11,4	13,0	11,4	16,6	16,5	16,6	17,2	16,0	Dry	16,6	16,3
<b>Herwen 100</b>	Dry	11,8	Dry	9,1	Dry	8,6	15,4	15,8	15,7	16,1	Dry		15,4	15,8
<b>Loo 10000</b>	Dry	12,8	13,1	12,8	13,2	12,8	Dry		Dry		Dry		Dry	
<b>Loo 100</b>	Dry	12,1	12,5	12,1	12,5	12,1	Dry		Dry		Dry		Dry	
<b>Spijk 10000</b>	14,2	13,2	13,6	13,1	13,6	13,1	16,7	16,5	16,7	16,5	16,9	17,2	16,9	17,2
<b>Spijk 1000</b>	Dry	13,1	13,2	13,1	13,2	13,1	16,7	16,9	16,7	16,9	16,7	16,8	16,8	17,0
<b>Spijk 100</b>	Dry	12,3	12,6	11,9	12,6	11,9	16,5	16,5	16,5	16,5	14,6	Dry	16,5	16,5
<b>Germany 2 10000</b>	15,1	14,9	13,4	13,1	13,1	13,0	Dry		Dry		Dry		Dry	11,6
<b>Germany 2 1000</b>	14,6	14,6	13,0	12,3	12,7	12,3	Dry		Dry		Dry		Dry	10,9
<b>Germany 2 100</b>	Dry	14,1	12,5	11,5	10,6	11,5	Dry		Dry		Dry		Dry	10,2

Table I-5 Water levels for 2D and the fast inundation model for other locations

	49		50		51		53_1		53_2		53_3		53_4	
Scenario	H_2D	H_0D												
<b>Gravensw 10000</b>	Dry	9,3	Dry											
<b>Gravensw 100</b>	Dry													
<b>Gravensw 1000</b>	Dry													
<b>Herwen 10000</b>	10,6	9,3	10,4		9,8		5,8		3,2		1,8		1,8	
<b>Herwen 100</b>	Dry													
<b>Loo 10000</b>	11,1	11,0	11,0	10,4	10,2	10,0	6,2	5,5	5,0	5,5	5,0	5,5	5,0	5,5
<b>Loo 100</b>	10,5	10,7	10,3	10,1	9,8	9,8	5,8	4,2	3,2	4,2	1,8	4,2	1,6	2,0
<b>Spijk 10000</b>	11,9	11,1	11,7	10,4	10,8	10,0	6,6	4,9	6,8	4,9	6,8	4,9	6,8	4,7
<b>Spijk 1000</b>	11,2	11,1	11,0	10,4	10,3	10,0	6,2	4,8	4,0	4,8	4,0	4,8	4,0	4,6
<b>Spijk 100</b>	9,6	10,4	Dry	9,7	Dry	8,5	Dry		Dry		Dry		Dry	
<b>Germany 2 10000</b>	11,0	11,0	10,8	10,4	10,2	10,0	6,2	5,0	4,0	5,0	4,0	5,0	4,0	5,0
<b>Germany 2 1000</b>	10,4	10,7	9,8	10,1	9,2	9,8	Dry	4,2	Dry	3,8	Dry	3,8	Dry	1,4
<b>Germany 2 100</b>	9,6	10,2	Dry	7,6	Dry									

## J Water level – damage curves

This Appendix shows all water level – damage curves used in the model. The water levels are the water levels in 2D, for the calculations made these were shifted by the average difference between 2D and the fast inundation model for all flood zones.

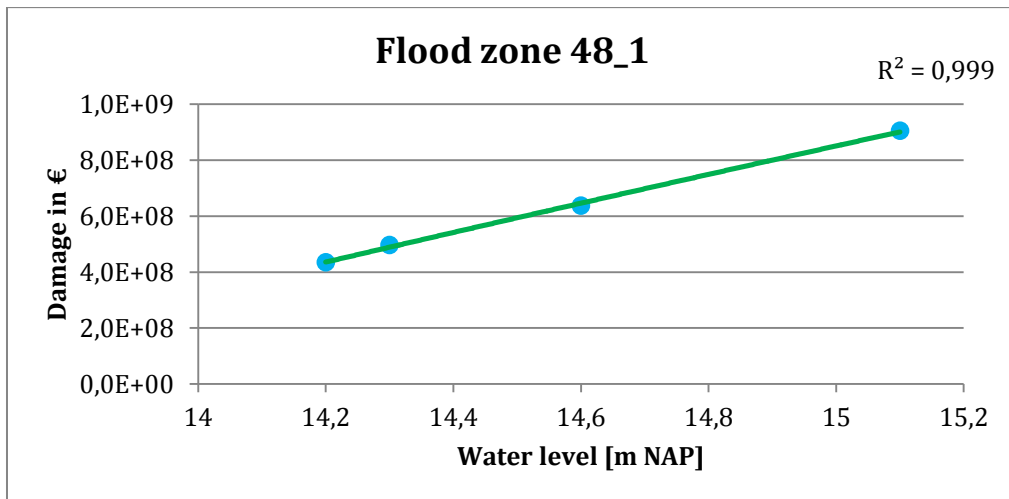


Figure J-23 Water level - damage curve for Flood zone 48\_1

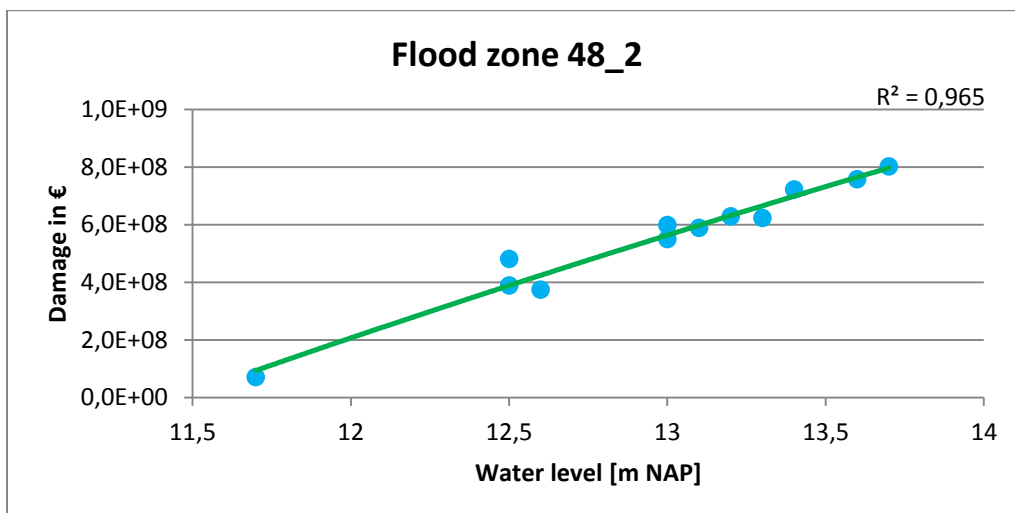


Figure J-24 Water level - damage curve for Flood zone 48\_2

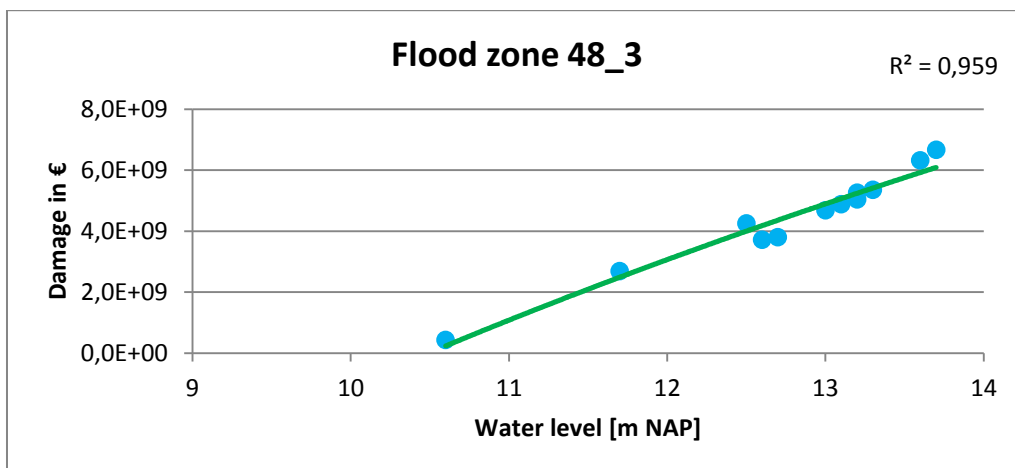


Figure J-25 Water level - damage curve for Flood zone 48\_3

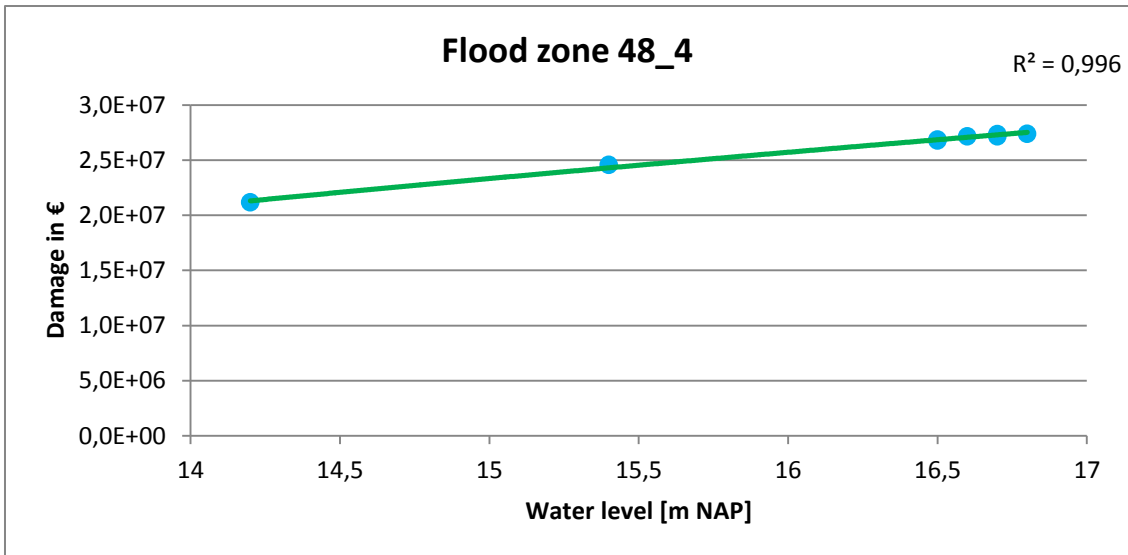


Figure J-26 Water level - damage curve for Flood zone 48\_4

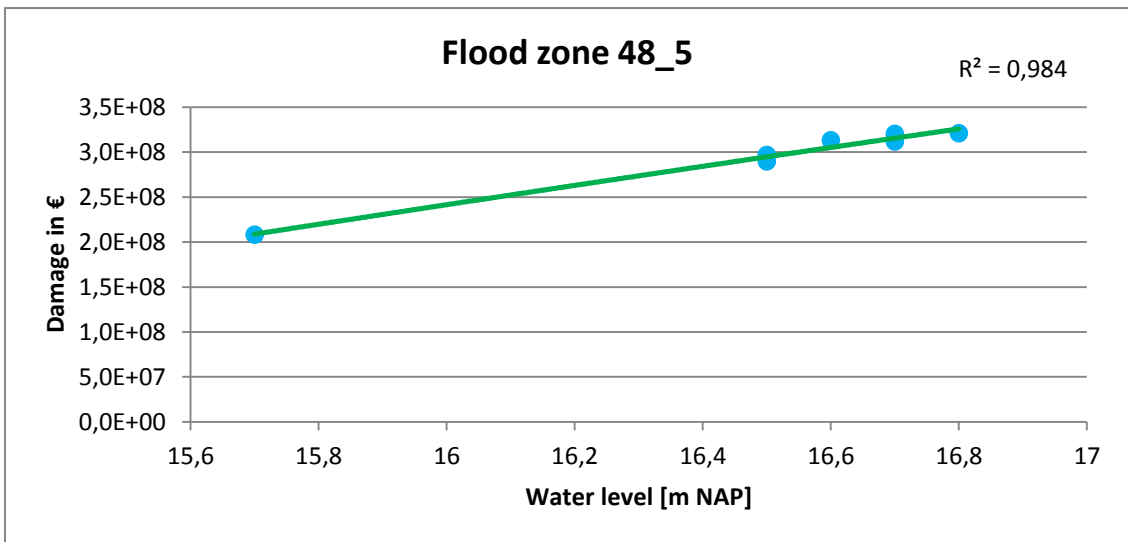


Figure J-27 Water level - damage curve for Flood zone 48\_5

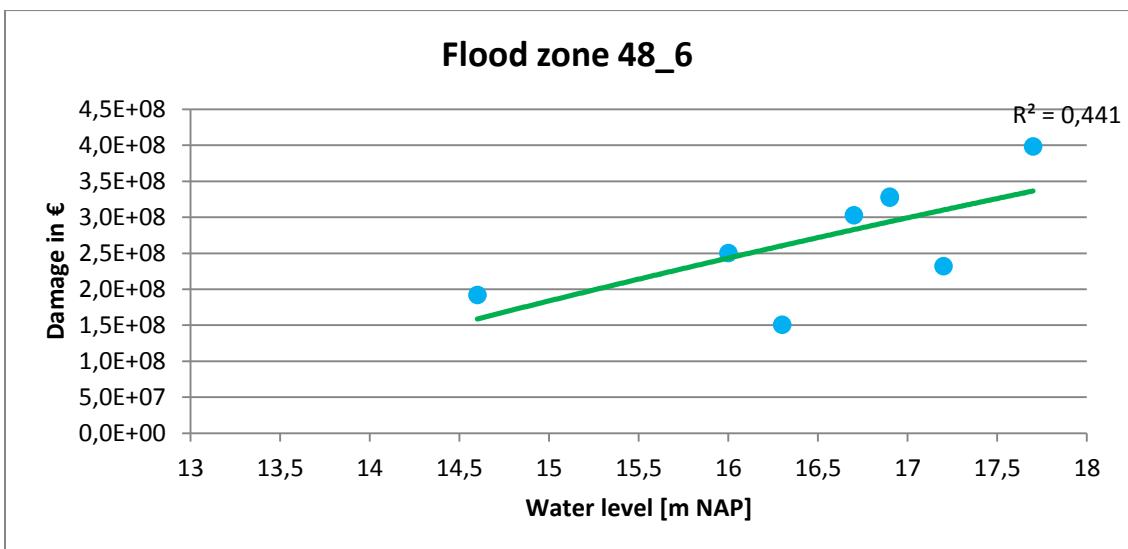


Figure J-28 Water level - damage curve for Flood zone 48\_6

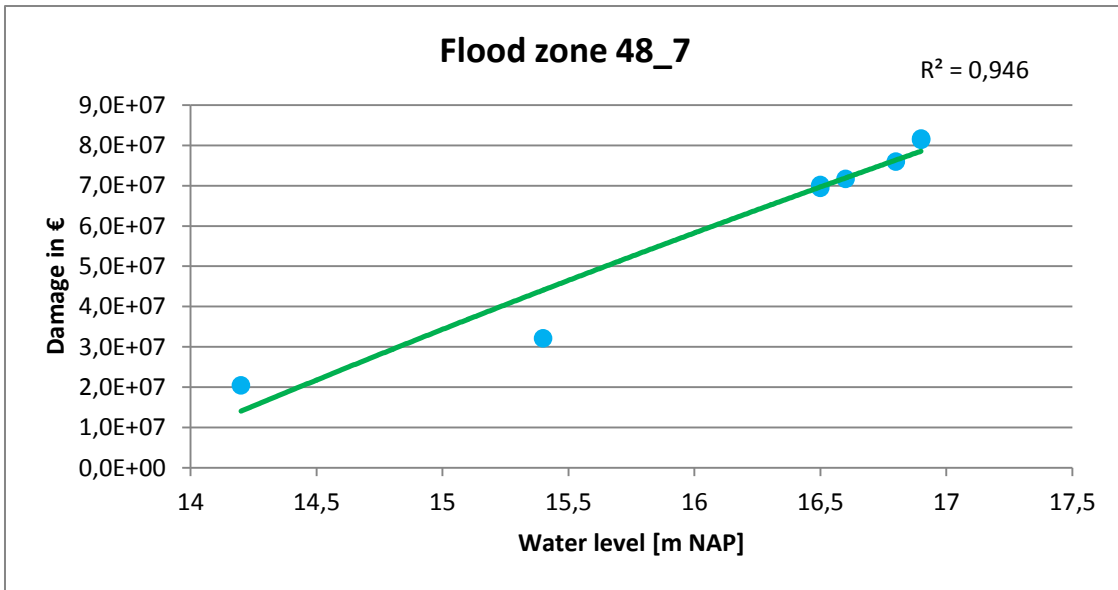


Figure J-29 Water level - damage curve for Flood zone 48\_7

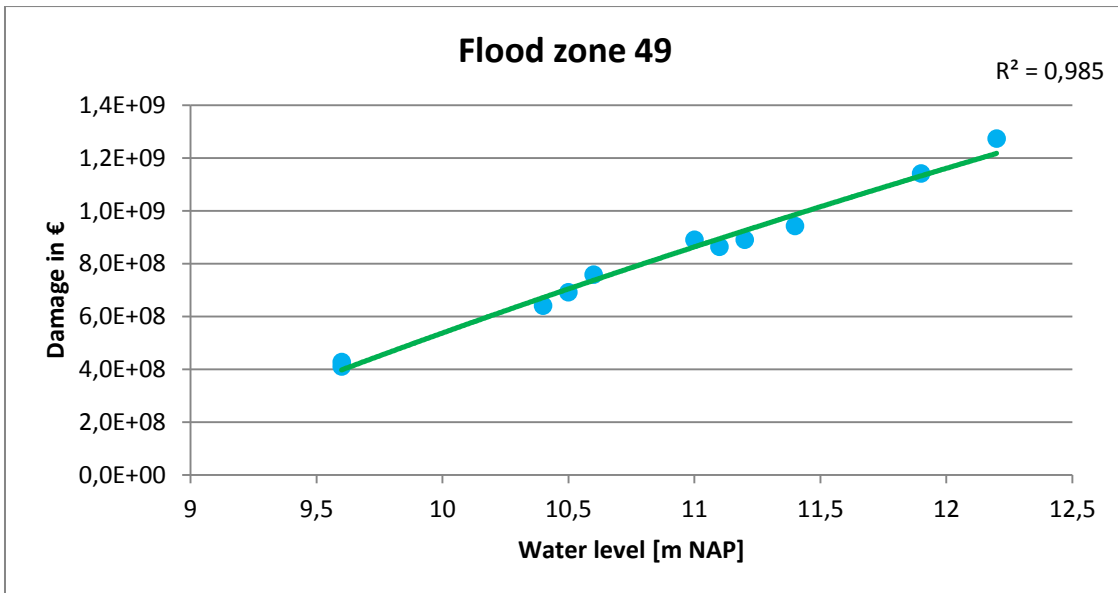


Figure J-30 Water level - damage curve for Flood zone 49

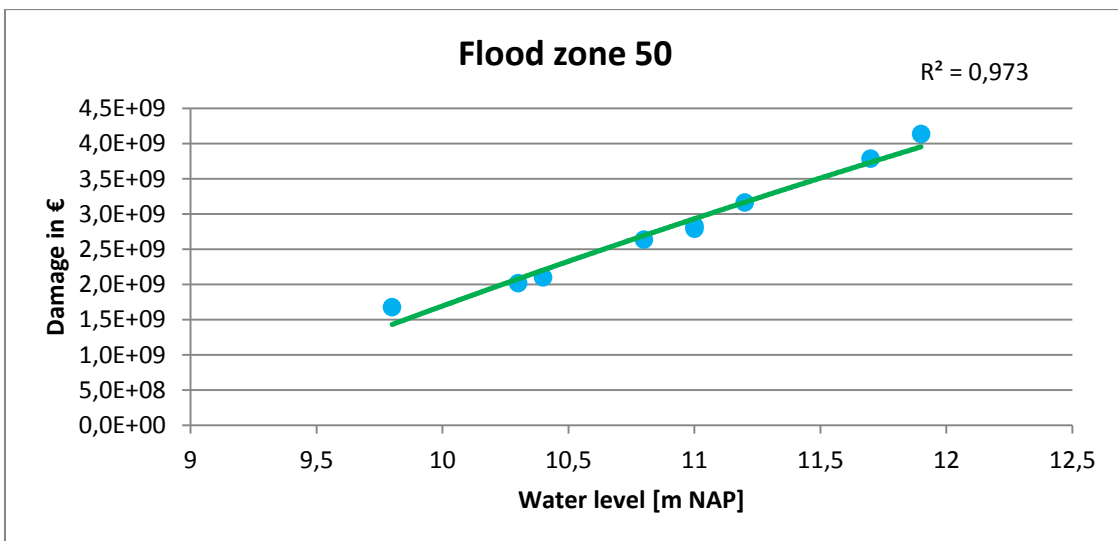


Figure J-31 Water level - damage curve for Flood zone 50

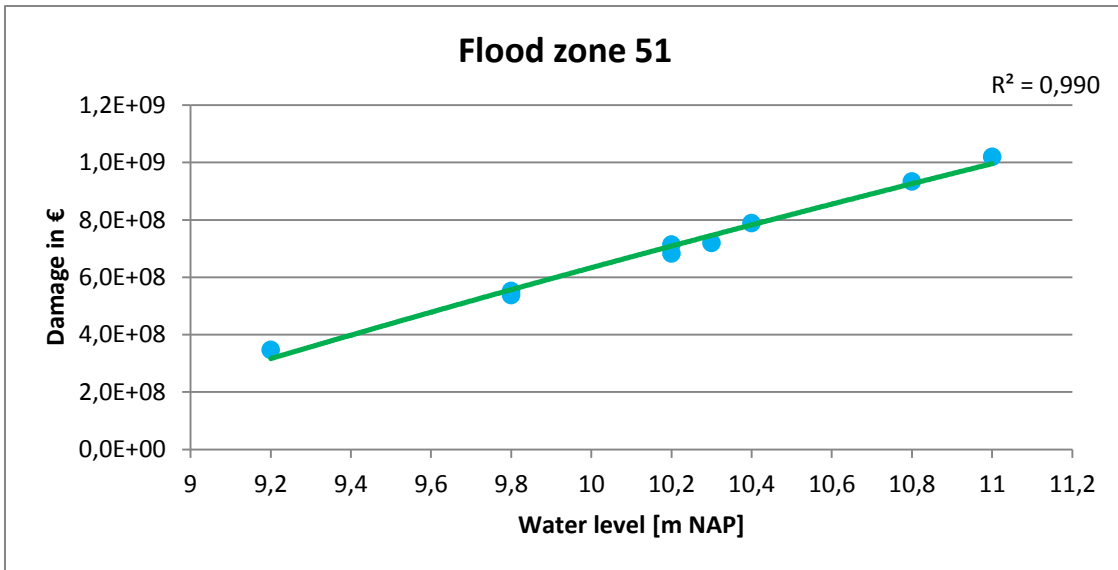


Figure J-32 Water level - damage curve for Flood zone 51

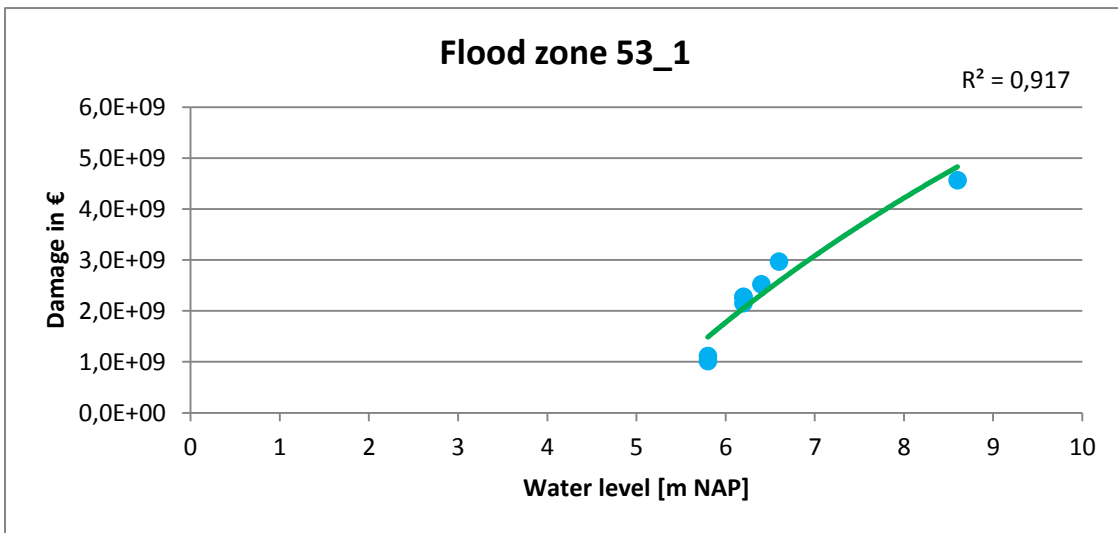


Figure J-33 Water level - damage curve for Flood zone 53\_1

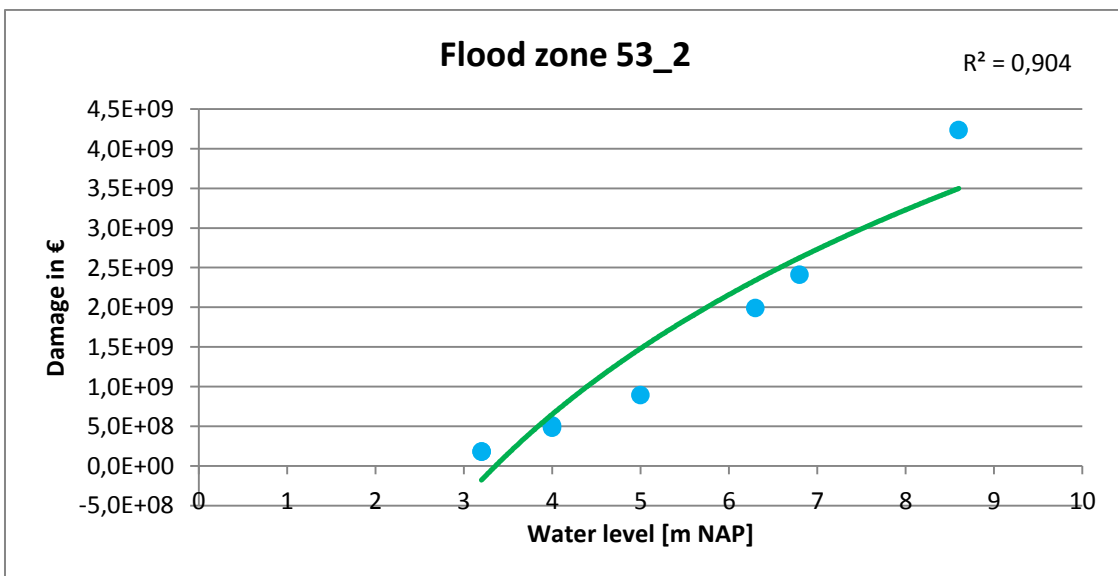


Figure J-34 Water level - damage curve for Flood zone 53\_2

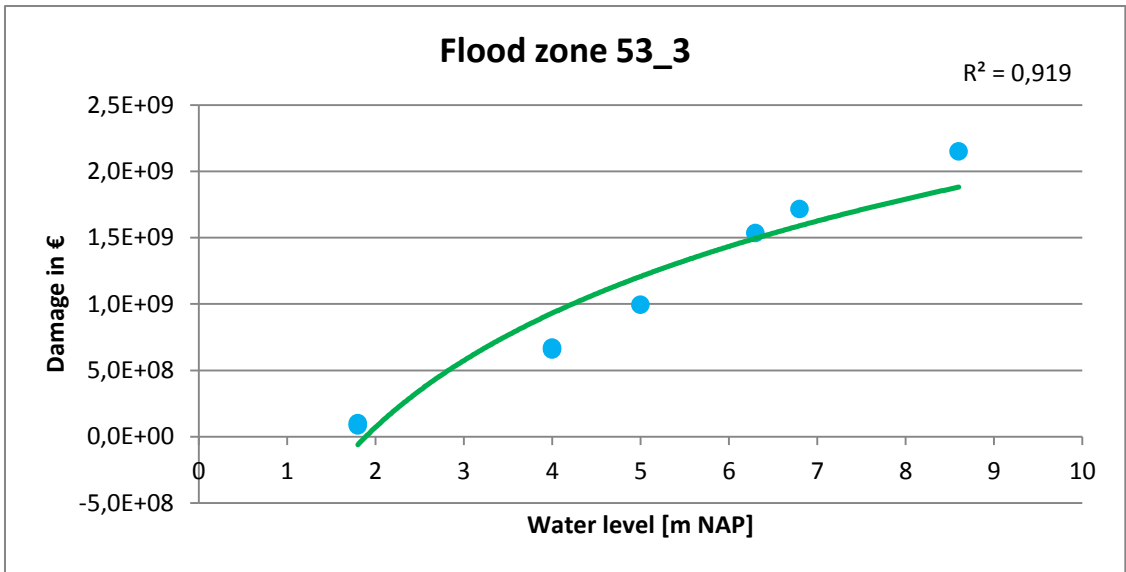


Figure J-35 Water level - damage curve for Flood zone 53\_3

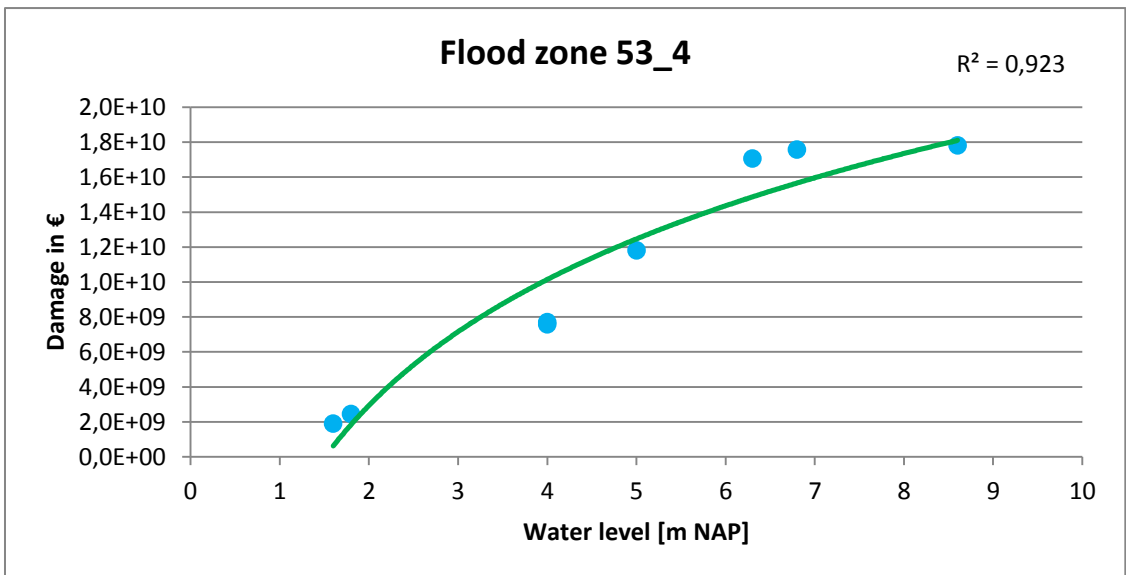


Figure J-36 Water level - damage curve for Flood zone 53\_4

## K Water level differences for all breach locations

This appendix shows the water levels for the different scenario's for most breach locations in the system. Not all are shown, as some are very close together and are practically the same.

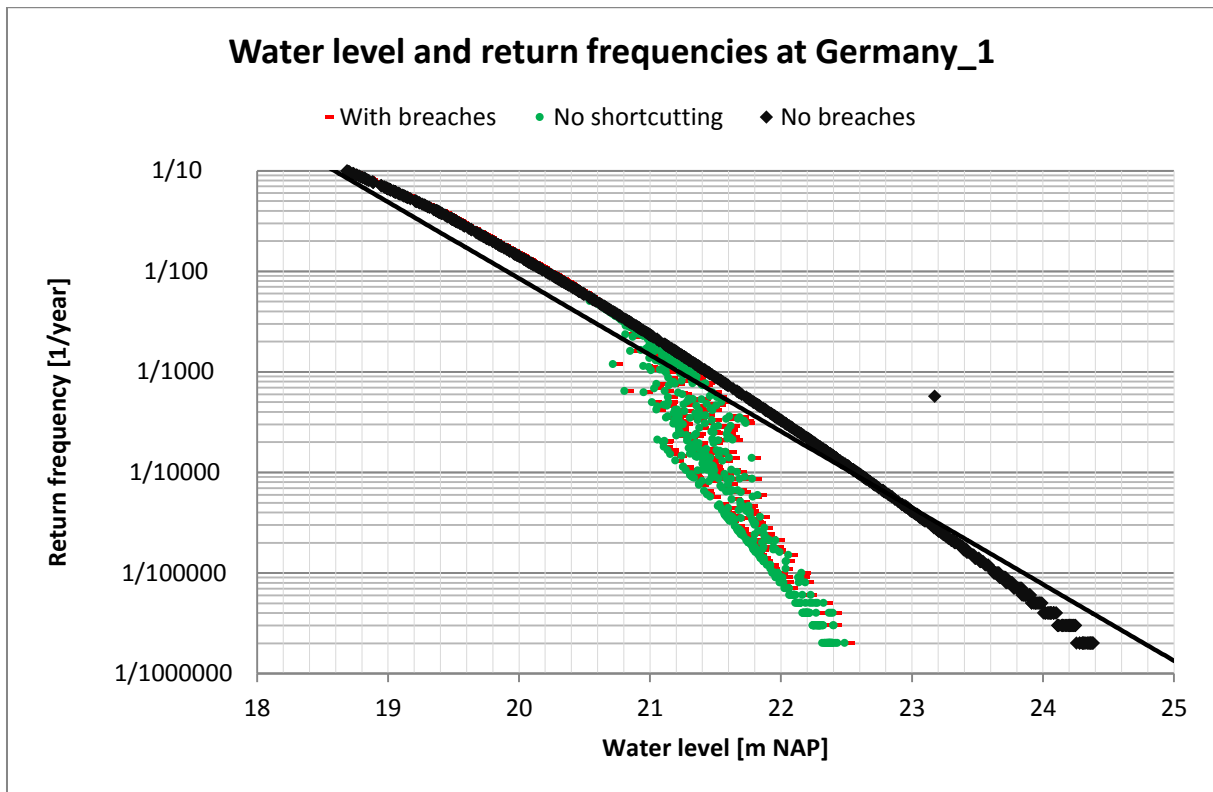


Figure K-37 Water level and return frequencies at Germany\_1

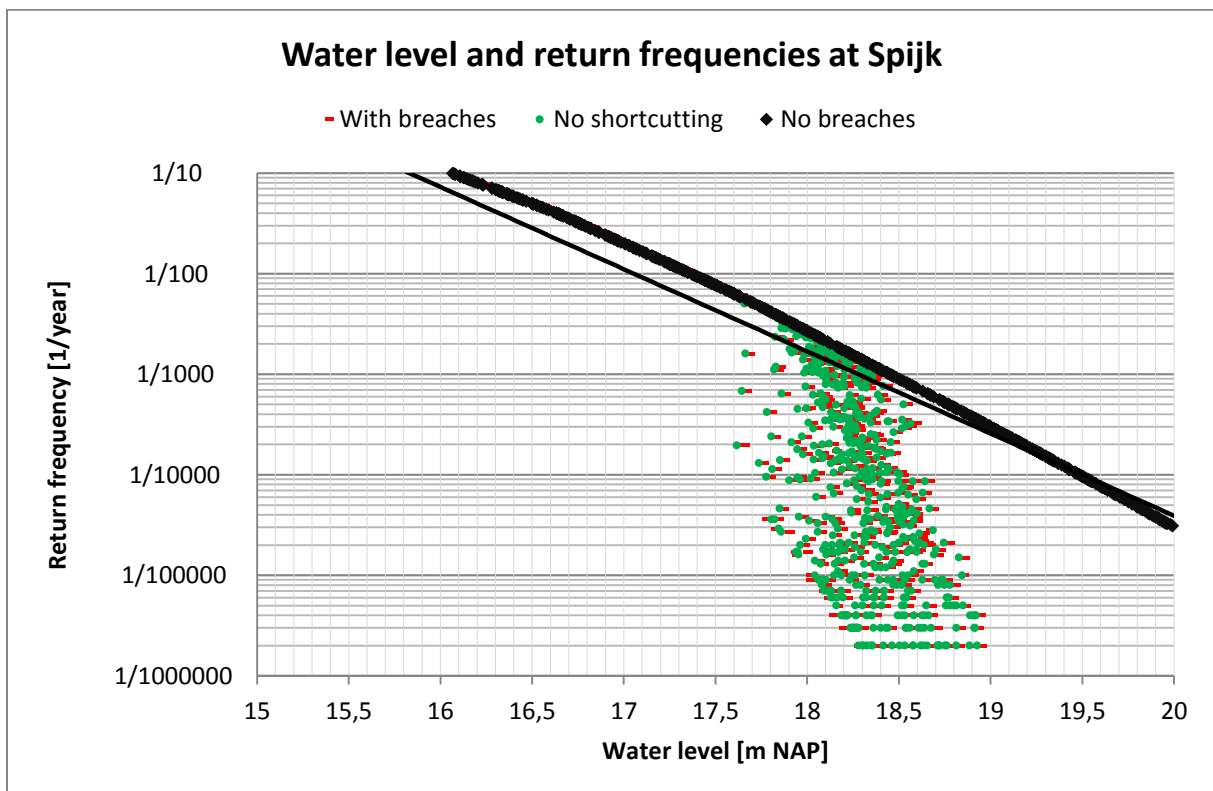


Figure K-38 Water level and return frequencies at Spijk

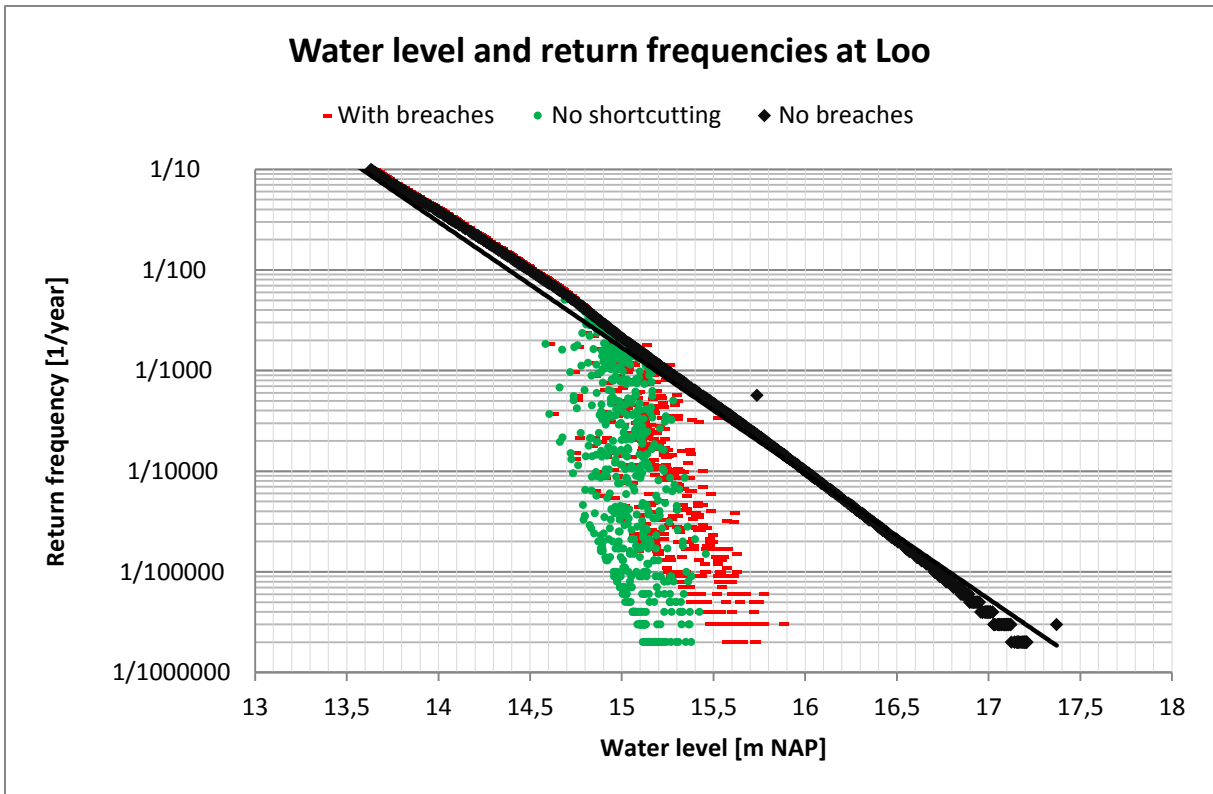


Figure K-39 Water level and return frequencies at Loo

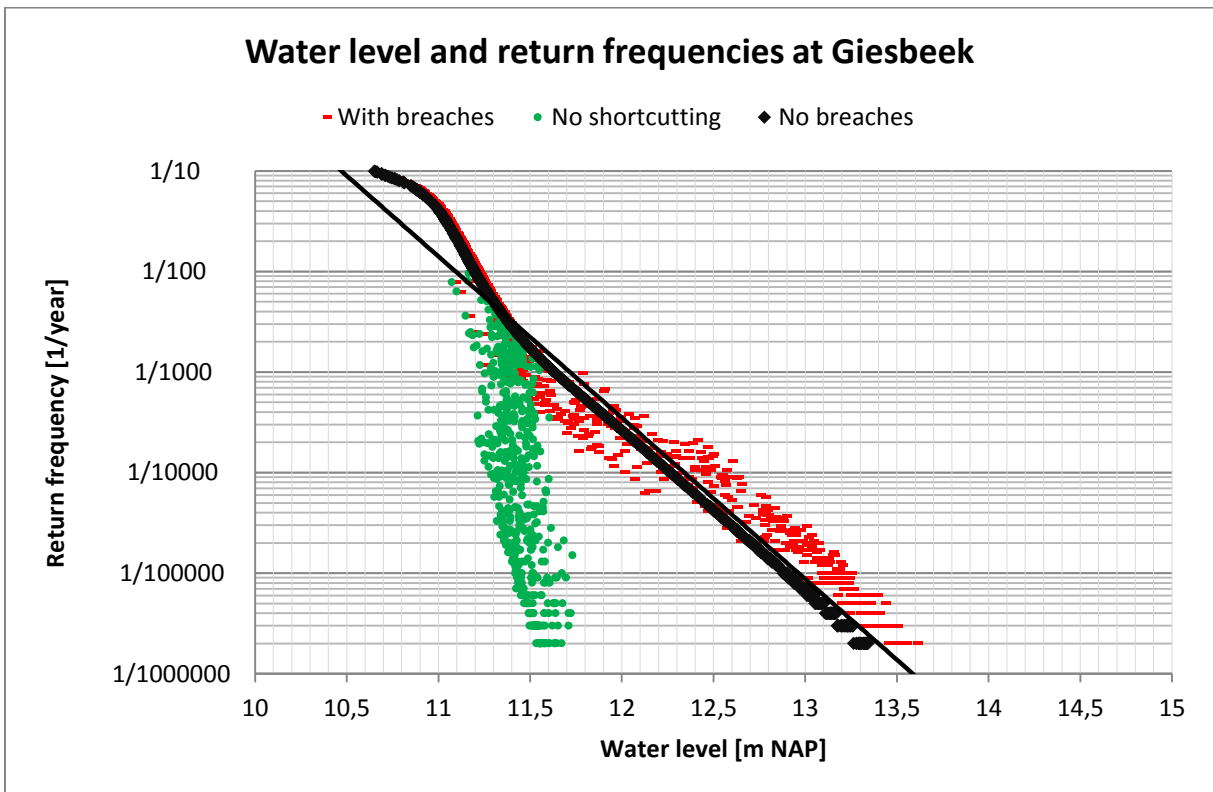


Figure K-40 Water level and return frequencies at Giesbeek

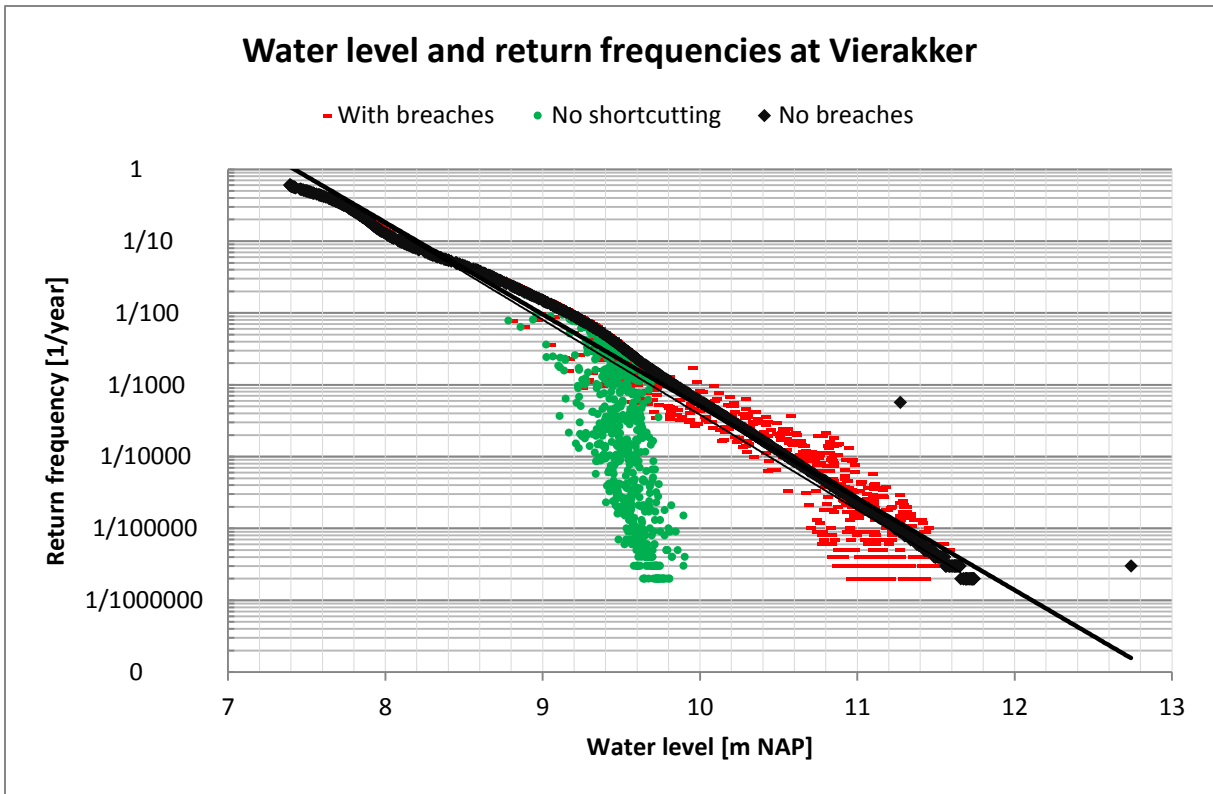


Figure K-41 Water level and return frequencies at Vierakker

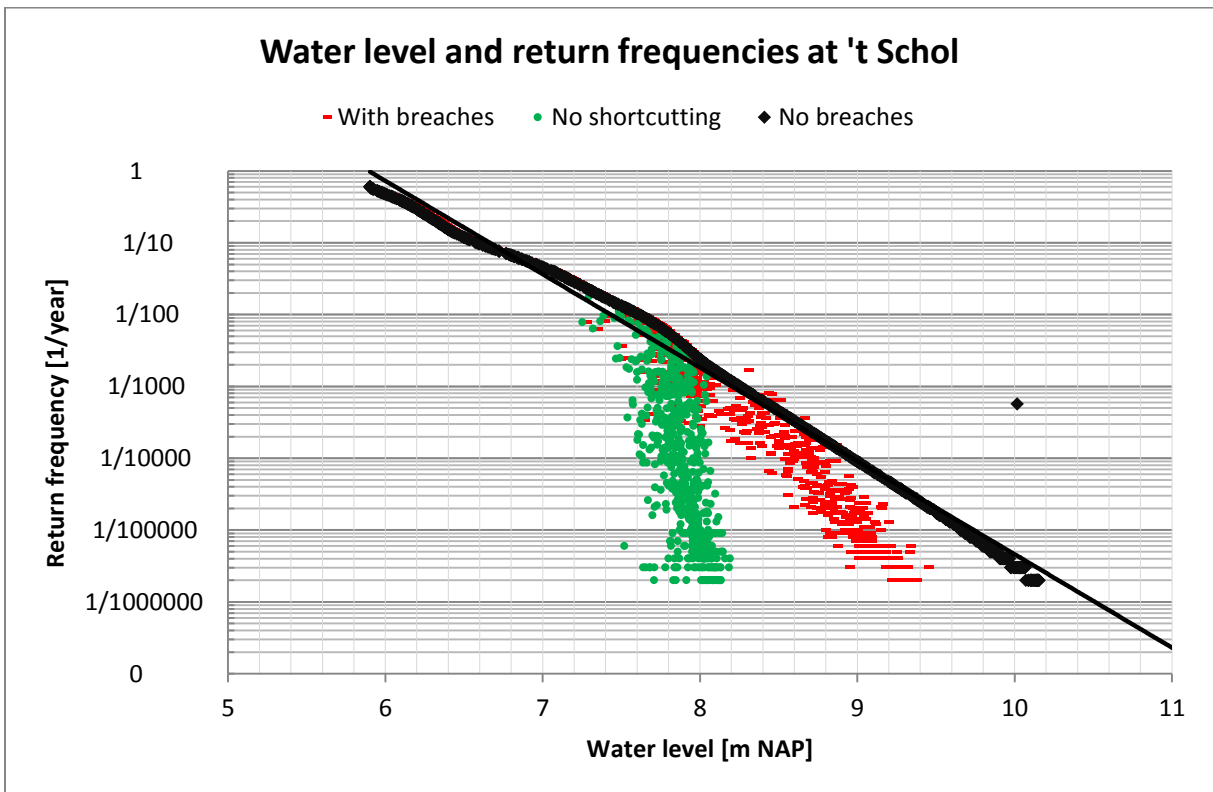


Figure K-42 Water level and return frequencies at 't Schol

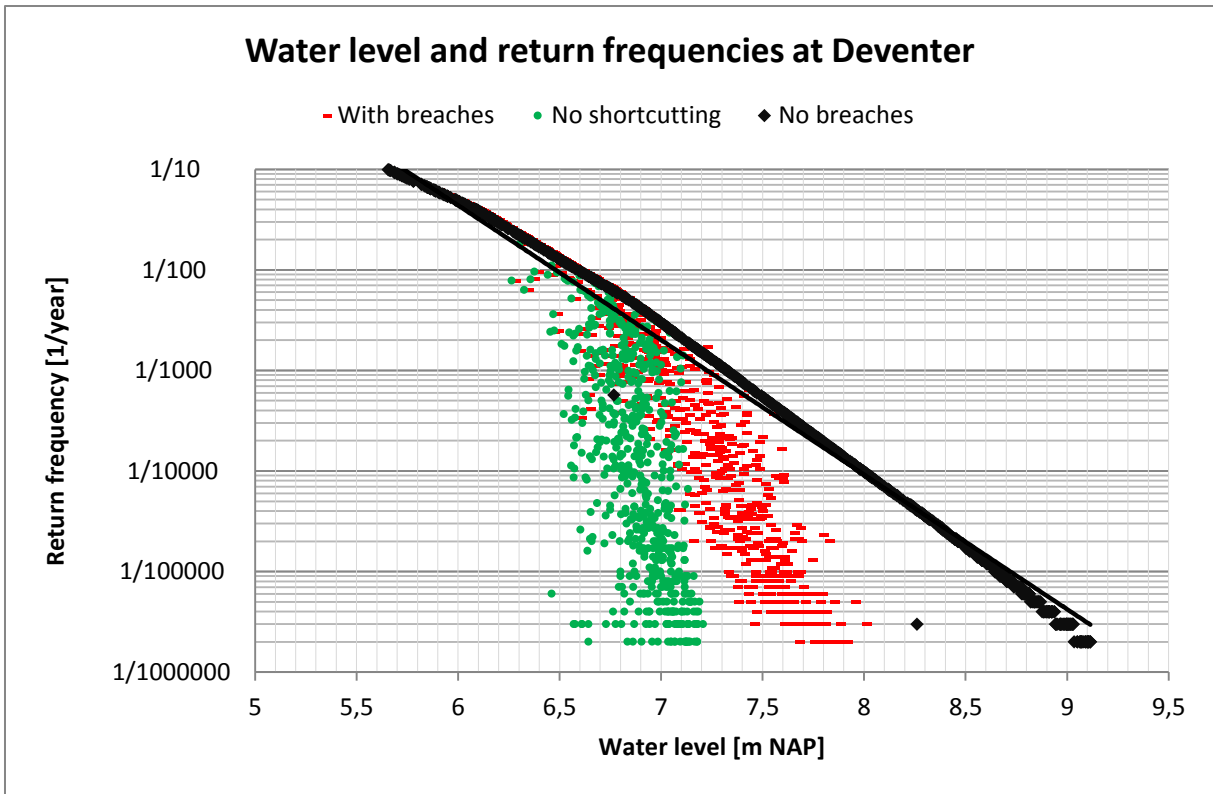


Figure K-43 Water level and return frequencies at Deventer

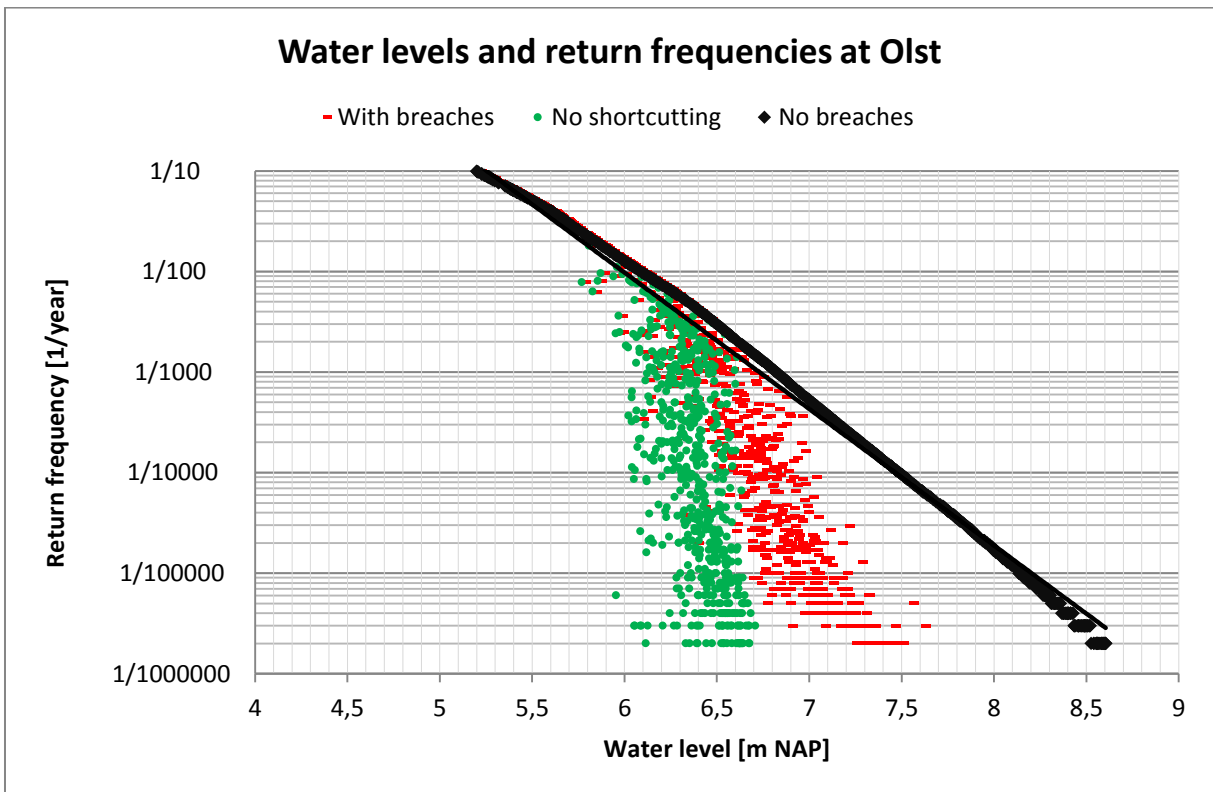


Figure K-44 Water level and return frequencies at Olst

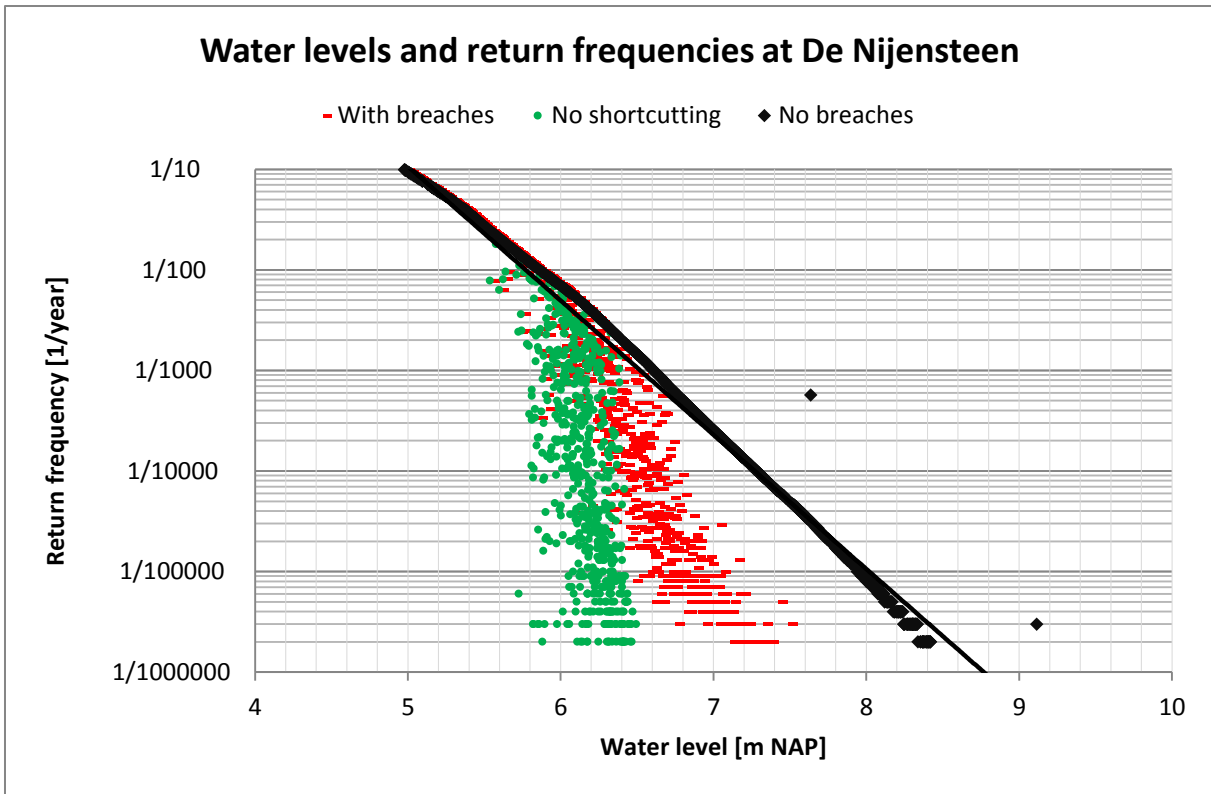


Figure K-45 Water level and return frequencies at De Nijenstein

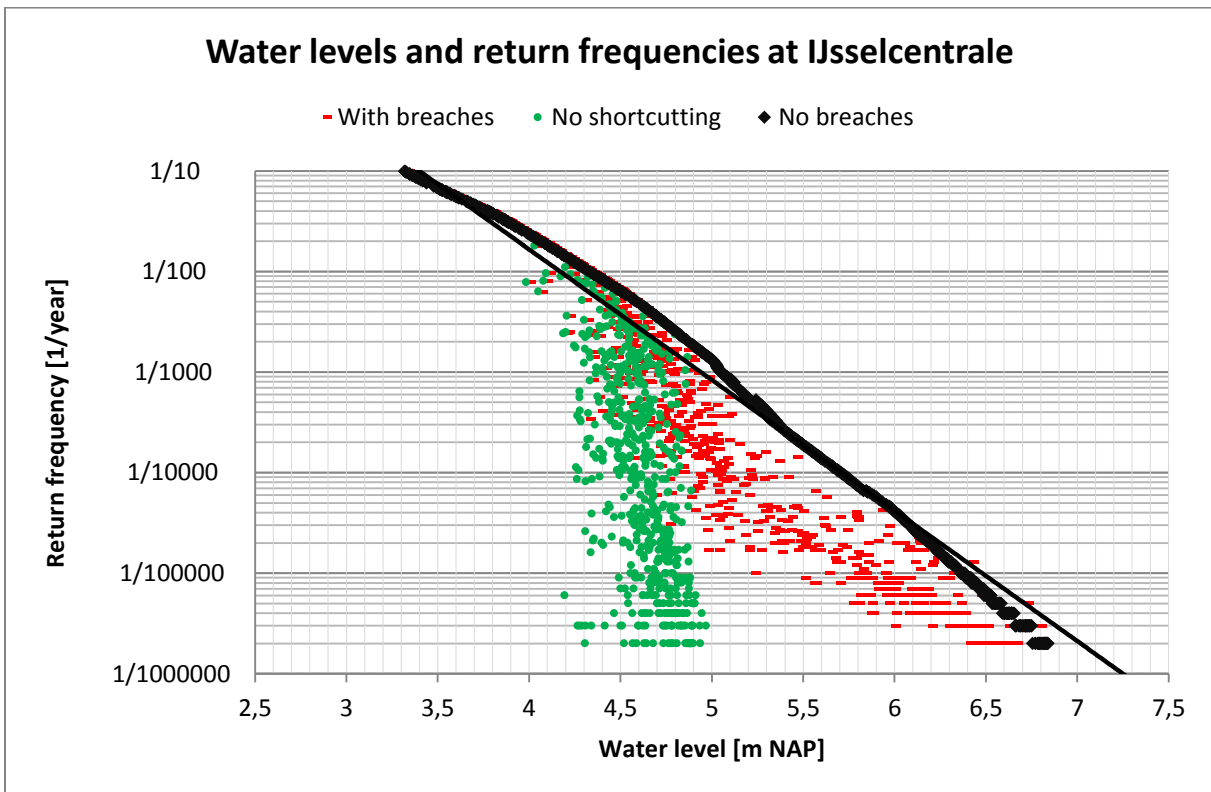


Figure K-46 Water level and return frequencies at IJcentrale

## L FD curves for dike rings 49, 50, 51 and 53

The FD curves for dike rings 49, 50, 51 and 53 were not shown in the main report. These curves can be found below.

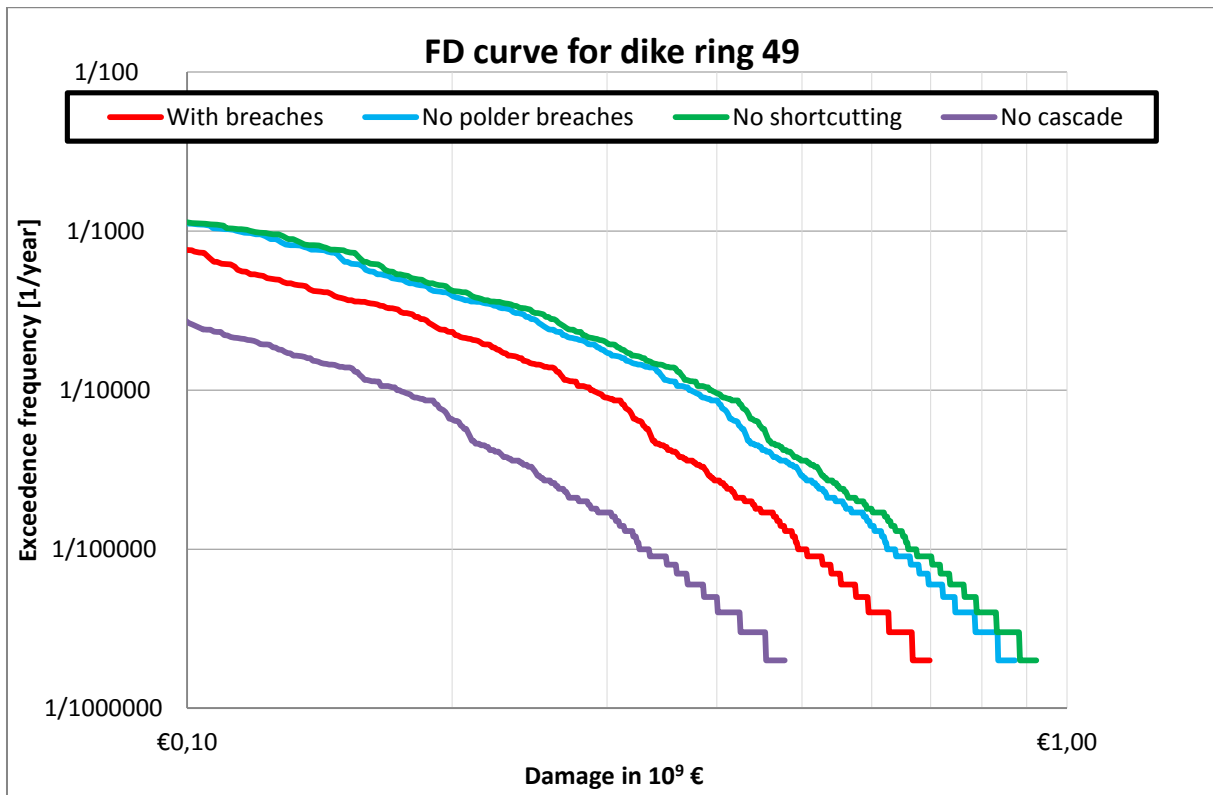


Figure L-47 FD curve for dike ring 49

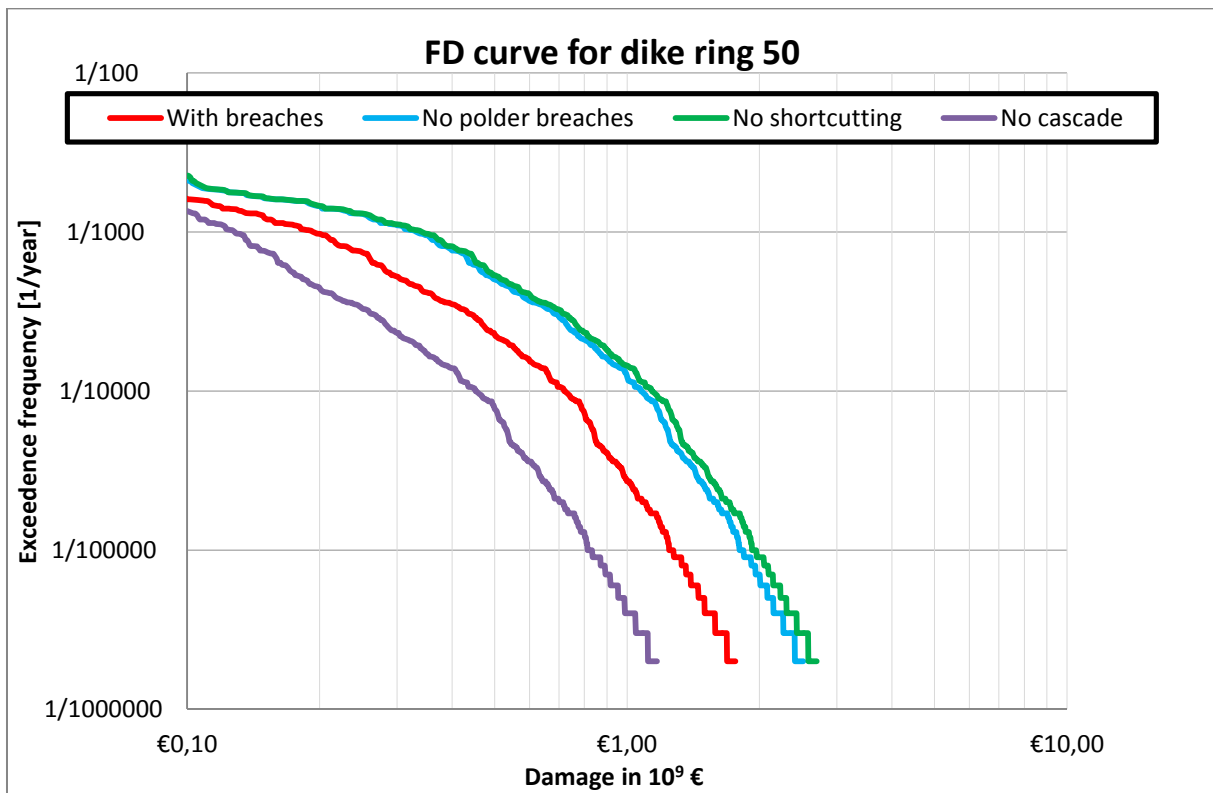


Figure L-48 FD curve for dike ring 50

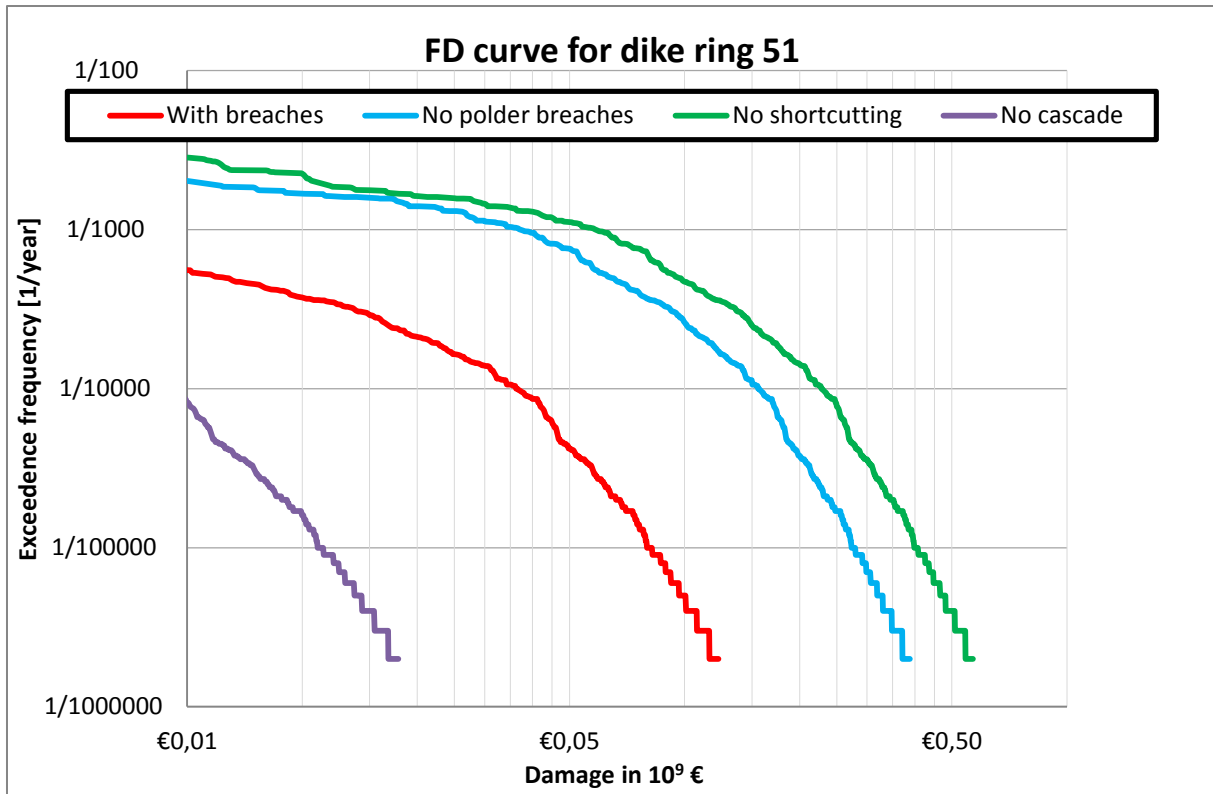


Figure L-49 FD curve for dike ring 51

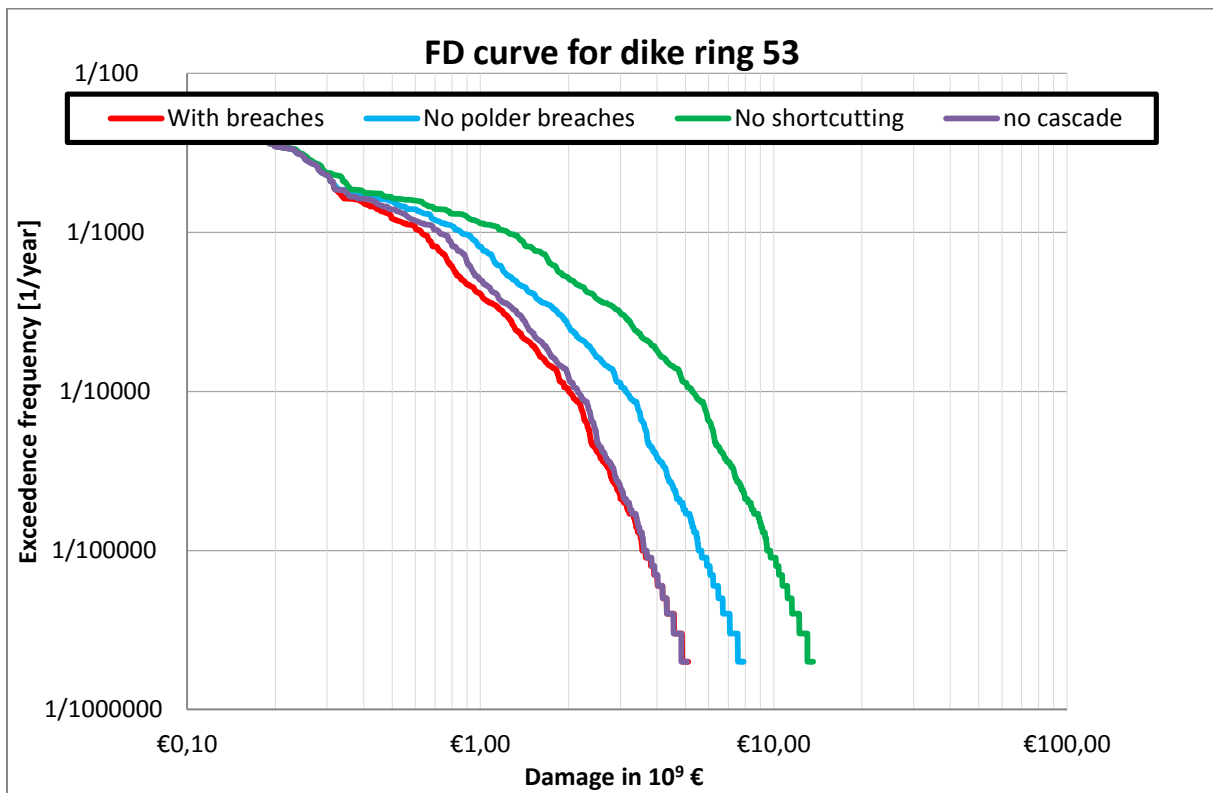


Figure L-50 FD curve for dike ring 53



